

**Identification of key genes involved in root knot
nematode (*M. incognita*) development for
effective resistance in plants using RNAi**

A THESIS

**submitted to Delhi Technological University
for the award of degree of**

DOCTOR OF PHILOSOPHY

in

BIOTECHNOLOGY

2019



By

DESHIKA KOHLI

**DEPARTMENT OF BIOTECHNOLOGY
DELHI TECHNOLOGICAL UNIVERSITY
(Formerly Delhi College of Engineering)
DELHI-110042 (INDIA)**

©DELHI TECHNOLOGICAL UNIVERSITY-2019

ALL RIGHTS RESERVED



Govt. of N.C.T of Delhi
DELHI TECHNOLOGICAL UNIVERSITY
(Formerly Delhi College of Engineering)
Delhi-110042

CERTIFICATE

This is to certify that the work embodied in this “Doctor of Philosophy” thesis entitled “**Identification of key genes involved in root knot nematode (*M. incognita*) development for effective resistance in plants using RNAi**” submitted by **Deshika Kohli** (Reg. No: 2K12/PhD/BT/04) to the Delhi Technological University (formerly DCE) is original work carried out under our supervision and has not been submitted earlier, either in part or full, for the award of any other degree or diploma to this university or to any other University or Institution. This is further certified that **Deshika Kohli** (Ph.D. candidate) has successfully completed Ph.D. course work as per Ph.D. ordinance of the Delhi Technology University.

Dr. Navneeta Bharadvaja
(Supervisor)
Assistant Professor
Department of Biotechnology
Delhi Technological University

Prof. R Srinivasan
(Co-supervisor)
Emeritus Scientist
ICAR-NRC on Plant Biotechnology
Pusa Campus, Delhi

Prof. Jai Gopal Sharma
Professor and Head
Department of Biotechnology
Delhi Technological University

DECLARATION

I hereby declare that the thesis entitled “**Identification of key genes involved in root knot nematode (*M. incognita*) development for effective resistance in plants using RNAi**” submitted by me for the award of degree of Doctor of Philosophy to Delhi Technological University, is a record of *bona fide* work carried out by me under the supervision of Dr. Navneeta Bharadvaja and Prof. R. Srinivasan. It has not been submitted earlier, either in part or full, for the award of any other degree or diploma to this university or to any other University or Institution.

Date:

Place:

Deshika Kohli

Ph.D. candidate

(Reg. No. 2K12/Ph.D/BT/04)

Dedicated to the memories of

My Mother

and

My Grandmother

for their heavenly blessings

ACKNOWLEDGEMENTS

*Six years of my doctoral research work have been overwhelming with a period of intense learning for me not only on scientific front but also at the personal level by shaping me into a better thinker. I am thankful to **Almighty** for giving me such blissful life. This experience has been possible with support; encouragement and love of many people who I feel have contributed to the success of this study and made it an unforgettable learning experience for me.*

*I would like to express my gratitude to my supervisor **Dr. Navneeta Bharadvaja**, Assistant Professor, Delhi Technological University, for her aspiring guidance and belief in me. This thesis would have not been possible without her support. I am thankful to her for providing me the opportunity to carry out my research work under her supervision. Her intellect and knowledge have helped me in carrying out the research work successfully and also in compiling the thesis. I am thankful to her for her patience and providing me the freedom to work on my own intellectual abilities during my Ph.D.*

*I am highly indebted to my co-supervisor **Prof. R. Srinivasan**, Emeritus Scientist, NRC on Plant Biotechnology for mentoring me and providing me the chance to learn under his wing. His constant support, guidance and enlightening ideas have shaped me into a better researcher. I am deeply thankful to him for helping me in solving the problems aroused during the course of my research work and for his incessant motivation for accomplishment of my research and thesis. I want to thank you for being a source of inspiration, building the scientific temperament in me and guiding me for choosing the right direction for carrying out the experiment.*

*I would like to offer my special thanks to **Prof. D Kumar**, DRC chairman, **Prof. Jai Gopal Sharma**, Head, Department of Biotechnology, Delhi Technological University and **Director, NRC on Plant Biotechnology**, New Delhi for permitting me to conduct my research work and providing me with all the facilities required during the course of my work.*

*I owe deepest gratitude to **Dr. P.K. Jain, Principal Scientist, NRC on Plant Biotechnology**, for allowing me to work in his laboratory and for providing the scientific facilities. I thank him for generously supporting my research work. His insightful comments and suggestions have enormously shaped my doctoral research work. Without his persistent help this thesis would have not been materialized. His concern and wholehearted help have made this thesis to reach completion stage into a possibility. I am particularly grateful for assistance given by **Dr. Anil Sirohi, Principal Scientist, Division of Nematology, IARI**. I thank him for permission to use microscope and access to other facility in his laboratory. I also appreciate the valuable feedback offered by him in structuring my research work and thesis compilation. He has been a great support throughout my research work in providing the final shape to my work.*

I thank Delhi Technological University and ICAR-NFBSRA (National Fund for Basic and Strategic Research in Agriculture) for funding this research work.

No research work perspective of its degree of complexity can function at its fullest efficiency in a laboratory without the group effort of all the fellow lab members. I would like to pay my heartfelt thanks to my friends Ila and Dr. P. Tej Kumar for their constant motivation and consistent support during my Ph.D through those insightful discussions. The struggle during research work was easier to face due to affection and care bestowed upon me by Ila. My particular thanks to Dr. Satheesh, Dr. Parameswaran and Ashish for that many rounds of discussions on research work that have greatly benefitted me. I admire the distinguished helping nature of Dr. Satheesh and Tej and feel lucky to have their support. I appreciated the support and thanks of my seniors in NRC on Plant Biotechnology, Dr. Nimmy (Scientist), Dr. Pooja, Dr. Suruchi, Dr. Vishwajith, Dr. Anil, Dr. Vajinder and Dr. Naresh. I would like to thank all the lab members and my loving affectionate juniors Akanksha, Heena, Parichita and Lal Bahadur for helping me in few experiments and for providing stimulating and fun-filled environment. I am greatly thankful to the help and assistance provided by the lab attendant Fayaz without him this will be incomplete.

*I would like to extend my gratitude to my senior in Delhi Technological University, Nupur ma'am, for being available 24*7 and for solving my doubts. I thank her for her selfless support in completing my thesis. I also thank Dr. Satish sir, for his words of wisdom and helping me when I really needed. I thank my friends Richa, Sanghmitra, Abhishek and Mansi for being a great support in my thesis. I am also thankful to my dear friend Gaurav for encouraging me throughout my research work and for boosting my confidence. I express my thanks to juniors Lakhan and Arpita for their help, support and providing healthy environment. This Acknowledgement will be partial without thanking the senior management and especially CB Singh sir and Jatinder sir for the technical support, without them this thesis completion would not have been possible.*

It's my fortunate to have Dr. Shikha Bakshi and Roopa Kishore as my close friends who have always showed faith in me. They both have helped in smoothening the tough time during research work through their witty nature and words to push me. This hard and long path was made easier by my beloved friends Rohit, Parul, Aditi, Nandita and Priyanka who have stood by my side and gave me wise advice and were reason for beautiful memories in my journey of doctoral research.

Words fail me to thank my father for his wise counsel and sympathetic ear every time I needed. You are always there for me and I know it. I can't thank you enough for keeping faith in me, acquainting me with my capabilities of which I was unaware and for never ending emotional support. I cannot forget his sacrifices and hardships he has under went in making me what I am today. I am blessed to have my twin sister (Devanshi Kohli) who is my true critic and have always cared for me. She has reminded me of life's true priorities during the inevitable ups and downs of my research work. I thank my sister for Inaaya, my little niece who is my greatest stress buster. I extend my heartfelt thanks to my dear Brother-in-law (Shobhit Gupta) for having faith in me and supporting me. I don't know that I ever be able to thank my aunt (Neelam Sabharwal) for her love and always wishing best for me. Words cannot express how grateful I am to my mother-in-law and father-in-law, to their prayers for me that helped me in sustaining so far. It is my pleasure to express my gratitude for all the love and affection bestowed upon me by them. I would like to extend my

heartfelt appreciation and thanks my sister-in-law, Isha di, for her concern and words of encouragement and love showered by dear Kuber (nephew). I am highly overwhelmed when it comes to express my appreciation for my beloved, my better other half, Dr. Nishant kakar (husband) who has spent sleepless nights during my moments of distress and have managed to cheer me up every time. I thank for his patience and faith in me, you have supported every moment. No words can ever be enough to express my affection and appreciation for you. You are doing a great job I can't ask for more.

*This thesis is a beginning of new opportunities and I am grateful to the almighty **God** and my guiding angel for guiding me all this way, providing me the will and bestowing the blessings upon me to complete this work. I bow my head before him.*

Deshika

TABLE OF CONTENTS

Title	Page No.
<i>List of Tables</i>	<i>i</i>
<i>List of Figures</i>	<i>ii-v</i>
<i>Abbreviation</i>	<i>vi</i>
<i>Abstract</i>	<i>vii-viii</i>
Chapter 1: Introduction	1-6
1.1 Relevance of the study	5
Chapter 2: Review of Literature	7-36
2.1 Nematodes and its phylogeny	7
2.2 Plant-parasitic nematode (infraorder– Tylenchomorpha; Order- Rhabditida; Suborder- Tylenchina)	9
2.3 Root-knot nematode (<i>Meloidogyne incognita</i>) and its general features	12
2.4 Global impact of Root-knot nematode on agriculture	14
2.5 Root-knot nematode distribution and its impact on Indian agricultural economy	15
2.6 Lifecycle of Root-knot nematode	17
2.7 Cuticle: essential element for <i>M. incognita</i> morphology and integrity	18
2.7.1 Cuticle collagen genes	20
2.8 Pharynx: organ for feeding and parasitism	21
2.8.1 Polyclonal development of pharynx during embryogenesis in nematodes	22
2.9 <i>Meloidogyne incognita</i> genome	25
2.10 <i>Dumpy (Dpy)</i> genes	25
2.11 <i>Glp-1</i> (abnormal germline proliferation-1) gene	27
2.12 Conventional methods for RKN management	28
2.13 RNAi - A strategy to leash the nematode infestation	30
2.13.1 Mechanism of siRNA	30
2.14 Different strategies for silencing a gene	32

2.14.1	Host-delivered RNAi (HD-RNAi) method	33
2.15	Silencing of development genes from <i>M. incognita</i>	36
Chapter 3: Materials and Methods		37-73
3.1	Materials	37
3.2	Instruments	38
3.3	Methods	38
3.3.1	Culturing of bacterial cells	
3.3.2	Plasmid DNA isolation by alkaline lysis method	
3.3.3	<i>E. coli</i> competent cells preparation by calcium chloride method	39
3.3.4	Transformation of <i>E. coli</i> cells by heat shock method	40
3.3.5	<i>Agrobacterium tumefaciens</i> competent cells preparation	40
3.3.6	Maintaining bacterial strains/clones for long term storage	41
3.3.7	Identification and confirmation of <i>M. incognita</i> culture	41
3.3.8	Maintenance of nematode pure culture and inoculum preparation	43
3.3.9	Identification of development-specific genes in <i>M. incognita</i> genome	45
3.3.9.1	Computational analyses for genes identification	
3.3.9.2	Prediction of gene and respective protein structure	46
3.3.9.3	Identification of conserved motifs	47
3.3.9.4	Multiple-sequence alignment and phylogenetic analyses	47
3.3.10	Genomic DNA isolation from adult <i>M. incognita</i> females	48
3.3.11	Genomic DNA quantification	49
3.3.11.1	DNA quantification using nanodrop	
3.3.11.2	DNA quantification using agarose gel electrophoresis	
3.3.12	Polymerase chain reaction (PCR)	49
3.3.13	Elution of DNA from agarose gel	50
3.3.14	Ligation into pGEMT-Easy vector	51
3.3.14.1	Transformation	52
3.3.14.2	Confirmation for presence of insert by colony PCR	52
3.3.15	Nematode sample collection and preparation	52
3.3.16	Isolation of total RNA from different stages of <i>M. incognita</i>	53
3.3.16.1	RNA quantification	54

3.3.16.2	Denaturing formamide agarose (FA) gel electrophoresis for RNA	54
3.3.17	Reverse transcription for cDNA preparation	54
3.3.18	Quantitative real-time PCR (qRT-PCR) analyses	55
3.3.19	Strategy for designing RNAi constructs that express dsRNA	56
3.3.19.1	Preparation of entry clones	
3.3.19.2	Preparation of destination clone using RNAi vector	58
3.3.19.3	Another strategy for designing RNAi constructs	59
3.3.19.4	Selection of positive clones by restriction digestion	60
3.3.20	Transformation of <i>Agrobacterium tumefaciens</i> cells	60
3.3.21	Transformation of <i>Arabidopsis thaliana</i> plants	61
3.3.21.1	Germination of <i>Arabidopsis</i> seeds	
3.3.21.2	Planting of <i>Arabidopsis</i> seedlings in soil	62
3.3.21.3	Preparation of <i>Arabidopsis</i> plants for floral-dip transformation	62
3.3.21.3.1	Preparation of <i>Agrobacterium tumefaciens</i> suspension	63
3.3.21.3.2	Floral-dip	63
3.3.21.3.3	Seeds harvesting, handling and preservation	64
3.3.21.4	Screening of transgenic RNAi lines	64
3.3.21.4.1	Screening of transgenic lines for kanamycin resistance	
3.3.21.4.2	Genomic DNA (gDNA) isolation from <i>Arabidopsis</i> transgenic plants	65
3.3.21.4.3	Screening of putative transformants for the gene integration	66
3.3.21.5	Detection of dsRNAs from transgenic plants-northern hybridization	66
3.3.21.5.1	Small RNA isolation	
3.3.21.5.2	Preparation of denaturing polyacrylamide gel (dPAGE)	67
3.3.21.5.3	Small RNA sample preparation	68
3.3.21.5.4	Transferring of small RNA by electroblotting	68
3.3.21.5.5	Crosslinking of small RNA	69
3.3.21.5.6	Pre-hybridization and probe preparation	69

3.3.21.5.7	Hybridization	70
3.3.21.5.8	Washing	70
3.3.21.5.9	Autoradiography	71
3.3.22	Silencing efficacy of RNAi transgenic lines	71
3.3.22.1	Plant growth conditions and nematode infection bioassays	
3.3.22.2	Transgene expression analyses in nematode infecting RNAi plants by qRT-PCR	73
3.3.23	Data analyses	73
Chapter 4: Results		74-112
4.1.1	Genes involved in cuticle and pharynx development in <i>M. incognita</i>	74
4.1.2	Protein sequence analysis and phylogenetic analysis of selected genes in nematode species	78
4.1.3	Presence of conserved domains	85
4.1.4	Protein-protein interaction	89
4.2.1	Isolation of <i>Mi-dpy-10</i> , <i>Mi-dpy-31</i> and <i>Mi-glp-1</i> from <i>M. incognita</i>	93
4.2.2	Transcript abundance of identified genes during developmental stages of <i>M. incognita</i>	94
4.2.3	Cloning of partial mRNA of selected genes in pGEM®-T easy vector	96
4.3.1	Development of dsRNA constructs	97
4.3.1.1	<i>glp-1</i> dsRNA constructs	98
4.3.1.2	<i>dpy-31</i> dsRNA constructs	99
4.3.2	Determining <i>glp-1</i> and <i>dpy-31</i> efficacy as candidate for gene silencing	101
4.3.2.1	Over-expression of <i>Mi-glp-1</i> and <i>Mi-dp-31</i> genes in <i>Arabidopsis thaliana</i>	
4.3.2.2	Nematode infection assay on <i>A. thaliana</i> RNAi lines	102
4.3.2.3	Molecular analyses of RNAi lines through qRT-PCR and northern blotting	106
4.3.2.4	Phenotypic evaluation of RNAi lines expressing nematode dsRNA of <i>glp-1</i> and <i>dpy-31</i> gene	108
4.3.3	Effect of silencing on <i>M. incognita</i> fecundity and next-generation J2s	109
Chapter 5: Discussion		113-121

Chapter 6: Summary and Conclusion 122-124

References 125-140

Appendices

List of Publications

Reprints of the Publications

LIST OF TABLES

<i>Table No.</i>	<i>Description</i>	<i>Page No.</i>
2.1	List of cuticle collagen genes identified in <i>C. elegans</i> on the basis of RNAi phenotype	21
2.2	Genes identified in pharynx development in <i>C. elegans</i>	24
2.3	List of RNAi mediated gene silencing in PPNs	36
3.1	List of materials used in this study	37
3.2	List of primers used in this research	42
4.1	Comparison of gene sizes of <i>dpy-10</i> and <i>dpy-31</i> of plant-parasitic nematodes to that of reported dumpy genes of free-living nematodes	75
4.2	Comparison of gene size of <i>glp-1</i> of plant-parasitic nematodes with that of reported <i>glp-1</i> gene of free-living nematodes	77
4.3	Size evaluation of females obtained from wild-type plants and <i>Mi-glp-1</i> transgenic RNAi lines	104
4.4	Size evaluation of females obtained from wild-type plants and <i>Mi-dpy-31</i> transgenic RNAi lines	106
4.5	Number of eggs counted for <i>M. incognita</i> feeding on wild-type plants and RNAi plants for calculating MF value	110
4.6	Adverse effect on J2s obtained from <i>M. incognita</i> females isolated from infected RNAi and wild-type plants	112

LIST OF FIGURES

<i>Figure No.</i>	<i>Description</i>	<i>Page No.</i>
2.1	Phylogenetic tree constructed on the basis of SSU rDNA sequences across nematode species	9
2.2	Evolution of parasitic nematodes based on ribosomal DNA	10
2.3	Phylogeny of <i>Meloidogyne</i> spp(s)	13
2.4	Representation of anterior part of second-stage juvenile (J2) of root-knot nematode	14
2.5	Area-wise distribution of PPNs infecting primary crops in India	16
2.6	Schematic diagram of events occurring in a life cycle of <i>M. incognita</i>	18
2.7	Structure of a nematode cuticle collagen	19
2.8	Schematic representation of structure of nematode cuticle collagen	20
2.9	Pharynx structure in <i>C. elegans</i>	22
2.10	Early pharyngeal development	23
2.11	Schematic diagram of siRNA mechanism in eukaryotes	31
2.12	Different dsRNA delivery methods	32
2.13	Diagram representing mechanism of plant-mediated RNAi in parasitic nematode	34
3.1	Confirmation of <i>M. incognita</i> culture	42
3.2	Maintenance of nematode culture	44
3.3	Physical map of pGEMT-Easy vector	51
3.4	Overview of gateway technology for generating dsRNA constructs	56
3.5	Graphical representation showing region selected for generating dsRNA construct for <i>glp-1</i> and <i>dpy-31</i>	57
3.6	Vector map for pHELLSGATE12 RNAi vector	58

Figure No.	Description	Page No.
3.7	Vector map for pBC6 vector	59
3.8	<i>Arabidopsis</i> plants bagged with butter paper for collecting seeds	64
3.9	<i>Arabidopsis</i> plants grown in a tray for nematode infection	72
4.1	Diagrammatic representation of predicted structures of proteins encoded by cuticle genes of <i>M. incognita</i>	78
4.2	Predicted transmembrane domain in <i>M. incognita</i> cuticle proteins	79
4.3	Prediction of signal peptide in Mi- DPY-10 and Mi- DPY-31	80
4.4a	Phylogenetic analysis of Mi-DPY-10	80
4.4b	Phylogenetic analysis of Mi-DPY-31	81
4.5	Diagrammatic representation of the predicted structures of the <i>glp-1</i> gene and its encoded protein	82
4.6	Predicted transmembrane domains in the <i>M. incognita</i> GLP-1 protein	82
4.7	Prediction of signal peptide in Mi- GLP-1	83
4.8	Multiple sequence alignment of GLP-1	84
4.9	Phylogenetic analysis of Notch-like receptors	85
4.10	Multiple sequence alignment of DPY-10 protein	86
4.11	Multiple sequence alignment of DPY-31 protein	87
4.12	Protein motifs of Notch receptor members	88
4.13	Protein-protein interaction of Mi-DPY-10	90
4.14	Protein-protein association of Ce-DPY10	91
4.15	Protein-protein association of Mi-DPY-31	91
4.16	Protein-protein association of Mi-GLP-1	92
4.17	gDNA isolated from the <i>M. incognita</i> females	93
4.18	PCR amplification of selected genes from gDNA	94

Figure No.	Description	Page No.
4.19	Total RNA isolated from the <i>M. incognita</i> females	95
4.20	Transcript profiling of <i>dpy-10</i> , <i>dpy-31</i> and <i>glp-1</i> genes at different developmental stages in <i>M. incognita</i>	95
4.21	Cloning of selected genes in pGEMT-Easy vector using gene-specific primers	96
4.22	Confirmation of <i>Mi-dpy-10</i> , <i>Mi-dpy-31</i> and <i>Mi-glp-1</i> insert in pGEMT Easy vector	97
4.23	PCR amplification of <i>Mi-glp-1</i> sense and antisense strands	98
4.24	Cloning of <i>Mi-glp-1</i> in sense and antisense orientation in pBC6 vector	99
4.25	PCR amplification of <i>Mi-dpy-31</i> sense and antisense strands	100
4.26	Cloning of <i>Mi-dpy-31</i> in sense and antisense orientation in pHELLSGATE12 vector for <i>Mi-dpy-31</i> -dsRNA construction	101
4.27	Confirmation of <i>dpy-31</i> -dsRNA constructs	101
4.28	T ₁ selection of <i>Arabidopsis</i> transformants on an antibiotic (kanamycin) selective MS media	102
4.29	PCR based confirmation of T ₁ <i>Arabidopsis</i> seedlings	102
4.30	Evaluation of nematode resistance in T ₃ <i>Arabidopsis</i> RNAi lines expressing <i>Mi-glp-1</i> -dsRNA	103
4.31	Females isolated from wild-type and <i>Mi-glp-1</i> RNAi transgenic plants	104
4.32	Evaluation of nematode resistance in T ₃ <i>Arabidopsis</i> RNAi lines expressing <i>Mi-dpy-31</i> -dsRNA	105
4.33	Females isolated from wild-type and <i>Mi-dpy-31</i> RNAi transgenic plants	106
4.34	RT-qPCR-based <i>glp-1</i> expression analysis of <i>M. incognita</i> females	107
4.35	RT-qPCR-based <i>dpy-31</i> expression analysis of <i>M. incognita</i> females	107

<i>Figure No.</i>	<i>Description</i>	<i>Page No.</i>
4.36	Molecular analyses of <i>M. incognita</i> isolated from transgenic <i>Arabidopsis</i> plants	108
4.37	Morphological evaluation of transgenic RNAi line compared to wild type plants as control	109
4.38	Altered phenotypes of stylets and pharynxes of J2s	111

LIST OF ABBREVIATIONS

BLAST	Basic local alignment search tool
bp	Base pair
cDNA	Complementary deoxyribonucleic acid
CTAB	Cetyl Trimethyl Ammonium Bromide
DEPC	Diethyl pyrocarbonate
DMSO	Dimethyl sulfoxide
DNA	Deoxyribonucleic acid
dNTP	Di-nucleotide triphosphate
EDTA	Ethylene diamine tetraacetic acid
EST	Expressed sequence tag
EtBr	Ethidium bromide
g	Gram
h	Hour
HD-RNAi	Host-delivered RNA interference
IPTG	Isopropyl-thio-galactoside
Kb	Kilo base pairs
J2s	Second stage juveniles
LA	Luria agar
LB	Luria bertani
mg	Milligram
MCS	Multiple cloning site
Min	Minute
MS	Murashige and Skoog medium
ng	Nanogram
NCBI	National center for biotechnology information
NOS	Nopaline synthase
<i>NPT II</i>	Neomycin phospho transferase
ORF	Open reading frame
PCR	Polymerase chain reaction
PVP	Polyvinyl pyrrolidone
PPNs	Plant-parasitic nematodes
RNA	Ribonucleic acid
RKNs	Root-knot nematodes
rpm	Revolutions per minute
RT-PCR	Reverse- Transcriptase-Polymerase Chain Reaction
TAE	Tris-acetate EDTA
TE	Tris-EDTA
Tris	Tris (hydroxymethyl) aminomethane
UV	Ultraviolet light
X-gal	5-bromo-4-chloro-3-indolyl- β -D-galactopyraanoside
YEP	Yeast extract peptone media
CaMV35S	Cauliflower mosaic virus 35S promoter

ABSTRACT

The southern root-knot nematode, *Meloidogyne incognita*, is sedentary endoparasite with an adverse social and economic impact worldwide. The cuticle and pharynx of plant-parasitic nematode is a less studied area of research with only few developmental genes identified till date. In this study, key genes involved in cuticle and pharynx development of *M. incognita* were identified and characterized. An orthologue of *Caenorhabditis elegans* *dpy-10* (dumpy), *dpy-31* and *glp-1* (abnormal germline proliferation) genes were identified in *M. incognita*. The phylogenetic analysis revealed evolutionary conserved nature of these genes throughout the phylum Nematoda. Successful partial mRNA cloning of these three genes in pGEMT-Easy vector confirms their presence in *M. incognita*. Temporal regulated expression of dumpy genes was revealed by qRT-PCR expression analyses. *Mi-dpy-10* showed higher expression at the second stage juveniles (J2s) of the nematode development in comparison to eggs and adult females. However, *Mi-dpy-31* gene revealed higher expression in adult females in *M. incognita* suggesting different roles of dumpy genes during moulting process in nematode development. While *Mi-glp-1* showed differential expression throughout the lifecycle of *M. incognita*, with relatively higher expression in the egg stage. The functional analysis of *Mi-dpy-31* and *Mi-glp-1* was conducted in a host-mediated gene silencing strategy by developing gene-specific dsRNA expressing RNAi lines. There was no significant reduction in terms of nematode infection in *Mi-dpy-31*-RNAi lines as equal number of galls, females and eggs were observed in RNAi and wild-type plants. The *Mi-glp-1*-RNAi lines on the other hand showed 47–50% reduction in the numbers of galls, females and egg

masses. Intriguingly, an adverse effect on the phenotype of second-generation J2s, which were descendants of the infected females from the *glp-1*-RNAi lines, was noticed. These J2s exhibited a significant decrease in the overall distance from the stylet to the metacarpus region, and disruption around the metacorporeal bulb of the pharynx. This indicates a role for this gene in organ (pharynx) development during embryogenesis in *M. incognita*. In Toto, these findings suggest that *Mi-dpy-10* and *Mi-dpy-31* play role in cuticle and *Mi-glp-1* in pharynx development in *M. incognita* and their potential use as a target in controlling plant-parasitic nematode infection in a host-mediated gene silencing approach.

Chapter 1
Introduction

1. INTRODUCTION

With an estimated rise of the global population to about 10 billion by 2050 (Elling, 2013), the world faces one of the biggest challenges of meeting the food requirements. There are major biotic and abiotic factors affecting both the yield and quality of economically important crops. There have been many practices adopted in order to enhance agronomical traits of these crops. With the advancements in improving crop yields, significant measures have been taken in improving stress management qualities of crop plants for better production (Atkinson and Urwin, 2012). Apart from abiotic stresses like drought, heat, cold, and salinity; biotic factors also play significant role in affecting the crop productivity around the world. Plant-parasitic nematodes (PPNs) are primary pests affecting the crop productivity, resulting in a loss of hundreds of billion dollars worldwide (Elling, 2013).

Nematodes, the most abundant multi-cellular animals, occupy nearly every habitat on earth owing to their resistant cuticle and ability to adapt. These are also known as round worms. Depending upon the species, nematodes are beneficial as well as parasites that are detrimental to plants, animals, and human health. PPNs are amongst the most damaging pest of the world causing serious problems in crop production. There are wide genera of PPNs depending upon their feeding organ and tissue type. The ectoparasitic nematodes that feed on plant tissues from outside, semi-endoparasitic nematode feeding on the plant tissue from inside by embedding its anterior portion inside the host and its posterior part remaining free in the soil and lastly, endoparasitic nematodes that feed from inside the host tissue. Endoparasitic nematodes feed on almost every part/tissue of vascular plants viz. bulb and stem (*Ditylenchus dipsaci*),

Bud and leaf (*Aphelenchoides spp.*), stems (*Bursaphelenchus*) and root (*Heterodera* and *Meloidogyne spp.*). Amongst them the sedentary root-knot and cyst nematodes are of great concern to biologists. Most widely studied species are *Meloidogyne spp.*, *Globodera* and *Heterodera spp(s)*.

Root-knot nematode (RKN) (*Meloidogyne spp.*) are obligate endoparasites, that locate the host, invade it through roots, select the site and then establish a feeding site inside the plant before being able to reproduce. At the time of infection infective juveniles pierce the root cell-wall through secretions to enter the host cells. In the pericycle it hacks the plant auxin pathway for inducing increased cell divisions. This results in the enlargement of cells in vascular cylinder. Development of a typical nurse cell system called 'Giant cell' or 'syncytium' or gall is triggered as a result of action of feeding by nematode. These galls are the underground symptom of root-knot nematode disease which are multinucleated with dense cytoplasm. These cells also consist of enlarged nuclei along with numerous mitochondrial and Golgi bodies that are metabolically active. By virtue of the broad host range RKN are one of the most hardened foes to almost every economically important crop.

The conventional approaches to managing the PPN infection are not enough. Nematicides used for preventing PPN are highly toxic and environmentally unfriendly. Agricultural practices like soil sanitization; crop rotation is insufficient and cannot effectively control the nematode infestation. Biological agents like nematode eating fungus and bacteria are not available for every nematode pathogen. For successful prevention of nematode infection, a thorough study of their morphology, biology and host parasitic relationship is necessary. Exploitation of genetic approaches to parasitism, as advocated by Bird (Bird et

al. 1999), could be a powerful route for novel methods of controlling PPNs. Nematode parasitism is based on a series of signaling events that leads to various changes in the nematode and complimentary in the host plant. Different plants have nematode resistance genes occurring naturally as a means of defense against PPNs. Use of host-plant resistance has been successful against nematode infection and is one of the most preferred method. But the nematode resistance is restricted against specific species of a particular nematode. In some cases, the genetic diversity within the nematodes limits the effectiveness of existing resistant cultivars.

Knowledge of genetic compliment of many crop plants and the availability of new molecular techniques has lead to the development of genetically based resistance to nematode diseases. In a classical piece of genetic engineering, a cyst resistant gene against *H. schachtii* was introduced from wild Beta species into sugarbeet (Cai et al. 1997), transgenic plants expressing proteinase inhibitors can impart effective resistant against several nematodes species (Atkinson et al. 2003). Use of resistant plant has been successful against nematode infection but it mainly depends upon the presence of resistance genes in the gene pool of crop plant that can be transferred via conventional breeding. For instance, the Mi gene for resistance in tomato against few species of *Meloidogyne viz. M. javanica, M. anenari* and *M. incognita*, is very effective (Williamson et al. 1994a; Kaloshian et al. 1995; Milligan et al. 1998). But breaking down of resistance in the field population of *M. incognita* and *M. javanica* has been reported (López-Pérez et al. 2006).

In the last decade, a new biotechnological approach i.e. RNA interference (RNAi) has attracted much attention from the researchers all over the world. The fundamental idea

includes an effective post-transcriptional gene silencing with complementary sequences by a potential double-stranded RNA (dsRNA) molecule. It was originally determined in free-living nematode, *Caenorhabditis elegans* (Fire et al. 1998). There is increasing documentation of RNAi efficiency against PPNs both in RKN and cyst nematodes (*Heterodera glycine* and *Globodera pallida*) (Urwin et al. 2002). Urwin et al (2002) targeted Cysteine protease and C-type lectin like genes in second juvenile stage of life cycle of *M. incognita*. A significant decrease in infection level along with the phenotypic effects like modified sexual fate, lower levels of specific transcript of these genes was noticed. 16D10, a conserved parasitism gene in RKN species, when targeted for gene silencing via host-mediated gene silencing showed 63% to 90% decrease in number of galls in *M. incognita* (Huang et al. 2006a). Similar effects were observed in *M. javanica*, *M. arenaria* and *M. hapla* (Huang et al. 2006a). Thus, pointing as a broad range resistance mechanism against RKNs.

Diverse secretory and effector genes were reported as efficient targets for developing nematode resistance for example, *Misp12* expressing in the dorsal esophageal gland, SXP/RAL-2 secretory protein expressed in subventral pharyngeal glands (Xie et al. 2016; Tytgat et al. 2004). Several studies on specific gene knockdown through RNAi for secretory genes influencing parasitism in PPNs are present (Kohli et al. 2018). But a few of the development genes have been targeted for RNAi based silencing for managing the PPNs. *Rpn7* gene, important for the integrity of 26S proteasome was targeted for controlling RKN *M. incognita* (Niu et al. 2012). *Mg-pat-10* and *Mg-unc-87* genes functioning in muscle contraction and maintenance of structure myofilaments, knock-downed in vitro through soaking, showed 91% and 87% reduction, respectively

in infected *M. graminicola* (Nsengimana et al. 2013). *nhr-48*, a nuclear receptor gene was suppressed in *M. incognita* as a result delayed development and reduction in its reproduction was observed (Lu et al. 2016). Research on RNAi based controlling of RKN is also focused on targeting secretory and effector proteins. There is a limited research documenting the potential of key developmental genes for host-mediated RNAi approach based nematode resistance.

1.1 Relevance of the study

Since *M. incognita* resides in host body throughout the life cycle, several significant changes in the organs and eventually at transcript levels of PPNs occur. Such infection-responsive genes are central to successful invasion by PPNs. Cuticle and pharynx developmental genes were considered as a target because it is by virtue of these organs that *M. incognita* enables to survive inside the host tissue withstanding plant defense attack. Thus, identifying and characterizing such genes that play a crucial role in the development of these vital organs will broaden our understanding of *M. incognita* development. The present study was aimed at identification and characterization of *glp-1*, *dpy-10* and *dpy-31* genes involved in development of *M. incognita*. The study also describes expression profiling of these genes at different development stages in *M. incognita*. The host-mediated RNAi silencing strategy was also adapted to evaluate the ability of *Mi-glp-1* and *Mi-dpy-31* as a probable candidate gene for control of nematode infection by developing nematode resistant transgenic *Arabidopsis* plants.

Thus, the present study entitled "Identification of key genes involved in root knot nematode (*M. incognita*) development for effective resistance in plants using RNAi" was undertaken with following objectives:

- I. In silico identification of the critical gene(s) of *Meloidogyne incognita* involved in development.
- II. Cloning and characterization of cuticle and pharynx genes and their transcript profiling.
- III. Evaluating the efficacy of these genes in *Arabidopsis thaliana* for nematode resistance against *M. incognita*.

Chapter 2
Review of Literature

2. REVIEW OF LITERATURE

2.1 Nematodes and its phylogeny

Members of phylum Nematoda (or Nemathelminthes) are a large group of invertebrates with over 25,000 species, including free-living, plant-parasitic and animal-parasitic species. These were once classified with a considerable divergent cluster of animals. These were all classified in a group based on their overall worm-like appearance, a pseudocoelom (structure of an internal body cavity), and absence of features such as cilia and a head that are present in nearly all animals. Nematodes, diversely accepted as Aschelminths or Pseudocoelomata, was once recognized as a natural one but not anymore. Presence of pseudocoelom as underived feature and a simple body plan is thought to have resulted most likely from reduction and simplification from more than one group of ancestral organisms (Wallace et al. 1996). Prevailing studies implies a close relation of nematodes to the arthropods and are recognized in a clade, the Ecdysozoa (Aguinaldo et al. 1997). These were further classified under the phylum "Nematoda" due to bilateral symmetry, triploblastic, unsegmented and pseudocoelomates body like features. Nematodes lack specialized circulatory or respiratory system.

Nematodes are multicellular animals having a soft body and can shed cuticle by a process known as moulting (Lambert and Bekal, 2002). After insects these are remarkably plenty in number and distinct animals exceeding their diversity. Majority of nematodes are free-living feeding on bacteria, fungi and protozoans (40% of the reported species). Most of them are beneficial nematode species which are recognized

as pollution indicators, there are others that aid in circulation of nutrients. However, many are parasites of animals (among vertebrates 44% of the described species) and plants (15% of the reported species). The PPNs were first identified in wheat seeds by Needham (1743). But it is after the discovery of root-knot nematodes on cucumber by Berkeley (1855) and cyst nematodes causing “beet-tired” disease on sugar beets by Schacht (1859), plant nematology came forth as a significant branch of scientific speciality.

Nematodes are present in almost every habitat *viz.* in marine, in freshwater and terrestrial environment. They are placed under clade Ecdysozoa in phylum Nematoda (Dunn et al. 2008). Due to diversity in the structure and feeding habitats of nematodes scientists resolve to small subunit ribosomal DNA (SSU rDNA) sequence analysis for establishing a phylogenetic relationship among the nematodes (Aleshin et al. 1998; Blaxter et al. 1998). Recently, Van Megan presented a phylogenetic tree based on 1,215 SSU rDNA sequences across the nematode species resembling that of constructed by Holterman dividing Nematoda into 12 clades (Holterman et al. 2006). It can be seen that PPNs have emerged independently in phylum Nematoda (**Figure 2.1**). The infraorder Tylenchomorpha is comprised of economically most important plant parasites which are a potential threat to world agriculture (van Megan et al. 2009).

It is very difficult to classify nematodes due to diversity in their structure and feeding habitats. Thus, prompting scientists to resolve to better and more authentic system for phylogenetic studies. Small subunit ribosomal DNA (SSU rDNA) sequence study is one such established method for developing phylogenetic relationship among nematodes (Aleshin et al. 1998; Blaxter et al. 1998).

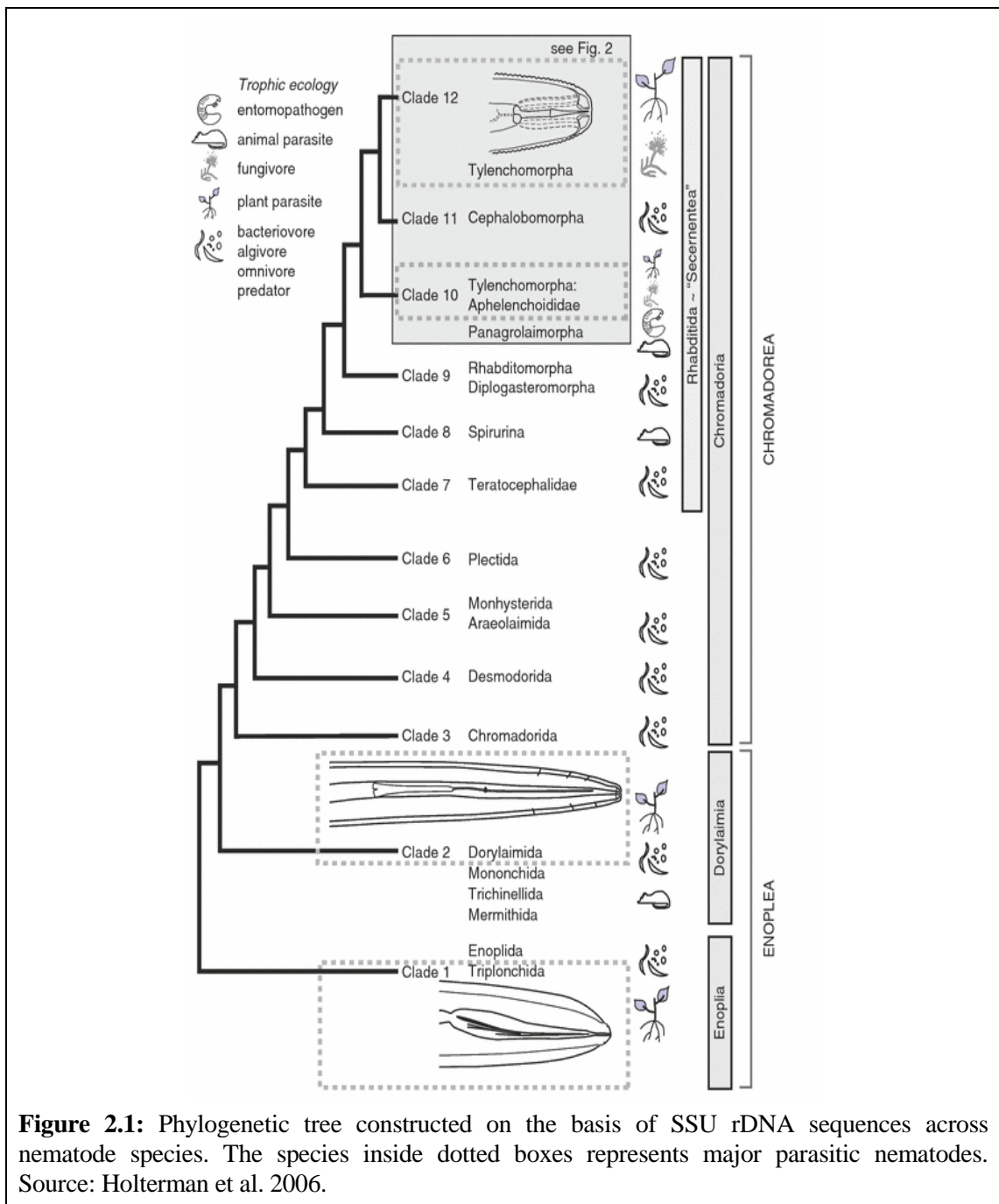
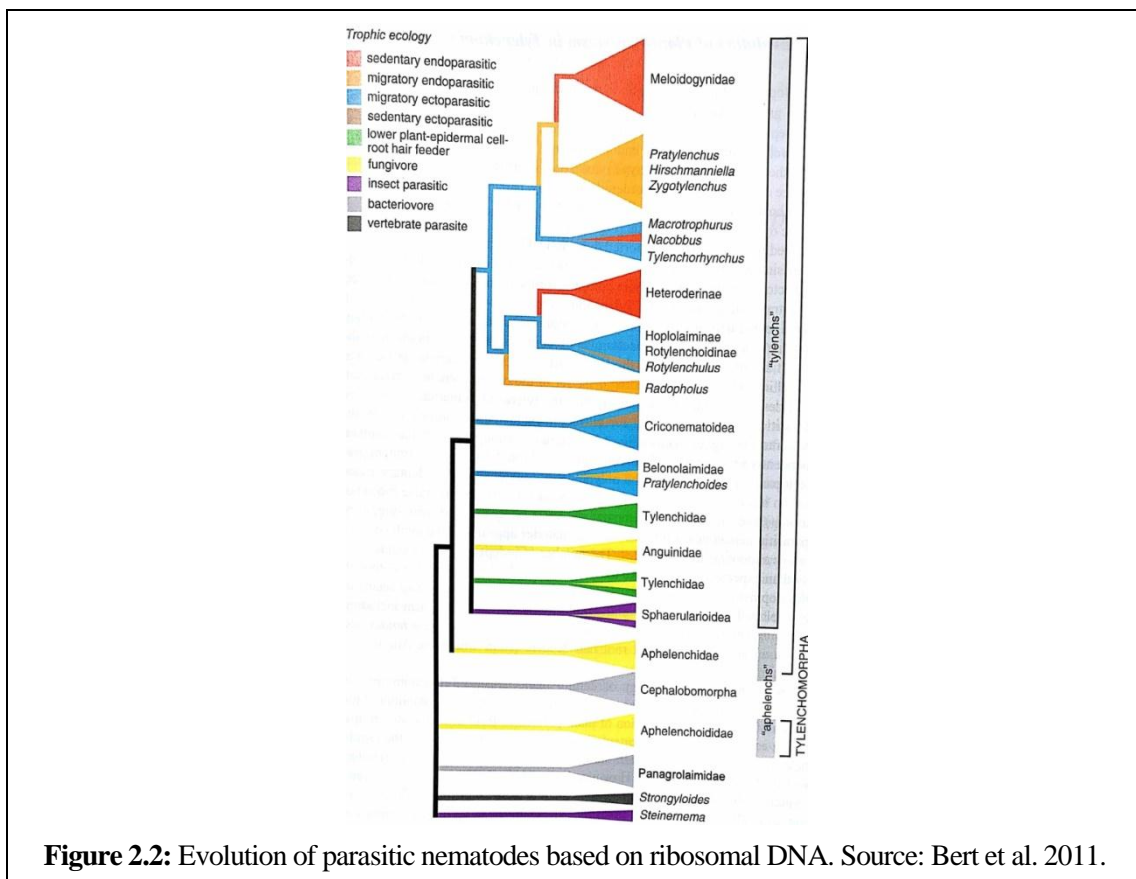


Figure 2.1: Phylogenetic tree constructed on the basis of SSU rDNA sequences across nematode species. The species inside dotted boxes represents major parasitic nematodes. Source: Holterman et al. 2006.

2.2 Plant-parasitic nematode (infraorder– Tylenchomorpha; Order- Rhabditida; Suborder- Tylenchina)

Nearly all species of PPNs belongs to the class Chromodorea, order Rhabditida and suborder Tylenchida. It is the most extensively investigated group within this order.

Several evolutionary relationships of Tylenchida were presented using various strategies. According to the Holterman phylogenetic tree, Meloidogynidae, Heteroderinae, and Pratylenchidae comprise of clades with most important plant-parasites (Bert et al. 2011) (**Figure 2.2**). PPNs are recognized as major pathogens causing an estimated world-wide crop loss of \$US157 billion per year (Singh et al 2015). They are usually small, soil borne pathogens with an extensive host range. There are 4100 PPNs species reported (Decraemer and Hunt, 2006). Plant-parasitic nematodes range from 250 μm to 12 mm in length, and about 15-35 μm in width. The outer appearance of nematode body appears to be segmented because of presence of annulations (accordion-like transverse grooves) on the cuticle. This helps PPN in binding without producing any kinks. Nematodes have an un-segmented body structure with no replication of any parts throughout its body (Lambert and Bekal, 2002).



PPNs can be further classified on the basis of their different feeding strategies as Ectoparasites, Semi-endoparasites, migratory endoparasites and sedentary endoparasites. Ectoparasites derive their nutrition through specialized structures called stylet for ingesting food material while remaining outside its host plant. For example, *Xiphinema* (Class- Enoplea) is an example of ectoparasite. They are motile in nature due to which are known to transmit viruses. Semi-endoparasites for example, *Rotylenchulus reniformis* are able to partially penetrate the root and form a permanent feeding cell. It is the anterior part of the nematode that remains inside the host. Another class of PPNs is of migratory endoparasites.

As the name suggests they remain motile and migrate through root tissues inducing a massive plant tissue necrosis. They feed through stylet only which helps in simply sucking out the plant cytoplasm. Thus the need for a permanent feeding site does not arise in this type of feeding strategy (for example, *Pratylenchus* or lesion nematode). But the most damaging nematodes are the sedentary endoparasites including two main groups of plant-parasitic nematodes viz. root-knot nematodes (RKNs) and cyst nematodes (CNs). These nematodes have a sedentary lifestyle i.e. once penetrating their host they complete their life cycle within the host tissue by forming a permanent feeding cells resulting from a repeated divisions as is the case in RKN or by the incorporation of neighboring cells into a syncytium which is formed by the breakdown of neighboring cell walls in case of CNs. Because of this type of feeding behavior host plants suffers a severe damage leading in a permanent loss of movement of fluids across the plant tissues.

2.3 Root-knot nematode (*Meloidogyne incognita*) and its general features

Root-knot nematodes (RKN), *Meloidogyne* spp., are obligate, biotrophic, sedentary endoparasites with majority of their life-cycle occurring within host-plant roots with an expansive plant host-range (Sasser, 1980). Thus this makes them the most damaging and economically important group of parasitic nematodes among the PPNs worldwide (Chitwood, 2003; Lilley et al. 2007). Following is the phylogenetic classification of *Meloidogyne incognita* as per Escobar et al (2015):

Phylum: Nematoda

Class: Chromadorea

Order: Rhabditida

Suborder: Tylenchina

Superfamily: Tylenchoidea

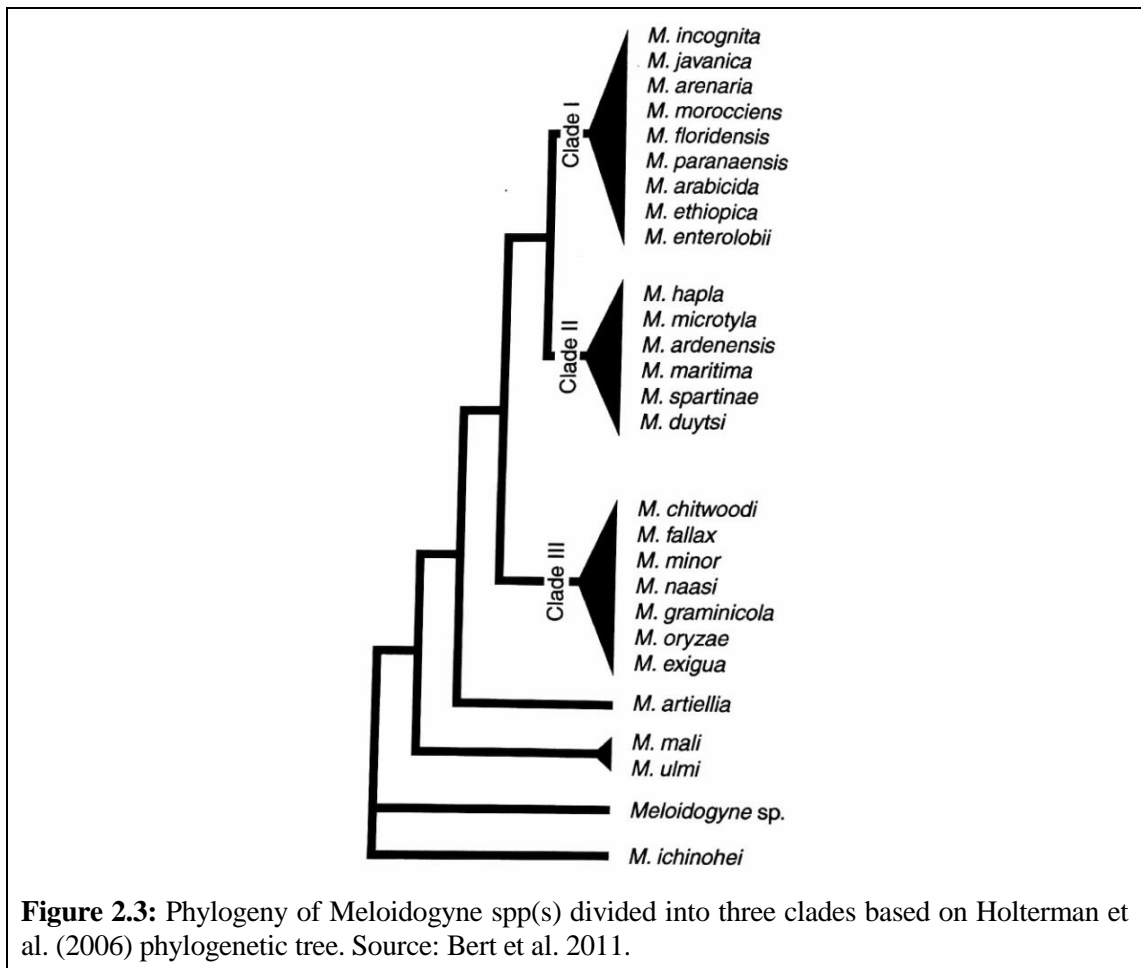
Family: Heteroderidae

Subfamily: Meloidogyninae

Genus: *Meloidogyne*

Meloidogyne is a Greek word meaning ‘apple-shaped female’. This genus with more than 90 species is comprised of three clades as defined by Tandingan et al (2002) (**Figure 2.3**). There are three particular *Meloidogyne* species that are deemed to have a stable existence in warm countries (ranging between 35 °S and 35 °N latitudes of the world) namely, *Meloidogyne javanica*, *Meloidogyne incognita* and *Meloidogyne arenaria* (Taylor and Sasser, 1978). Thus, four *Meloidogyne* spp. namely, *M. incognita*, *M. javanica*, *M. arenaria* (belonging to Mediterranean and tropical areas) and *M. hapla*

(the temperate species) are the four most important polyphagous species with most damaging effect on agriculture.



The most common above ground field symptoms of RKN infection are the yellowing of leaves and restricted growth while it is the infected roots that show development of galls or knot like structure indicating the attack of RKNs. Due to complex life cycle of *Meloidogyne incognita*, the body morphology changes from vermiform juvenile to adult swollen pear-shaped sedentary female (**Figure 2.4**). The body wall consists of cuticle. The mouth opening has a specialized structure stylet which is in continuous with pharynx, the digestive tract.

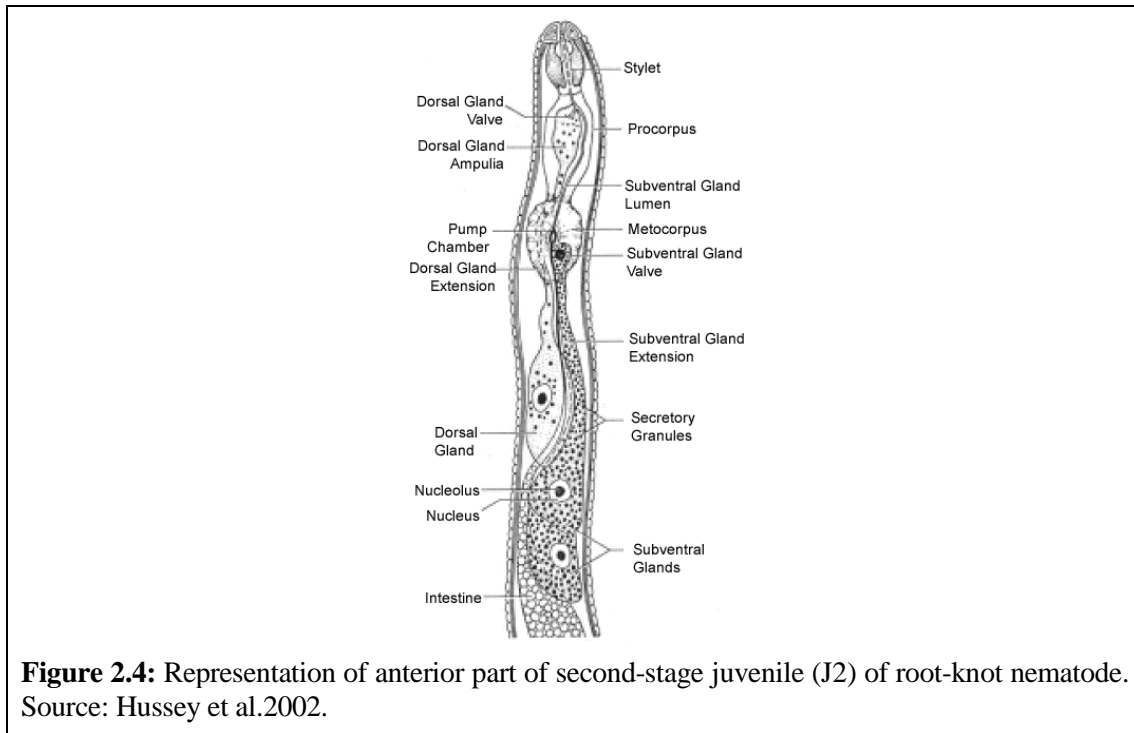


Figure 2.4: Representation of anterior part of second-stage juvenile (J2) of root-knot nematode. Source: Hussey et al.2002.

2.4 Global impact of root-knot nematode on agriculture

PPNs are distributed globally surviving almost in every climatic condition from Mediterranean to tropical and even in the temperate regions. Some of these PPNS are cosmopolitan adapted to varied regions such as *Meloidogyne* spp. whereas; some are restricted to certain geographical regions like that of *Nacobbus* spp. And yet there are few which have highly specific host and hence, specific region such as *Heterodera carotae*, infecting carrots only. Thus, the widespread distribution and varied host range makes PPNS one of the largest dangerous pests (Webster, 1987). Among the RKN, *Meloidogyne incognita* is extensively spread in tropical and subtropical regions. It is known to infect more than 3000 wild and cultivated plant species along with about 138 species of weeds (Hussey and Janssen 2002; Rich et al. 2009). One of the largest *Meloidogyne* species i.e. *M. hapla* is found in northern United States, Europe, parts of Asia, Canada as well as in South America that are known for the cool climates with

temperature between 0 °C to 15 °C or above. Whereas as the equator approaches, *M. incognita* and *M. javanica* are the most common RKN found. Globally, estimated crop loss due to plant-parasitic nematode is of \$80 billion (Handoo et al. 1998). In USA, up to 25 % loss to crops is due to nematode attack alone. In economic terms, nematodes cause loss of about \$157 billion annually to world agriculture (Singh et al. 2015). However, extensive information on accurate economic loss is often lacking. One of the main stumbling blocks for this is the notable absence of above ground symptoms of PPN infestation on infected crops. Not only this, damage occurring from PPN is often difficult to notice than that triggered by other pests or diseases (McCarter, 2009; Nicol et al. 2011).

2.5 Root-knot nematode distribution and its impact on Indian agricultural economy

In India, various crops are infested by different species of root-knot nematodes. The first report of any plant-parasitic nematodes was that of root-knot nematode identified at that time as *Heterodera radiculicola*, on tea from Kerala (Barber, 1901). Then *M. incognita* infecting jute was recorded for the first time in India from West Bengal by Chattopadhyay and Sengupta (1955). The reports on occurrence of root-knot nematode (*Meloidogyne* spp.) on various crops in different states of India were reported by different biologists thereafter. In India, the loss due to nematode infection is predicted at about 14.6% going upto as high as 50- 80% in some crops. About \$40.3 million is the estimated amount attributed to nematode attack as the national loss (Singh et al. 2015). The distribution of *M. incognita* and other PPNs species infecting major crops in India is shown in **Figure 2.5** indicating the severity of the plight caused by RKN infection.

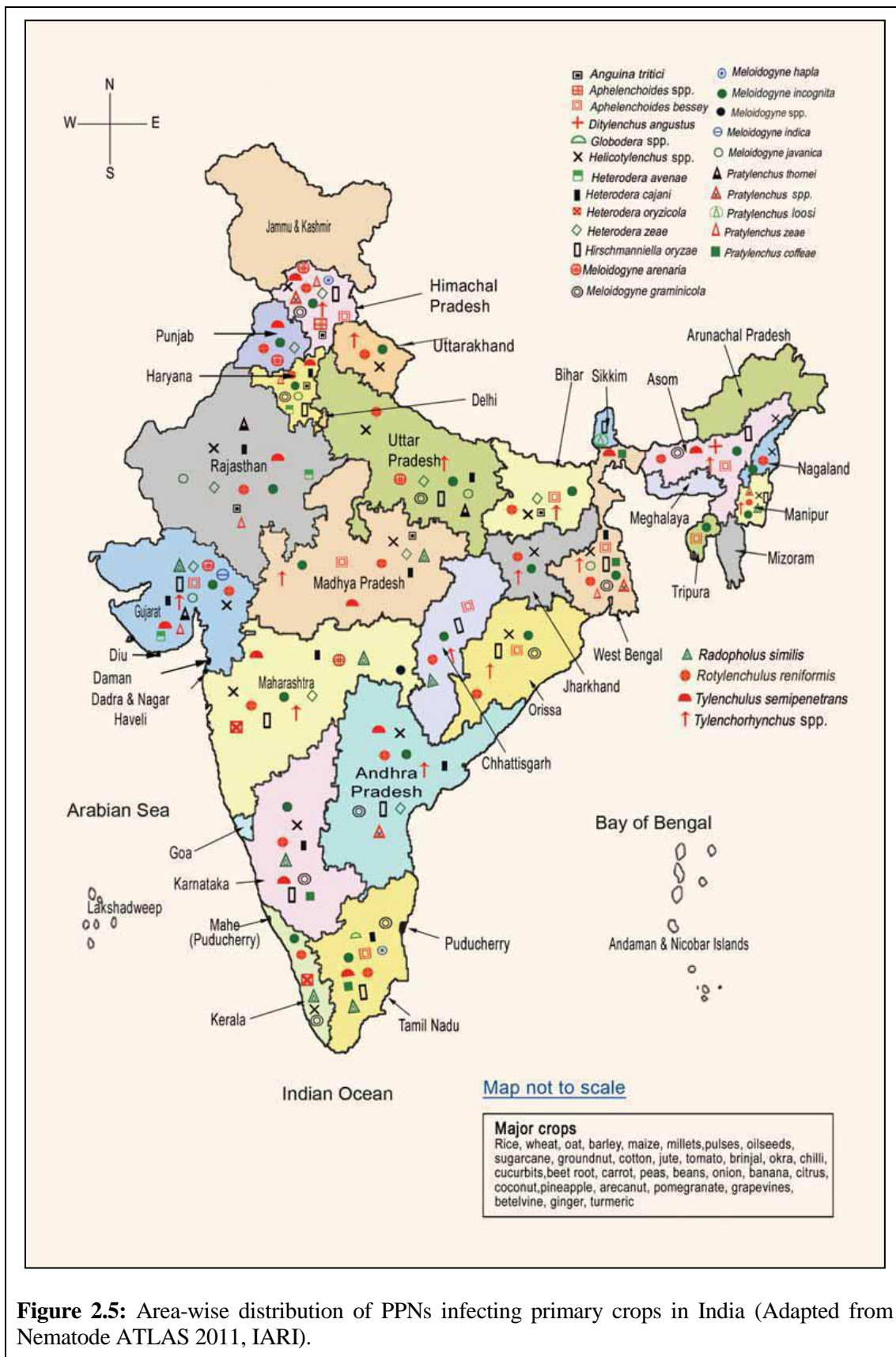


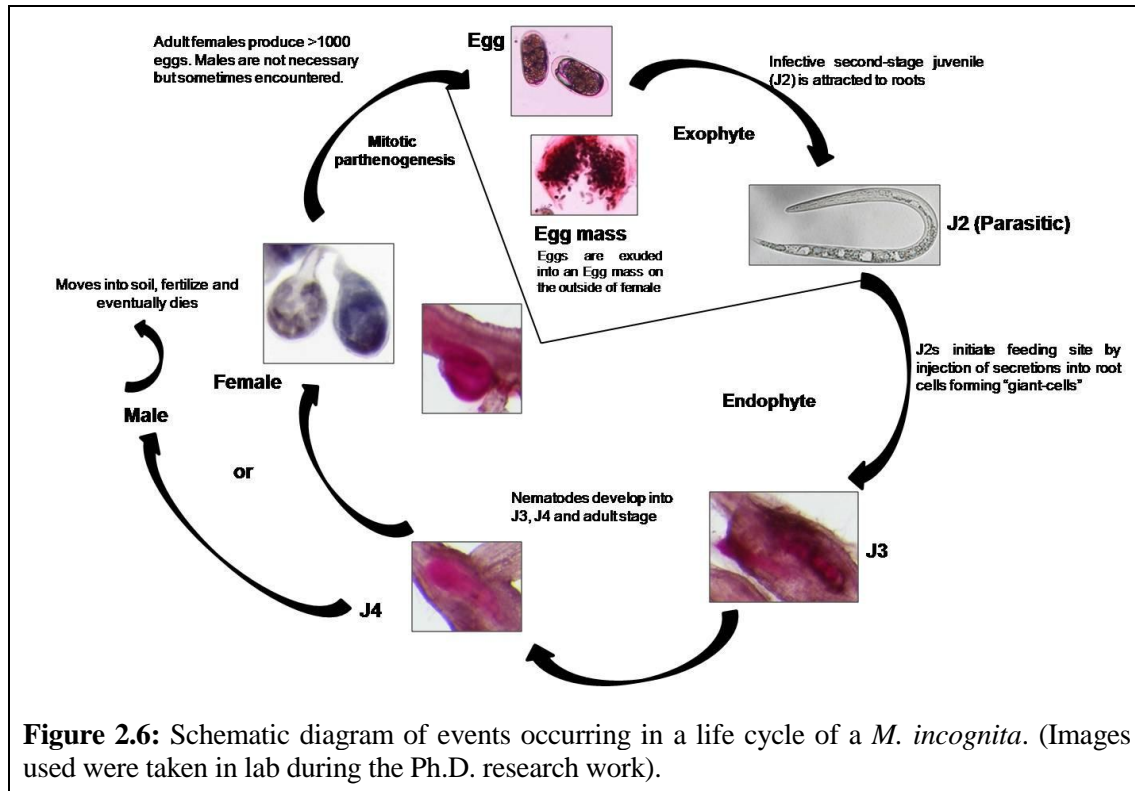
Figure 2.5: Area-wise distribution of PPNs infecting primary crops in India (Adapted from Nematode ATLAS 2011, IARI).

2.6 Lifecycle of root-knot nematode

As sedentary endoparasite, *M. incognita* infects the internal region of host roots and resides permanently in roots for survival that is to complete its life cycle by deriving nutrients; it has developed a specialized organ for it called the stylet (**Figure 2.6**). Females lay eggs into glycoprotein gelatinous matrix which are on the surface of the feeding site of roots. Apart from providing protection against environment, egg masses are known to have antimicrobial properties (Orion and Kritzman, 1991). The first-stage juvenile (J1) is produced inside the egg before moulting to second-stage parasitic J2. Moulting is a process in which synthesis of cuticle occurs at each development stage. In the life cycle of RKN moulting is reported to occur five times during its development (Davis et al. 2004). It is required for the progression between the larval stages in the life cycle of nematodes. The hatching of these infective J2s is temperature, moisture and other factors such as availability of root exudates dependent. Once hatched pre-parasitic J2 then penetrates roots by secreting cell-wall degrading enzymes through stylet (Abad et al. 2003) and migrates intercellularly between cortical cells before reaching vascular cylinder to form a permanent feeding site.

In the vascular cylinder both the protoxylem and protophloem cells undergoes differentiation to develop into nurse cells namely, giant cells functioning as a specialized sinks, providing nutrient supply to the growing nematode (Caillaud et al. 2008). The giant cells or knots are the only visible symptom of RKN attack on the infected plant. Once feeding site is established migratory J2s transformed to sedentary nematode and begins feeding. The giant cell walls thicken and increase in its surface area for more absorption of nutrients. After this stage nematode increase in size and undergoes moulting to the third-stage J3 and then to fourth-stage J4 and finally to

another moult to reach to the reproductive mature adult stage. RKN reproduce by parthenogenesis. Due to unfavourable conditions if males develop, they are vermiform and migrate out of the plant (Castagnone-Sereno, 2006).

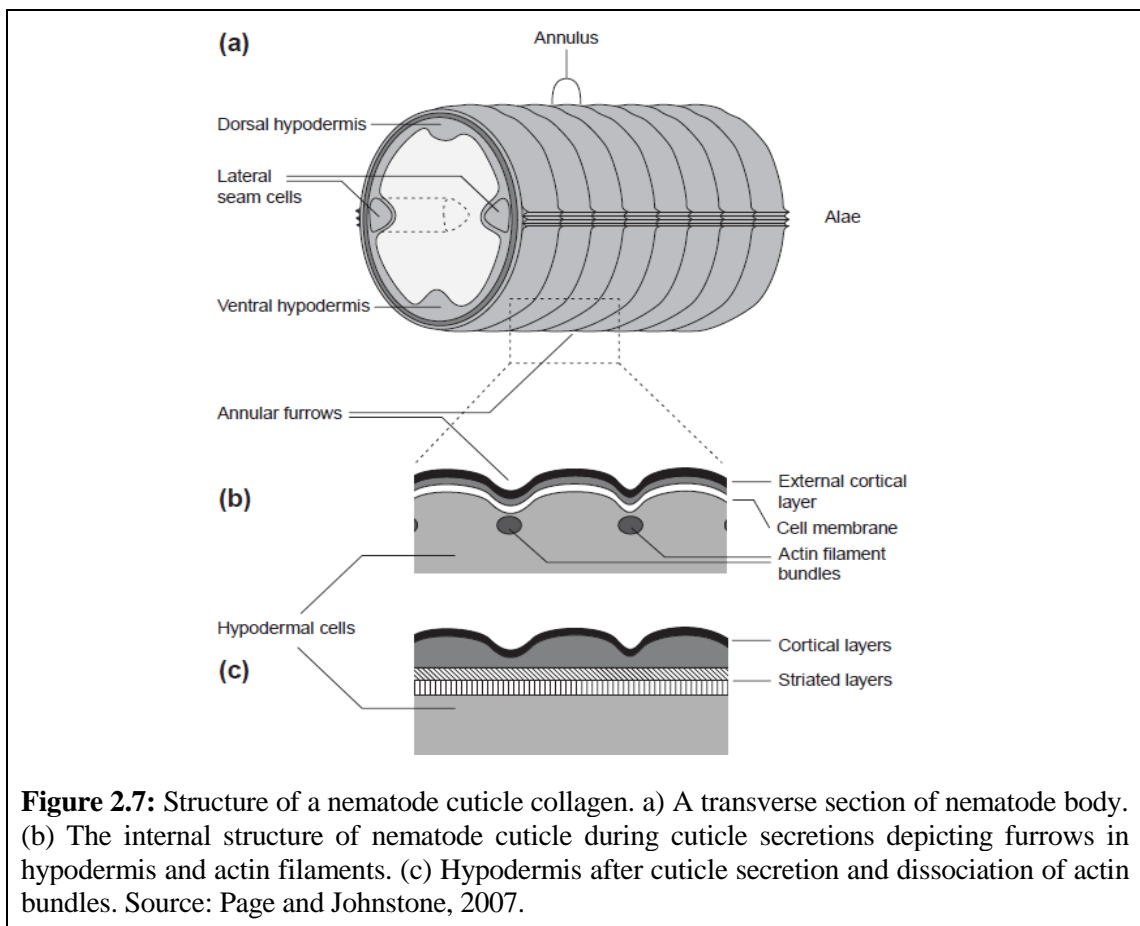


2.7 Cuticle: essential element for *M. incognita* morphology and integrity

Root-knot nematodes have a complex life cycle, their morphology changes from one-celled zygote to a vermiform, juvenile which undergoes four moulting to reach adult reproductive stage. Size of nematodes ranges from 400-1000 μm (Vanholme et al. 2004). Among the three life stages of RKN, J2s and males are vermiform. It is the females which are different in shape. Females have pear-shaped body with neck region muscled. The body wall in female protects her from the environment while in J2s and males it also helps in movement through the soil. Three major layers in body wall namely cuticle, hypodermis and somatic muscles are present (Bird, 1971). According to

the life stages, thickness of these layers varies ranging from 0.3-0.4 μm in J2s to 1.5 μm thick in males and up to 4-6 μm thick in the females.

The nematode cuticle is a multifunctional exoskeleton which is a highly impervious barrier between nematode and its environment. It is formed by an underlying ectodermal cell layer termed as the hypodermis (**Figure 2.7**).

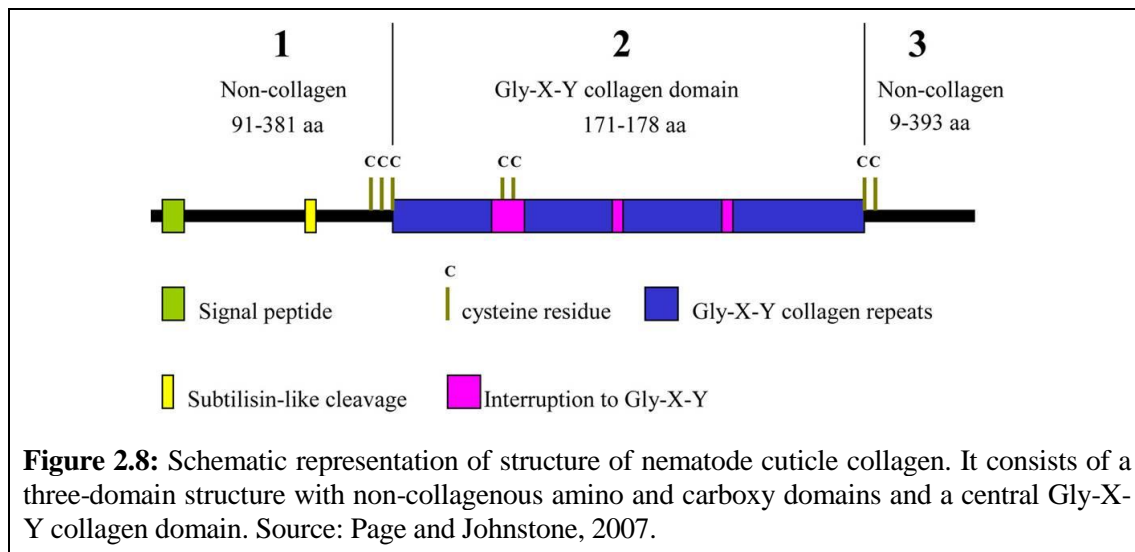


Interestingly, in a life cycle of plant-parasitic nematode synthesis of cuticle occurs five times during its development and this process is known as moulting. It is required for the progression between the larval stages in the life cycle of nematodes (Davis et al. 2004). The cuticle synthesis occurring second round time and henceforth occurs

underneath an existing cuticle unlike the initial round of synthesis. It is an extracellular matrix, where collagen constitutes as one of the major components.

2.7.1 Cuticle collagen genes

Cuticle, one of the major outer layers of nematode is composed of cuticle collagen proteins. These cuticle collagens proteins are encoded by over 170 members belonging to a gene family of cuticle collagen. Collagens are structural proteins with glycine-X-Y tripeptide repeats, where X- proline and Y- mostly hydroxyproline or proline surrounded by conserved cysteine residues (Johnstone, 2000) (**Figure 2.8**).



In *C. elegans*, about 21 cuticle collagen genes were identified through mutants of these genes (Page and Johnstone, 2007). These mutated genes include phenotype as DumPY(Dpy), Ray AbnorMal (Ram), RoLler (Rol), BLIster (Bli), SQuaT (Sqt) and LONG (Lon) (**Table 2.1**). Some of the members belonging to the cuticle collagen family are expressed throughout the life cycle while many collagen genes are required at a different time point of the moulting stage thus exhibiting specific function at a specific time. The studies have revealed cuticle collagen genes are expressed in a

defined temporal series with a repeated pattern at each synthetic period (Johnstone and Barry, 1996). Thus on the basis of time expression they are grouped as early, intermediate, or late, cuticle genes corresponding to their respective mRNA abundance.

Table 2.1: List of cuticle collagen genes identified in *C. elegans* on the basis of RNAi phenotype.

Gene	Cosmid	Group	Phenotypes
<i>sqt-1</i>	B0491.2	1	Dpy, RRol, LRol, Lon, Dom
<i>dpy-17</i>	F54D8.1	1	Dpy
<i>lon-3</i>	ZK836.1	1	Lon
<i>rol-6</i>	T01B7.7	1	RRol, Dpy, Dom
<i>dpy-5</i>	F27C1.8	1	Dpy
<i>bli-1</i>	C09G5.6	1	Bli
<i>dpy-9</i>	T21D12.1	2	Dpy
<i>sqt-2</i>	C01B12.1	2	wDpy/ RRol
<i>rol-8</i>	ZK1290.3	2	LRol
<i>bli-2</i>	F59E12.12	2	Bli
<i>dpy-3</i>	EGAP7.1	2	Dpy, DLRol
<i>ram-3</i>	F38A3.1	2	Ram/Dpy
<i>rol-1</i>	Y57A10A.11	3	LRol/wDpy
<i>ram-4</i>	F36A4.10	3	Ram
<i>sqt-3</i>	F23H12.4	3	Dpy, LRol, Dom
<i>dpy-13</i>	F30B5.1	3	Dpy
<i>dpy-4</i>	Y41E3.2	3	Dpy
<i>dpy-7</i>	F46C8.6	<i>dpy-7</i>	Dpy, DLRol
<i>dpy-8</i>	C31H2.2	<i>dpy-7</i>	Dpy, DLRol
<i>dpy-2</i>	T14B4.7	<i>dpy-2</i>	Dpy, DLRol
<i>dpy-10</i>	T14B4.6	<i>dpy-2</i>	Dpy, DLRol, LRol, Dom

Source: Page and Johnstone, 2007

2.8 Pharynx: Organ for feeding and parasitism

The pharynx organ is a bilobed, linear tube structure which is sheathed in a basement membrane (**Figure 2.9**). The pharynx structure is continuous with the stylet lumen in *M. incognita* (Eisenback and Hunt, 2009) and is one of the vital organ for its development. Pharynx has six regions which are defined as follows starting from the stylet - buccal cavity, procorpus, metacarpus, isthmus, terminal bulb and pharyngeal-intestinal valve. It is composed of 95 nuclei which are grouped into seven cell types: arcade cells, muscles, epithelia, neurons, glands, marginal cells and valves. The gland

cells of pharynx are vital for establishing host-parasite relationship (Albertson and Thomson, 1976). It is the metacarpus region that helps in pumping the secretions from gland cells into the host and substances from the host into its intestine and these secretions from gland cells have been of great interest for developing nematode managing strategies.

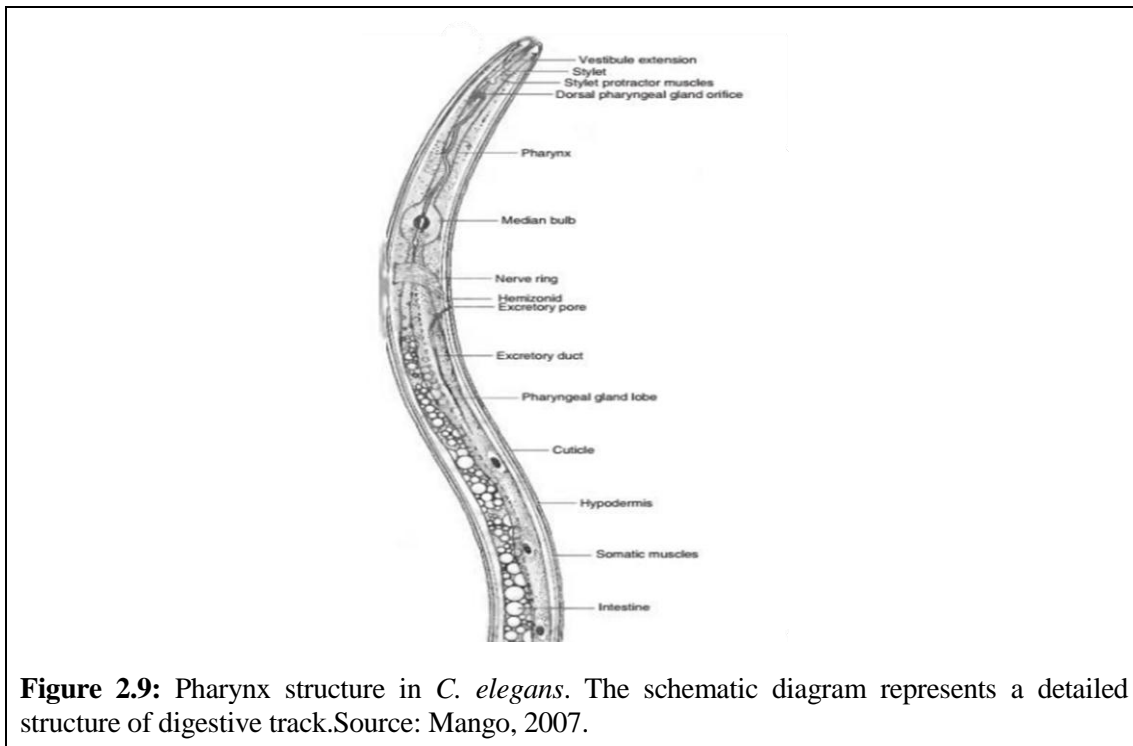


Figure 2.9: Pharynx structure in *C. elegans*. The schematic diagram represents a detailed structure of digestive track. Source: Mango, 2007.

2.8.1 Polyclonal development of pharynx during embryogenesis in nematodes

Pharynx development during embryogenesis in *C. elegans* is very well studied. Two sister blastomeres, AB and P₁ are the first product of fertilized eggs after undergoing first cleavage in *C. elegans* (Sulston et al. 1983). These two sister blastomeres although originates from a same egg they differ extensively in their sub sequential development. For instance, P₁ produces intestinal cells but AB does not. Asecond round of cleavage, AB results in ABa and ABp blastomeres, where ABa produces pharyngeal cells (Priess

et al. 1987). Pharynx composed of cells of different embryonic origins (Mango, 2007) that is produced by two different cell lineages at 4-cell stage viz. ABa and EMS pathways (**Figure 2.10**). These cells produce pharyngeal together with non-pharyngeal cells. ABa and EMS pathways are responsible for producing pharyngeal cells via atleast two defined molecular pathways (**Table 2.2**).

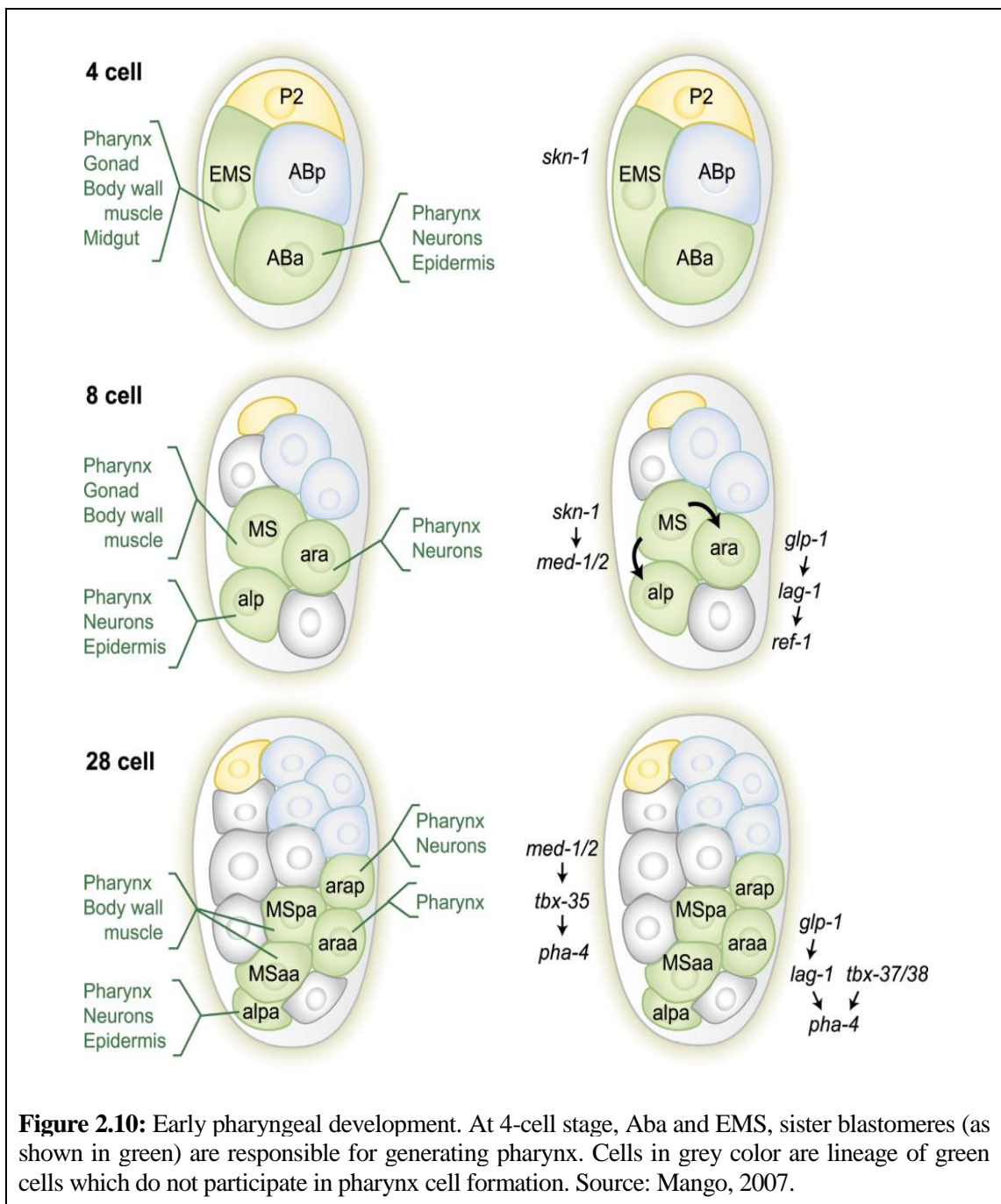


Table 2.2: Genes identified in pharynx development in *C. elegans*.

Gene	Homology	M/Z	Expression (initiation)	Pha phenotype	Targets	Binding sequence	Upstream genes	References
<i>glp-1</i>	Notch Rcp	M	ABa@4	Aph	<i>ref-1</i> <i>pha-4</i>	N/A	?	Kalb et al., 1998; Mango et al., 1994; Pries et al., 1987
<i>lag-1</i>	Su(H) TF	M	Broadly	Aph	<i>ref-1</i> <i>pha-4</i>	RTGGGAA	<i>glp-1</i>	Christensen et al., 1996; Smith and Mango, 2006
<i>skn-1</i>	Zipper TF	M	EMS@4	Pha	<i>ref-1</i> <i>end-1</i>	G/ATCAT + A/T	?	Bowerman et al., 1992; Maduro et al., 2005b; Mango et al., 1994; Neves and Pries, 2005
<i>med-1/2</i>	GATA-like Zn TF	M, Z	EMS@4 and maternal	Ppa	<i>end-1/3</i> <i>hth-25</i>	RRRAGT-ATAC	<i>skn-1</i>	Brottman-Maduro et al., 2005; Maduro et al., 2001
<i>ref-1</i>	bHLH TF	Z	ABa@26 ABp@4 EMS@24	none	<i>tbx-37</i> <i>tbx-2</i>	CANNTG	<i>lag-1</i>	Neves and Pries, 2005; Smith and Mango, 2006
<i>tbx-37/38</i>	T-box	Z	ABa@24	Aph	<i>pha-4?</i>	?	<i>ref-1</i> in some cell types	Good et al., 2004
<i>pha-4</i>	FoxA	Z	ABa@44 MS@28	Pha	<i>many</i>	TRTTKRY	<i>lag-1</i> <i>tbx-37/38</i> <i>med-1/2</i> <i>glp-1</i>	Gaudet and Mango, 2002; Good et al., 2004; Maduro et al., 2005b; Mango et al., 1994; Smith and Mango, 2006
<i>htz-1</i>	H2A.Z histone variant	Z	Broadly from the 28-cell stage	Delayed activation	<i>myo-2</i> , <i>R07B1.9</i>	N/A	?	Updike and Mango, 2006
<i>tbx-2</i>	T-box	Z	ABa@8E	ABa muscles absent	<i>pha-4</i> <i>ceb-22?</i>	?	<i>ref-1</i> in some cells <i>tbx-37/38?</i>	Chowdhury et al., 2006; Smith and Mango, 2006
<i>ceb-22</i>	Nkx2-5 Homeobox TF	Z	pm3-5, pm7	Indistinct BM Around pharynx	<i>myo-2</i>	CACTTAT	<i>pha-4</i> <i>ceb-22</i> <i>ceb-2</i> <i>pha-2</i>	Kalb et al., 1998; Mango et al., 1994; Okkema and Fire, 1994; Okkema et al., 1997
<i>peb-1</i>	FLYWCH Zn TF	Z	Broadly	Glands distended	<i>myo-2</i>	YDTGCCRW	?	Beaster-Jones and Okkema, 2004; Thatcher et al., 2001
<i>daf-12</i>	NHR Zn TF	Z	Broadly	Daf	<i>myo-2</i> <i>ceb-22</i>	AGTGCA	<i>daf-9</i>	Ao et al., 2004

Source: Mango, 2007.

The ABa pathway is dependent on intercellular signaling between the Notch receptor orthologue *glp-1* (abnormal germline proliferation) and blastomeres (Mango, 2007). *Glp-1* is a notch receptor gene and induces germline proliferation during pharyngeal

embryonic development. While the EMS pathway is *glp-1* independent and depends on two maternal genes, namely *skn-1* and *pop-1* to develop pharyngeal cells (Mango, 2007).

2.9 *Meloidogyne incognita* genome

Whole genome sequencing of *M. incognita* revealed a genome size of 86 Mb that comprises 2,817 supercontigs using whole-genome shotgun approach (Abad et al. 2008). In the assembly absence of DNA characteristic of any bacterial genome (specifically endosymbiont) was notable. The study also identified 19,212 protein-coding genes in its genome. Genes involved in parasitic interactions were identified, among them were 61 plant cell wall-degrading, carbohydrate-active enzymes (CAZymes), 21 cellulases and six xylanases from family GH5, two polygalacturonases from family GH28, 30 pectate lyases from family PL3, and four were secreted chorismate mutases. The study found similar genes in *M. incognita* that lead to fatal RNAi phenotype as reported in *C. elegans*. It also reported orthologs of several known nematode nuclear receptors that are present in *C. elegans* (Abad et al. 2008).

2.10 *Dumpy* (*Dpy*) genes

Cuticle genes are categorized into six groups based on the motifs and presence of Gly-X-Y region. Of the 154 cuticle genes identified in *C. elegans*, 68 belong to Group 1, 12 to Group 1a, 38 to Group 2 and 31 to Group 3. Apart from these there are two other groups namely, *dpy-7* and *dpy-2* group having three and two members, respectively. Major of the cuticle genes have been identified by mutation using RNAi experiments. Among them Group 1 genes are *bli-1*, *sqt-1* and *rol-6*; *bli-2* forms Group 2; Group 3 genes are *dpy-13* and *sqt-3*. The other two groups are named based on the genes constituting these groups namely, *dpy-7* Group having single gene *dpy-7* and *dpy-2*

Groupbut is having two genes, *dpy-2* and *dpy-10*. Group 1a genes are not identified based on mutational studies. All the identified cuticle genes by mutation are involved in formation of the basic collagen structure i.e. main blocks of Gly-X-Y collagen; each separated by cysteine residues thus forming domains namely I, II and III.

In *C. elegans* more than 50 genes affecting overall biological structure have been identified by mutation and genetic mapping (Von Mende et al. 1988). The most common mutant class is DumPY (Dpy) and genes responsible to this phenotype have been characterized as cuticle collagen genes as identified in *C. elegans*. Dumpy class of genes is a family of zinc metalloproteases also known as Astacins. A member of astacin family was first time described in crayfish and was revealed as a digestive enzyme (Titani et al. 1987). Astacin family is a divergent group having digestive enzymes, hatching enzymes with other astacins that are determined in *C. elegans* (Park et al. 2010). *C. elegans* zinc metalloproteases were distinguished into six subgroups formed as per the domain organization, especially that are present in C-terminal extensions next to the catalytic site. In *C. elegans* astacins, three basic structural and functional moieties can be distinguished: pre pro portion, the central catalytic chain and long C-terminal extensions with apparently regulatory functions. In these the regulatory moiety certain domains and motifs have been distinguished namely, astacin domain, EFG-like, CUB domains and others. Subgroup I members (*nas-1* to *nas-5*; Nematode astacin protease (*nas*)) lack additional domains. Subgroup II (*nas-6* to *nas-15*) is indicated by SXC/ShK toxin domains. Members of subgroup III (*nas-16* to *nas-30*) mostly known for one EGF as well as one CUB domain. Subgroup IV (*nas-31* and *nas-32*) comprised of single SXC/ShK toxin domain besides EGF and CUB domains, while subgroup V (*nas-33* to *nas-38*) are identified by presence of TSP1 domain instead. Subgroup VI (*nas-39*) has

only one BMP- 1/Tolloid domain as studied in *C. elegans* (Park et al. 2010). Among the identified *C. elegans* astacin genes, the members of Subgroup V, majorly nas-36 and nas-37, are found to play role in moulting process. Another member of this subgroup viz. nas-35 or *dpy-31* is very well characterized in parasitic nematodes for example in *B. malayi*. *Dpy-31* gene is reported to be involved during shedding of cuticle layer (Park et al. 2010).

2.11 *Glp-1* (abnormal germline proliferation-1) gene

Glp-1, abnormal germline proliferation gene, is one of the key gene associated with pharynx development via ABa pathway during embryogenesis. This pathway is determined by intercellular signaling between blastomeres and *glp-1*, the Notch receptor orthologue. The product of *glp-1* gene induces certain AB descendents to differentiate into pharyngeal cells. *Glp-1* is a homolog of the *Drosophila* Notch gene and induces germline proliferation during pharyngeal embryonic development (Priess et al. 1987; Priess and Thomson, 1987; Roehl et al. 1996). *Glp-1* is crucial for cell interactions during embryogenesis in nematodes. It is a part of conserved family comprising transmembrane proteins such as LIN-12 in *C. elegans* (Yochem and Greenwald, 1989), Notch in *Drosophila* (Wharton et al. 1985b; Kidd et al. 1986), and several homologs in vertebrates that includes humans (Stifani et al. 1992). It is structurally and functionally identical to another Notch-related receptor, *lin-12*, which has similar conserved motifs, imparting functional roles to both of them as membrane-bound receptors required in Notch signalling. Studies have shown that both the notch signalling receptors namely, GLP-1 and LIN-12 have binding sites for LAG-1 (Yochem and Greenwald, 1989). During early embryogenesis, GLP-1 is required between the 4- to 28-cell stages. There are evidences that suggest the involvement of GLP-1 in

inductive interactions between posterior and anterior blastomeres to specify several anterior cell fates (Evans et al. 1994). In embryo, *Glp-1* RNA is contributed maternally which is then carefully translated in ABa and eventually to its sister ABp blastomere (Mango, 2007). Thus, the *glp-1* gene donates a regulated maternal mRNA to the early embryo (**Figure 2.10**). It is reported that *glp-1* mRNA is distributed in anterior region. GLP-1 function in the embryo is stringently dependent on maternal *glp-1* expression (Austin and Kimble, 1987; Priess et al. 1987). By Northern blot analysis, *glp-1* mRNA is found to be present in both the germline and early embryo (Ahringer et al. 1992). In the *C. elegans* germline, function of GLP-1 is related with mitosis and/or in repression of meiosis. Loss of *glp-1* creates a critical germline proliferation deformity and entry into meiosis (Austin and Kimble, 1987).

2.12 Conventional methods for RKN management

There are numerous ways that are broadly practiced in managing these parasitic nematodes. The conventional approaches to manage the PPN infection are not enough. Albeit usage of chemical nematicides in regulating nematode infection is a useful method of late, controversies related to contagious groundwater, environmental poisoning and its remnant in food have led to formulation of rigorous mandates of their use in agriculture. Not even this certain countries have also prohibited the commercialization of nematicides (Tamilarasan and Rajam, 2013). Other cultural practice like crop rotation, non-host crop are generally enough by itself in regulating nematode infection overextending at economically devastating state. Nonetheless, correct determination of nematode species is crucial for recognizing its hosts and non-host plants (Yepsen, 1984; Mary, 1996; Wang et al. 2004). Method like crop rotation is not enough in eliminating nematode infestations completely due to the wide host range of root-knot nematodes. Another method is

fallowing i.e. leaving land for a period of time. Although it is most effective when done during hot, dry weather has some negative effects such as soil erosion and loss of soil moisture and nutrients. Soil sanitation involves destroying infested plant thereby restricting expansion of infected soil to un-infected one. But this alone is not enough for eliminating the pathogen. Other control measures like use of biological agents such as nematode fungal parasites (*Dactylella oviparasitica*) or bacterial parasites (*Pasteuria penetrans*) that feed on PPNs are not effective worldwide (Sayre, 1986).

Genetic engineering method involves identification and manipulation of natural occurring defense genes like R genes, proteinase inhibitors, lectins and Bt toxin genes which imparts resistance against nematodes in plants. For instance, *Mi-1* gene identified in tomato was used against parasitic nematode to generate nematode resistance plants (Williamson et al. 1994a; Milligan et al. 1998). This gene have been used against few species of *Meloidogyne* for example, *M. javanica*, *M. anenari* and *M. incognita* but there are already reports of breaking down of resistance in the field population of *M. incognita* and *M. javanica* (Lopez-Perez et al. 2006). Resistance genes against cyst nematodes have been well identified. $Hs1^{pro-1}$ gene identified from *Beta procumbens* showed resistance against *H.schachtii* (Cai et al. 1997). Transgenic potato plants expressing *Hero A* gene (isolated from tomato) showed >95% and 80% reduction against *G. rostochiensis* and *G. pallida*, respectively (Sobczak et al. 2005). Use of host resistant plant has been successful against nematode infection but it mainly depends upon the availability of resistant genes in the gene pool of a crop plant that can be transferred via conventional breeding. Thus, the plant resistance is restricted to specific species of a particular nematode. In some cases, the genetic diversity within the nematodes limits the effectiveness of existing resistant cultivars. Hence, the natural

resistance against PPNs is unavailable for every crop. Not only this, certain nematode species have the ability to infect even the resistant host.

2.13 RNAi - A strategy to leash the nematode infestation

For successful management of nematodes, a thorough study of their morphology, biology and host-parasitic relationship is necessary. An integrated approach combining cultural, biological, and chemical methods towards controlling these devastating pathogens is needed. The constraints associated with the conventional methods cater a scope for biotechnologists to initiate new compelling but persistent strategy for nematode inhibition. RNA interference (RNAi) is new biotechnological strategy in managing nematodes infection. RNAi mechanism was originally observed in plants where this phenomenon was named as post-transcriptional gene silencing- PTGS (Jorgensen et al. 1996; Waterhouse et al. 1998). However, it was initially discovered in *C. elegans* by Fire and his group (1998). It is a defense mechanism exhibiting naturally against double-stranded RNA (dsRNA) targeting cellular and viral mRNAs. It is a specific and sequence-dependent targeted gene silencing activity. Once double-stranded RNA enters the cell, it is cleaved by an RNaseIII endonuclease like enzymes, Dicer into short double-stranded fragments of 20-25 basis pairs. In an ATP dependent step, the dsRNA become integrated into a protein complex, known as RNA induced silencing complex (RISC) which guides the siRNA to target sequence with assistance from other proteins majorly Agronautes (Nykanen et al. 2001; ketting, 2011).

2.13.1 Mechanism of siRNA

The basic RNAi pathway involves initiation and effector phase. In the initiation phase, the dsRNA molecules are cleaved by Dicer (ribonuclease III) and produce small

interfering RNAs (siRNAs) (21-23 nucleotides) which bear 5' phosphate groups and 2 nucleotide overhangs at 3' essential for subsequent siRNA induced silencing through RNA induced silencing complex (RISC). The second phase i.e. effector phase consists of events involving, unwinding of siRNA presumably by RNA helicase enzyme resulting in RISC assembly. This result in activation of protein complex, which recognizes the target by siRNA-mRNA base pairing and cleaves the target gene leading to sequence-specific mRNA degradation (**Figure 2.11**) (Hannon, 2002).

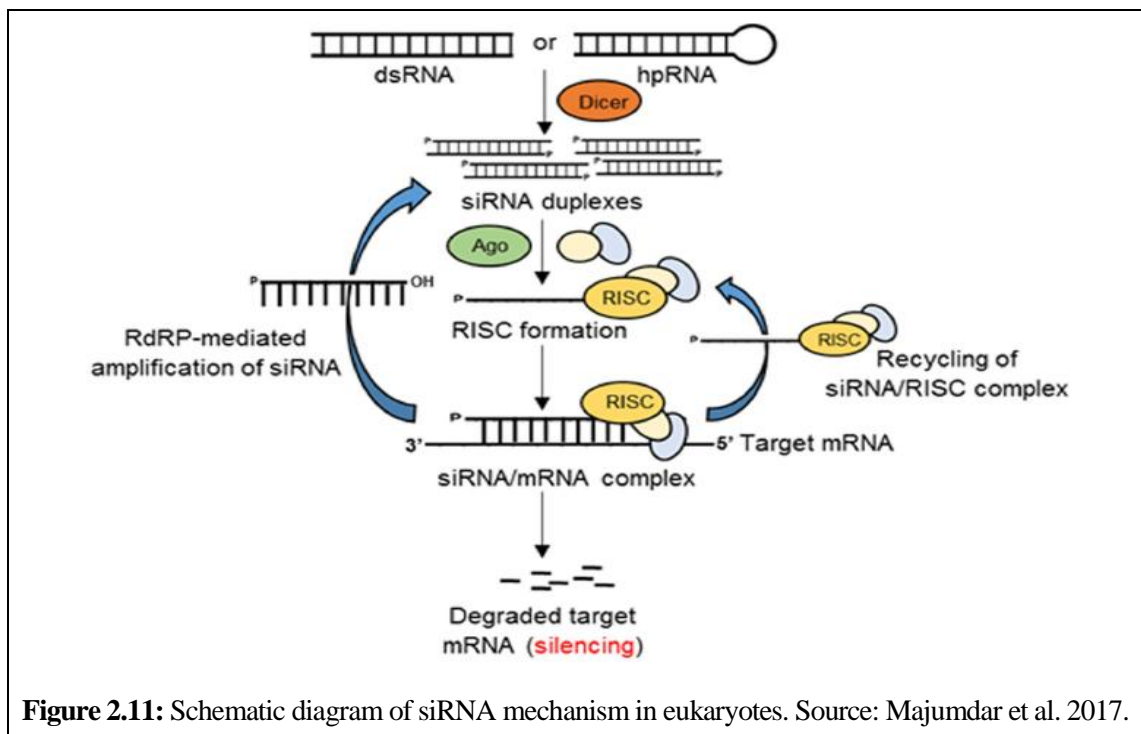


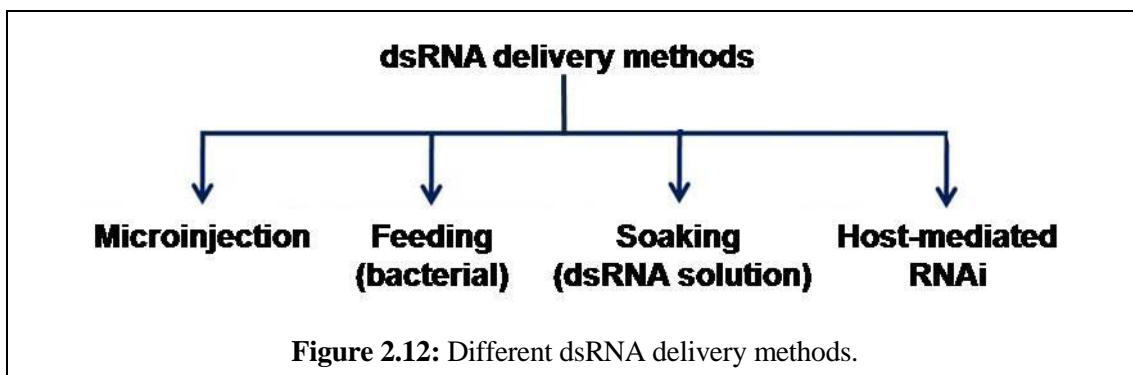
Figure 2.11: Schematic diagram of siRNA mechanism in eukaryotes. Source: Majumdar et al. 2017.

Amidst of discovery of siRNA-mediated silencing pathway, presence of secondary siRNA molecules was reported (Hunter et al. 2002). These secondary molecules were found to be formed from the action of RNA-dependent RNA polymerases (RdRPs) on the target transcript resulting in the amplification of silencing response. Secondary siRNAs are antisense to the target mRNA with a 5'- triphosphate. They function in association with specific argonaute proteins. Thus, only few dsRNA molecules are enough to trigger

silencing generating an altered phenotype. Although generation of secondary siRNAs follows different mechanism in different organisms but transitivity process appears to be common. This process depends on RdRP wherein initial target mRNA acts as template resulting in transitive RNAi as observed in plants and nematodes.

2.14 Different strategies for silencing a gene

Since PPNs are sedentary endoparasites, they reach out to their respective host and infect to develop a host-parasite interaction. Hence, various genes play significant role in establishing such relation between plant and nematode. Secretory genes and other genes having critical role in development or in signaling are of great interest as a target for RNAi approach. But firstly developing a dsRNA construct of such genes is of utmost importance. A number of different strategies have been employed for delivering dsRNA into host for a successful RNAi experiment. Such strategies are Microinjection, Feeding, Soaking and Host-mediated RNAi with each having its own advantages and limitations (**Figure 2.12**). The silencing efficiency of a gene depends a lot on dsRNA delivery method used.



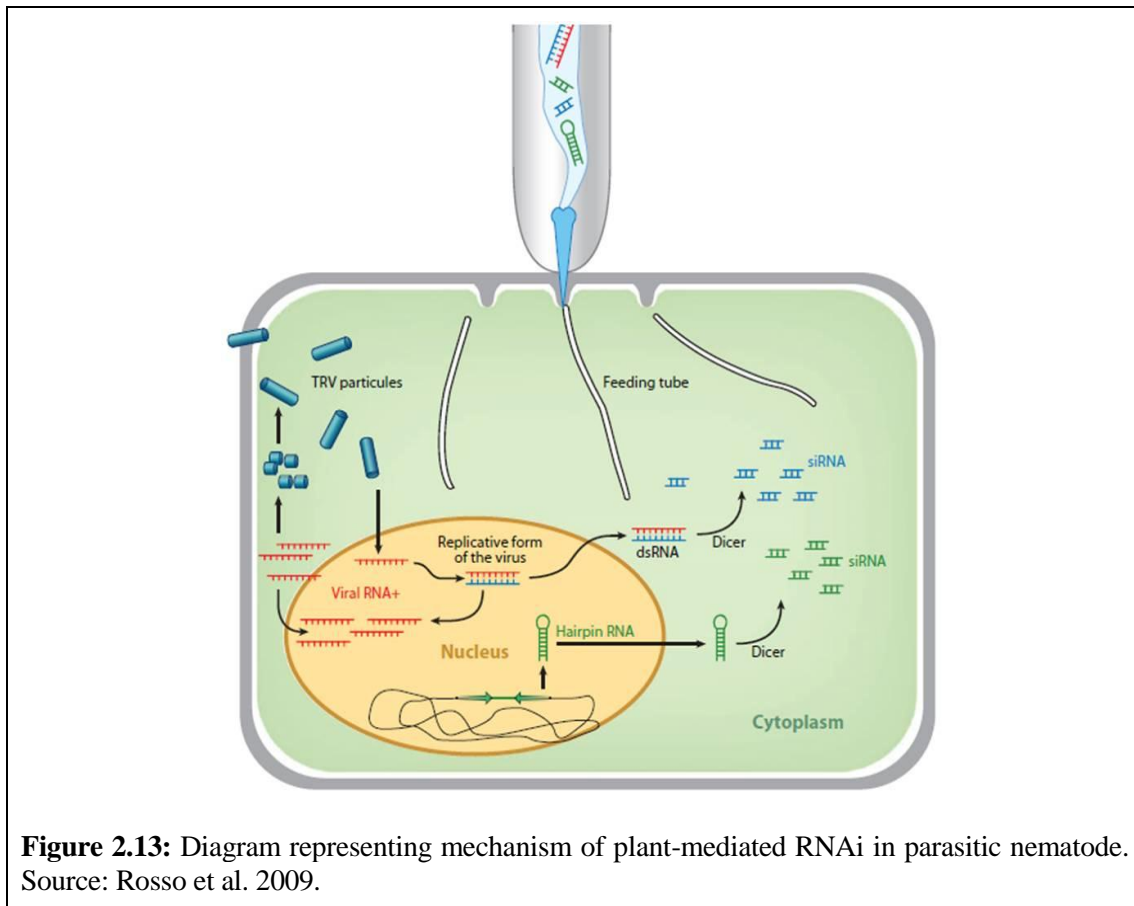
Methods like microinjection, feeding and soaking are a success in case of *C. elegans* but have limitations with respect to parasitic nematodes. The microinjection has not

proven to be successful and efficient in case of plant-parasitic nematodes. This is due to fact that infective second-stage J2(s) are smaller in size along with that are unable to uptake fluid in absence of host plant infection (Banerjee et al. 2017). Similarly parasitic nematodes do not feed upon bacteria for deriving the nutrients thus is of not much significance in case of parasitic nematodes. However, soaking the nematodes in dsRNA solution has shown some success but this too has a limitation. The infective juveniles of PPNs do not ingest dsRNA orally with that ease from the dsRNA solution. There are reports of inducing oral uptake of dsRNA via neuroactive compounds like octopamine, resorcinol and serotonin in PPNs (Urwin et al. 2002; Huang et al. 2006a). This soaking method using such compounds has proved to be successful in both RKN and CNs (Rosso et al. 2005). However, this method is concentration dependent and leads to a transient and unstable silencing as the time duration for which nematodes have been exposed significantly alters the silencing efficiency.

2.14.1 Host-delivered RNAi (HD-RNAi) method

Host-delivered RNAi is the most successful and efficient method for imparting gene silencing in nematodes wherein targeted gene belonging to a pathway or organ development is silenced via host that is being damaged. In this method the first part of RNAi partially occurs *in planta* and partially in PPNs ingesting nutrients from the transgenic expressing dsRNA for the targeted gene (**Figure 2.13**). Parasitic nematodes feed on transgenic plants through stylet. The transgenic plants produce siRNAs by their RNAi machinery which is then ingested by these feeding PPNs (Li et al. 2011). This technique depends upon the PPNs ability of ingesting macromolecules from the host. This technique involves construction of dsRNA for the target gene which is achieved by cloning some part in sense and antisense direction separated by an intron or spacer region driven by either constitutive or tissue-specific promoter in binary RNAi vector. DsRNA construct thus

produced is used for developing transformed plants either by *Agrobacterium*-mediated transformation for some crops or by using other screening systems like hairy-root method employed for producing transgenics for cultivated crops like sugarbeet, tomato and soybean. Considerable number of reports has successfully produced resistant transgenic plants against nematode infection by utilizing this time-consuming yet efficient strategy.



Varied genes involved in development, signaling pathway, associated with mRNA metabolism, house-keeping genes and most importantly secretory genes are targeted using this approach. The first successful HD-RNAi experiment came into light in 2006 wherein a transgenic tobacco line expressing *M. incognita* integrase and splicing factor gene was silenced (Yadav et al. 2006). The selected genes were proved as fatal targets against *M. incognita* feeding on transgenic *Arabidopsis* lines (Kumar et al. 2017). Other house-keeping

genes such as *prp-17*, ribosomal proteins etc have been effectively silenced against parasitic nematodes (Banerjee et al. 2017). Reports have shown success of some of the critical effector genes as efficient targets against *Meloidogyne spp(s)*, for instance, suppression of 16D10 exhibited 63-90% reduction in *M. incognita* infection in transgenic *Arabidopsis*, while a decrease in number of eggs was noticed on silencing 16D10L in *M. chitwoodi* using plant-mediated or host-mediated RNAi strategy in transgenic *Arabidopsis* and potato plants (Huang et al. 2006a; Li et al. 2011; Dinh et al. 2014a and 2014b).

Not only RKNs, HD-RNAi mediated nematode management have shown some success in case of CNs. A 68% decrease in egg number was noticed in *H. glycines* when infected on transgenic soybean plants expressing major sperm protein (Steeves et al. 2006). The attenuation of four parasitism genes - ubiquitin-like (4G06), CBP (3B05), SKP1-like (8H07) and ZF protein (10A06) in *Heterodera schachtii* led to reduction in number of females in RNAi transgenic *Arabidopsis* plants (Sindhu et al. 2009). Thus, plethora of studies silencing genes using RNAi methodology for developing nematode control strategy is present. Suppression of another class of genes i.e. neuropeptides like *flp-14* and *flp-18* resulted in 50–80% reduction in terms of *M. incognita* infectivity on introducing it to transgenic tobacco lines (Papolu et al. 2013). Esophageal proteins silenced by HD-RNAi against *H. glycines* showed reduced reproduction (Bakhetia et al. 2007). In other studies genes silenced using this approach are Mj-Tisll, tyrosine phosphatase and mitochondria stress 70 protein precursor against *M. incognita* (Papolu et al. 2013).

Although there are reports of CNs management using this technique, it is more successful in RKNs due to aspects like more RNAi sensitivity and larger size exclusion limit of RKNs than in CNs. This plant-mediated based RNAi approach for curbing the

menace caused by PPNs endeavors a new strategy for raising nematode resistant varieties of cultivated crops.

2.15 Silencing of development genes from *M. incognita*

In one of the most recent studies conducted by Junhui Niu et al (2012), a developmental gene, Rpn7 critical for the integrity of 26S proteasome was targeted for controlling root-knot nematode *M. incognita*. It resulted in reduced negative impacts on reproduction and motility rate of *M. incognita*. These several successful studies on silencing of specific gene through RNAi for some parasitic genes in PPNs propose that RNAi technology and other genetic approaches together will be helpful in developing a promising and effective method for management of PPNs. Nevertheless, a few of the development genes have been targeted for RNAi based gene silencing for managing plant parasitic nematodes (Li et al. 2010a; Xue et al. 2013; Kumar et al. 2017) (Table 2.3).

Table 2.3: List of RNAi mediated gene silencing in PPNs.

Gene name/ accession no.	Function of target gene	Nematode species	Delivery method	Phenotype and reduction %	Plant system	Reference
Col-1, Lemmi-5	Structure and development of cuticle	<i>M. incognita</i>		Reduction in nematode infection	Tomato	Banerjee et al. 2018
Pat-10, unc-87	Muscle contraction and structure of myofilaments in body wall muscle	<i>P. penetrans</i>	<i>In vitro</i>	Reduction number of nematodes	Soybean	Vieira et al. 2015
Pat-10, unc-87	Muscle contraction and structure of myofilaments in body wall muscle	<i>M. graminicola</i>	<i>In vivo</i>	Inhibition in nematode motility		Nsengimana et al. 2013
Rpn-7	Integrity of 26S proteasome	<i>M. incognita</i>	<i>In vivo, In vitro</i>	Reduction in reproduction and motility	Tomato	Niu et al. 2012
3B05, 8H07, 10A06, 4G06	Cellulose binding protein, SKP1-like, Zinc finger protein, ubiquitin-like	<i>H. schachtii</i>	<i>In vivo</i>	Reduction in female number	Arabidopsis	Sindhu et al. 2009
Flp	FMRF amide-like peptides	<i>G. pallida</i>	<i>In vivo</i>	Inhibition of motility	Potato	Kimber et al. 2007
MSP	Major sperm protein	<i>H. glycines</i>	<i>In vitro</i>	Up to 68 % reduction in eggs	Soybean	steeves et al. 2006
AY013285	Chitin synthase	<i>M. artiellia</i>	<i>In vivo</i>	delayed egg hatch		Fanelli et al. 2005

Chapter 3
Materials and Methods

3. MATERIALS AND METHODS

3.1 Materials

Experimental materials used in the present study are mentioned in **Table 3.1**.

Table 3.1: List of materials used in this study

Materials	Source
Chemicals and Enzymes	From different sources that includes Amersham Biosciences USA, Applied Biosystems, USA, Fermentas, Germany; USA; Himedia, India; Invitrogen, USA; Thermo Scientific Corp, USA; Merck, Germany; New England Biolabs Inc., USA; Sigma Aldrich, USA; Qiagen Inc., USA etc.
Primers	Sigma
Vectors pHELLSGATE12 pGEMT [®] -Easy pDONR221 pBC-6	Dr. Tushar K Dutta, Scientist, Nematology Division, IARI Promega Inc. Invitrogen, USA Dr. Subhramaniam, IIT, Kanpur
Nematode strain <i>Meloidogyne incognita</i>	Available in the lab (NRCPB)
Plant material <i>Arabidopsis thaliana</i> ecotype <i>Columbia</i> (<i>Col-0</i>) <i>Solanum lycopersicum</i> cv Pusa Ruby (Tomato)	Available in the lab (NRCPB) National Seeds Corporation, IARI, India
Radioisotope α -p32 dCTP	JONAKI, Regional Centre, BRIT, Hyderabad
Soilrite	Keltech Energies Ltd.

Other commercial kits and reagents used are mentioned in the text with the respective description.

3.2 Instruments

The entire instrument facilities required to carry out this research was available at the NRCPB, Pusa Campus, New Delhi and Department of Biotechnology, DTU, Delhi. The microscopic photographs of the plant tissues were taken under stereo zoom microscope available at Division of Nematology, IARI, New Delhi.

3.3 Methods

3.3.1 Culturing of bacterial cells

All the *Escherichia coli* (*E. coli*) cells were grown on Luria Agar (LA) or Luria Broth (LB) with appropriate antibiotics. The detailed compositions of the LA and LB media are provided in the (**Appendix Table 1 and 2**). The *E. coli* strain DH5 α from glycerol stock was streaked on freshly prepared LA plates containing nalidixic acid (15 mg/ml) and incubated at 37 °C overnight. A single colony was always used for subsequent culturing in this study. The *Agrobacterium tumefaciens* cells (strain GV3101) were cultured on freshly prepared Yeast Extract Peptone (YEP) medium (**Appendix Table 3**) containing rifampicin (25 mg/ml) and gentamycin (15 mg/ml) and incubated at 28 °C for 48 h in an incubator. The liquid cultures were incubated at a shaking speed of 180 to 250 revolutions per minute (rpm). For storage of bacterial strains and clones, a single colony was inoculated overnight in liquid medium with appropriate antibiotics. To 1.0 ml of overnight culture, glycerol was added to a final concentration of 15% in 2 ml sterilized screw cap tubes. The cultures were mixed thoroughly and snap frozen in liquid nitrogen and stored at -80 °C freezer for long-term storage.

3.3.2 Plasmid DNA isolation by alkaline lysis method

Plasmid DNA was isolated using an alkali lysis method as mentioned in Sambrook et al. (1989). Overnight grown recombinant *E. coli* (DH5 α strain) culture in LB medium

(**Appendix Table 1**) supplemented with appropriate antibiotics was pellet down at 5000 rpm, 10 minutes (min) at room temperature (RT). The supernatant was discarded and the pellet was re-suspended in 100 µl of solution I (**Appendix Table 4**) and vortex to lyse the cells. After lysis, 200 µl of solution II (**Appendix Table 4**) was added and mixed with gentle swirling and was incubated at RT for 5 min with subsequent mixing after every 2 min. To it, 150 µl of Solution III (**Appendix Table 4**) was added and mixed gently until the clear solution was formed followed by centrifugation at 13,000 rpm for 10 min. The supernatant was collected then equal volume of phenol: chloroform: isoamyl alcohol (PCI) was added in the ratio 25:24:1 (volume/volume/volume; v/v/v) and mixed by vortexing followed by centrifugation at 12,000 rpm for 5 min. The upper aqueous layer was collected and 800 µl of isopropanol was added to it and incubated at -20 °C for 30 min. The mixture was centrifuged at 13,000 rpm at RT for 15 min and supernatant was discarded. The pellet was washed at 13,000 rpm for 5 min at RT. The pellet was air dried and suspended in 25 µl of sterile H₂O.

3.3.3 *E. coli* competent cells preparation by calcium chloride method

E. coli strain DH5α was cultured in Luria Broth (LB) media (**Appendix Table 1**) containing kanamycin (10 mg/ml). For the preparation of competent cells, a single colony of *E. coli* was streaked out on an LB- plate and grown overnight at 37 °C. Next day a single colony was inoculated into a 10 ml of SOC in 50 ml Falcon tube and incubated at 37 °C for 250 rpm as starter culture. 1 ml of this starter culture was used to inoculate 100 ml LB medium in a 500 ml culture flask and again incubated at 37 °C for 250 rpm till mid log phase i.e. O.D. A₆₀₀= 0.4-0.6 was observed. Growth was arrested by chilling the cells on ice for 10-15 min before pelleting down at 5000 rpm at 4 °C for 10 min. The supernatant was carefully poured out without disturbing the pellet. The pellet in each tube was gently suspended in half of the volumes (of initial culture) of ice

cold 100 mM CaCl₂ and incubated on ice for 30 min. The cells were collected by centrifugation as above and suspended in 1 volume of ice cold 100 mM CaCl₂ by gently swirling of tubes. Finally, 100µl of this suspension was aliquoted into the pre-chilled microcentrifuge tubes containing 40% glycerol and stored at -80 °C till future use (Sambrook and Russell, 2001).

3.3.4 Transformation of *E. coli* cells by heat shock method

Heat shock method (Mandel and Higa, 1970; Cosloy and Oishi, 1973) was employed for performing transformation throughout out this study. All the steps of transformation were carried out in laminar hood under sterile conditions. For *E. coli* transformations, approximately 100 ng of plasmid DNA was mixed with 100 µl competent cells and incubated in ice for 30 min. The tube was then transferred to 42 °C water bath for 90 seconds (sec) to give heat shock, and quickly chilled on ice for 5 min. To the sample tube, 900 µl of LB medium was added under sterile conditions and incubated at 37 °C at 120 rpm for 1 h for the cell recovery. The cells were then pelleted at 6000 rpm at room temperature (RT), approximately 900 µl of the supernatant was discarded and the pellet was suspended in the remaining 100 µl of supernatant. It was spread onto LA medium plates, containing the appropriate concentration of antibiotics. Plates were incubated at 37 °C overnight for the transformed cells to grow. A transformation control was maintained in which no DNA was added, to check for contamination (if any).

3.3.5 *Agrobacterium tumefaciens* competent cells preparation

The vector constructs used in this study were cloned into different binary-based plant transformation vectors and were mobilized into competent *Agrobacterium tumefaciens* strain GV3101 prepared by the standard CaCl₂ method. A single colony of GV3101 was inoculated in 5.0 ml of liquid YEP medium with rifampicin (1 µl/ml, 25 mg/ml stock) and

gentamycin (1 µl/ml, 15 mg/ml stock) and was incubated at 28 °C for 24 h at 250 rpm as a starter culture. 1.0 ml of the starter culture was inoculated into 100 ml of fresh YEP media containing rifampicin, gentamycin (1:100 w/w) concentration and incubated at 28 °C in a shaker at 250 rpm for 4-6 h till the OD₆₀₀ reached to 0.5 to 1.0. The *Agrobacterium* culture was chilled on ice for 30 min and centrifuged at 5000 rpm for 10 min at 4 °C. Supernatant was discarded and pellet was rinsed with 1 ml of ice cold 20 mM CaCl₂. The *Agrobacterium* cells were then centrifuged at 5000 rpm for 10 min at 4 °C to remove antibiotics. Again supernatant was discarded and cell pellet was dissolved in 2 ml of ice cold 20 mM CaCl₂. To this 500 µl 60% glycerol stock was added. The cells were dispensed into 100 µl aliquots into fresh pre-chilled 1.5 ml microcentrifuge tubes and snap frozen in liquid nitrogen. The tubes were then stored at -80 °C until further use.

3.3.6 Maintaining bacterial strains/clones for long term storage

The bacterial strains/clones were incubated in the respective media with appropriate antibiotic selection (if any) and grown to mid log phase. In the cryo-vials 1 ml of culture was mixed with 1 ml of 60% glycerol to get the final concentration of 30% (v/v) and kept at -80 °C.

3.3.7 Identification and confirmation of *M. incognita* culture

The *M. incognita* females were confirmed by studying the perineal pattern (Eisenback et al. 1980). The females were isolated from the roots of infected tomato plants and incision at the posterior part was made under the microscope. The cut part was placed in 45% lactic acid and mounted onto the slide. The perineal pattern was observed under the microscope 10x objectives (**Figure 3.1a**). The further identification of these females as *M. incognita* was examined by carrying out a polymerase chain reaction (PCR) of DNA isolated from these females using RBC kit (detail protocol is described in section

3.3.10). The PCR was performed using the species-specific primers (Table 3.2) (Dong et al. 2001). The amplified product of desired length (1350 bp) as reported confirmed the worms as *M. incognita* (Figure 3.1b). These females were used for maintaining the nematode pure culture.

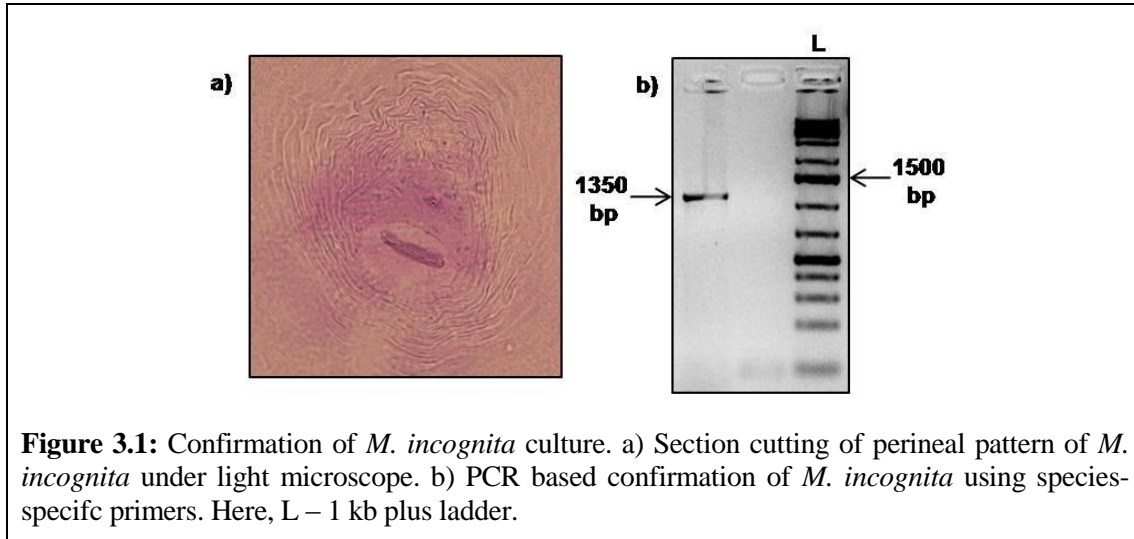


Table 3.2: List of primers used in this research.

Primer	Sequences (5'-3')
Mi ss-F	TAGGCAGTAGGTTGTCGGG _a
Mi ss-R	CAGATATCTCTGCATTGGTGC _a
Mi-G1-F	CGTTGTCTCTTTGATGGTTTCG
Mi-G1-R	TTAAAGGCATATTTGAAGAAGCAC
dp-10 F	GATGGTGAAGAAGAAAGATATAACC
dp-10 R	CATAAATAGAACTCCCTCCACCT
dp36-31 F	GAATTTGACAGCCGAGGAAATG
dp36-31 R	AACCTACATTTCGAATTCACC
Mi 18S QRT F 1	GGTCATGGTGGAAAGTATG
Mi 18S QRT R 1	CCCCAGTGTAATGTCCTTTG
Mi-actin_F	GCTTTGCTATGTTGCTTTGG
Mi-actin_R	TGTAAGAAGTCTCGTGAATACC
qGlp2_F	CGTTGTCTCTTTGATGGTTTCG
qGlp2_R	CTGATCGCATTGCCCATTTG
qD10_F	GCTTATCAATTTGTTGCTGGTATTC
qD10_R	TGTTGTTTGTGTTCTACTATGC

Primer	Sequences (5'-3')
qD31_F	TGTTGATGGGTGTGCTTCT
qD31_R	CGTGTGCAATAACGCCTAATC
g1 sense –F	TCTGCAGGATCCGATGGTGGCGAATGTTCAAC
g1 sense –R	TCTGCACTCGAGCCTTCCTCATCGACAGAAAGTG
g1 antisense –F	TCTGCAGAGCTCGATGGTGGCGAATGTTCAAC
g1 antisense – R	TCTGCAGGTACCCCTTCCTCATCGACAGAAAGTG
attB1_adapter	GGGACAAGTTTGTACAAAAAAGCAGGCT
attB2_adapter	GGGACCACTTTGTACAAGAAAGCTGGGT
12attB1-DP31n_F	AAAGCAGGCTTCAGGAAAGACGATGAGCCTAAAG
12attB2-DP31n_R	AGAAAGCTGGGTTATCGTAGGGAAGTCCAGAATT
NPTII F	GCAATTACCTTATCCGCAACTTC
NPTII R	CTCGTCCTGCAGTTCATTCA
CaMV F	CAACAAGTCAGCAAACAGACAG
CaMV R	TGCATGGCCTTAGATTTCAGTAG
Pdk-F	AACAAAGCGCAAGATCTATCA
atR2-F	TCATAGTGACTGGATATGTTGTGT
G78/260rB-F	CGGGAAAAGTTCTTCTGGTTGT
G78/260rB-R	AAATGCCCTCGACTAGCTGA

a: sequence as reported in Dong et al. 2001

3.3.8 Maintenance of nematode pure culture and inoculum preparation

Solanum lycopersicum cv Pusa Ruby (Tomato) seeds were sterilized by soaking in sterile distilled H₂O for 20 min followed by treating with 70% ethanol for 5 min. Seeds were then soaked in 5% NaOCl and 0.1% Tween 20 for 15 min and subsequently washed four times in sterile distilled H₂O. Sterilized seeds were then germinated on a cocopeat, vermiculite and sand (1:1:1) mixture in glass house at National Phytotron Facility, Indian Agricultural Research Institute (IARI) (**Figure 3.2a**). Two-week-old tomato seedlings were infected with a pure culture of *M. incognita* (pre-parasitic J2s) confirmed (section 3.3.8) and maintained in our lab (Kumar et al. 2017). After 35 days of infection tomato plants were uprooted and roots were washed with double distilled H₂O until absolutely clean (**Figure 3.2b**). Adult females and egg masses of *M.*

incognita were hand-picked from the galled roots of these infested plants under dissecting microscope. The egg masses kept in a cavity block were placed in the shaker and maintained until hatching at 28 °C in Petri plates containing 10-15 ml of sterile H₂O to collect second stage juveniles (J2s) of *M. incognita*. The freshly hatched J2s were collected in a beaker in suspension and were counted and calibrated per ml. An average of 3 aliquots was taken and used for further inoculums. These J2s were then used for expression studies and subsequent inoculation assays using transgenic *Arabidopsis* lines. Females hand-picked were immersed in 100 µl Trizol reagent (Invitrogene, USA) and snap frozen in liquid nitrogen for further studies.

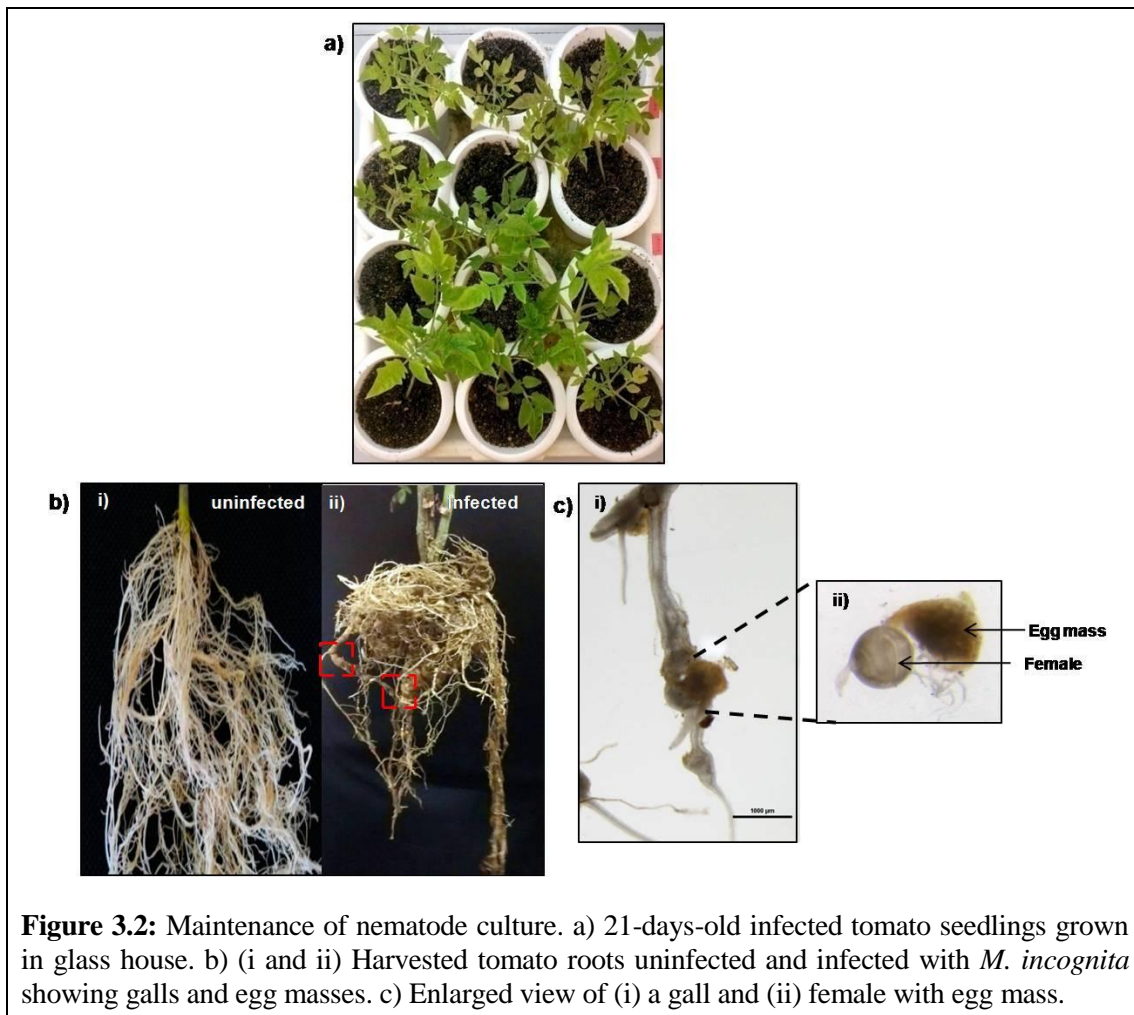


Figure 3.2: Maintenance of nematode culture. a) 21-days-old infected tomato seedlings grown in glass house. b) (i and ii) Harvested tomato roots uninfected and infected with *M. incognita* showing galls and egg masses. c) Enlarged view of (i) a gall and (ii) female with egg mass.

3.3.9 Identification of development-specific genes in *M. incognita* genome

3.3.9.1 Computational analyses for genes identification

The *M. incognita* genome database was downloaded from http://www6.inra.fr/Meloidogyne_incognita (Abad et al. 2008). Local nucleotide and protein *M. incognita* database was created in a bioedit local BLAST search for identifying the *glp-1*, *dpy-10* and *dpy-31* genes in *M. incognita*. The *C. elegans glp-1*, *dpy-10* and *dpy-31* sequences (retrieved from NCBI) were used as a query as it is a representative of nematodes. A tblastn search was conducted using the *Ce-glp-1* (CAA79620.1), *Ce-dpy-10* (T14B4.7) and *Ce-dpy-31*(R151.5) genes as a query against these databases using default parameters. An e-value and cut off (default parameters) was the selection criterion and hits with lower e-value were discarded. All sequences that met the requirements were analyzed for gene prediction using GeneMark and FGENSEH analysis, followed by removal of those genes that did not contain the known conserved domains and motifs using the Pfam database (<http://pfam.janelia.org/>) (Finn et al. 2016). Based on this search a contig (Minc15911) was found as probable *dpy-10* and two contigs namely, Minc01936 and Minc03986 as probable *Mi-dpy-31* were obtained. In case of *glp-1* gene, MiV1ctg1087 (Minc16055) a single contig obtained with the maximum possible score was selected as the probable *Mi-glp-1* for further experiments. The sequences were retrieved from the *M. incognita* genome database and their detailed study was carried out.

For gene conservation, we tried to identify *glp-1*, *dpy-10* and *dpy-31* gene in other PPNs especially in *Meloidogyne* genus. For this all the available ESTs, transcriptome and genome databases of PPNs were retrieved from various sites. Along with *M. incognita* (Minc16055), we were able to identify *glp-1* orthologs in four other *Meloidogyne* species (spp.) viz. *M. hapla* (Mh10g200708_Contig1018), *M. floridensis* (nMf_1_1_scaf00321), *M. javanica* (MJ01378, MJ05005), *M. Chitwoodi* (MC01544, MC00257), and

in *Globodera pallida* (GPLIN_000999900.1), a cyst nematode, using their genome, transcriptome and/or EST databases. The derived sequences were downloaded from their genome assembly or transcriptomic databases or EST (Expressed sequence tags) clusters available at either NCBI, NEMBASE4 (www.nematode.org) and/or nematode.net V4.0 (Opperman et al. 2008; Elsworth et al. 2011; Cotton et al. 2014; Lunt et al. 2014; Martin et al. 2014). Similarly, probable *dpy-10* and *dpy-31* genes were identified in Meloidogyne spp. and other plant-parasitic nematodes. We able to identify *dpy-31* in *M. hapla* (MhA1_Contig704.frz3.gene1) and *M. floridensis* (nMf.1.1.scaf07709-augustus-gene-0.3) and sequences were retrieved. Interestingly, the analysis did not reveal *dpy-10* orthologs in other Meloidogyne spp(s).

3.3.9.2 Prediction of gene and respective protein structure

A gene prediction algorithm GeneMark and FGENSH were employed separately for prediction of these genes structure. Gene architecture for *dpy-10*, *dpy-31* and *glp-1* was designed using the online Gene Structure Display Server 2.0 (<http://gsds.cbi.pku.edu.cn/>) (Hu et al. 2015) with the help of coding sequences and corresponding genomic sequences, which depict the exon/intron arrangement, gene length, and upstream/downstream region.

Protein sequences were analyzed with Pfam (<http://pfam.sanger.ac.uk/>) and SMART (<http://smart.emblheidelberg.de/>) databases to confirm the presence of conserved motifs. SignalP3.0 and TMHMM server v. 2.0 were employed to predict the presence of signal peptide sequence and the transmembrane domain, respectively. Two other software programs (Kd and Protscale) based on different algorithms were also used for

determining the presence of transmembrane domains to further authenticate the results (Kyte and Doolittle, 1982; Gasteiger et al. 2005).

3.3.9.3 Identification of conserved motifs

The motif-based sequence analysis tool MEME 4.11.2 (<http://meme.sdsc.edu/meme/meme.html>) (Bailey et al. 2015) was used to identify conserved motifs in the *glp-1*, *dpy-10* and *dpy-31* genes of *M. incognita* with the following parameters: optimum width, 10–300 amino acids, and the maximum number of motifs set to 10. NCBI conserved domain database was used for identifying other conserved domains within the *Mi-glp-1*, *Mi-dpy-10* and *Mi-dpy-31* genes. The Isoelectric Point (pI), molecular weight and grand average of hydropathy (GRAVY) of the amino acid sequences were predicted by Sequence Manipulation Suite (SMS) V2 available at gene infinity web server (<http://www.genefinity.org/index.html?dp=5>). The subcellular localization of GLP-1, DPY-10 and DPY-31 proteins was predicted using WoLFPSORT a protein Subcellular Localization Prediction Tool available at <http://www.genscript.com/wolf-psort.html>.

3.3.9.4 Multiple-sequence alignment and phylogenetic analyses

The identified GLP-1, DPY-10 and DPY-31 amino acid sequences in *M. incognita* were aligned in MUSCLE with their orthologs identified and reported in other nematodes across the phylum using the default parameters (Edgar, 2004). The unrooted phylogenetic tree was constructed by the Neighbor-Joining (NJ) method using MEGA 7.0 software (<http://www.megasoftware.net/>), with Poisson correction, pairwise deletion and bootstrap value set to 2000 replicates for analyzing the clustering pattern as parameters (Kumar et al. 2016). For GLP-1 protein, phylogenetic tree was constructed using orthologs identified in *M. hapla*, *M. floridensis*, *M. javanica*, *M. chitwoodi*, and

G. pallida, along with the reported GLP-1 sequences in free-living nematode species, viz. *C. elegans*, *C. briggsae*, *C. japonica* and *C. remanei*, and the Notch-like protein of *Priapulid caudatus*, a marine worm (retrieved from NCBI).

In case of DPY-10 and DPY-31 genes, following are the nematodes used for constructing phylogenetic tree viz. *C. elegans*, *C. briggsae*, *C. japonica*, *C. brenneri* and *C. remanei* (retrieved from NCBI), *M. hapla*, *M. floridensis* (retrieved from our tBLASTn analysis), *Brugiya malayi*, *Pristionchus pacificus* and *Onchocerca volvulus* (retrieved from Wormbase).

3.3.10 Genomic DNA isolation from adult *M. incognita* females

About 30 females, handpicked from infected tomato plants, were immersed in M9 buffer (100 µl) (**Appendix Table 5**) in 1.5 ml micro centrifuge tube and were snap-frozen in liquid nitrogen. These females were used for isolating genomic DNA using QIAGEN DNeasy Blood tissue kit (QIAGEN, USA) according to manufacturer's instructions. Frozen females were homogenized in 180 µl buffer ATL. For complete lyses 20 µl of proteinase K was added to it and incubated at 56 °C for 10 min with vortexing every 2 min. Then 200 µl of buffer AL was added to the sample and again incubated at 56 °C for 10 min. This mixture was pipetted onto Mini spin column in a 2 ml collection tube and centrifuged at 8000 rpm for 1 min. Flow-through was discarded and column was washed using 500 µl buffer AW1 by centrifuging at 8000 rpm for 1 min. Second wash was done by adding 500 µl buffer AW2 and centrifuging at maximum speed, i.e. 14,000 rpm for 3 min. After discarding the flow-through, column was dried spin by centrifuging for 2 min at maximum speed. For the elution of nucleic acid, spin column was transferred onto a new 1.5 ml micro centrifuge tube, and 25 µl

buffer AE was added. It was incubated at RT for 2 min and centrifuged for 1 min at 8000 rpm. This step was repeated for better elution of genomic DNA.

3.3.11 Genomic DNA quantification

3.3.11.1 DNA quantification using nanodrop

Before proceeding with any molecular work involving the extracted DNA, both its quality and quantity was checked. For DNA quantification, NanoDrop 2000C (Thermo Scientific, USA), a full spectrum spectrophotometer was used. Absorption at 260 and 280 nm of DNA samples were recorded against Buffer AE or DEPC treated H₂O as blank and quantity was calculated.

3.3.11.2 DNA quantification using agrose gel electrophoresis

Agrose gel electrophoresis separates DNA fragments according to their size. For preparation of 0.8% agrose gel, 0.8 g agrose was added to 100 ml 1x TAE buffer (**Appendix Table 6**) and boiled in microwave oven till complete dissolution. After cooling the solution to about 60 °C 0.5 µl of 10 mg/ml stock of ethidium bromide (EtBr) buffer was added and was mixed. The gel was poured slowly from a corner in casting tray with combs already fitted into it. It was left for solidification for approximately 45 min. 1 µl of isolated genomic DNA mixed with 1µl of 6X loading dye (Bromophenol blue and xylene cyanol) was prepared and loaded onto the gel immersed in 1X TAE buffer. Electrophoresis was carried out under electric current (60-80 V) till blue dye reached the end.

3.3.12 Polymerase chain reaction (PCR)

Integrity of selected three genes was confirmed by polymerase chain reaction using gene-specific primers (**Table 3.2**). The gene-specific primers were designed using Primer Express (v3.0) software (Applied Biosystems, Foster city, CA) from the respective

nucleotide sequences retrieved from the *M. incognita* database available at http://www6.inra.fr/Meloidogyne_incognita. Primers designed had GC content 40-60%, T_m 50-60 °C and primer length of 20-25 nucleotides. For the PCR reaction, 50 ng of isolated DNA was used as template in a 10 µl reaction volume performed in 200 µl PCR tube. Following was the PCR reaction mix, 1x buffer (with 1.5mM MgCl₂), 0.3 µM dNTP mix, 0.6 µM gene-specific forward and reverse primers and 0.5 U *Taq* DNA polymerase (GeNei™, India) mixed in nuclease free H₂O (to make up the 10 µl final volume). The reaction mixture was kept in a thermal cycler (G-STORM) and subjected to the following thermal conditions; initial denaturation of 95 °C for 2 min, 35 cycles of a three-temperature PCR cycle of (94 °C; 30 sec (final denaturation): 58 °C 45 sec, as annealing and 72 °C 1 min), followed by 72 °C for 10 min as final extension. 5 µl of amplified PCR product was mixed with 2 µl of 6X loading dye and electrophoresed on 1% TAE/EtBr agarose gel for size confirmation.

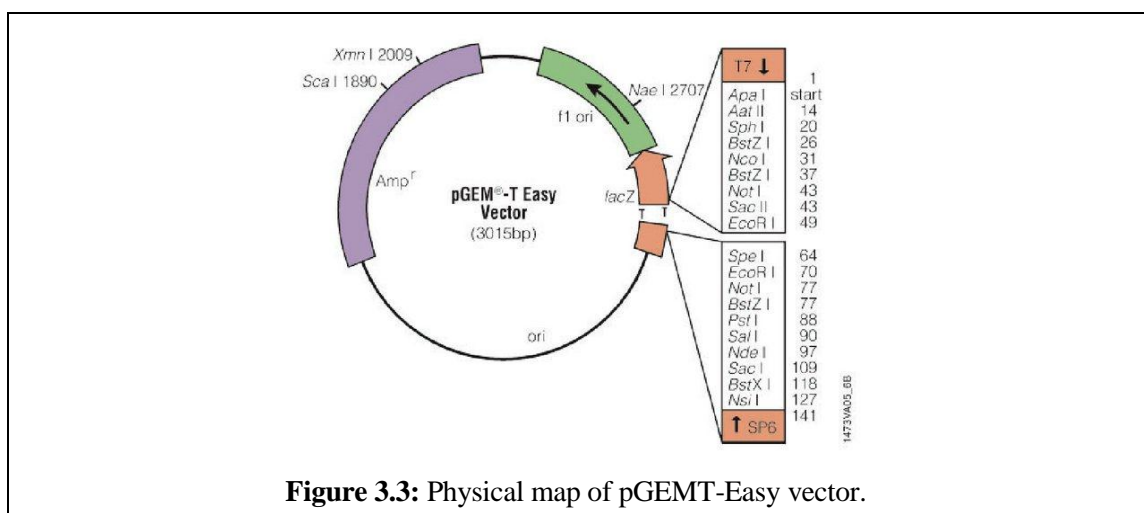
3.3.13 Elution of DNA from agarose gel

The PCR amplified products (for *glp-1*, *dpy-10* and *dpy-31* genes) were fractionated on 1% agarose gel. The gel slices containing the respective desirable bands were cut by using sterile blade and each collected in separate 1.5 ml sterile microcentrifuge tubes and their weight was recorded. DNA elution was carried out according to manufactures instructions (Qiagen, Germany). Three volumes of buffer QG was added to 1 volume of gel (for one volume of gel, 100 mg or approximately 100 µl) and incubated at 50 °C for 10 min with subsequent mixing the tubes at every 2–3 min using vortex during the incubation time till the gel slice was dissolved completely. 1 gel volume of isopropanol was added to the solution and mixed by inverting the tube 6-8 times. This solution was added to the column kept on 2 ml collection tube, and centrifuged at 13,000 rpm for 1 min. The flow-through was discarded and 500 µl of Buffer QG was added to the spin column and centrifuged for 1 min. The flow-through was discarded and the column was

placed back in the same collection tube. To wash the column, 750 μ l of Buffer PE was added to the column and centrifuged for 1 min. The flow-through was discarded and the column was again centrifuged for an additional 2 min at 13,000 rpm to remove the residual ethanol. The column was placed into a clean 1.5 ml microcentrifuge tube and 20 μ l of pre-warmed buffer EB (elution buffer) was loaded directly on the membrane. The column was incubated for 5 min at RT, and then centrifuged at 13,000 rpm for 2 min. The eluted amplicon obtained as flow through was stored in -20 $^{\circ}$ C till further use.

3.3.14 Ligation into pGEMT-Easy vector

To facilitate cloning in pGEMT-Easy vector which is a suitable TA-cloning vector, addition of Adenine (A) residues to the insert was essential. Since PCR products were obtained by *Taq* polymerase, terminal A nucleotides were added at the end of the each amplicon separately. All the three genes were partially cloned in pGEMT-Easy vector. For cloning of PCR amplified DNA in T/A cloning vector (pGEMT-Easy) (**Figure 3.3**), ligation reaction containing 50 ng vector DNA, 3-fold molar excess of insert DNA, 2X ligation buffer and 3U T4 DNA ligase was prepared in a final volume of 20 μ l and mixed by quick spin. The reaction was incubated at 4 $^{\circ}$ C for overnight.



3.3.14.1 Transformation

For *E. coli* transformations, ligated product of the three genes was mixed separately with 100 μ l *E. coli* competent cells, prepared as aforementioned, in the laminar air flow cabinet and transformation was carried out using heat shock method (see section 3.3.4). The *E. coli* cells were spread onto LA medium plates, containing the ampicillin (1 μ l/ml, 100 mg/ml stock), X-gal (5 μ l/ml, 20 mg/ml stock) and IPTG (0.5 μ l/ml, 100 mM stock). Plates were incubated at 37 °C overnight for the blue-white colonies. White transformed colonies were tested for the confirmation of ligated product by colony PCR.

3.3.14.2 Conformation for presence of insert by colony PCR

The colony PCR was performed by using insert specific primers for these three genes. Individual white colonies were picked with the help of toothpick from the overnight grown plates and mixed in 7.3 μ l dH₂O. The colonies were initially denatured to 95 °C for 10 min before setting up the colony PCR. To the denatured colonies 1x buffer, dNTP mix(100 μ M), primers (0.3 μ M each) and 0.5 U *Taq* polymerase (GeNei™, India) was added and reaction was set up. The final PCR cycle is as follows; initial denaturation of 95 °C for 2 min, 35 cycles of a three-temperature PCR cycle of (94 °C; 30 sec (final denaturation): 60 °C 45 sec, as annealing and 72 °C 1 min), followed by 72 °C for 10 min as final extension and the PCR product was checked on 0.8% agrose gel. Plasmid of the positive clones was isolated using alkaline lysis method and further confirmed by Sanger sequencing outsourced by company.

3.3.15 Nematode sample collection and preparation

Egg masses hand-picked from infected tomato roots were washed with distilled H₂O. 1 ml M9 buffer was added and vortexed for 30 sec. It was centrifuged for 3 min at 5000

rpm. The supernatant was discarded and pelleted eggs were again washed with dH₂O. For the maceration of egg masses, 1 ml of (0.1%) sodium hypochloride was added and vortexed for 30 sec, followed by centrifugation at 5000 rpm for 3 min. Supernatant was discarded and subsequently washed with dH₂O thrice. The eggs were stored in 100 µl of Trizol reagent (Invitrogen) and snap-frozen in liquid nitrogen. The vials were stored at -80 °C till further use.

3.3.16 Isolation of total RNA from different stages of *M. incognita*

Frozen egg masses, J2s and females were crushed in liquid nitrogen with a micro pestle without letting it thaw. Total RNA from these samples was isolated using a Pure Link RNA Mini Kit (Ambion, USA) according to the manufacturer's instructions, followed by DNase treatment using the Qiagen DNase enzyme. 10 µl of β-mercaptoethanol was added to 1 ml of lysis buffer. For the complete lysis of the samples, 300 µl of this lysis buffer mix was added into each sample. Equal volume of 70% ethanol was added and entire solution was passed onto the column. It was centrifuged at 12,000 rpm for 30 sec at RT and flow-through was discarded. To the column 300 µl of wash buffer I added and centrifuged for 30 sec at 12000 rpm. Samples were then preceded with on-column DNase treatment. For this, 70 µl of buffer and 10 µl of DNase I enzyme (Qiagen, USA) was added on to the column followed by incubation at 37 °C for 30 min. To it 300 µl buffer I was added and centrifuged at 12,000 rpm for 30 sec. Flow-through was again discarded and 300 µl wash buffer was added. It was centrifuged for 30 sec at 12,000 rpm and flow-through was discarded. The column was air dried by spinning it for 2 min at maximum speed. Total RNA was eluted by adding 30 µl DEPC-treated H₂O (prewarmed) and centrifuging at 12,000 rpm for 1 min. Total RNA was stored in -80 °C refrigerator till further use.

3.3.16.1 RNA quantification

1 µl of RNA was diluted 500 times by adding 1 ml DEPC-treated H₂O. Absorption at 260 and 280 nm of diluted RNA samples were recorded against DEPC treated H₂O as blank using spectrometer and RNA quantity was calculated using following formula-

Concentration of RNA (microgram/ml) or (µg/ml) = 40 X Absorbance of the sample at 260 nm

Purity of RNA was checked by determining the Absorbance at 230, 260 and 280 nm wavelength. The RNA was considered as pure if the ratio of Absorbance (260/280) ranged between 1.8-2.0 and Absorbance (260-230) was > 2.0.

3.3.16.2 Denaturing formamide agarose (FA) gel electrophoresis for RNA

Denaturing agarose gel electrophoresis was used to check the size and integrity of RNA preparations. Total RNA was run in 1.2% formamide agarose (FA) gel. For preparation of gel 1.2 g agarose was added to 100 ml 1X MOPS (**Appendix Table 7**) buffer and boiled in microwave oven till complete dissolution. Once temperature comes down to 60 °C 3 ml formaldehyde (37%) was added and contents were mixed by swirling. The gel was poured slowly from a corner in casting tray with combs already fitted into it. It was left for solidification for approximately 45 min. The RNA samples were prepared by mixing 2µl of total RNA with 2 µl of 2X RNA loading dye (Fermentas, Germany). The samples were heat denatured at 65 °C for 5 min and immediately chilled on ice and loaded on to the gel. Electrophoresis was carried out at 6 Volts/Cm² for 5 h in 1x MOPS.

3.3.17 Reverse transcription for cDNA preparation

5 µg of total RNA of each sample was reverse transcribed into cDNA. cDNA was synthesized using the SuperScript® III First-Strand Synthesis System (Invitrogen,

USA). Total RNA was mixed with 1 μ l each of oligo(dT)₂₀ (50 μ M) and 10 mM dNTP mix in a 10 μ l of total volume in a 200 μ l volume PCR tube. It was incubated at 65 °C for 5 min and immediately placed on ice for 1 min. To each sample following cDNA synthesis mix was added; 2 μ l 10x RT buffer, 4 μ l MgCl₂ (25mM), 2 μ l 0.1 M DTT, 1 μ l RNaseOUT (40 U/ μ l) and 1 μ l SuperScript III RT (200 U/ μ l). The solution was then incubated at 55 °C for 1 h, followed by 85 °C for 5 min. To stop the reaction 1 μ l of RNase H was added to each tube and incubated for 20 min at 37 °C before proceeding to other applications.

3.3.18 Quantitative real-time PCR (qRT-PCR) analyses

Quantitative real-time PCR was performed on *M. incognita* cDNA samples of egg masses, infective stage juveniles (J2s), and mature females and roots of infected plants harvested at different time points after inoculation for evaluating the expression levels at different development stages (J3 and J4). Third stage juveniles (J3s) and fourth stage juveniles (J4s) were analyzed from nematodes within the roots of infected plants harvested at 10 and 21 days post inoculation (dpi), respectively. After the 10th day post-inoculation, the second molt occurs, giving rise to J3s, and the third moulting to J4 occurs approximately 16 days post inoculation (Moens et al. 2009; Martinuz et al. 2013). SYBR-based chemistry was adopted to perform qRT-PCR in a StepOne Plus™ real-time PCR System. The primers of *M. incognita*-specific Actin and 18S rRNA genes were used as a reference (Nguyễn et al. 2014; Ye et al. 2015) (**Table 3.2**). Three biological and three technical replicates were used per sample. The thermal cycle was as follows: 95 °C for 3 min, 40 cycles of 95 °C for 3 sec, 60 °C for 30 sec. The

specificity of the reactions was verified by melting curve analysis. The data were analyzed using the $2^{-[\Delta\Delta C(T)]}$ method, and real-time data were reported as the means \pm standard error (SE) of three biological replicates per sample (Livak and Schmittgen, 2001).

3.3.19 Strategy for designing RNAi constructs that express dsRNA

3.3.19.1 Preparation of entry clones

Plasmids expressing dsRNA of *dpy-31* gene was constructed through gateway technology (**Figure 3.4**). Entry clone carrying selected regions of *dpy-31* gene was generated by performing a BP recombination reaction between pDONRTM221 vector and *attB*-PCR product of respective genes. Gene-specific primers were designed with *attB* sites *viz.* *attB1* site (GGGGACAAGTTTGTACAAAAAAGCAGGCT) and *attB2* site (GGGGACCACTTTGTACAAGAAAGCTGGGT) on the 5' end of each primer for cloning (**Figure 3.5; Table 3.2**).

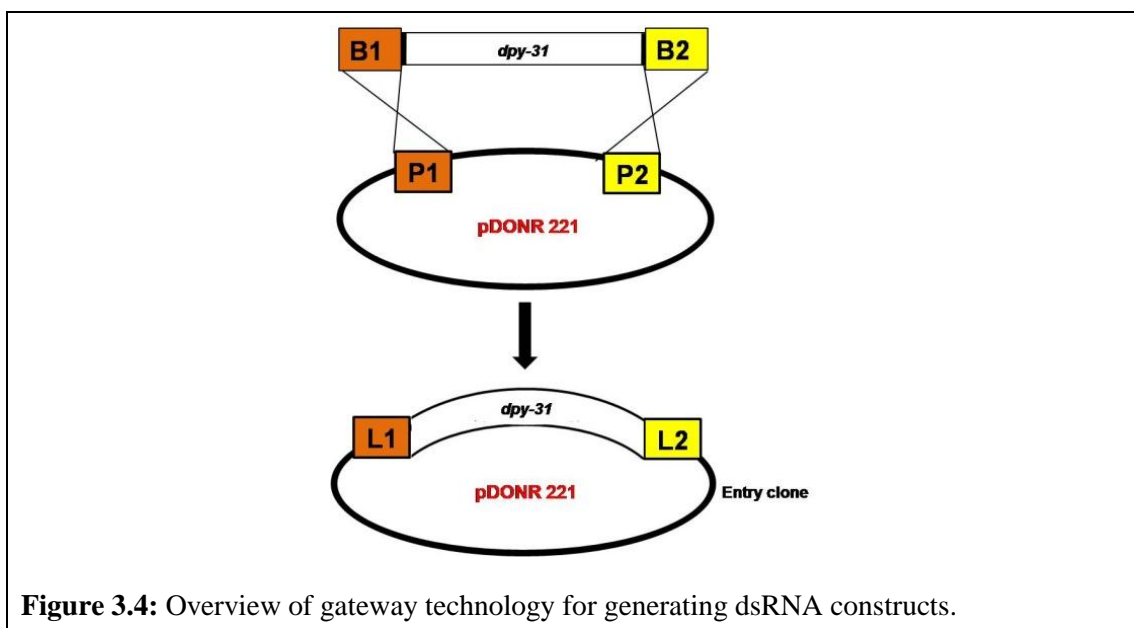
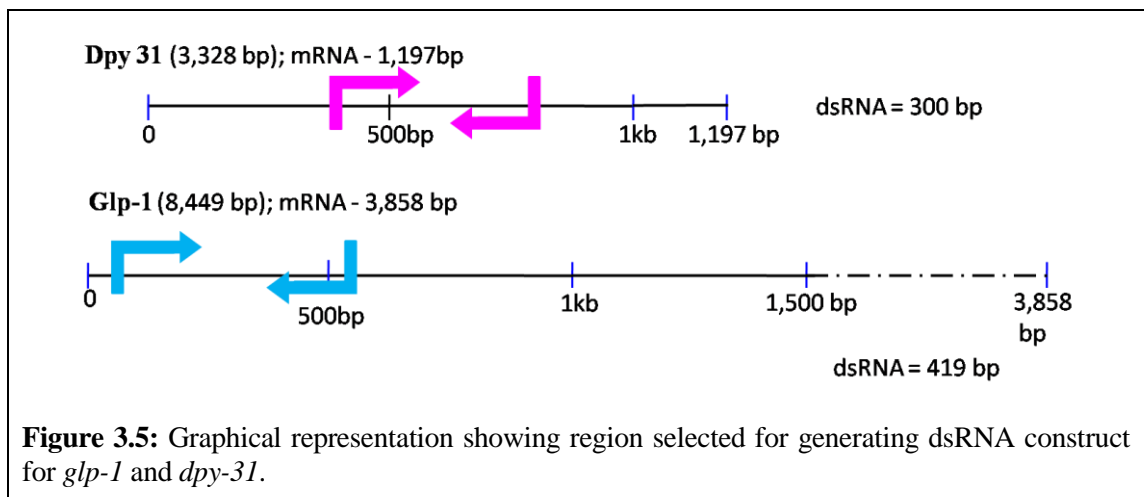


Figure 3.4: Overview of gateway technology for generating dsRNA constructs.

One of the advantage of using gateway cloning methodology was that only one single PCR product could be used for cloning both sense and antisense strands of the selected gene (for clear understanding refer **Figure 3.4**). *attB*-product was PCR amplified using reaction mixture as follows- 2 μ l 5x buffer, 0.2 μ M dNTP mix, 0.3 μ l DMSO, 0.4 μ M gene-specific forward and reverse primers and 0.5 U Phusion DNA polymerase (ThermoFisher Scientific, USA) mixed in nuclease free H₂O (to make up the final volume of 10 μ l). The mixture was subjected to following reaction cycle- initial denaturation of 95 °C for 2 min, 5 cycles of a three-temperature PCR cycle of (94 °C, 15 sec; 45 °C, 30 sec and 68 °C, 1 min), followed by 25 cycles of (94 °C, 15 sec; 52 °C, 30 sec and 68 °C, 1 min) and 68 °C, 10 min as final extension.

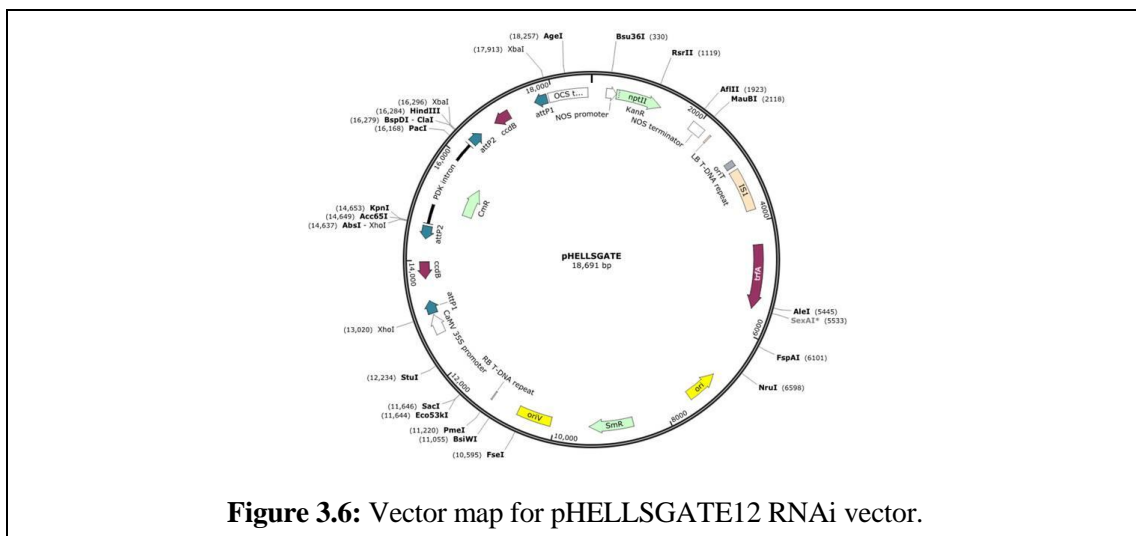


The *attB*-PCR product was then used for BP recombination reaction as follows- 50 ng *attB*-PCR product, 1 μ l pDONRTM 221 vector, 2 μ l BP clonase II enzyme and TE buffer to make up the final volume 8 μ l. The reaction was incubated at 25 °C for 1 h preceded by addition of 1 μ l Proteinase K solution incubating at 37 °C for 10 min. The amplified PCR product was eluted using QIAGEN gel elution kit for subsequent

cloning. The BP product was cloned into DH5 α *E. coli* competent cells and plated onto LA medium plates, containing the kanamycin antibiotic (50 mg/ml stock) (as in section 3.3.4). The positive colonies for entry clone were selected using colony PCR by M13F and M13R universal primers (sequences present in vector) (**Table 3.2**) and resultant amplicon was checked by running it on agrose gel.

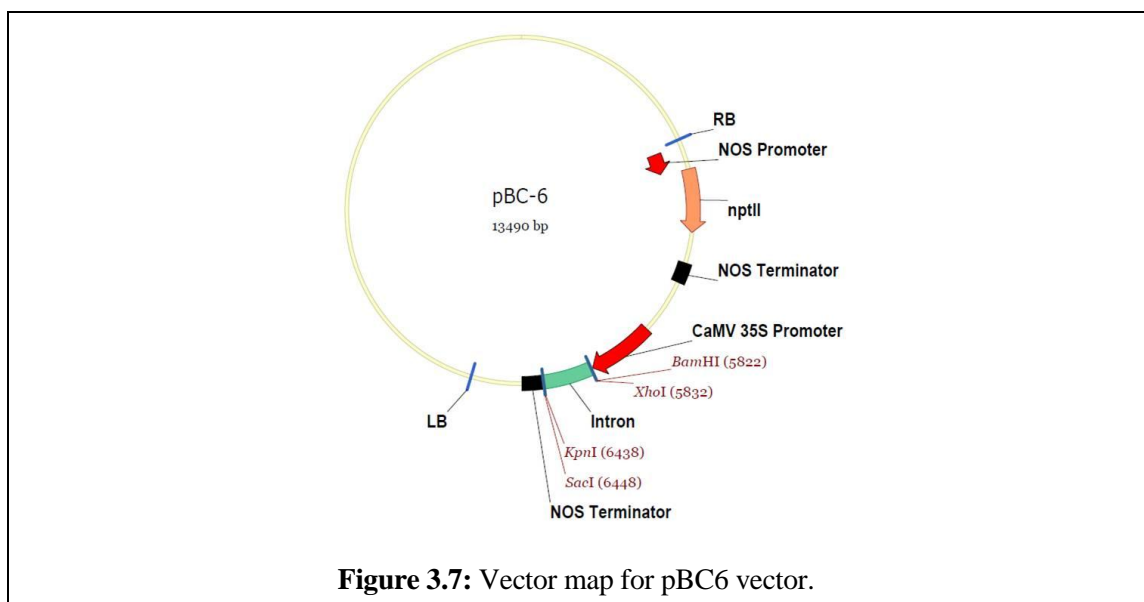
3.3.19.2 Preparation of destination clone using RNAi vector

The positive entry clone carrying selected regions of *dpy-31* gene was further cloned into pHELLSGATE12 RNAi vector (**Figure 3.6**). The LR recombination reaction was set as follows- 100 ng of entry clone, 1 μ l of pHELLSGATE12 (100 ng), TE buffer (pH 8.0) to make up the total volume 8 μ l and 2 μ l LR Clonase II enzyme. The reaction mix was incubated at 25 $^{\circ}$ C for 1 h. To it 1 μ l Proteinase K (2 μ g/ μ l stock) was added and incubated for 10 min at 37 $^{\circ}$ C. 2 μ l of LR reaction was transformed into *E. coli* and plated onto LA medium containing spectinomycin antibiotic (100 mg/ml stock) (as in section 3.3.4). The positive clones were selected by colony PCR using vector specific primers (**Table 3.2**).



3.3.19.3 Another strategy for designing RNAi constructs

For *glp-1* gene, conventional cloning strategy was employed for designing dsRNA construct. Another RNAi vector namely, pBC6 (Yadav et al. 2006) was used for generating dsRNA construct (**Figure 3.7**). Sense and anti-sense gene-specific primers were designed. The primers for sense strands had *Bam*HI restriction sequence on the 5' end of the forward primer and *Xho*I restriction site sequence on the reverse primer (**Figure 3.5**). Similar strategy was employed while designing primers for amplifying antisense strands; restriction sites for *Kpn*I and *Sac*I were added at the 5' end of the forward and reverse primer, respectively. *Glp-1* sense and antisense strands were amplified using PCR reaction. The amplified product was eluted in TE buffer (pH8.0).



pBC6 vector was digested using *Bam*HI, *Xho*I, *Kpn*I and *Sac*I restriction enzymes. In a 100 µl of ligation reaction, eluted *glp-1* sense and antisense strands were ligated with pBC6 vector, incubated at 4°C for overnight. The ligated product was successfully cloned into DH5α*E. coli* cells and cells plated on to LA medium containing kanamycin

antibiotic (50 mg/ml stock) selection (see section 3.3.4). The positive clones were selected using colony PCR by vector specific primers (**Table 3.2**).

3.3.19.4 Selection of positive clones by restriction digestion

The positive clones of RNAi vector carrying both the sense and antisense strand of *dpy-31* gene were selected by restriction digestion reaction. For the sense strand *XhoI* and for antisense strand *XbaI* restriction enzymes were used. For the *glp-1* gene, double restriction digestion using *BamHI*, *XhoI*, *KpnI* and *SacI* restriction enzymes were used. For sense strand, the pBC6 vector was double digested using restriction enzymes *BamHI* and *XhoI* and was ligated with sense strand. For the antisense strand, now the same pBC6 vector carrying sense strand of *glp-1* gene, and amplified *glp-1* product was again double digested using *KpnI* and *SacI* followed by ligation of these two. Following reaction was set up for the restriction- 1 µl 10x buffer, 1 µl plasmid DNA (300 ng), 0.4 µl each restriction enzyme (10U) and nuclease-free H₂O to make up the reaction volume to 10 µl. The mix was then incubated at 37 °C overnight in a thermal PCR machine. 2 µl of restricted product was electrophoresed on 0.6% agarose gel for observing restricted insert.

The selected positive clones were sent for Sanger sequencing for further confirming the cloning. The clones showing 100% similarity were selected for generating transgenic *Arabidopsis thaliana* plants.

3.3.20 Transformation of *Agrobacterium tumefaciens* cells

Frozen *Agrobacterium tumefaciens* competent cells were thawed on ice and 2 µl of 150 ng of recombinant plasmid DNA was added to the cells. These cells were incubated on ice for 5 min followed by snap frozen in liquid nitrogen for 5 min. The cells were

thawed immediately at 37 °C in water bath for 5 min. 1.0 ml of LA media was added to the cells and the tube was incubated at 28 °C for 4 h with gentle shaking for the cell recovery (200 rpm). This period allowed bacterial cells to express antibiotic resistance genes and to overcome the stress due to heat and cold shocks. The tube was centrifuged for 30 sec at 5000 rpm and supernatant was discarded. The cell pellet was re-suspended in 100 µl of fresh LA media and spread on LA containing rifampicin (1 µl/ml, 25 mg/ml stock), gentamycin (1 µl/ml, 15 mg/ml stock) and kanamycin (1 µl/ml, 50 mg/ml stock; in case of pBC6 vector) and spectinomycin (1 µl/ml, 100 mg/ml; in case of pHELLSGATE12 vector), for bacterial and plasmid selections. The plates were incubated at 28 °C for 48 h for the colonies to grow. Colony PCR was carried out for screening of colonies containing recombinant vectors.

3.3.21 Transformation of *Arabidopsis thaliana* plants

glp-1-dsRNA and *dpy-31*-dsRNA specific constructs mobilised into *Agrobacterium tumefaciens* strain GV3101 (by freeze thaw method) were used for developing *Arabidopsis* transgenics by floral-dip method.

3.3.21.1 Germination of *Arabidopsis* seeds

Seeds sterilization

Arabidopsis thaliana seeds (T_0) were thoroughly washed with sterile distilled H₂O; surface sterilized by washing for 1 min in 70% ethanol followed by washing with sterile distilled H₂O. After this, the seeds were treated with 0.1% SDS-HgCl₂ for 7 min followed by subsequent washing with sterile distilled H₂O until foam is disappeared (approximately 5 times). The surface sterilized seeds were then suspended in 0.1% agarose solution and incubated at 4 °C for 48 h for cold treatment to break the dormancy

of seeds. After two days seeds were evenly spread on MS medium on Petri plates. These plates were incubated in the culture room maintained at ± 22 °C at a photoperiod of 16 h light and 8 h of darkness for the germination of seedlings.

3.3.21.2 Planting of *Arabidopsis* seedlings in soil

Pots (4 cm diameter) were filled with soilrite, without compressing to give a uniform and soft bed, covered with aluminum foil and were autoclaved at 15 psi, 120 °C for 20 min. Each pot was arranged in a tray and saturated with Hoagland's solution (Himedia, India). Two-weeks-old seedlings grown on MS plates were gently picked and transplanted on saturated pot (3 seedlings per pot). Pots were then covered with saran wrap to maintain high humidity. The trays containing these pots were placed in growth chambers maintained at a temperature 20-23 °C and a photoperiod of 16 h light/8 h darkness at National Phytotron facility, IARI. A relative humidity of 60-75% was maintained. The soil was kept moist by regularly pouring Hoagland's solution in the tray. The plants formed rosettes and after 3-4 weeks inflorescence stalks appeared and soil was allowed to dry out periodically so as to control algal and fungal growth with regular supply of H₂O alternated with that of Hoagland's solution. The plants were harvested within 8 weeks of transferring into soilrite. In case of aphid infestation, 0.1% MetasystoxTM (Bayer, Germany) was sprayed.

3.3.21.3 Preparation of *Arabidopsis* plants for floral-dip transformation

For *in planta* transformation of *Arabidopsis*, floral-dip protocol (Clough and Bent, 1998) was followed. The plants were placed in pots at a density of 3 plants per pot. The first inflorescence shoots were cut as soon as they emerged so as to encourage growth of more shoots method called pruning. In a week, the plants were ready for transformation.

3.3.21.3.1 Preparation of *Agrobacterium tumefaciens* suspension

Three days prior to plant transformation, a 5 ml LA broth containing appropriate antibiotics was inoculated with *Agrobacterium tumefaciens* carrying the RNAi vector (pHELLSGATE12 and pBC6) and incubated at 28 °C with vigorous agitation. After 2 days, 1 ml of this culture was inoculated in 200 ml of LA containing the same antibiotics taken in a 1 l flask and incubated again at 28 °C with vigorous agitation (180 rpm) for 24 h. *Agrobacterium* was pelleted by centrifugation at 6000 rpm for 10 min and the cell pellet was re-suspended in 400 ml of 5% freshly prepared sucrose. Silwet L-77 (0.05%) was added to this suspension and it was mixed thoroughly for frothing.

3.3.21.3.2 Floral-dip

The *Agrobacterium tumefaciens* suspension was transferred to a 500 ml plastic beaker. Before immersing the plants into the suspension, soilrite was pressed tightly so that it doesn't fall into the suspension while inverting the pots. All the siliques and open flowers were cut with scissors and only unopened buds were left. Whole plants were dipped into the suspension by inverting the pots in the solution such that all the above ground parts were dipped in the suspension. The plants were left in that position for 1 min. The same suspension was used for approximately 6 pots. After treatment with *Agrobacterium*, the plants were kept in horizontal position in a tray and covered with the polythene to maintain high humid conditions for the next 24 h in dark. After 24 h, the leaves were washed with H₂O to remove excess *Agrobacterium* and the plants returned to their normal growing conditions kept in Phytotron facility, IARI. The seeds from these plants were collected in about 3-4 weeks.

3.3.21.3.3 Seeds harvesting, handling and preservation

For seed collection, the inflorescences were bagged into long inverted butter paper bags (**Figure 3.8**). The base of the bags was cut open and the mouth was fastened to the base of the plants. Seeds were harvested by cutting the entire inflorescence at its base after all the siliques matured and turned brown. The harvested plant material was allowed to dry in 37 °C for a few days in the bags before threshing. Seeds were sieved to separate them from chaff and cleaned by gentle blowing. The seeds were then further air dried for 1-3 weeks at RT to reduce the moisture content. Dried seeds were dispensed in micro centrifuge tubes and sealed tightly with PARAFILM™ and stored in desiccators at 4 °C.



Figure 3.8: *Arabidopsis* plants bagged with butter paper for collecting seeds.

3.3.21.4 Screening of transgenic RNAi lines

3.3.21.4.1 Screening of transgenic lines for kanamycin resistance

Harvested T₁ seeds were sterilised and germinated on MS media plate supplemented with kanamycin (1 µl/ml, 50mg/ml) (as in section 3.3.21.1). Wild type seeds were

germinated on MS media without any antibiotics. The ratio of kanamycin resistance and sensitivity for each mutant was calculated by counting number of kanamycin resistant and susceptible seedlings in each plate. In the presence of kanamycin, resistant plants grew normally while the sensitive plants become yellow by losing their chlorophyll and died within 10 days of germination. The green resistant plants were then shifted into pots filled with soilrite for seed harvesting.

3.3.21.4.2 Genomic DNA (gDNA) isolation from *Arabidopsis* transgenic plants

gDNA was isolated from fresh leaves harvested from T₁ transgenic as well as untransformed (wild type) *Arabidopsis* plants by cetyltrimethylammonium bromide (CTAB) method described by Doyle and Doyle (1990). The CTAB buffer was prepared freshly from the stocks (**Appendix Table 8**) as follows; 10 ml (100 mM) 1M Tris-Cl (pH 8.0), 4 ml (20 mM) 0.5 M sodium EDTA, 28ml (1.4 M) 5 M NaCl, 2 gm CTAB and autoclaved distilled H₂O to make up the volume to 100 ml. Approximately 1 gm of leaf tissues were frozen in liquid nitrogen and ground to fine powder in pre-chilled mortars and pestle. The powder was transferred to 2 ml of pre-warmed extraction buffer with 0.2% β-Mercaptoethanol freshly added in 2 ml micro centrifuge tubes. The tissue samples were mixed properly by vortexing and incubated at 65 °C for 1 h. The lysed tissues were cooled down to RT and equal volume of chloroform, isoamyl alcohol (CIA) (24:1 v/v) solution was added with gentle mixing by inverting the tubes. The tubes were centrifuged at 12,000 rpm for 20 min at RT. The aqueous phase was pipetted into fresh 2 ml micro centrifuged tubes and the CIA treatment was repeated followed by centrifugation. The supernatant was transferred into fresh tubes and mixed with equal volumes of isopropanol. The tubes were kept at -20 °C for 2 h to facilitate DNA precipitation followed by centrifugation at 12,000 rpm for 20 min. The DNA pellet was

washed with 2 ml of 70% ethanol, centrifuged for 10 min at 10,000 rpm and air-dried. The DNA was dissolved in 30 µl of 10 mM Tris-Cl buffer (pH 8.0). The gDNA was treated with 10 µl of RNase A (10 mg/ml) and incubated at 37 °C for 1 h to get rid of RNA contamination. The quality and quantity of isolated gDNA were checked by 0.8% agarose/EtBr gel electrophoresis and NanoDrop (Thermo Scientific, USA), respectively and before using for further molecular analysis.

3.3.21.4.3 Screening of putative transformants for the gene integration

The *Arabidopsis* transgenic (T₁) plants were primarily screened for the presence of T-DNA insert by PCR (Section 3.3.11) using gene-specific primers (*glp-1/dpy-31*) (**Table 3.2**). The presence of T-DNA was also confirmed in the T₂ plants using *NPT II* gene-specific region (**Table 3.2**) by PCR analysis. For the PCR screening, 50 ng of DNA from untransformed control and transgenics were used and mixed with following reagents- 100 nM of forward and reverse primers (*glp-1/dpy-31* and *npt-II* genes), 1X buffer, 2mM MgCl₂, 100 µM dNTP mix and 0.5 U *Taq* polymerase (GeNei™, India) in a 10 µl volume of reaction. The PCR products were analyzed on a 1% agarose gel and documented by Gel Doc (Syngene).

3.3.21.5 Detection of dsRNAs from transgenic plants-northern hybridization

3.3.21.5.1 Small RNA isolation

Low molecular weight (LMW) small RNA was isolated from the leaves of RNAi transgenic and wild-type (as control) plants according to the method described by Rosas-Cárdenas et al. (2011). 100 mg of frozen tissue was pulverized using liquid nitrogen and 500 µl each LiCl extraction buffer and acid phenol pH 8.0 was added. The composition of LiCl extraction buffer (**Appendix Table 9**) is as follows 100 mM Tris-

HCl (pH 9.0), 1% SDS, 100 mM LiCl and 10 mM EDTA. The solution was mixed for 1 min using vortex and incubated at 60 °C for 5 min followed by centrifugation at 14,000 rpm for 10 min at 4 °C. The upper phase was transferred to new 1.5 ml micro centrifuge tube and 600 µl of chloroform-isoamyl alcohol (24:1; v/v) was added. It was again centrifuged at 14,000 rpm for 10 min at 4 °C. Again the upper phase was transferred to a new 1.5 ml centrifuged tube and left for incubation at 65 °C for 15 min. To it 50 µl NaCl (5M) and 63 µl 40% polyethylene glycol 8000 (w/v) (**Appendix Table 9**) was added. The solution was mixed well and incubated on ice for 30 min. It was then centrifuged for 10 min at 14,000 rpm at 4°C. The supernatant containing LMW RNA was transferred to a new 1.5 ml micro centrifuge tube and 500 µl phenol-chloroform-isoamyl alcohol (25:24:1; v/v/v) was added. It was again centrifuged at 14,000 rpm for 10 min at 4 °C. To precipitated LMW RNA supernatant obtained was transferred into new tube and 50 µl sodium acetate pH 5.2 (3M) and 1200 µl ethanol was added and left for overnight incubation at -20 °C. The next day tube was centrifuged at maximum speed at 4 °C for 10 min. Supernatant was discarded and pellet was air-dried for 5 min. LMW RNA was re-suspended in 20 µl RNase-free H₂O. The enrichment and integrity of the small RNAs were checked by running on a 1.5% 1x MOPS agarose gel (section 3.3.14.2). The purity of LMW RNA was determined by measuring their absorbance at 230, 260 and 280 nm using a spectrophotometer NanoDrop, ND-1000 (NanoDrop Technologies) (section 3.3.14.1).

3.3.21.5.2 Preparation of denaturing polyacrylamide gel (dPAGE)

For preparing 15% PAGE 20 ml final volume of urea PAGE 7.5 ml of 40% acrylamide-bisacrylamide (29:1; v/v), 8.4 g urea (7 M), 1 ml 10xTBE, 11.4 ml of DEPC-treated H₂O

were added in a small beaker and mix well by shaking and the whole mixture was heated in oven for dissolving crystals. Then to it 10 μ l TEMED and 40 μ l 25% APS was added. Immediately gel was poured in the vertical setup and gel was left for polymerization for 1 h. Once polymerized comb was removed and a pre-run in 0.5x TBE for about 30 min at 90 V was carried. Leached urea was flushed from the wells just prior to loading sRNA samples.

3.3.21.5.3 Small RNA sample preparation

20 μ g of small RNA (sRNA) was resolved in 15% polyacrylamide/1X MOPS.LMW RNA samples were denatured in 2x RNA loading dye (Fermentas, Germany) comprised of 50% deionised formamide with bromophenol blue tracking dye at 65 °C for 5 min and placed back on ice immediately until they were loaded. Similar volume of H₂O and loading dye was also loaded in empty slots. Samples were run at a constant 90V for 3 h at RT until the blue loading dye reached near to the bottom of the gel. Once the small RNA was run far enough the gel rig was disassembled, it was stained with ethidium bromide solution for 5 min. After documenting the RNA gel in Gel Doc/UV transilluminator, the gel was de-stained in 1x MOPS buffer for 2 min.

3.3.21.5.4 Transferring of small RNA by electroblotting

Four 3MM Whatman filter papers and positively charged Hybond-N⁺ membrane nylon (Amersham) was cut according to the size of the gel. Electroblotting was carried out in Hoefer miniVE Blot Module (AA Hoefer, Inc.). The transfer stack was assembled as follows: a packing sponge (on the cathode side), a wet filter paper (cut in exactly of gel size), gel was carefully placed on the filter paper, a pre-wet positively charged nylon membrane; once placed glass rod used to remove air bubbles and above it wet filter

paper was placed. The stack was closed with two packing sponge and module was closed. To the module 350 ml 1x MOPS buffer was poured and placed carefully into the tank. Pre-chilled de-ionised H₂O used to fill the tank which served as heat sink during electrotransfer. The small RNA was transferred at a constant 20V/400mA for 45 min.

3.3.21.5.5 Crosslinking of small RNA

Small RNA was chemically cross-linked onto the nylon membrane (Rosas-Cárdenas et al. 2011). A 3MM sheet cut slightly larger than the nylon membrane was soaked in 1-Ethyl-3-(3-dimethylaminopropyl) carbodiimide (EDC) cross-linking reagent (**Appendix Table 9**). The elctroblotting unit was disassembled and the nylon membrane was placed on top of the EDC cross-linking reagent-saturated 3MM, with RNA side up i.e. the membrane surface onto which small RNA has been blotted should not be the side in direct contact with the 3MM sheet. EDC is quite unstable in H₂O and should be prepared immediately before use. This assembly was wrapped in Saran wrap and placed in incubator at 60 °C for 2 h. After cross-linking, membrane was washed with excess RNase-free H₂O and preceded to pre-hybridization and hybridization.

3.3.21.5.6 Pre-hybridization and probe preparation

PerfectHybTM Plus (Sigma) was used for pre-hybridization and was added at the rate of 0.2ml/sq cm in the hybridization bottles. The bottles were then incubated at 42 °C for 2 h in the hybridization oven.

Block-ItTM RNAi designer (<https://rnaidesigner.thermofisher.com/rnaiexpress>), siRNA wizard (<http://www.invivogen.com/sirnazizard/>) and siDesign center (<http://dharmacon.gelifesciences.com/design-center/>) tools were used to identify the regions suited for

siRNA target design. Primers for probe preparation were designed from the region marked most suitable for siRNA targeting (**Table 3.2**). To generate specific DNA probes, ^{32}P - α -dCTP labeling was performed with a mega prime DNA labeling kit (GE Healthcare Amersham) using gene-specific antisense fragments (**Table 3.2**). The labeling reaction was performed in 50 μl reaction mixture. The 25 ng DNA template was mixed with 5 μl primers with H_2O to make up the volume to 50 μl and denatured at 95 $^\circ\text{C}$ for 5 min. To it 5 μl labeling buffer, 5 μl Radiolabeled dCTP (^{32}P - α -dCTP) and 2 μl klenow fragment of DNA polymerase (1 U/ μl) was added and incubated at 37 $^\circ\text{C}$ for 10 min. The labelled probe was stored in -20 $^\circ\text{C}$ until further use.

3.3.21.5.7 Hybridization

Before performing hybridization using labeled probe, it was firstly purified using Microspin G-25 column (Amersham). The column was vortexed gently to re-suspend the resin. The cap was loosened by $\frac{1}{4}$ turn and bottom of the column was snapped off. It was then placed in the 1.5 ml screwcap eppendorf tube. The column was pre-spin for 1 min at 3000 rpm. 5 μl stop buffer (Blue Dextran and Orange-G in 1 ml EDTA, pH 7.0) was added to the probe reaction to stop the reaction (**Appendix Table 10**). The labeled probe was then poured slowly onto the centre of resin bed and centrifuged for 2 min at 3000 rpm. Column was discarded and flow-through having labeled probe was used. The hybridization was performed at 42 $^\circ\text{C}$ overnight in PerfectHybTM Plus buffer using ^{32}P - α -dCTP labelled DNA fragment.

3.3.21.5.8 Washing

The hybridization buffer was discarded and membrane was washed two times briefly with 2x SSC, 0.1% SDS for 20 min at 37 $^\circ\text{C}$ and last wash with 0.5x SSC, 0.1% SDS at

RT for 15 min and counts were checked before subsequent wash. The washed membrane was dried on filter paper and wrapped in clean plastic bag.

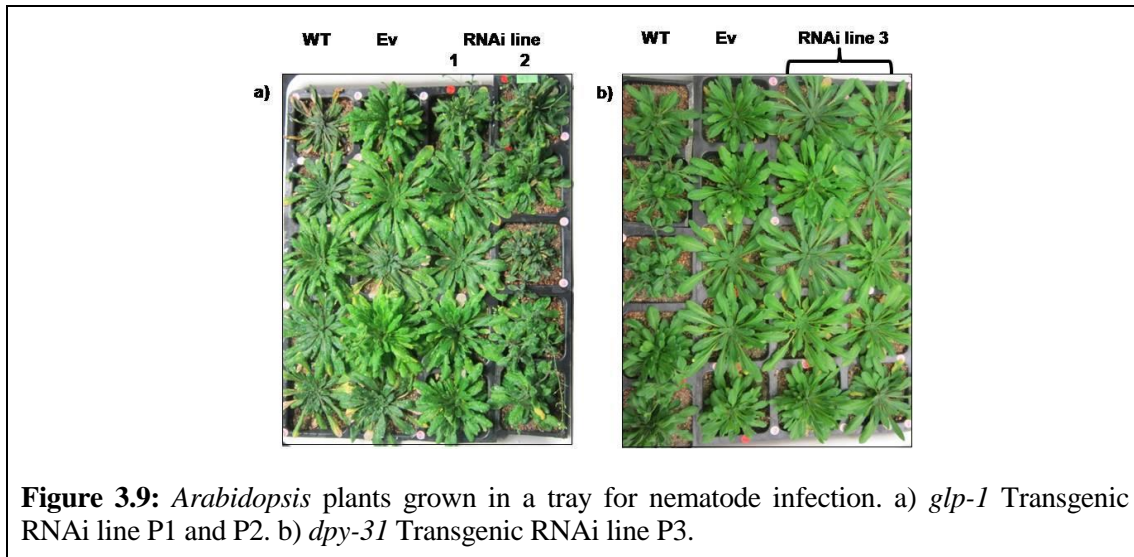
3.3.21.5.9 Autoradiography

The dried membrane was then placed in a lead cassette and exposed to X-ray film (Kodak) -80 °C for 16 h. The autoradiograph was developed as per X-ray films manufacturer's instructions. For repeated hybridization, membrane was stripped with 0.5% SSC, 0.5% SDS for 30 min at 80 °C.

3.3.22 Silencing efficacy of RNAi transgenic lines

3.3.22.1 Plant growth conditions and nematode infection bioassays

Transgenic RNAi and wild type *Arabidopsis* T₃ seeds were surface sterilized (section 3.3.19.1) before germination on MS medium. Plates were maintained at 21°C under a 16 h light/8 h dark photoperiod. Twelve-days-old seedlings were transferred from the petri plates to a 24-slot tray, per slot 2 inch in diameter (one plant per slot), containing a suitable mixture of sand, vermicompost, cocopeat (1:1:1 w/w) maintained in a growth chamber with a 16 h light/8 h dark photoperiod (**Figure 3.9a and b**). After 2 weeks of transplantation each plant was infected with 1000 freshly hatched J2s of root-knot nematodes using 1 ml pipette. The infected roots were harvested after 45 days post infection (45-dpi). Root characteristics, galling, molecular assays and morphometric studies were performed on these uprooted infected plants. The number of galls per plant, as well as the number of females and egg masses per gram root fresh weight, were counted under a dissection microscope and used as a measure for determining the nematode infection.



Nematodes within the infected roots of all samples were stained with acid fuchsin (Bybd et al. 1983) and photographed using a Nikon microscope. To determine the level of susceptibility towards nematode infection in RNAi lines and wild-type plants, reproductive potential of *M. incognita* infecting these plants was determined (Kumari et al. 2016). For this nematode multiplication factor (MF) of *M. incognita* was calculated as follows:

$$(\text{number of egg masses} \times \text{number of eggs per egg mass}) \div \text{nematode inoculum level}$$

Two independent sets of nematode feeding bioassays were carried out for all lines; in any given assay 10 progenies per each RNAi line was calculated. Thus each data point represents the average of at least 20 infected roots per line. The size of stained females isolated from the infected plant samples was measured using a 10x objective on the Nikon microscope equipped with measurement software (NIS element D) (Eisenback and Hunt, 2009; Kaur and Attri, 2013). The stylet and pharyngeal structures of J2 progeny of females feeding on transgenic RNAi lines (expressing *glp-1*- and *dpy-31*-

dsRNA) and control plants were also observed with Zeiss Axio microscope Imager.M2m coupled to an AxioCam using a 40x objective.

3.3.22.2 Transgene expression analyses in nematode infecting RNAi plants by qRT-PCR

Total RNA was isolated from the females infecting transgenic RNAi lines and control plants using Pure Link RNA Mini Kit (Ambion, USA) according to the manufacturer's instructions, followed by DNase treatment using the Qiagen DNase enzyme (see section 3.3.14). SYBR green chemistry based qRT-PCR was performed to determine the level of transcription of nematode transgene (*glp-1/dpy-31*) in the *M. incognita* females infecting transgenic and control plants following the same protocol as described in section 3.3.16, with Actin and 18S rRNA genes used as the reference genes for the qRT-PCR analysis.

3.3.23 Data Analyses

All the results were obtained from at least three independent experiments. The data represented the average (mean) with standard error from all the experiments. Statistically significant differences between the means of replicates of samples were determined by ANOVA and Student's t-test to check the level of significance at $p < 0.05$ and/or $p < 0.01$.

Chapter 4
Results

Objective 1: In silico identification of critical gene(s) of *Meloidogyne incognita* involved in development

4.1.1 Genes involved in cuticle and pharynx development in *M. incognita*

Dpy-10* and *dpy-31* orthologs identified in *M. incognita

We identified two cuticle collagen genes namely, *dpy-10* and *dpy-31* gene in *M. incognita* as the orthologs of *Ce-dpy-10* and *Ce-dpy-31* genes using in silico approach. The sequences were retrieved from the genomic database of *M. incognita* and were further analyzed. The local TBLASTN in Bioedit revealed a single hit for the *dpy-10* (Minc15911) gene and two hits for *dpy-31* (Minc01936 and Minc03986). The BLAST analysis revealed >95% similarity between Minc01936 and Minc03986 both at the gene as well as amino acid level present at different coordinates as retrieved from Gbrowse. Genes enlisted in OrthoMCL search database carried out by Abad et al also revealed *Ce-dpy-10* and *Ce-dpy-31* genes ortholog in *M. incognita* genome (2008).

Mi-dpy-31

A recent report also predicted Minc01936 as *dpy-31* gene in *M. incognita* while identifying *dpy-31* in ovine gastrointestinal nematode *Teladorsagia circumcincta* (Stepek et al. 2015). At the gene level, *Mi-dpy-31* (Minc01936) is a 3.328 kb long sequence, comprising of 12 exons and 10 introns and *Mi-dpy-31* (Minc03986) is 3.721 kb long gene, comprising of 14 exons and 13 introns. Whereas its ortholog in *C. elegans* is a 5kb long gene, interestingly comprising of 8 exons and 7 introns. The 3.328 kb DNA segment of *dpy-31* is predicted to encode a 1.197 kb long mRNA while Minc03986 encodes 1.148 kb long (**Table 4.1**).

Table 4.1: Comparison of gene sizes of *dpy-10* and *dpy-31* of plant-parasitic nematodes to that of reported dumpy genes of free-living nematodes.

Gene	Organism	Accession number	Gene size (kb)	mRNA size (kb)	Protein size (amino acid residues)
<i>dpy-10</i>	<i>Caenorhabditis elegans</i>	T14B4.7 (isoform a)	2.072	1.586	356
	<i>Caenorhabditis briggsae</i>	CBG11227 (isoform a)	2.556	1.679	135
	<i>Caenorhabditis japonica</i>	CJA05199	1.530	1.338	354
	<i>Caenorhabditis remanei</i>	CRE26236	1.217	1.071	356
	<i>Meloidogyne incognita</i> *	Minc15911	1.903	1.181	352
<i>dpy-31</i>	<i>Caenorhabditis elegans</i>	R151.5 (isoform a)	5.004	2.015	592
	<i>Caenorhabditis briggsae</i>	CBG16621	4.299	2.005	593
	<i>Caenorhabditis japonica</i>	CJA10004	7.351	1.785	594
	<i>Caenorhabditis remanei</i>	CRE25103	2.741	1.791	596
	<i>Meloidogyne incognita</i> *	Minc01936	3.328	1.197	391
		Minc03986	3.721	1.148	375
	<i>Meloidogyne hapla</i> #	MhA1_Contig704.frz3.gene1	N.A.	N.A.	362
<i>Meloidogyne floridensis</i> #	nMf.1.1.scaf07709-augustus-gene-0.3	N.A.	0.687	228	

* indicates cuticle genes which have been experimentally proved in this study

indicates cuticle genes which have been predicted computationally in this study

Mi-dpy-10

While *Mi-dpy-10* showed gene length of 1.903 kb comprising of 8 exons and 7 introns and *Ce-dpy-10* is reported as 2.072 kb long interestingly comprising of only 4 exons and 3 introns. *Mi-dpy-10* mRNA is 1.181 kb long which are shorter in length in comparison to *Ce-dpy-10* mRNA which is 1.586 kb long (**Table 4.1**). Even with the disparity in the number of exons and coding length between *C. elegans* and *M. incognita* cuticle genes, gene structure analysis indicated the presence of a similar length of the conserved domains in both the cuticle genes identified in *M. incognita*. The partial mRNA sequence of *Mi-dpy-10* (1.031 kb) and *Mi-dpy-31* (1.116 kb) were successfully cloned in pGEMT easy vector and both the sequences were confirmed by Sanger sequencing.

***glp-1* orthologs identified among RKN and other nematode species**

In order to identify ortholog of *glp-1* in *M. incognita* tblastn analysis was performed against the *M. incognita* genome with the *C. elegans* GLP-1 protein as a query (retrieved from wormbase) and a few hits were selected following Pfam analysis. Among these hits, MiV1ctg1087, the only contig with a high bit score, showed 100% similarity with the Minc16055 enlisted in the OrthoMCL analysis of *M. incognita* as a *Ce-glp-1* ortholog by Abad et al (2008). Thus, functional annotation studies were carried out for the selected gene. The Mi-GLP-1 (Minc16055 or MiV1ctg1087) is a member of the LIN-12/Notch family receptors and is composed of a series of motifs that are conserved among all Notch receptors. The size of the *Ce-glp-1* and *Mi-glp-1* genes was found to be nearly identical, 7.458 kb vs. 7.449 kb, respectively. However, the number of introns and exons differed in these orthologous, with *Ce-glp-1* comprising only 9 exons and 8 introns (Rudel and Kimble, 2001) and *Mi-glp-1* having 18 exons and 17 introns, as based on our computational analysis. The exon/intron structures of these orthologous genes are thus not well-conserved among the nematodes. At the mRNA level, *Mi-glp-1* is 3.252 kb long, whereas *Ce-glp-1* is 4.326 kb long. Recently, another gene named GLP-4, was identified as a new member of the Notch GLP protein family, in *C. elegans* (Rastogi et al. 2015). To date, GLP-4 has been identified only in *C. elegans* and *C. briggsae* (Mango, 2007; Rastogi et al. 2015) and not in plant-parasitic nematodes. The genome-wide search in this study identified only a single *glp-1* contig, as is the case with *C. japonica* and *C. remanei*, wherein each has a single *glp*.

Since *glp-1* is a vital gene involved in pharyngeal development during embryogenesis, we also performed a comprehensive species-wide search for this gene in the genomes

and ESTs of various other *Meloidogyne* species available in NCBI and/or Nematode.net using tblastn. Among the *Meloidogyne* spp., a *glp-1* homolog was identified in *M. hapla*, *M. floridensis*, *M. javanica*, *M. chitwoodi* and in *G. pallida*, another plant-parasitic nematode (details in **Table 4.2**). We also included free-living nematodes, including *C. elegans*, *C. briggsae*, *C. japonica* and *C. remanei* and a marine worm (*Priapulus caudatus*) Notch receptor gene in our phylogenetic analysis. It was observed that among the *Meloidogyne* spp., *M. hapla* has all the domains present that were identified in the *Ce-glp-1* gene, unlike *Mi-glp-1*, which does not have an EGF domain. A motif search conducted in all the species used for analysis in this study revealed conserved ANK repeats.

Table 4.2: Comparison of gene size of *glp-1* of plant-parasitic nematodes with that of reported *glp-1* gene of free-living nematodes.

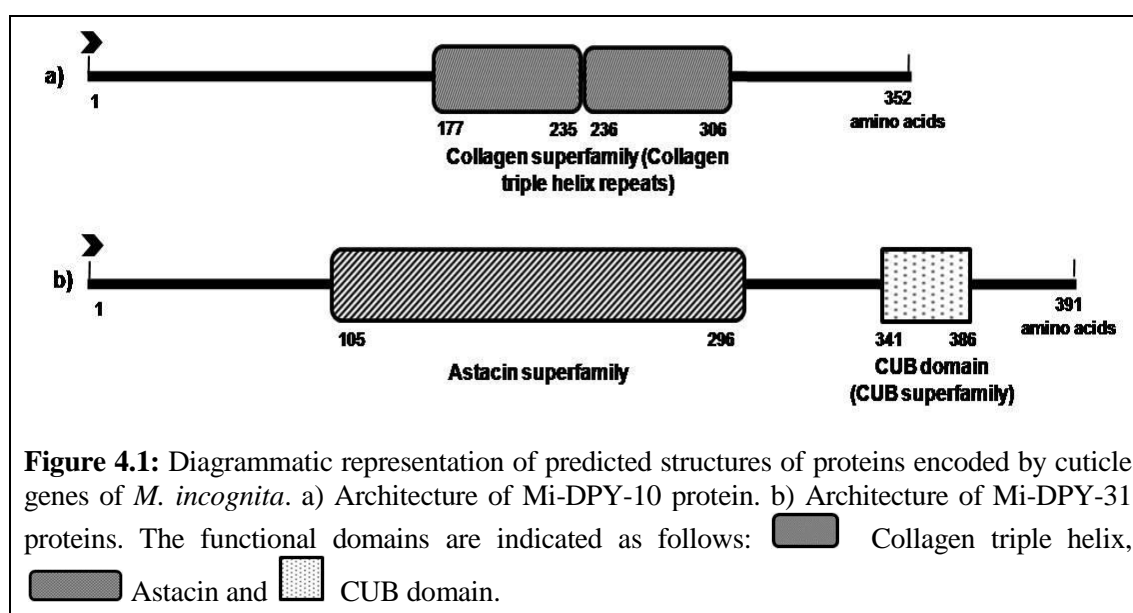
Organism	Accession number	Gene size (kb)	mRNA size (kb)	Protein size (amino acid residues)	Source
<i>Caenorhabditis elegans</i>	CAA79620.1	7.45	4.32	1295	retrieved from Wormbase
<i>Caenorhabditis briggsae</i>	CBG06809	6.61	4.43	1326	retrieved from Wormbase
<i>Caenorhabditis japonica</i>	CJA09628	11.48	3.94	1294	retrieved from Wormbase
<i>Caenorhabditis remanei</i>	CRE29209	6.12	4.32	1308	retrieved from Wormbase
<i>Meloidoyne incognita</i> *	MiV1ctg1087	7.44	3.25	1083	identified in this study
<i>Meloidogyne hapla</i> #	Mh10g200708_Contig1018	5.8	2.27	757	identified in this study
<i>Globodera pallida</i> #	GPLIN_000999900.1	N.A.	3.75	1250	identified in this study
<i>Meloidogyne floridensis</i> #	contig nMf_1_1_scaf00321	N.A.	2.69	898	identified in this study

* indicates pharyngeal genes which have been experimentally proved in this study

indicates pharyngeal genes which have been predicted computationally in this study

4.1.2 Protein sequence analysis and phylogenetic analysis of selected genes in nematode species

Although the identified *dpy-10* and *dpy-31* genes in *M. incognita* are the orthologs of *C. elegans*, we noticed some difference in their cuticle protein composition. In order to analyze the biochemical properties of these two genes molecular weight, isoelectric point (pI) and subcellular localization were predicted. The identified *dpy-10* encodes a protein of 352 amino acids long (**Figure 4.1a**). The two probable paralogs of *dpy-31* identified viz., Minc01936 and Minc03986 encode a protein of 391 and 375 amino acids, respectively (**Figure 4.1b**). The predicted molecular weight of DPY-10, DPY-31(Minc01936) and DPY-31(Minc03986) proteins are 36.83 kDa, 45.43 kDa and 43.44 kDa with predicted isoelectric point (pI) of 5.20, 6.65 and 6.17, respectively. A negative grand average of hydropathicity (GRAVY) scores of -0.683, -0.808 and -0.771 for DPY-10, DPY-31 (Minc01936 and Minc03986) proteins, respectively indicated the hydrophilic nature of these proteins.



The sub-cellular localization prediction of both the cuticle collagen genes suggested that both are probably located in nuclear and extracellular (including cell-wall) regions. As reported earlier, the expression of *dpy-31* in the hypodermis was noticed and is reported to process cuticle components (Mohrlen et al. 2003; Novelli et al. 2004; Park et al. 2010; Suzuki et al. 2004). The prediction software indicated the presence of transmembrane domain in Mi-DPY-10 similar to that of Ce-DPY-10 protein (**Figure 4.2a**). In case of Mi-DPY-31, no transmembrane domain was predicted this was in accordance with Ce-DPY-31 protein (**Figure 4.2b**). While the signal peptide sequence was notably absent in both Mi-DPY-10 and Mi-DPY-31 (**Figure 4.3a and b**).

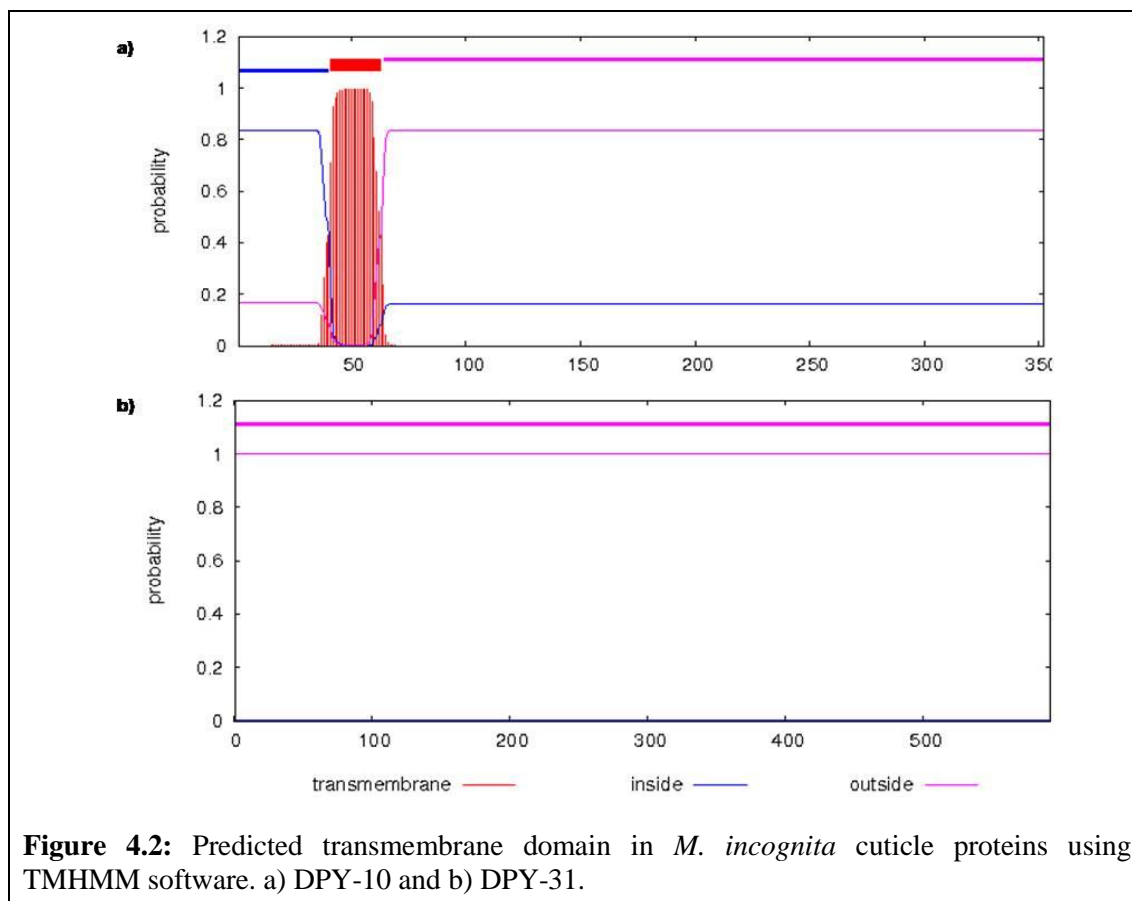


Figure 4.2: Predicted transmembrane domain in *M. incognita* cuticle proteins using TMHMM software. a) DPY-10 and b) DPY-31.

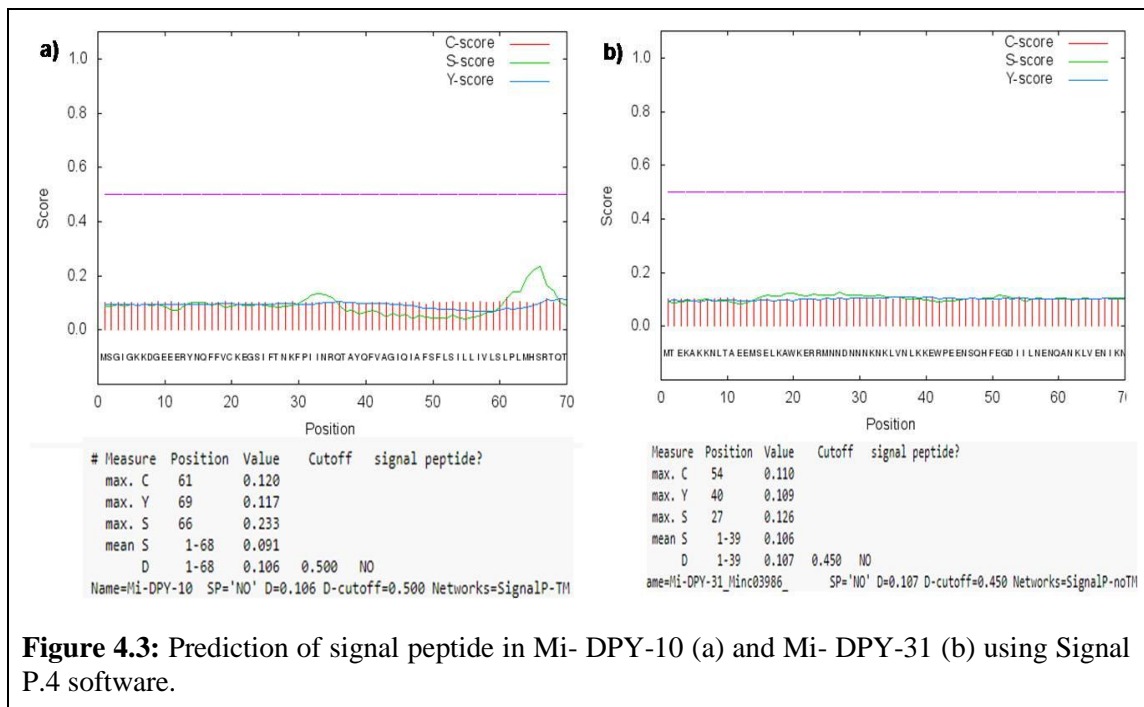


Figure 4.3: Prediction of signal peptide in Mi- DPY-10 (a) and Mi- DPY-31 (b) using Signal P.4 software.

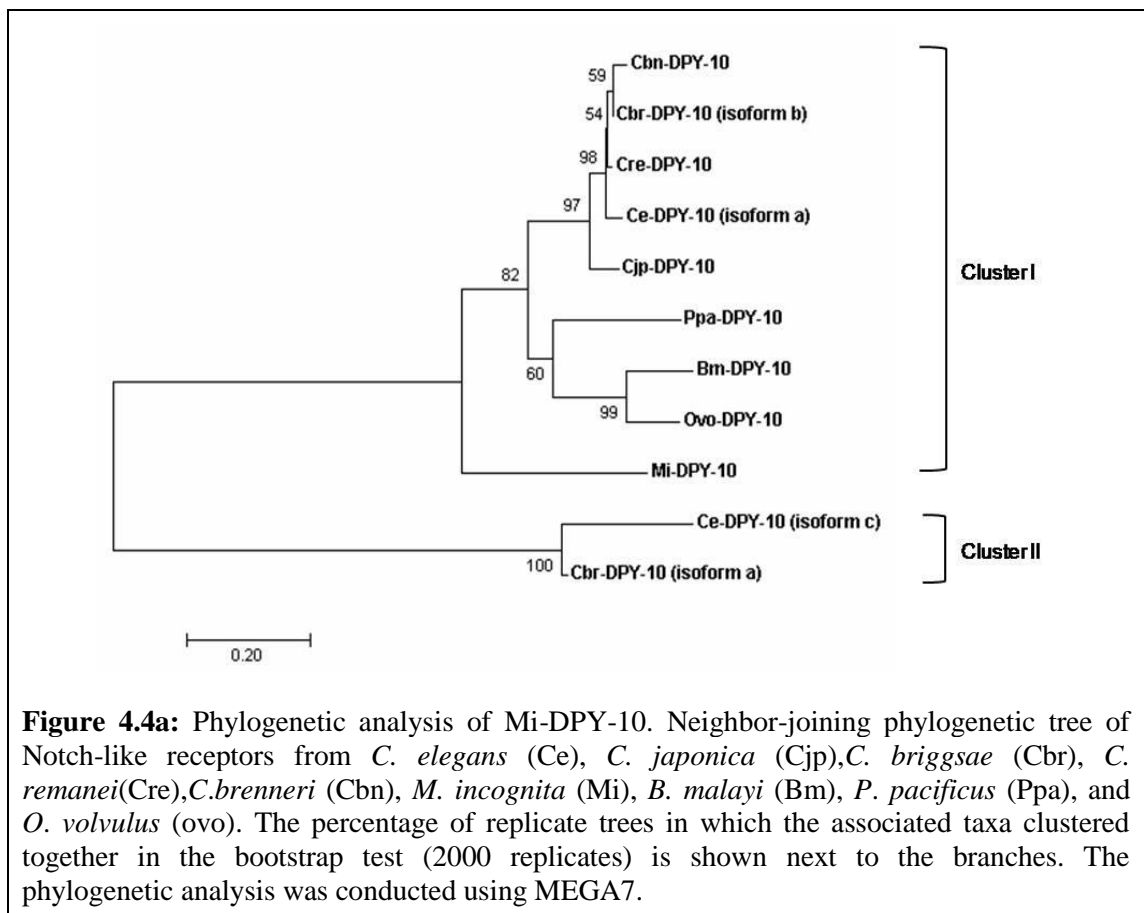
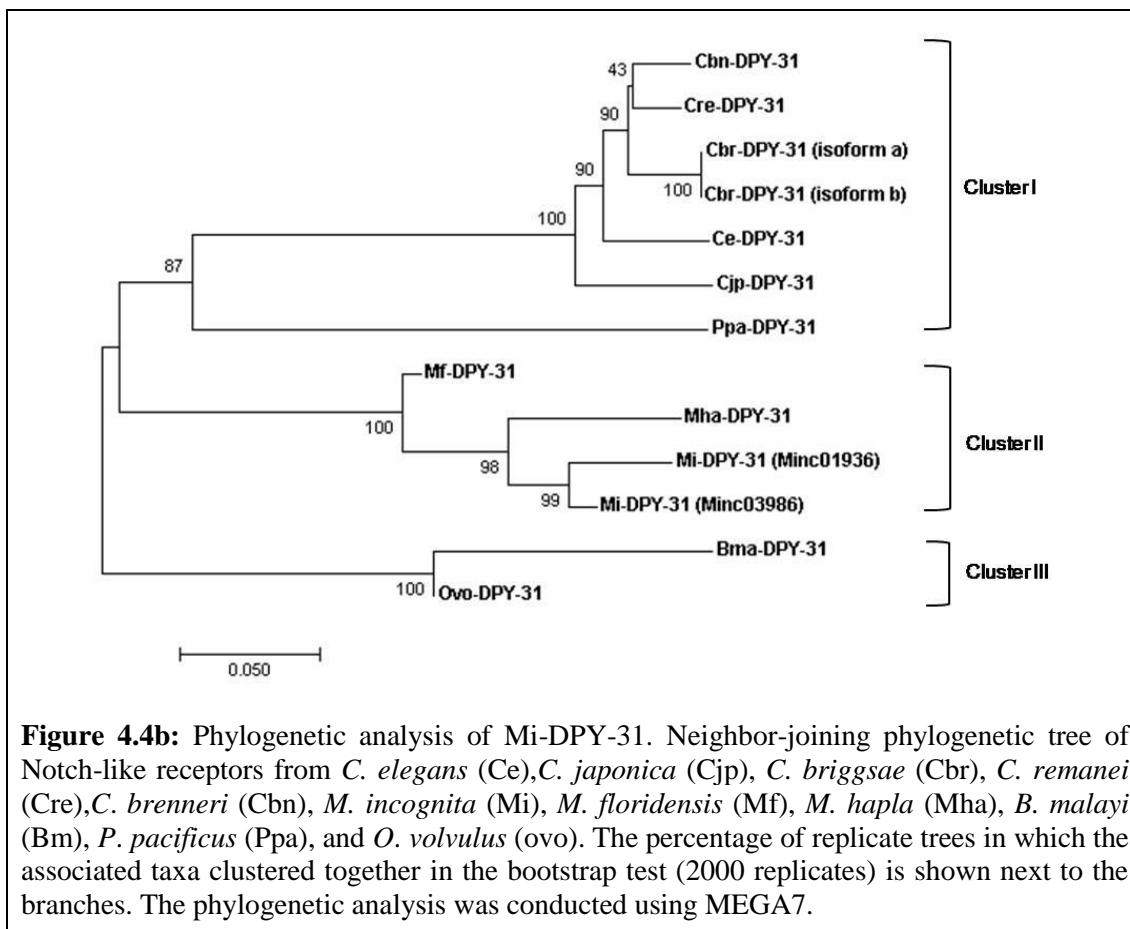


Figure 4.4a: Phylogenetic analysis of Mi-DPY-10. Neighbor-joining phylogenetic tree of Notch-like receptors from *C. elegans* (Ce), *C. japonica* (Cjp), *C. briggsae* (Cbr), *C. remanei* (Cre), *C. brenneri* (Cbn), *M. incognita* (Mi), *B. malayi* (Bm), *P. pacificus* (Ppa), and *O. volvulus* (ovo). The percentage of replicate trees in which the associated taxa clustered together in the bootstrap test (2000 replicates) is shown next to the branches. The phylogenetic analysis was conducted using MEGA7.

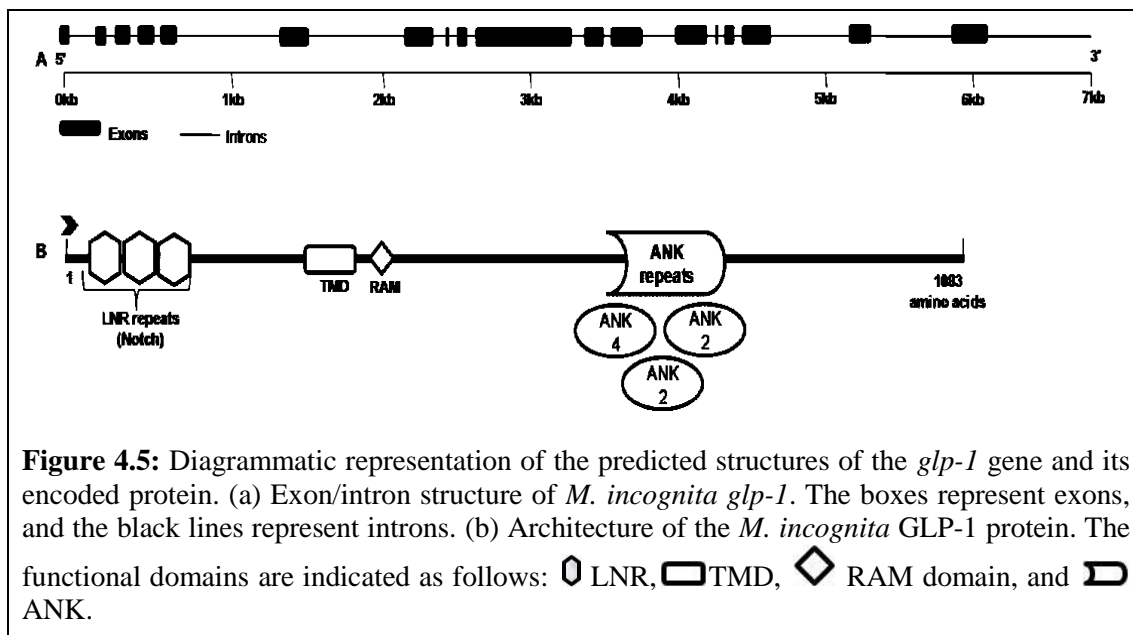
The phylogenetic analysis of these genes was on the basis of high similarity within the conserved collagen domains. Both the probable paralogs of Mi-DPY-31 (Minc01936 and Minc03986) grouped together forming one cluster with other *Meloidogyne spp.* The phylogenetic tree indicates the presence of DPY-10 and DPY-31 throughout the different nematode phylum and strongly points to their conserved function (**Figure 4.4a and b**).



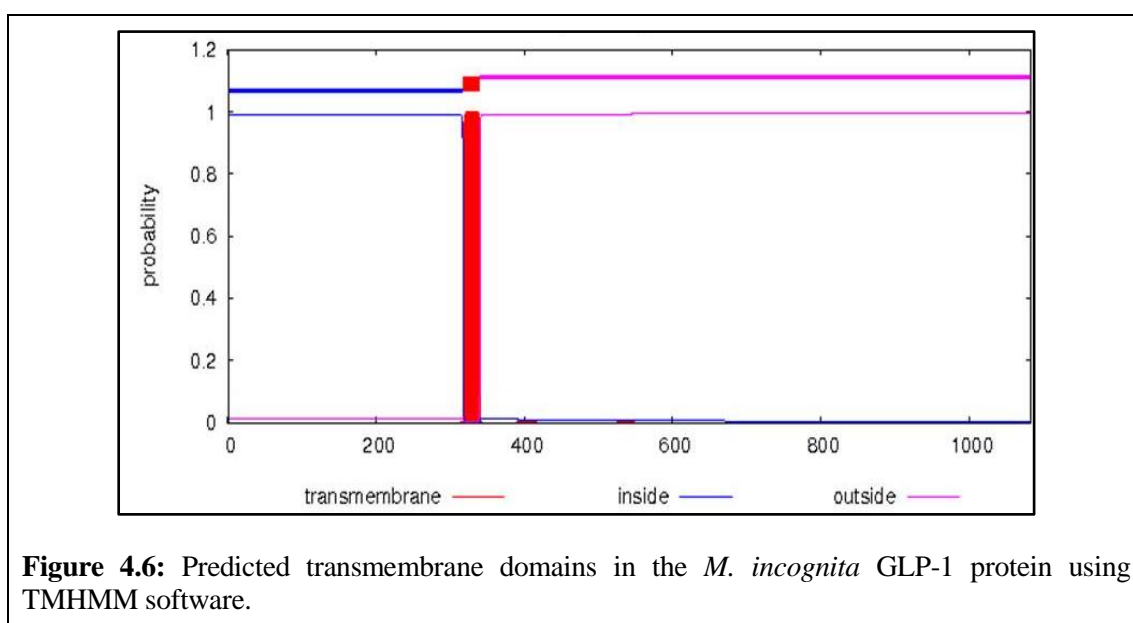
In Mi-glp-1

The *Mi-glp-1* gene encodes a protein of 1083 amino acids in length, as determined by Pfam analysis, in contrast to *Ce-glp-1*, which is composed of 1295 amino acids (**Figure 4.5a and b**). The molecular weight of Mi-GLP-1 protein is 120.67 kDa with predicted isoelectric point (pI) of 7.25 and a negative grand average of hydropathicity (GRAVY)

score of -0.532 indicated its hydrophilic nature. The subcellular localization prediction software indicated the probability of GLP-1 as a nuclear protein.



The transmembrane software and Pfam analysis suggested the presence of transmembrane domain (**Figure 4.6**) but no N-terminal signal peptide was found in the Mi-GLP-1 protein (**Figure 4.7**).



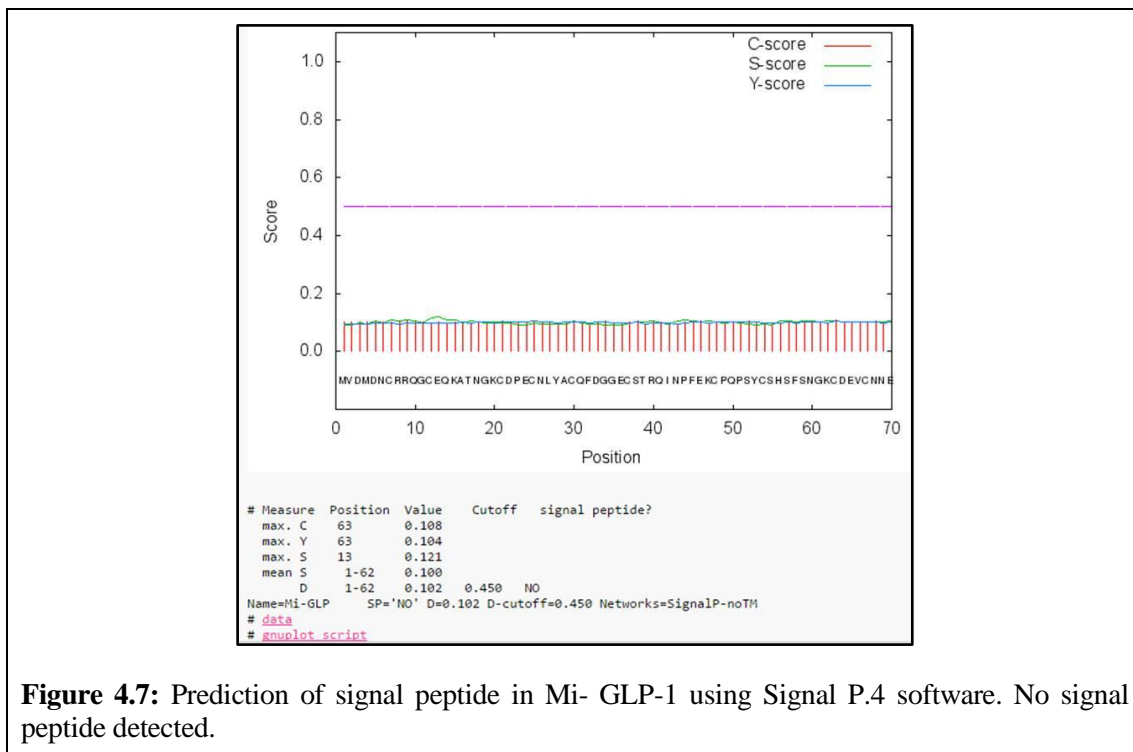


Figure 4.7: Prediction of signal peptide in Mi-GLP-1 using Signal P.4 software. No signal peptide detected.

All identified GLP-1 protein sequences belonging to the different nematode species were aligned using MUSCLE (**Figure 4.8**). The alignment revealed several conserved motifs present among these parasitic and free-living nematodes, with two motifs showing maximum amino acid conservation. Phylogenetic analysis using the amino acid sequences was performed with the goal of understanding the patterns of relatedness of the *glp-1* gene among the nematodes under study.

Phylogenetic analysis through the neighbor-joining method of GLP-1 in *Meloidogyne* and in other species revealed a separate cluster comprised of Mi-GLP-1, Gp-GLP-1, Mh-GLP-1 and Mf-Notch-like protein. As observed in the phylogenetic tree, Mi-GLP-1 appears to be most closely related to the Mf-Notch-like protein. However, there was a higher degree of similarity among the conserved domains between Mi-GLP-1 and Gp-GLP-1, thereby conclusively demonstrating that these as two closely related genes (**Figure 4.9**).

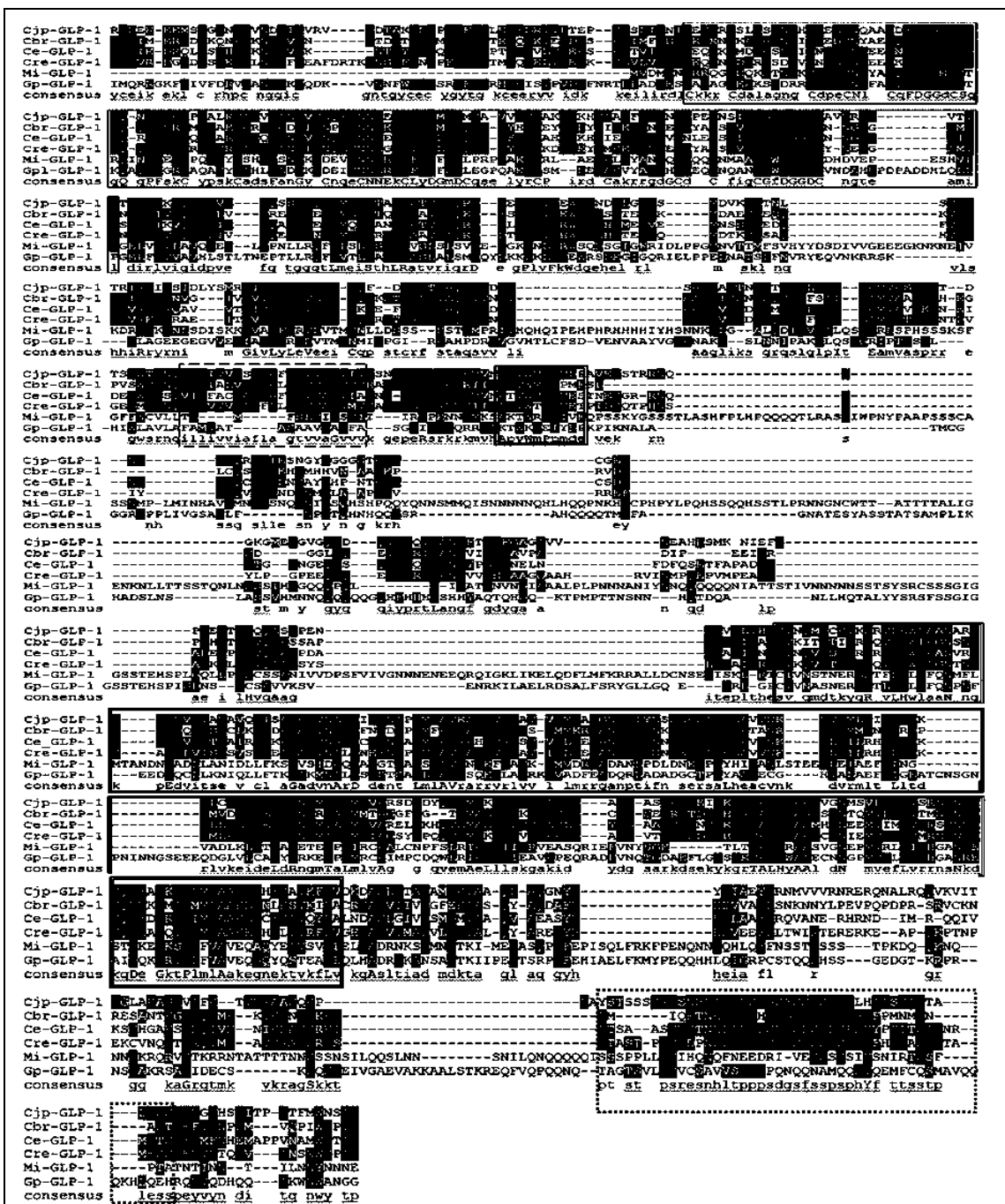


Figure 4.8: Multiple sequence alignment of GLP-1 in free-living and plant-parasitic nematodes. Black shading indicates conserved amino acids. Rectangular boxes represent different motifs conserved in GLP-1 in these species (□-LNR, □-TMD, □-RAM domain, □-ANK and □-PEST domain). Ce- *Caenorhabditis elegans*, Cbr- *Caenorhabditis briggsae*, Cjp- *Caenorhabditis japonica*, Cre- *Caenorhabditis remanei*, Mi- *Meloidogyne incognita* and Gp- *Globodera pallida*.

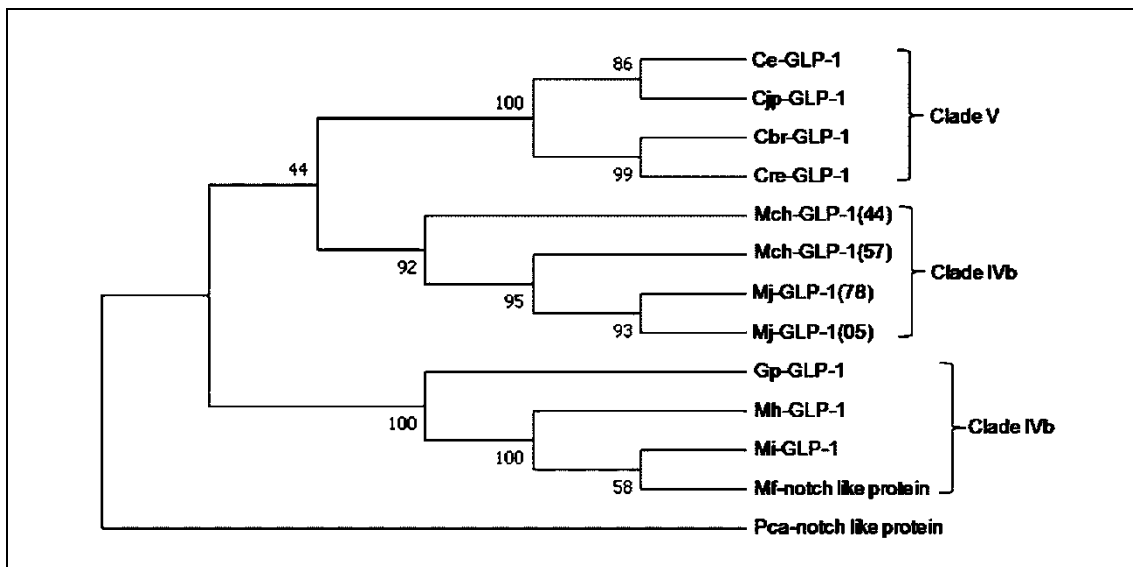


Figure 4.9: Phylogenetic analysis of Notch-like receptors. Neighbor-joining phylogenetic tree of Notch-like receptors from *C. elegans* (Ce), *C. japonica* (Cjp), *C. briggsae* (Cbr), *C. remanei* (Cre), *M. chitwoodi* (Mch), *M. javanica* (Mj), *G. pallida* (Gp), *M. incognita* (Mi), *M. floridensis* (Mf), *M. hapla* (Mhp), and *P. caudatus* (Pca, as an outgroup). The percentage of replicate trees in which the associated taxa clustered together in the bootstrap test (2000 replicates) is shown next to the branches. The phylogenetic analysis was conducted using MEGA7.

4.1.3 Presence of conserved domains

In cuticle proteins

Proteins of DPY family have a diverse role ranging from development to processes like extracellular matrix components. Protein structure analysis of DPY-10 reveals the presence of collagen superfamily domain which contains copies of Gly-X-Y to form a triple helix (**Figure 4.10**). Each Gly-X-Y repeats flanked by conserved cysteine residues as observed in reported Ce-DPY-10. The pattern of Gly-X-Y repeats of Mi-DPY-10 resembles that of Dpy-2 group as classified on the basis of the pattern of conserved cysteines (Johnstone, 2000). In Mi-DPY-10 the size of Gly-X-Y repeats between first and second cysteine cluster is 47 amino acids and between second and third cluster is 131 amino acids. It was also observed that proline content was more in the Gly-X-Y pattern in Mi-DPY-10 which is a typified character of nematodes.

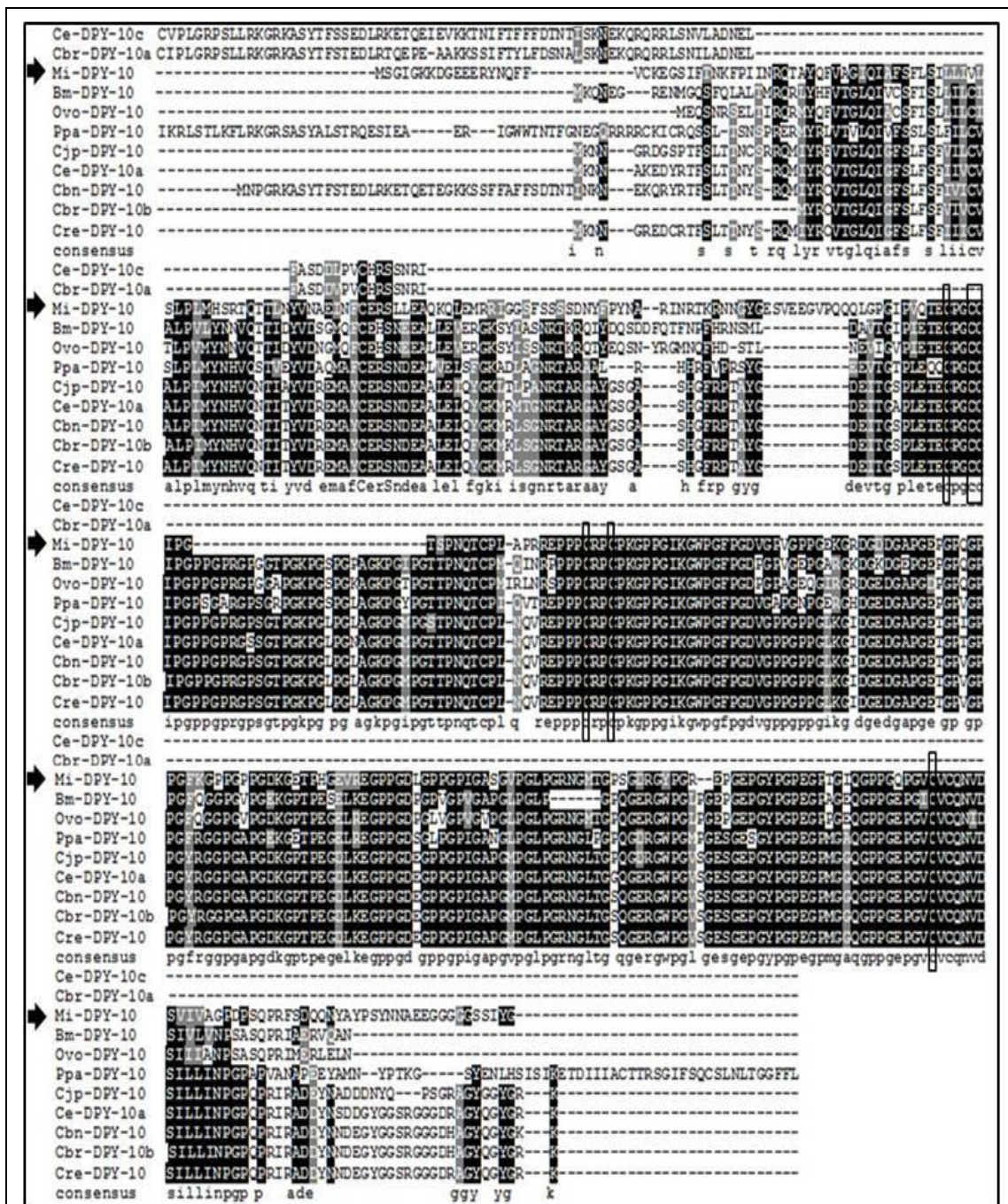


Figure 4.10: Multiple sequence alignment of DPY-10 protein in free-living and plant-parasitic nematodes. Black shade indicates conserved amino acids. Rectangular boxes represent conserved cysteine residues in between Gly-X-Y repeats. Here, Ce- *Caenorhabditis elegans*, Cbr- *Caenorhabditis briggsae*, Cjp- *Caenorhabditis japonica*, Cre- *Caenorhabditis remanei*, Cbn- *Caenorhabditis brenneri*, Mi- *Meloidogyne incognita*, Bm- *Brugiya malayi*, Ppa- *Pristionchus pacificus* and Ovo- *Onchocerca volvulus*. Arrow indicates Mi-DPY-10 protein.

Astacin domain is a characteristic of members of DPY family proteins. In both the Mi-DPY-31 proteins (Minc01936 and Minc03986), astacin domain is comprised of 193 amino acid residues (Figure 4.11).

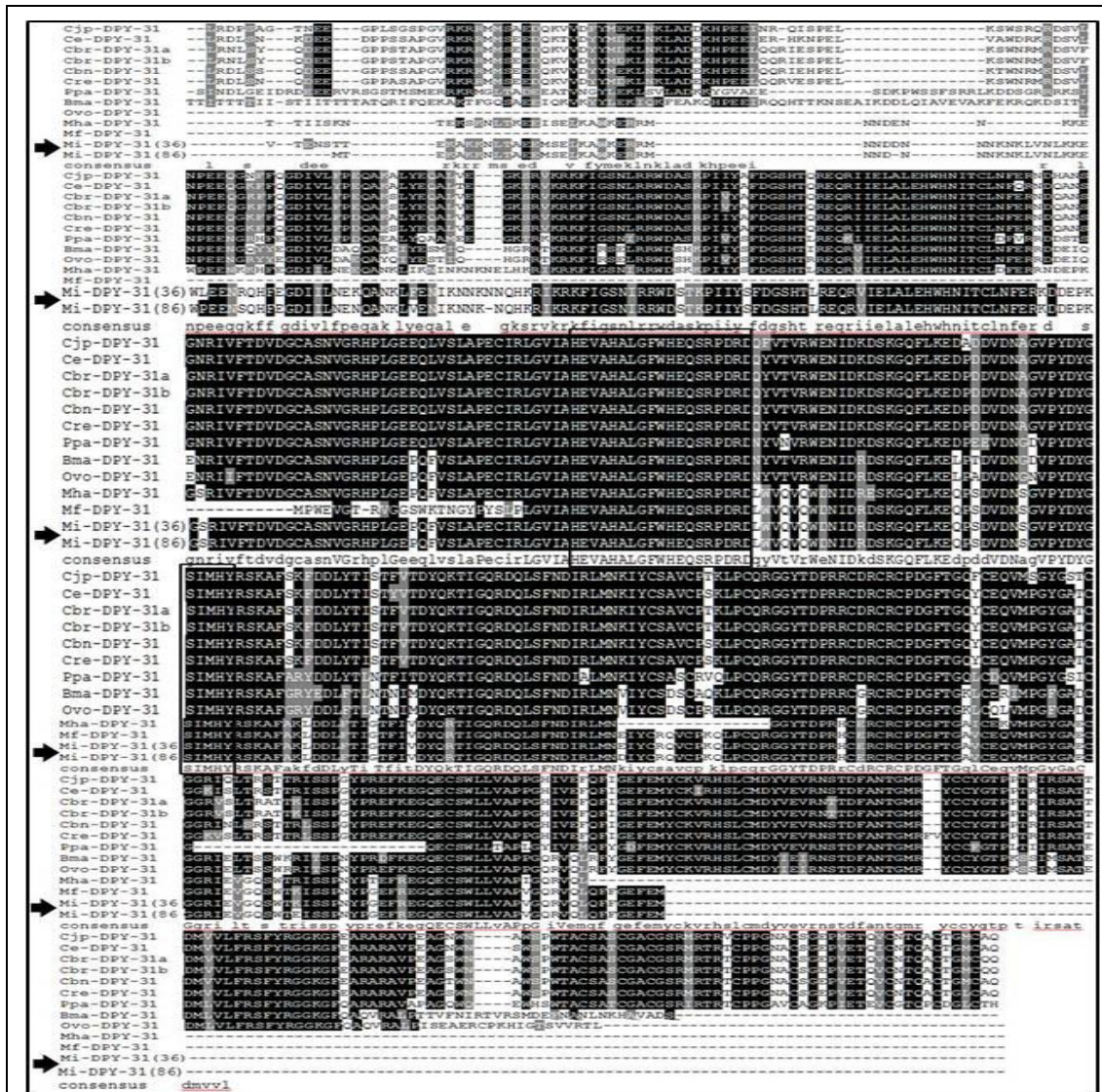


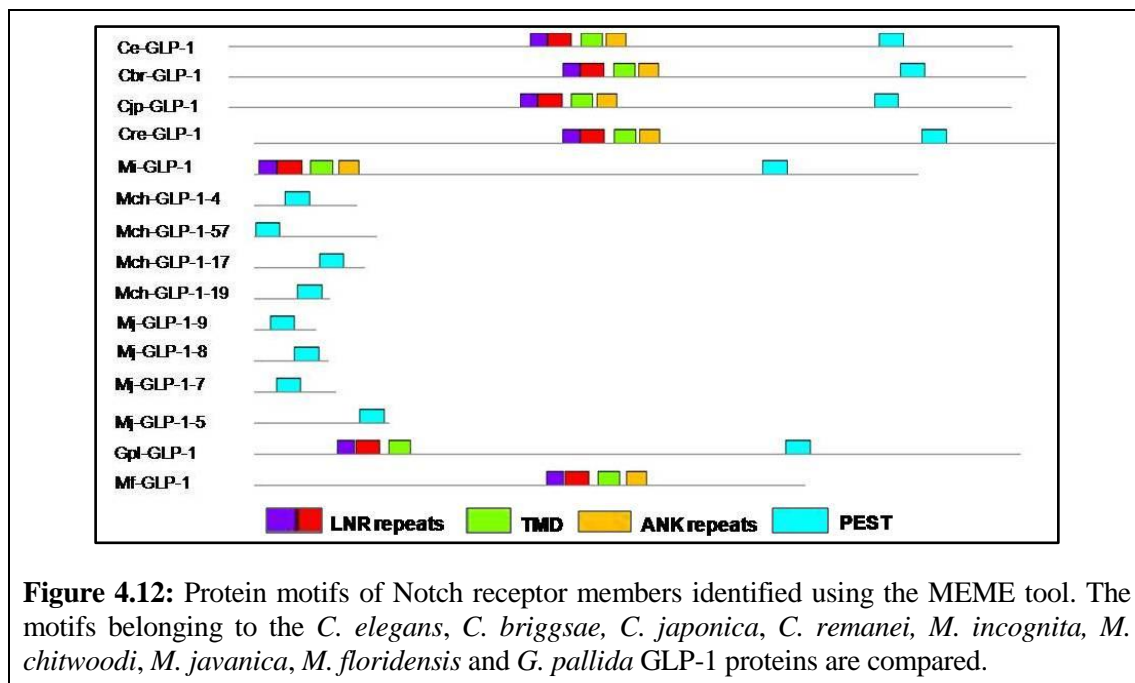
Figure 4.11: Multiple sequence alignment of DPY-31 in free-living and plant-parasitic nematodes. Black shade indicates conserved amino acids. Rectangular boxes represent zinc-binding active site (HExxHxxGFxHExxRxDRD) and methionine-turn (SxMHY) motifs conserved in these species in dumpy genes. Here, Ce- *Caenorhabditis elegans*, Cbr- *Caenorhabditis briggsae*, Cjp- *Caenorhabditis japonica*, Cre- *Caenorhabditis remanei*, Cbn- *Caenorhabditis brenneri*, Bm- *Brugiya malayi*, Ppa- *Pristionchus pacificus*, Ovo- *Onchocerca volvulus*, Mi- *Meloidogyne incognita*, Mha- *Meloidogyne hapla* and Mf- *Meloidogyne floridensis*. Arrows indicates Mi-DPY-31(36) - Minc01936 and Mi-DPY-31(86) - Minc03986 protein.

Astacin containing proteins are proteases that require zinc for catalysis and hence, the name metalloprotease proteins. Presence of astacin domain indicates towards the peptide cleavage role of Mi-DPY-31. The motif search analysis showed same motifs of similar sizes in these two probable copies of DPY-31. Apart from astacin domain, motif analysis search also revealed the presence of CUB domain (for complement C1r/C1s, Uegf, Bmp1) at C-terminal of both the copies of Mi-DPY-31, thus classifying it under subgroup V according to the classification by Park et al (2010). The proteins with astacin and CUB domain are generally membrane proteins known to be involved in development. Thus, Mi-DPY-31 could also be a membrane protein although no transmembrane domain was predicted in Mi-DPY-31 which is in accordance to Ce-DPY-31. DPY-31 is thought to be responsible for C-terminal cleavage of the cuticular collagen SQT-3 (Novelli et al. 2004), a function reminiscent of the role of BMP-1 in cleaving fibrillar collagens in vertebrates (Park et al. 2010; Reddi, 1996).

In GLP-1 protein

On the other hand, amino acid sequence analysis of the *M. incognita* GLP-1 protein revealed a single transmembrane domain (TMD), an extracellular domain containing Lin-12/Notch repeats (LNR), ankyrin repeats (ANK), which is an intracellular domain, and a Pro-Glu-Ser-Thr domain (PEST) (**Figure 4.12**). The LNR and ANK repeats have been described in *C. elegans* in terms of their molecular and biological functions (Austin and Kimble, 1989; Roehl et al. 1996). Thus, the presence of these motifs in Mi-GLP-1 indicates its probable role in embryogenesis. Specific primers from the LNR region were designed, and the region was successfully amplified, confirming the presence of these repeats in *M. incognita*. Interestingly, the presence of a conserved "C" cysteine as the first residue marking the beginning of the LNR motif was found to be

present in the *glp-1* in all nematode species evaluated in this study (**Figure 4.8**). Mi-GLP-1 had one ANK domain with three copies, three LNR domains present at the 5' end, a transmembrane domain, and a RAM domain; however, an epidermal growth factor (EGF) domain was not found. GLP-1 induces downstream transcriptional regulators and interacts with them to mediate signaling. In our sequence analysis, we found an "RTGGGAA" DNA binding site and a RAM domain in *Mi-glp-1*. These sites have been proposed as a binding site for the LAG-1 (Lin-12 and Glp-1) protein, which is required during embryogenesis for regulating pharyngeal development (Christensen et al. 1996).

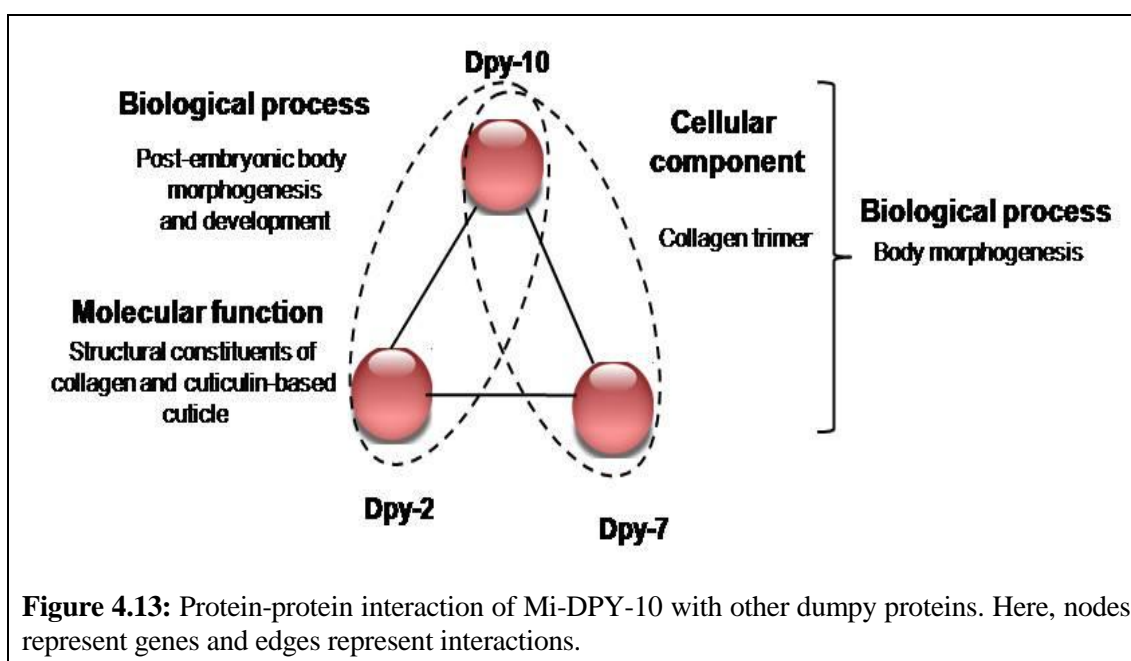


4.1.4 Protein-protein interaction

Cuticle proteins

To determine the probable function of DPY-10 and DPY-31 in *M. incognita*; a protein-protein association network was carried out using STRING software. For this, we

identified and retrieved other *dumpy* genes from the *M. incognita* genome using *C. elegans dumpy* genes as query. The analysis revealed a direct interaction between Mi-DPY-2, Mi-DPY-7 and Mi-DPY-10 (**Figure 4.13**). To further confirm our result we also performed protein-protein interaction analysis for Ce-DPY-10 and Ce-DPY-31 genes with other cuticle genes using STRING. The analysis revealed a direct interaction between Ce-DPY-10, Ce-DPY-7 and Ce-DPY-2. However, an indirect network between Ce-DPY-10 and other proteins like NOAH-1, NOAH-2, MLT-11, DPY-3, ACN-1 and IPR-3 (**Figure 4.14**) was noticed. Nevertheless, we were unable to identify these sequences in *M. incognita* genome and therefore no such network was established between Mi-DPY-10 and other respective protein sequences. Interestingly, Mi-DPY-31 displayed a direct interaction with only Mi-SQT-3 protein (sequence identified and retrieved in our BLAST analysis) similar to the predicted interaction network indicated by the Ce-DPY-31 (**Figure 4.15**).



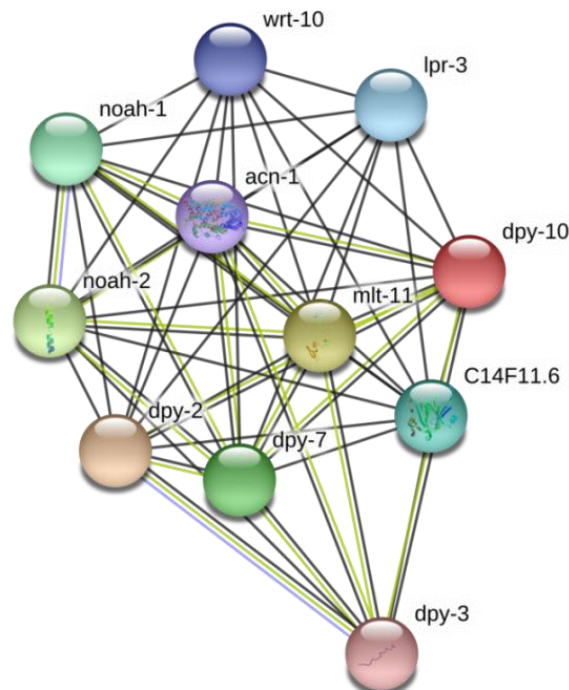


Figure 4.14: Protein-protein association of Ce-DPY10. Direct protein interaction network of Ce- DPY-10 with other cuticle genes. Here, nodes represent genes and edges represent interactions.

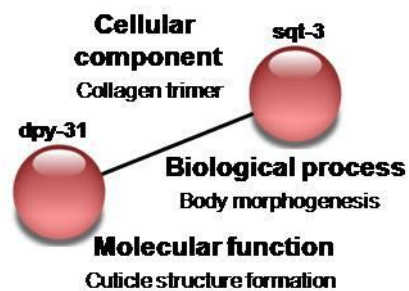
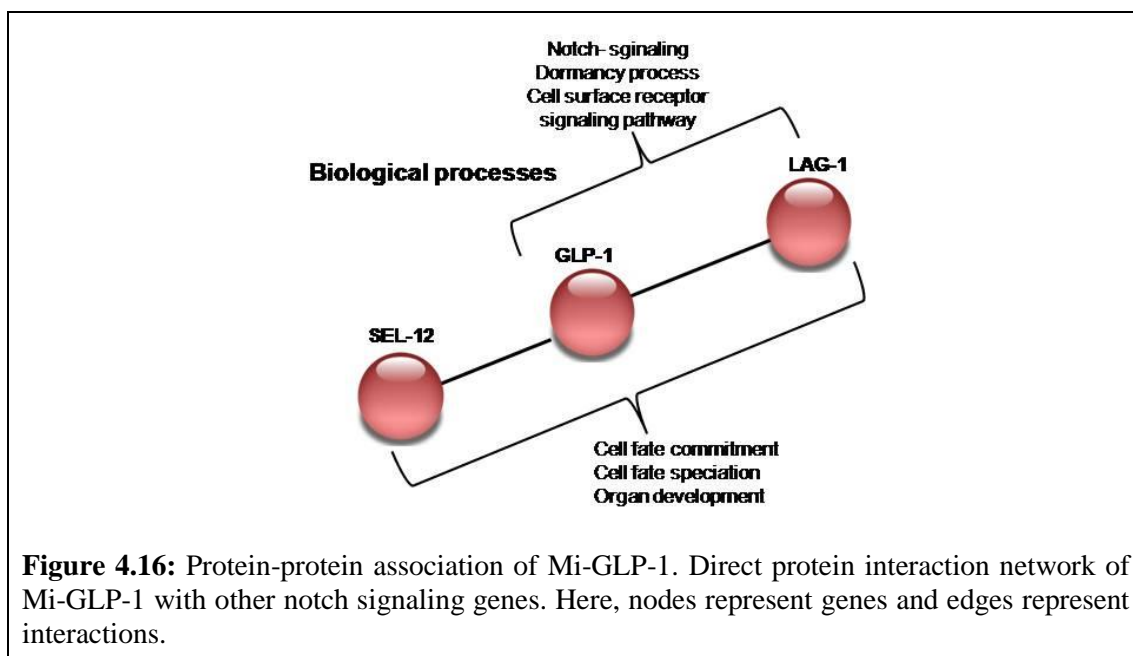


Figure 4.15: Protein-protein association of Mi-DPY-3. Direct protein interaction network of Mi-DPY-31 with other cuticle genes. Here, nodes represent genes and edges represent interactions.

GLP-1 protein

A protein-protein interaction network was predicted to identify the probable association of *glp-1* with other genes. For this we identified *Mi-lag-1* and *Mi-sel-12* in our computational analyses and retrieved corresponding sequences from the *M. incognita* genome. It was observed that the probable genes having direct interaction with *glp-*

were not having any association among themselves. A similar pattern of protein-protein interaction for Ce-GLP-1 was also detected. The analysis clearly demonstrated a direct and vital interaction of GLP-1 with LAG-1 for performing vital processes in *M. incognita* (**Figure 4.16**). Biological processes involving cell fate commitment, notch-signaling pathway and cell-surface receptor signaling pathways requires a direct interaction between GLP-1 and LAG-1. Thus, there is a good match between our motif search analysis revealing LAG-1 binding DNA sequence sites and protein-protein association of GLP-1 and LAG-1. Together, these results indicate LAG-1 as an important ligand for GLP-1 in performing significant functions involving organ development.



Objective 2: Cloning and characterization of cuticle and pharynx genes and their transcript profiling

4.2.1 Isolation of *Mi-dpy-10*, *Mi-dpy-31* and *Mi-glp-1* from *M. incognita*

Total DNA was isolated from *M. incognita* adult females hand-picked from the infected tomato cv pusa ruby plants and run on an agarose gel to check the quality of DNA (Figure 4.17). PCR amplification was carried out using this DNA to confirm the integrity of predicted *dpy-10*, *dpy-31* and *glp-1* genes in *M. incognita* genome. PCR product or amplicon was evaluated on agarose gel. The expected amplification of the amplicon of respective genes (Figure 4.18a, b and c) confirmed the genes identified through in silico analyses. The amplicon lengths of genes *dpy-10*, *dpy-31* and *glp-1* are 1.031 kb, 1.116 kb, and 1 kb, respectively.

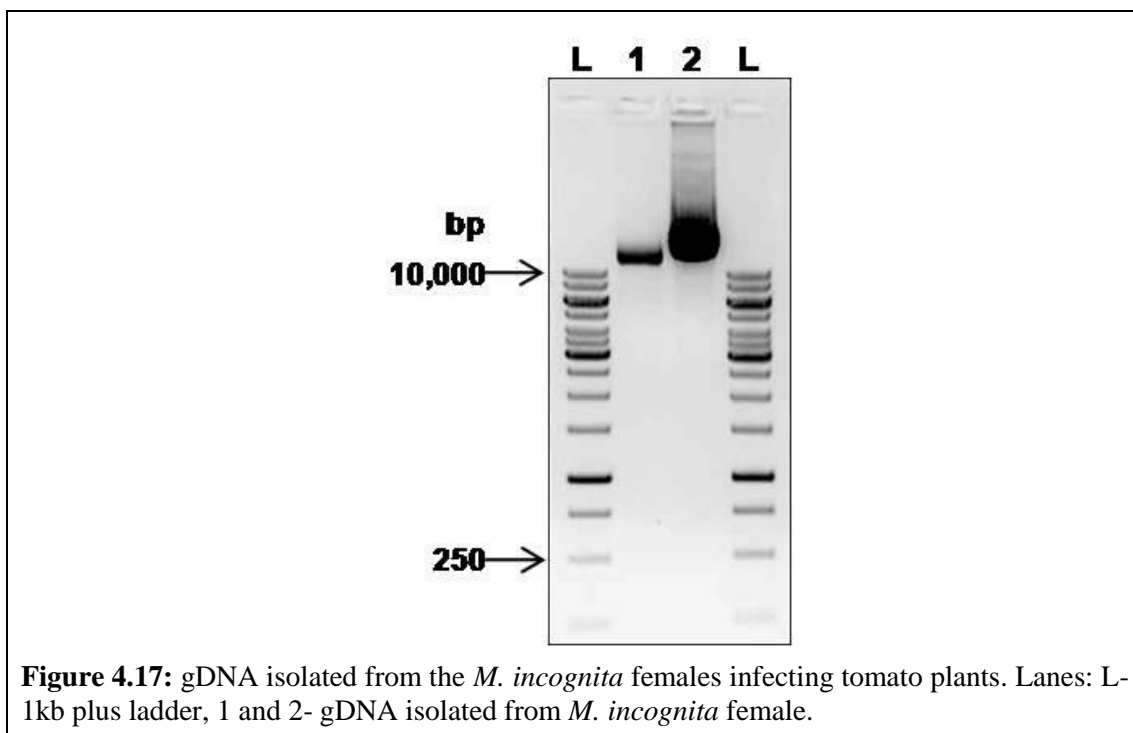
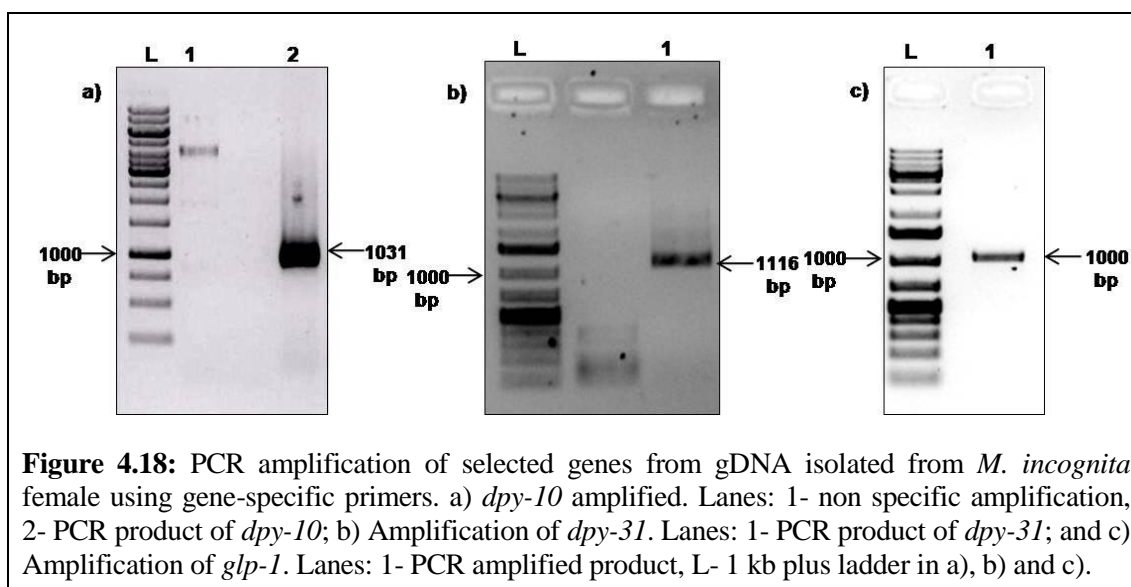


Figure 4.17: gDNA isolated from the *M. incognita* females infecting tomato plants. Lanes: L- 1kb plus ladder, 1 and 2- gDNA isolated from *M. incognita* female.



4.2.2 Transcript abundance of identified genes during developmental stages of *M. incognita*

The expression pattern of *dpy-10*, *dpy-31* and *glp-1* in *M. incognita* was studied at five different development stages: egg masses, J2s, mature females, J3s and J4s (infected roots of plant samples harvested after 10 dpi and 21 dpi). Total RNA was isolated from these samples and run on formaldehyde agarose gel to check the quality of the RNA (**Figure 4.19a and b**). In *dpy-10* higher expression at J2 stage (7.5 relative fold) was observed indicating its possible role during an early stage of moulting (**Figure 4.20a**). The *dpy-31* transcript levels were found higher in adult females as compared to that in early stages (**Figure 4.20b**). Thus, indicating possible role of *Mi-dpy-31* during the fourth round of moulting in the nematode life cycle. Interestingly, *glp-1* showed higher expression levels during the early development of *M. incognita*, i.e., in egg masses (**Figure 4.20c**). This finding is consistent with the previous studies reporting that the *glp-1* is abundant at early developmental stages in *C. elegans* embryos (Austin and Kimble, 1989; Crittenden et al. 1997). The qRT-PCR analysis also revealed that *glp-1* transcript levels showed an increase in mature females, indicating its possible role even at this later stage in *M. incognita*.

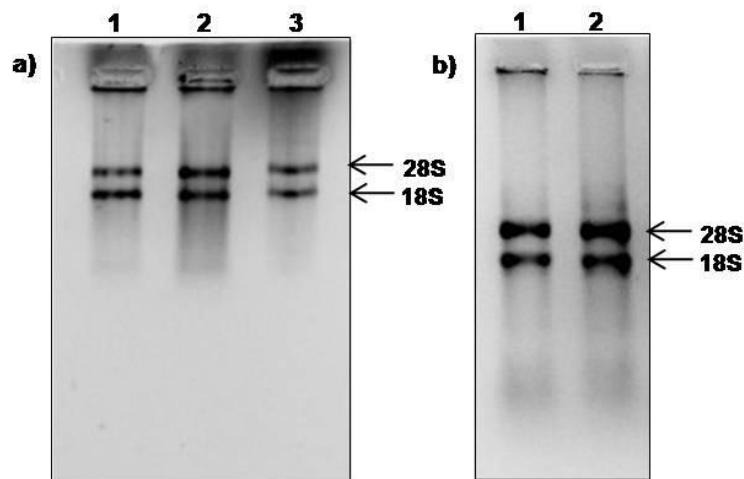


Figure 4.19: Total RNA isolated from the *M. incognita* female infecting tomato plants. Lanes represent RNA isolated from five different samples. a) Lanes: 1- egg mass, 2- J2s, 3- adult females; b) Lanes: 1- infected roots of plant samples harvested after 10 dpi (J3s), 2- infected roots of plant samples harvested after 21 dpi (J4s).

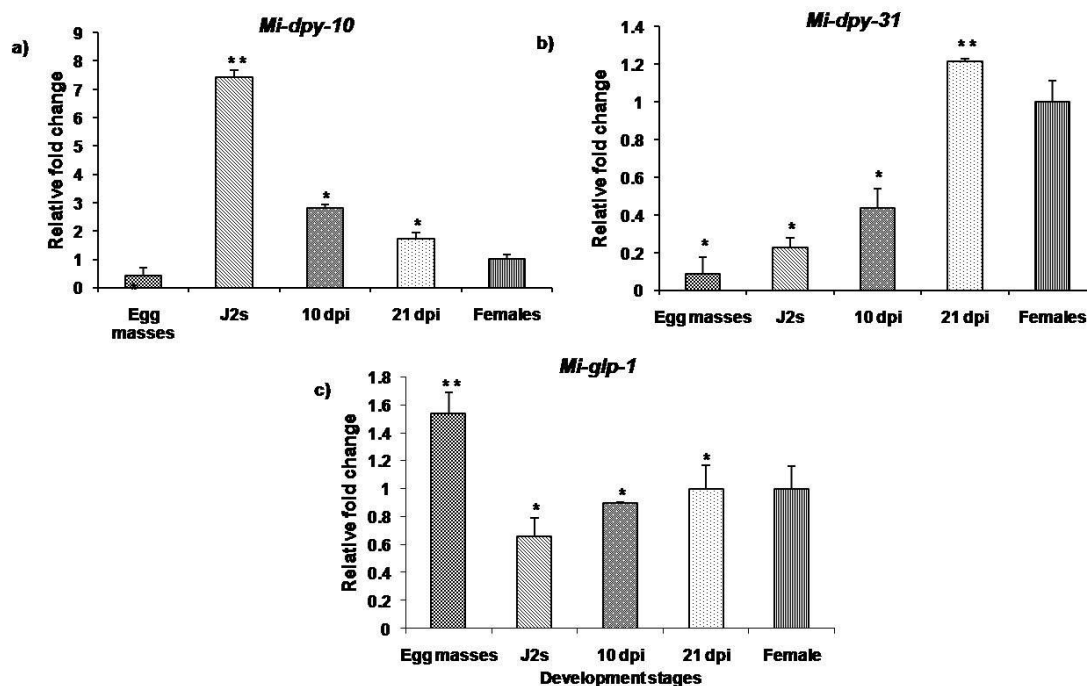
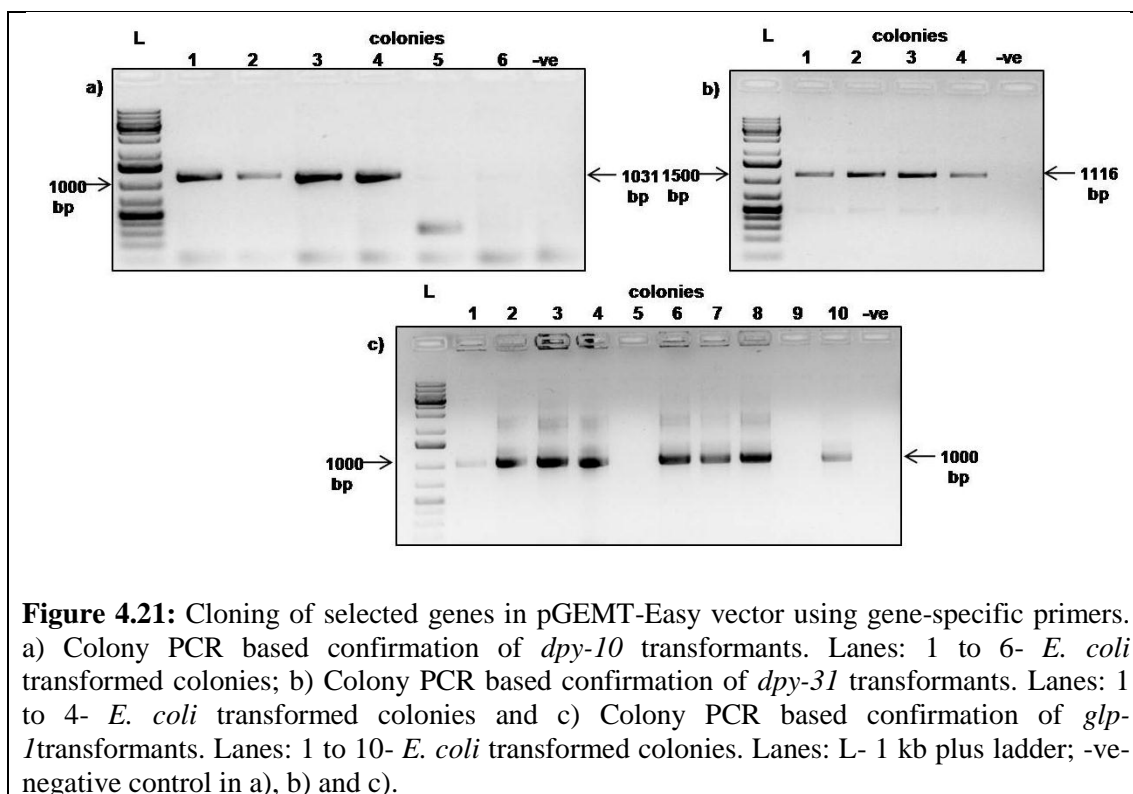
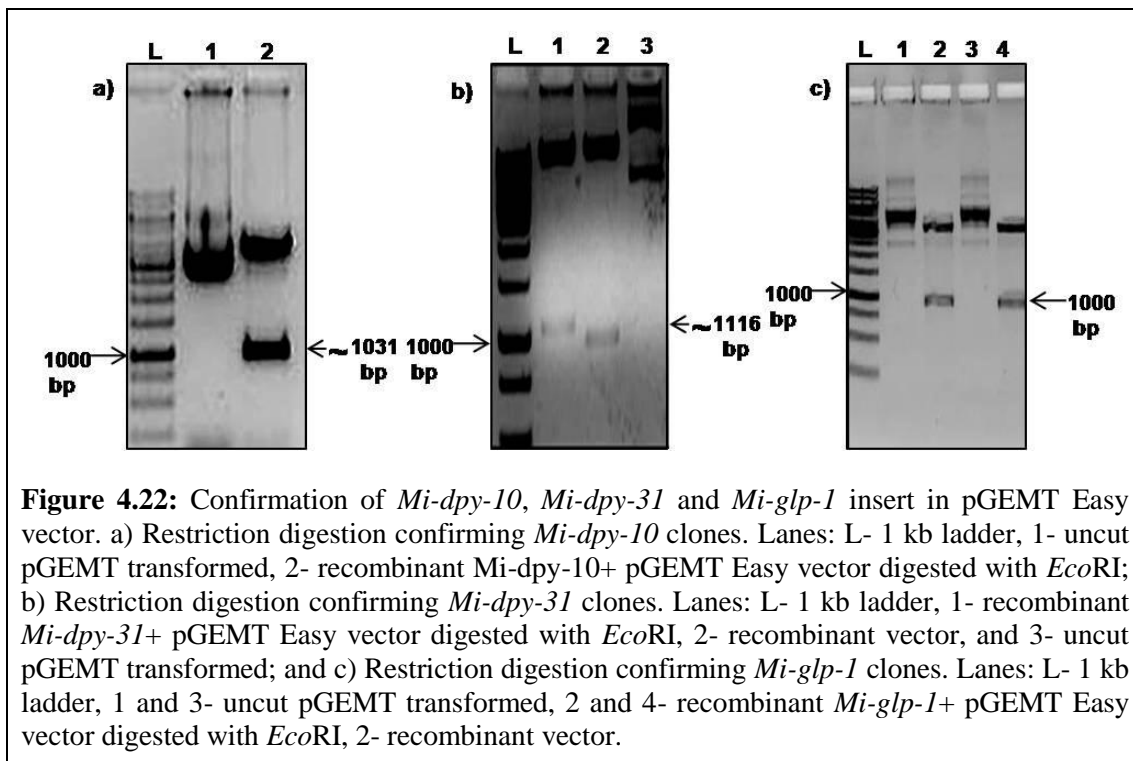


Figure 4.20: Transcript profiling of *dpy-10*, *dpy-31* and *glp-1* genes at different developmental stages in *M. incognita*. a) qRT-PCR based expression of *Mi-dpy-10*; b) qRT-PCR based expression of *Mi-dpy-31*; and c) qRT-PCR based expression of *Mi-glp-1*. The histogram indicates the relative fold change ($2^{-\Delta\Delta CT}$ value) normalized based on the actin gene as an endogenous gene and the female ΔCt value as a calibrator. The asterisks * and ** indicate significant differences at $p < 0.05$ and $p < 0.01$, respectively.

4.2.3 Cloning of partial mRNA of selected genes in pGEM®-T easy vector

The partial mRNA sequence of *dpy-10* (1.031 kb), *dpy-31* (1.116 kb) and *glp-1* (1 kb) were amplified with appropriate primers designed from the retrieved sequences. The amplified fragments were cloned in TA cloning vector pGEM®-T easy and recombinant clones were confirmed by colony PCR using gene specific primers (**Figure 4.21a, b and c**). The colonies which showed amplification of the desired length were then used for isolating plasmid and further verified by restriction digestion using *SacII* and *NotI* enzymes (**Figure 4.22**), followed by Sanger sequencing using universal primers namely, M13F and M13R primers. The vector sequence was removed from the obtained sequences using the Vecscreen software. Thus, a 1.031 kb, 1.116 kb, and 1 kb size of partial mRNA of *dpy-10*, *dpy-31*, and *glp-1* genes, respectively was successfully sequenced.





Objective 3: Evaluating the silencing efficacy of these genes in *Arabidopsis thaliana* confer the nematode resistance against *M. incognita*

4.3.1 Development of dsRNA constructs

The identified *dpy* genes have been reported to play a critical role in cuticle and *glp-1* gene in pharynx development in nematodes. Thus, targeting these genes for silencing might hamper the overall growth and development of *M. incognita* and thereby, aiding in controlling the infection. To achieve this objective, dsRNA constructs carrying sense and antisense strands of the selected gene were generated. For the development of *Mi-dpy-31* RNAi construct, gateway cloning technology was used, while *Mi-glp-1* RNAi construct was developed through conventional cloning strategy but first the partial mRNA sequences of these three genes were cloned into a pGEMT easy vector as described previously and sequenced using Sanger sequencing platform.

4.3.1.1 *glp-1* dsRNA constructs

A dsRNA expression construct of the *glp-1* gene was designed in the pBC vector (Yadav et al. 2006). Sense and antisense strands of *glp-1* each of 419 bp in size were amplified using gene-specific primers having restriction enzyme site at their 5'end (Figure 4.23). The sense and antisense strand of *glp-1* gene was successfully cloned into pBC6 RNAi vector driven by a CaMV35S promoter. The positive clones were confirmed by colony PCR, restriction digestion (Figure 4.24a and b) and by Sanger sequencing. The positive clones were restricted with *Bam*HI and *Xho*I to release sense strand of approximately (~) 400 bp long and on restriction digesting these clones with *Kpn*I and *Sac*I released antisense strand also of ~400 bp long. All the clones that released the same size of product after restriction were confirmed by sequencing. The positive clone was mobilized into *Arabidopsis* via *Agrobacterium* mediated transformation (Figure 4.24c).

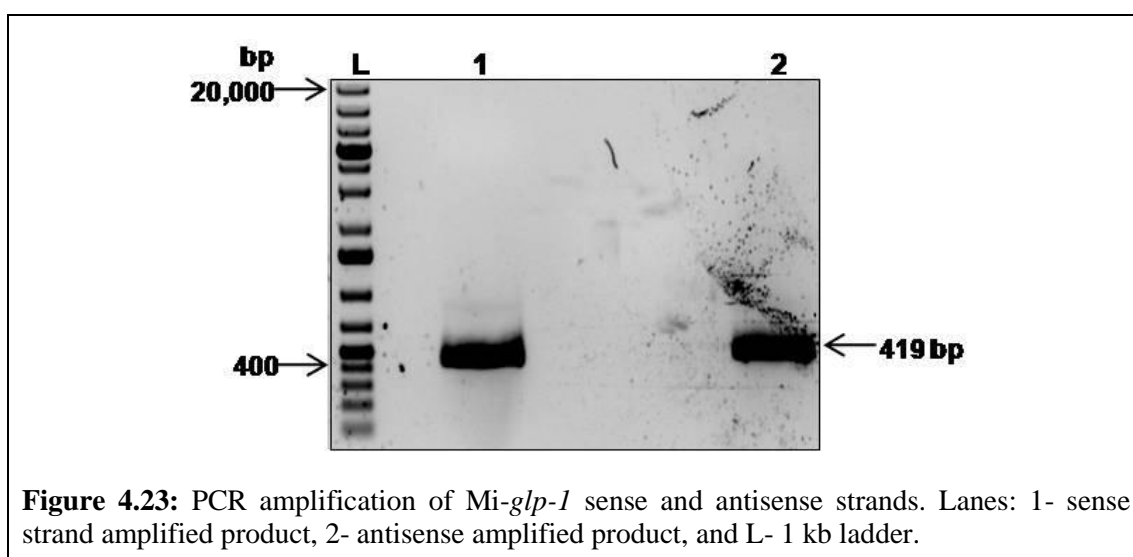


Figure 4.23: PCR amplification of Mi-*glp-1* sense and antisense strands. Lanes: 1- sense strand amplified product, 2- antisense amplified product, and L- 1 kb ladder.

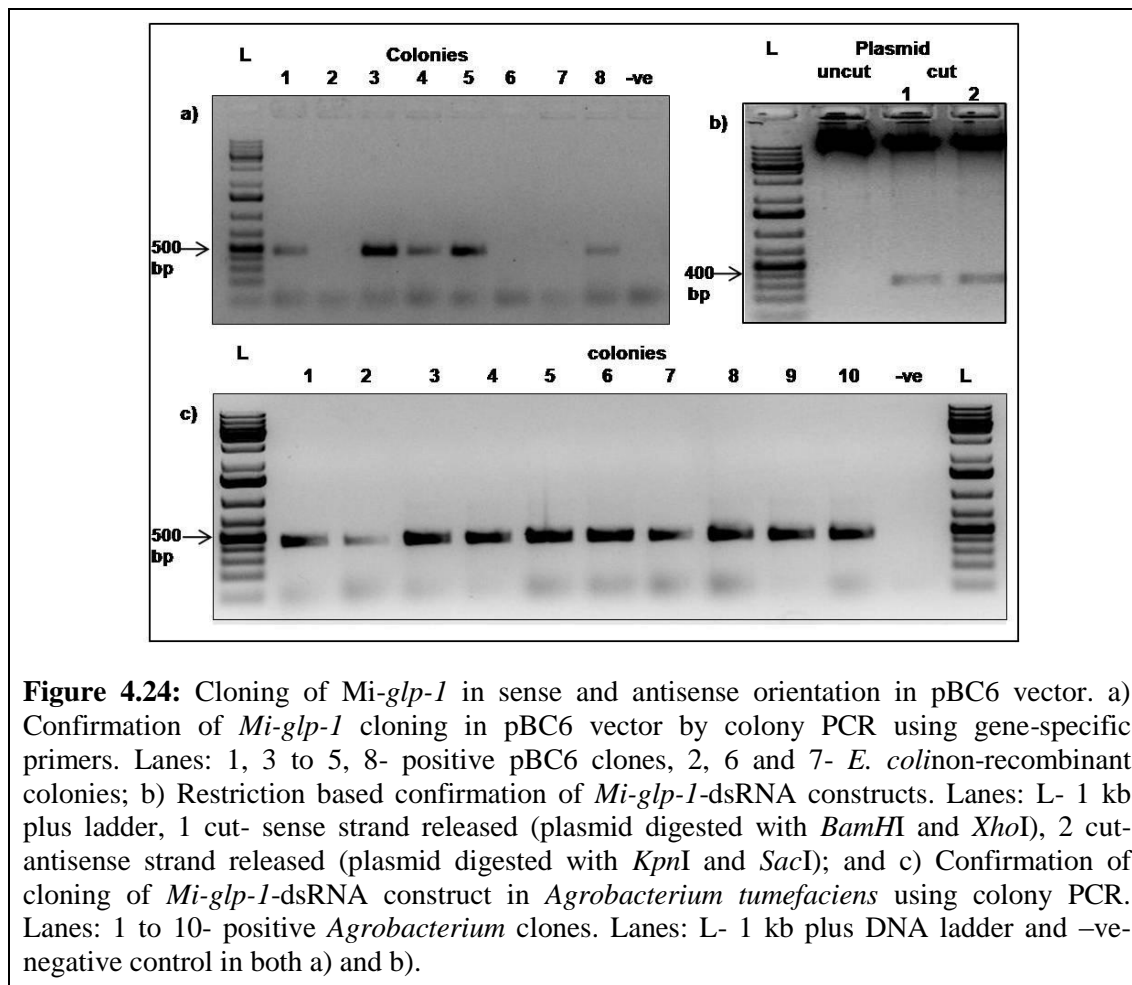
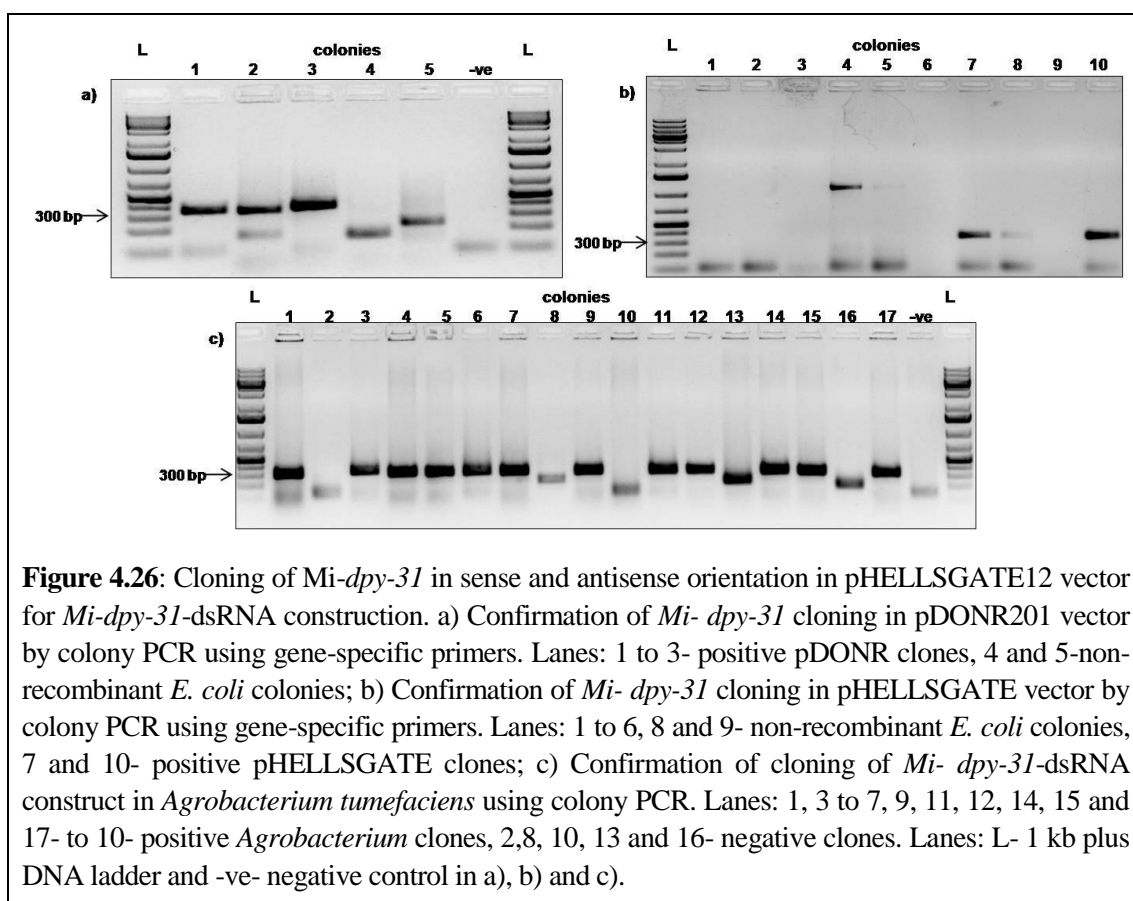
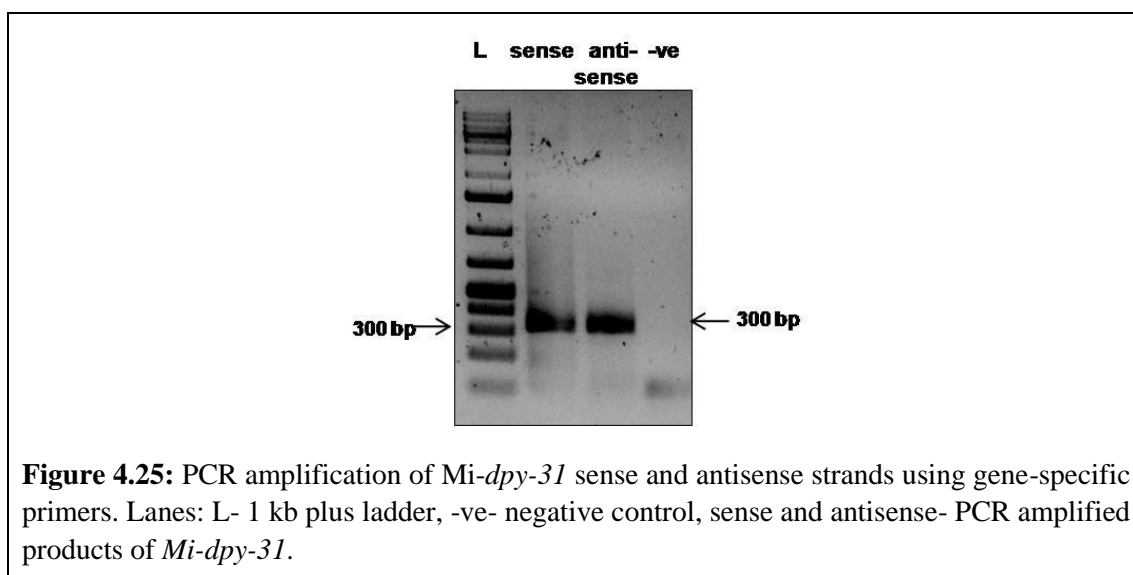


Figure 4.24: Cloning of *Mi-glp-1* in sense and antisense orientation in pBC6 vector. a) Confirmation of *Mi-glp-1* cloning in pBC6 vector by colony PCR using gene-specific primers. Lanes: 1, 3 to 5, 8- positive pBC6 clones, 2, 6 and 7- *E. coli* non-recombinant colonies; b) Restriction based confirmation of *Mi-glp-1*-dsRNA constructs. Lanes: L- 1 kb plus ladder, 1 cut- sense strand released (plasmid digested with *Bam*HI and *Xho*I), 2 cut- antisense strand released (plasmid digested with *Kpn*I and *Sac*I); and c) Confirmation of cloning of *Mi-glp-1*-dsRNA construct in *Agrobacterium tumefaciens* using colony PCR. Lanes: 1 to 10- positive *Agrobacterium* clones. Lanes: L- 1 kb plus DNA ladder and -ve- negative control in both a) and b).

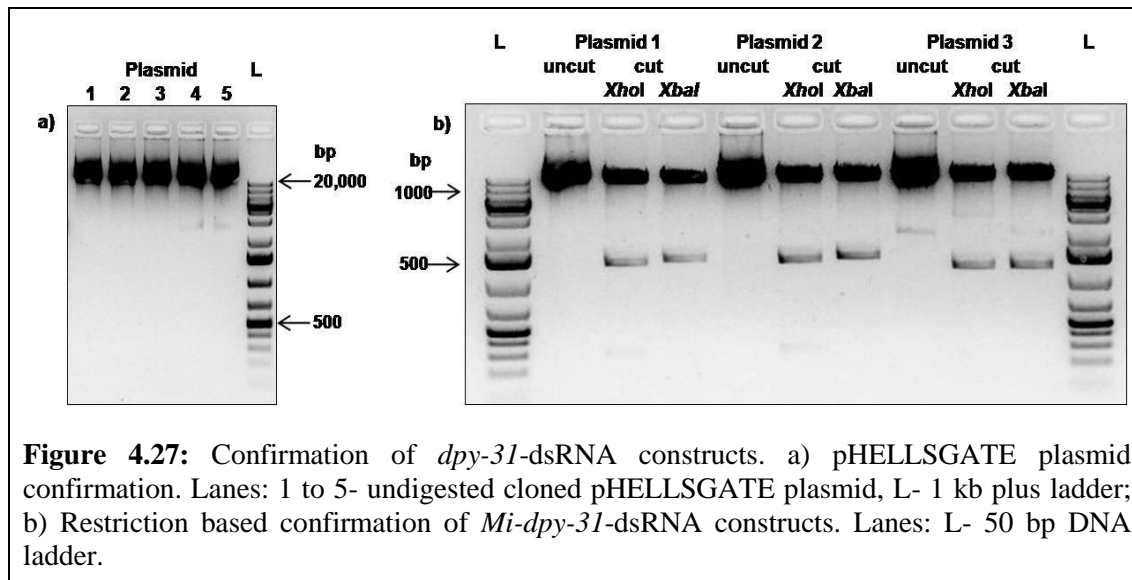
4.3.1.2 *dpy-31* dsRNA constructs

pDONR121 vector was inserted with sense and antisense strand of *dpy-31* gene each of approximately of 300 bp in length. For this, the PCR amplification was carried out using gene-specific primers and the amplified product was cloned into pDONR121 by a recombinant reaction. Thus, this way we were able to clone both the sense and antisense strands of *dpy-31* in a single reaction into this vector (**Figure 4.25**). The recombinant clones were confirmed by colony PCR and Sanger sequencing. Further by recombination reaction using LR recombinase enzyme *dpy-31* RNAi construct was prepared in pHELLSGATE12 vector (**Figure 4.26a, b and c**).



The positive clones were similarly confirmed by colony PCR, double digesting the plasmids using restriction enzymes *Xho*I (for sense strand) and *Xba*I (for antisense

strand) followed by Sanger sequencing (**Figure 4.27a and b**). The sense and antisense strands each of ~500 bp (300 bp (gene insert) + ~200 bp (vector sequence)) in length were released on double digestion of positive clones with restriction enzymes.



4.3.2 Determining *glp-1* and *dpy-31* efficacy as candidate for gene silencing

4.3.2.1 Over-expression of *Mi-glp-1* and *Mi-dpy-31* genes in *Arabidopsis thaliana*

RNAi lines expressing *Mi-glp-1* and *Mi-dpy-31*-dsRNA constructs were generated by transforming *Arabidopsis* plants. These lines were confirmed by kanamycin selection (**Figure 4.28a and b**) and integration of *Mi-glp-1* and *Mi-dpy-31* as transgenes in *Arabidopsis thaliana* was further confirmed by PCR amplification of gDNA isolated from each T₁ lines using respective gene-specific primers (**Figure 4.29a and b**). The over expression of genes under 35S promoter forms RNAi *glp-1* lines P1 and 2 and RNAi *dpy-31* lines P3 and P5.

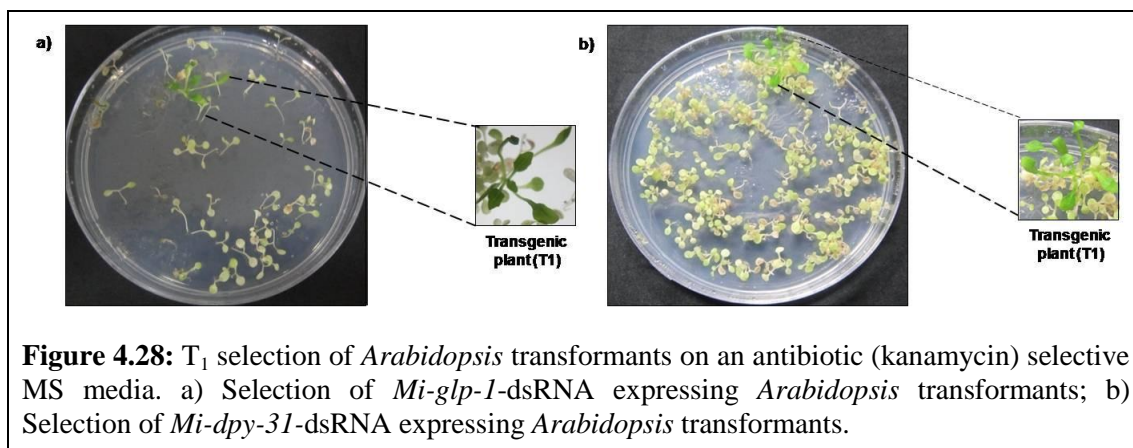


Figure 4.28: T₁ selection of *Arabidopsis* transformants on an antibiotic (kanamycin) selective MS media. a) Selection of *Mi-glp-1*-dsRNA expressing *Arabidopsis* transformants; b) Selection of *Mi-dpy-31*-dsRNA expressing *Arabidopsis* transformants.

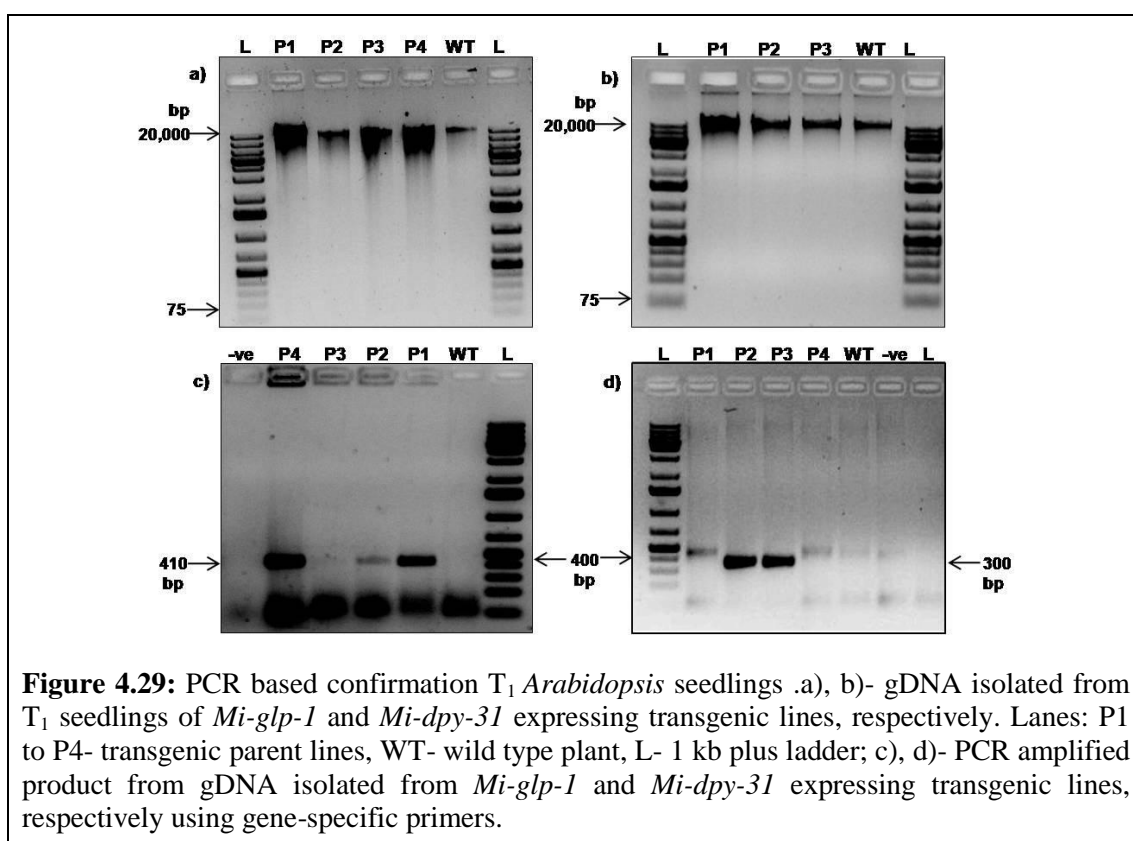


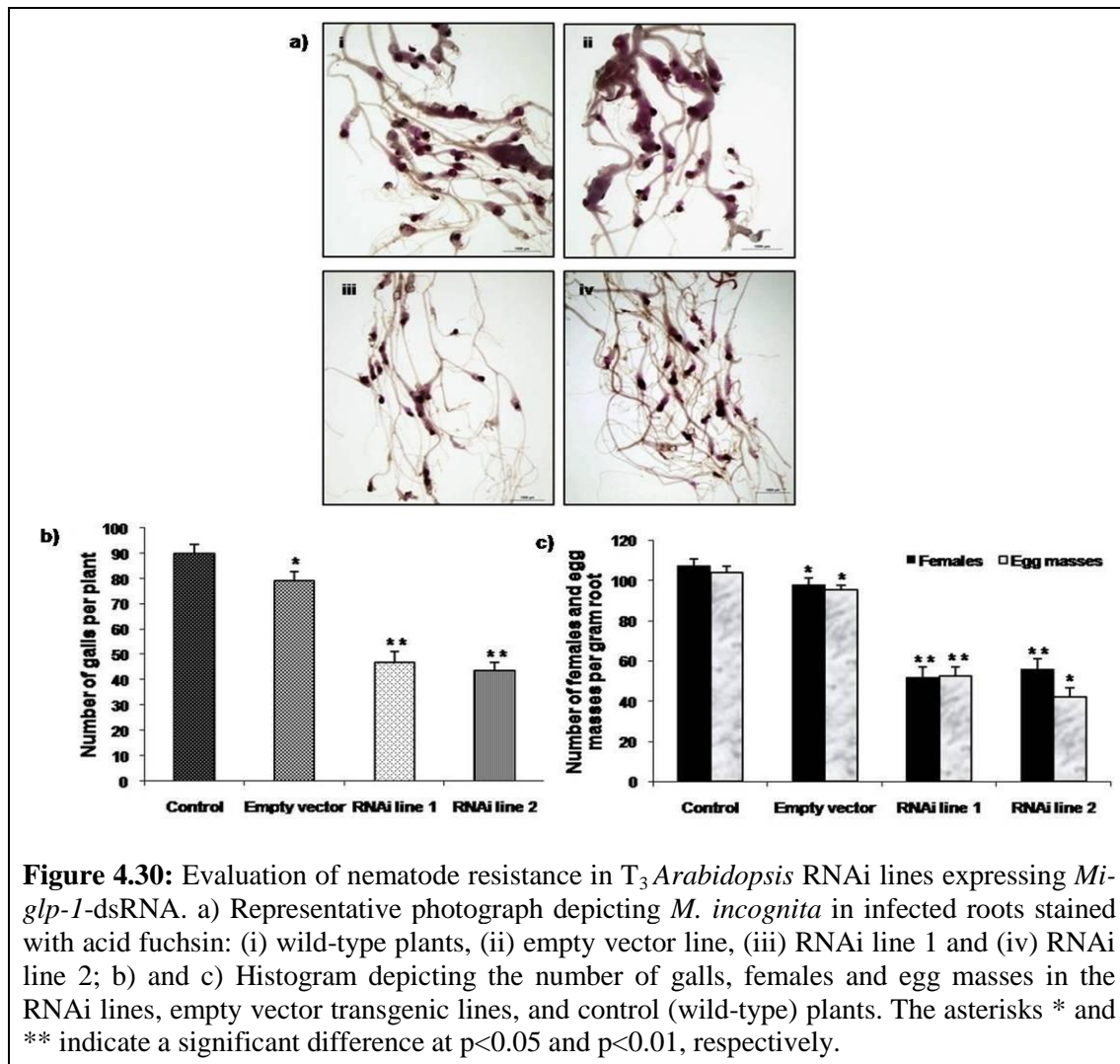
Figure 4.29: PCR based confirmation T₁ *Arabidopsis* seedlings .a), b)- gDNA isolated from T₁ seedlings of *Mi-glp-1* and *Mi-dpy-31* expressing transgenic lines, respectively. Lanes: P1 to P4- transgenic parent lines, WT- wild type plant, L- 1 kb plus ladder; c), d)- PCR amplified product from gDNA isolated from *Mi-glp-1* and *Mi-dpy-31* expressing transgenic lines, respectively using gene-specific primers.

4.3.2.2 Nematode infection assay on *A. thaliana* RNAi lines

Mi-glp-1

For evaluating the silencing efficacy of *Mi-glp-1*, T₃ seedlings of two independent transgenic lines were chosen and subjected to infection by parasitic juveniles. Two *glp-1* RNAi lines (RNAi line P1 and line P2) were evaluated, for which the nematodes

inside their roots were stained for determining the level of infection (**Figure 4.30a**). The *glp-1* RNAi lines exhibited a reduction in the number of galls (47.8 and 51.3%), females (51.5 and 47.79%) and egg masses (49.3 and 59.4%) compared to control and transgenic plants harboring empty vector (**Figure 4.30b and c**).



Altogether, both the transgenic RNAi lines had the significant reduction in number of galls, females and egg masses indicating a deleterious effect of silencing of this targeted gene on the growth and development of nematodes. The adult female nematodes were isolated, and their sizes were analyzed to determine any phenotypic effects, if any, on *M. incognita*.

Length and width were measured for each female using a scale on a Nikon microscope (**Figure 4.31**). The females dissected from control plants had an average length and width of 396.27 μm and 248.18 μm , respectively. However, females isolated from RNAi lines were significantly smaller and had an average length and width of 231.9 μm and 140.36 μm , respectively (**Table 4.3**). Therefore, there was a reduction of 41.4% and 43.4% in their length and width, respectively, in the nematode females feeding on RNAi lines.

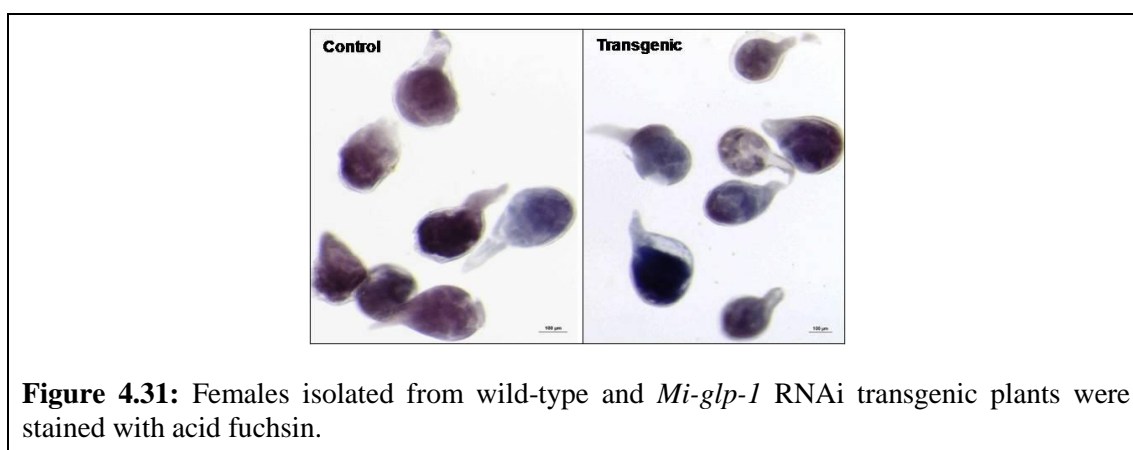


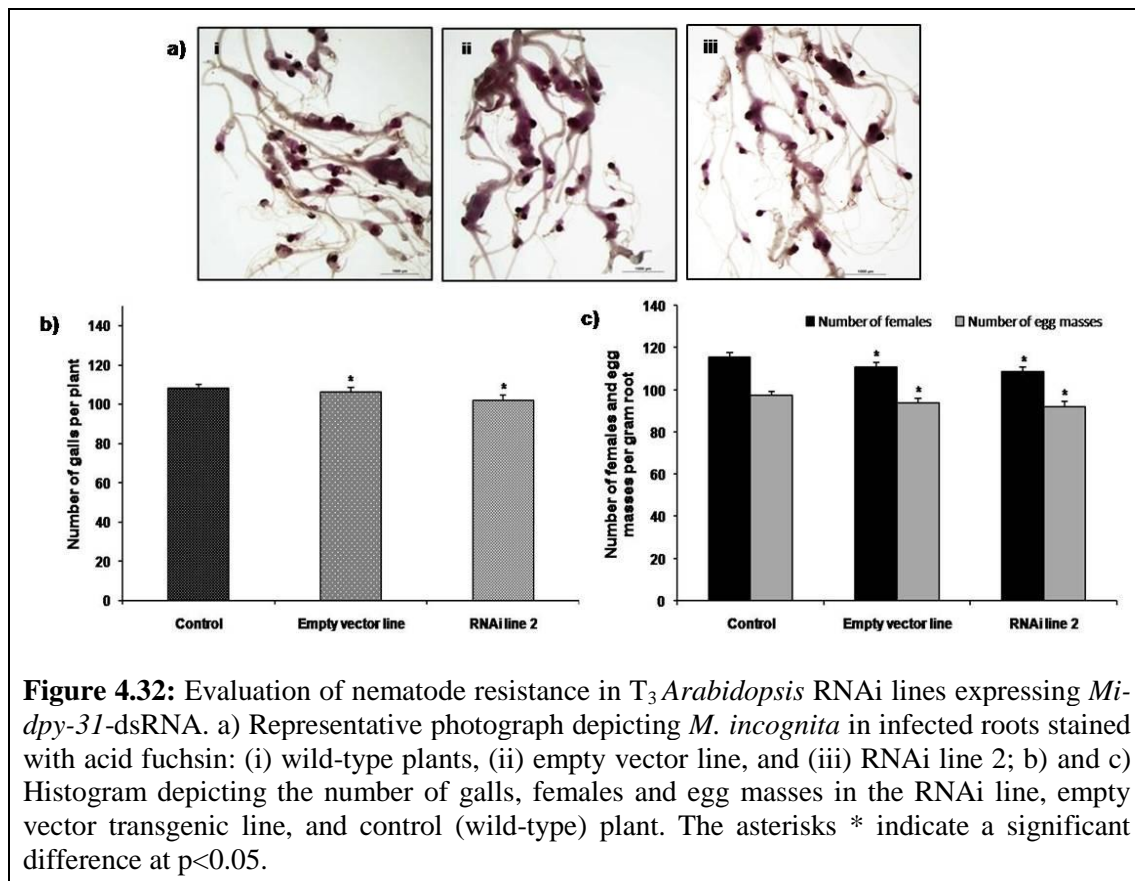
Figure 4.31: Females isolated from wild-type and *Mi-glp-1* RNAi transgenic plants were stained with acid fuchsin.

Table 4.3: Size evaluation of females obtained from wild-type plants and *Mi-glp-1* transgenic RNAi lines.

Female	Wild type		RNAi line	
	Length (μm)	Breadth (μm)	Length (μm)	Breadth (μm)
1	343	206	249	180
2	442	299	181	130
3	243	295	263	164
4	530	368	234	142
5	462	350	253	135
6	515	308	213	111
7	498	342	183	114
8	443	338	287	136
9	488	233	242	124
10	355	196	267	187
11	374	390	179	121
Average	426.64	302.273	231.9	140.36

Mi-dpy-31

In case of *dpy-31*, the silencing efficacy was evaluated by growing T₃ transgenic lines P3 and P5 on soilrite. The J2(s) were sterilized and each plant was inoculated with 1000 J2(s). The *dpy-31* RNAi line 3 and RNAi line 5 exhibited a reduction of only 6.93 and 2.7 %, respectively in terms of a number of galls (Figure 4.32a). These lines exhibited a reduction in the females (4.3 and 1.8%) and egg masses (3.4 and 5.3%) compared to control and transgenic plants harboring empty vector (Figure 4.32b and c). Thus, the *dpy-31* RNAi lines did not show significant resistance to nematodes. Even the length and breadth for each adult female was when measured using a scale on a Nikon microscope, not much difference was observed (Figure 4.33; Table 4.4). Thus, no phenotypic effect was noticed.



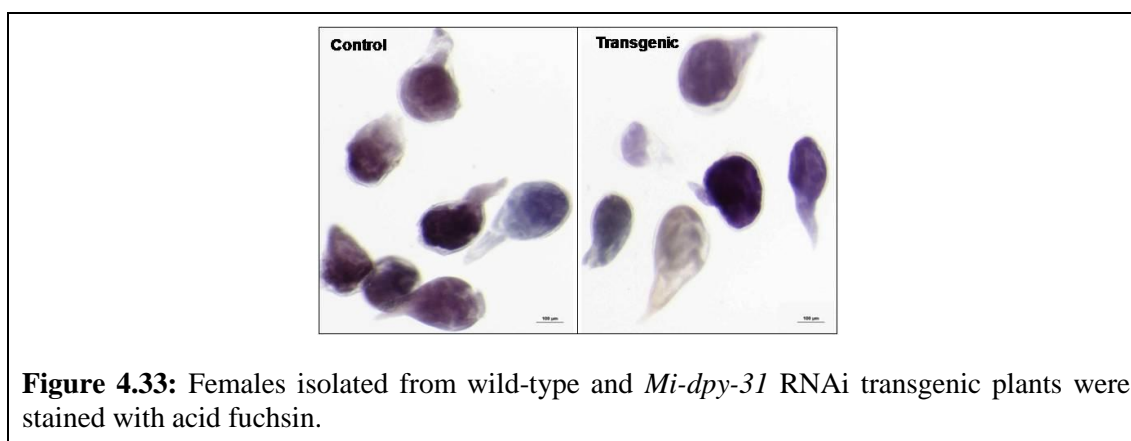


Figure 4.33: Females isolated from wild-type and *Mi-dpy-31* RNAi transgenic plants were stained with acid fuchsin.

Table 4.4: Size evaluation of females obtained from wild-type plants and *Mi-dpy-31* transgenic RNAi lines.

Female	Wild type		RNAi line	
	Length (µm)	Breadth (µm)	Length (µm)	Breadth (µm)
1	343	206	289	272
2	442	299	397	354
3	243	295	454	257
4	530	368	409	312
5	462	350	471	303
6	515	308	423	284
7	498	342	383	270
8	443	338	512	376
9	488	233	495	307
10	355	196	340	211
11	374	390	401	362
Average	426.64	302.273	415.818	300.727

4.3.2.3 Molecular analyses of RNAi lines through qRT-PCR and northern blotting

The transcript abundance of the *glp-1* gene in females isolated from both the RNAi lines showed an approximately 60% reduction compared to females isolated from control plants (**Figure 4.34**).

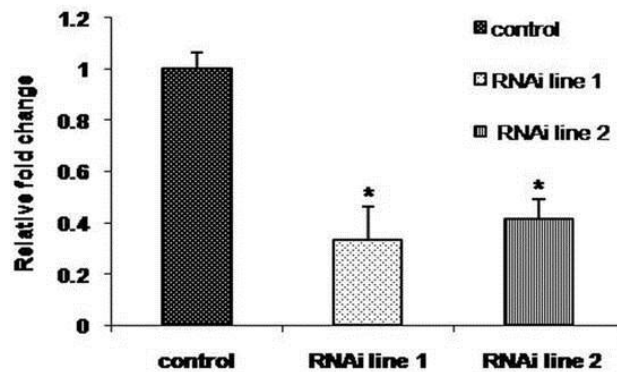


Figure 4.34: RT-qPCR-based *glp-1* expression analysis of *M. incognita* females isolated from infected roots of RNAi lines 1 and 2 and females isolated from control plants.

This decrease in the transcript levels of *glp-1* in females feeding on RNAi lines demonstrates the effect of its silencing through Host-delivered dsRNA. Although not much decrease in the infectivity of *M. incognita* on *dpy-31* RNAi lines was observed, a 35% reduction at the transcripts levels of *dpy-31* was observed in females extracted from the infected RNAi lines compared to females isolated from control plants (**Figure 4.35**).

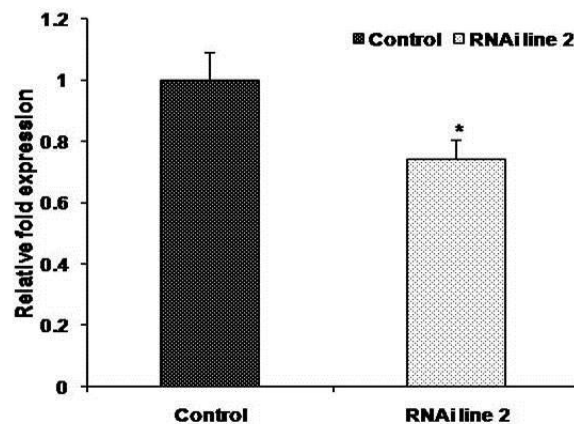
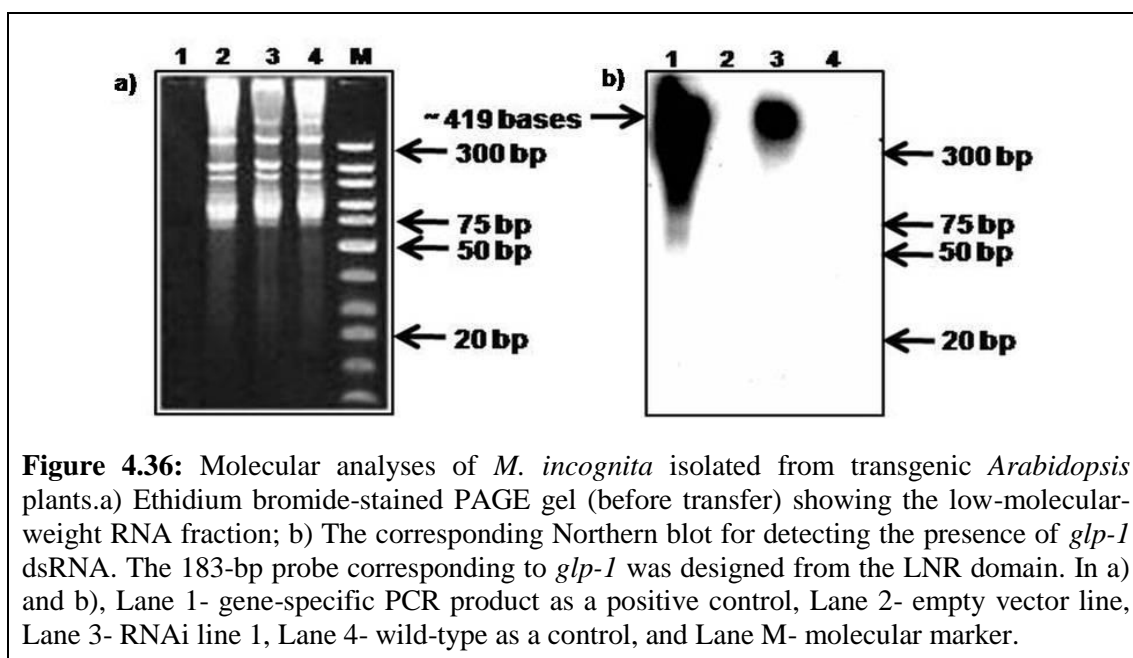


Figure 4.35: RT-qPCR-based *dpy-31* expression analysis of *M. incognita* females isolated from infected roots of RNAi line 2 and females isolated from control plants.

With the aim to determine the accumulation of *glp-1*-specific dsRNA in RNAi lines expressing *glp-1* partial cDNA, the transformants were analyzed through Northern

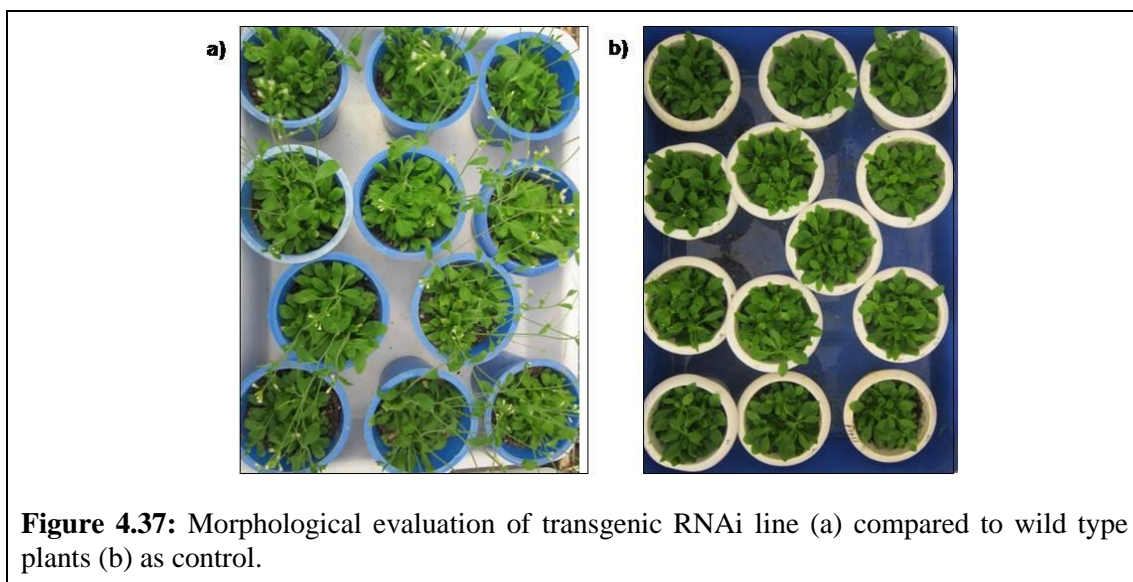
hybridization. Low molecular weight RNAs isolated from the RNAi line, empty vector line, and control plant were transferred to nylon membrane. The hybridization confirmed the presence of *glp-1* dsRNA in RNAi line 1 which would be processed into siRNAs (**Figure 4.36a and b**). One of the key components of host-mediated RNAi was the 419-bp dsRNA of *glp-1*, which was detected in the transgenic RNAi line. Also, no signal was observed in the case of control and empty vector RNAi lines. However, detection of dsRNAs or siRNAs was not preceded with *dpy-31* RNAi lines due to the non significant reduction in *M. incognita* infection level exhibited by these lines.



4.3.2.4 Phenotypic evaluation of RNAi lines expressing nematode dsRNA of *glp-1* and *dpy-31* gene

Although RNAi is believed to be highly sequence-specific and the region utilized in the present study has been rigorously evaluated *in silico* for homology searches, host-derived

siRNAs may elicit off-target effects (Charlton et al. 2010). In order to ascertain whether the manipulation of plant genome/ production of siRNAs have any adverse effect on plant development, the selected RNAi lines were compared morphologically with the control plants. No significant visible phenotypic anomalies were observed between the *glp-1*-RNAi line, *dpy-31*-RNAi line and control plant (**Figure 4.37a and b**). Moreover, these lines also successfully completed their life cycle by producing viable seeds.



4.3.3 Effect of silencing on *M. incognita* fecundity and next-generation J2s

The females feeding upon *glp-1* RNAi lines produced fewer numbers of egg masses compared to wild-type plants. The number of eggs present in these egg masses was further evaluated to determine the deleterious effect, if any, of silencing the *glp-1* gene. A 26% reduction in the number of eggs was noted in the *glp-1* RNAi lines. Nematode multiplication factor (MF) was then calculated to determine the reproductive potential of *M. incognita* in RNAi lines and wild-type plants. The MF value of *M. incognita* infecting transgenic RNAi lines was calculated as 11.57, whereas that of nematodes

infecting wild-type plants was 31.1 (Table 4.5). Several J2s isolated from *glp-1* RNAi lines showed aberrations around the metacarpus region, along with a shorter distance from the stylet to the metacarpus region of pharyngeal structures (Figure 4.38; Table 4.6). Thus, it can be deduced that adverse effects on J2s is due to the inherent nature of RNAi inherited from one generation to the next. There are studies in *C. elegans* that show inherited effects of silencing even in the absence of the original trigger (Bird et al. 2009). The persistence of silencing effects has also been observed when the *Mi-1* gene of tomato was suppressed (Gleason et al. 2008). However, MF value for *dpy-31* did not reveal much effect on silencing.

Table 4.5: Numbers of eggs counted for *M. incognita* feeding on wild-type plants and RNAi plants for calculating MF value.

Number of egg masses			Number of eggs per egg mass		
	Wild type	Transgenic line 2		Wild type	Transgenic line 2
1	87	45	1	283	188
2	125	39	2	307	213
3	102	50	3	337	250
4	117	54	4	326	168
5	92	57	5	335	256
6	96	37	6	318	245
7	114	80	7	239	148
8	100	53	8	314	217
9	89	82	9	264	278
10	109	29	10	277	237
Average	103.1	52.6	Average	300	220

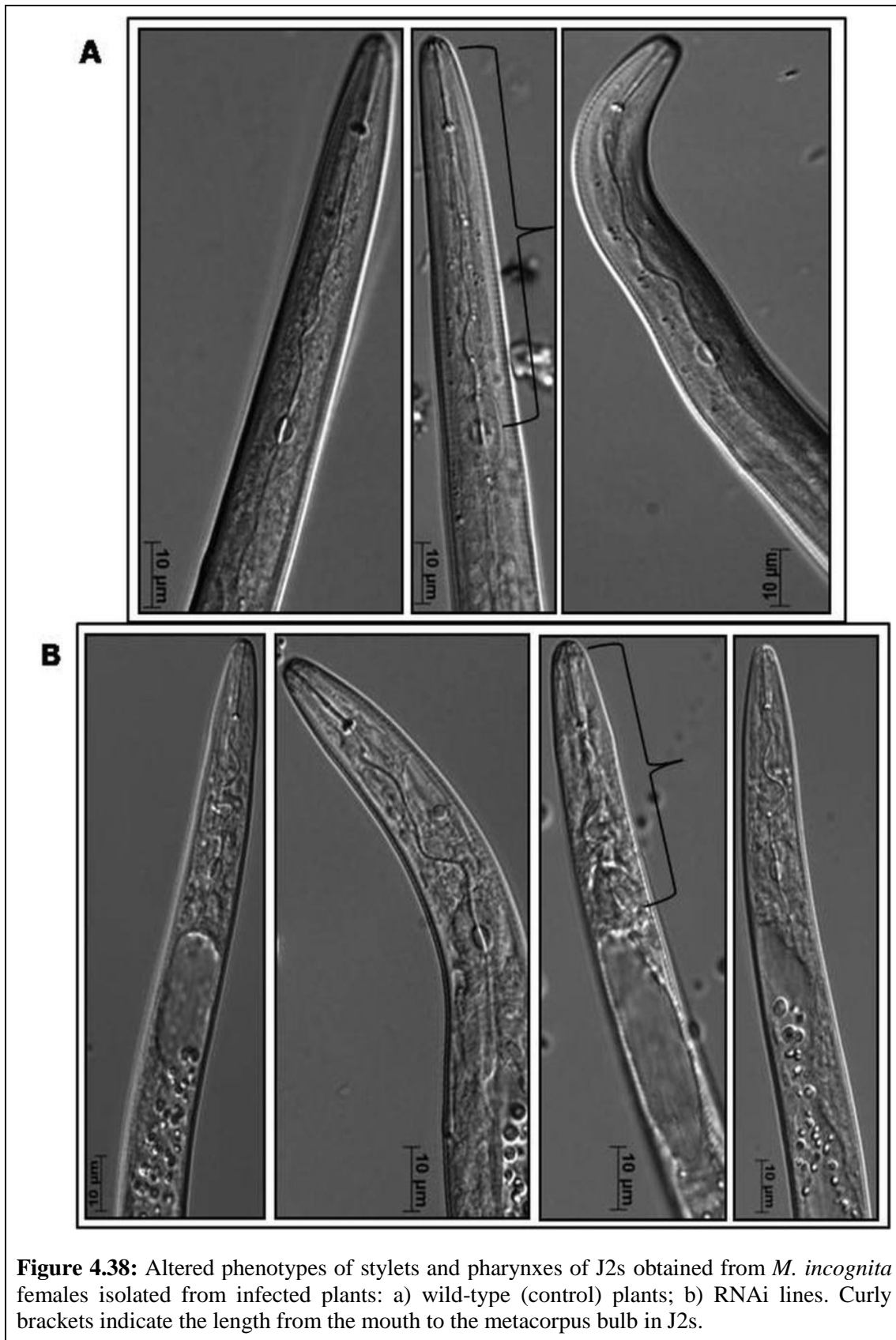


Figure 4.38: Altered phenotypes of stylets and pharynxes of J2s obtained from *M. incognita* females isolated from infected plants: a) wild-type (control) plants; b) RNAi lines. Curly brackets indicate the length from the mouth to the metacarpus bulb in J2s.

Table 4.6: Adverse effect on J2s obtained from *M. incognita* females isolated from infected RNAi and wild-type plants.

		Stylet length	Length from Mouth to metacarpus
wild type J2s	1	10	45
	2	14	47
	3	11	46
	4	11	44
	5	16	54
	6	11	58
	7	11	47
	8	16	65
	9	14	63
	10	16	68
RNAi J2s	1	10	41
	2	8	35
	3	9	39
	4	9	39
	5	11	42
	6	10	45
	7	10	42
	8	14	45
	9	15	56
	10	13	46

Chapter 5
Discussion

5. DISCUSSION

Very few genes that have a decisive function in the organ development of a plant-parasitic nematode that aids during infestation are known. Thus, the main concern of this study was to examine genes that have a crucial role in the development of cuticle and pharynx of *M. incognita*. Because it is by virtue of these organs *M. incognita* is able to establish an endoparasitic sedentary relationship with its plant host for successfully completing its life cycle inside the host. Our work here suggests that two cuticle genes identified viz. *Mi-dpy-10* and *Mi-dpy-31* functions in the formation of cuticle and have an important role in moulting. Another gene, *Mi-glp-1* identified is responsible in embryonic development of pharynx in *M. incognita*. The work was not focussed only on indentifying and characterizing these genes but also to evaluate their potential as a novel target in developing nematode resistant plants.

Astacin metalloprotease genes for cuticle development in *M. incognita*

Dumpy (DPY) class of proteases is also known as astacins proteins. The presence of astacins in different nematodes indicates conserved function and expansion of astacin protein family in nematodes for example, on basis of in silico analysis 30 astacins present in *M. hapla*, 37 in *M. incognita*, 13 in *B. malayi* and some in *M. chitwoodi*, *Parastronglyoides trichosuri* and *Trichinella spiralis* were reported (Craig et al. 2007; Park et al. 2010). From previous reports it is evident that genes responsible for synthesis of nematode cuticle are found similar in free-living as well as parasitic-nematodes, hence, *Mi-dpy-10* and *Mi-dpy-31* reported in this study are ortholog of *Ce-dpy-10* and *Ce-dpy-31*, respectively. *Mi-dpy-10* despite encoding protein of similar number of

amino acids as *Ce-dpy-10*, disparity in the size of the gene between the two was noticed in our analysis. The most likely explanation of this difference might be due to assembly of *M. incognita* genome in scaffold forms which resulted in truncated sequence. The presence of genome assembly in this form could also be a reason for obtaining two hits of *Mi-dpy-31* in our analysis, both showing more than 70% similarity to *Ce-dpy-31*. But the presence of these hits at two different scaffolds may indicate these two as different copies of *dpy-31* gene that might have resulted from an event of duplication during speciation. Nonetheless, 95% similarity both at the nucleotide as well as amino acid level was revealed when the two sequences were compared. Moreover, EGF domain that is reported in *Ce-DPY-31* was absent in both these copies of *Mi-DPY-31* protein.

Dumpy genes have been grouped into different subgroups based on the domain organization (Park et al. 2010). From our motif search output it was evident that *Mi-dpy-10* and *Mi-dpy-31* belongs to *dpy-2* and subgroup V, respectively (Johnstone, 2000; Park et al. 2010). *dpy-2* subgroup consists of only two members having a defined function in post-embryonic development stages. Whereas, members of subgroup V have been shown to express in hypodermis and involved in collagen processing for cuticle formation. The motif search revealed the presence of conserved Gly-X-Y repeats interrupted by cysteines residues in *Mi-DPY-10* which is noticed in accordance with *Ce-DPY-10*. It also showed presence of a longer C-terminal tail than average which is a characteristic of *DPY-10* protein. Apart from astacin and CUB domains, regions like conserved zinc-binding active site (HExxHxxGFxHExxRxDRD) and methionine-turn (SxMHY) domain which are characteristic of *DPY-31* was found in our motif search. This study reports the conserved sequence of catalytic and methionine-turn sites in *Mi-DPY-31* for the first time, HEVAHALGFWHEQSRPDRD and SIMHY, respectively.

The highly conserved nature of these sites was further disclosed from the multiple sequence alignment analysis which revealed a 100% identity in these two sites among all the nematodes across different phylum. All the domains identified in both cuticle genes have been well studied in cuticle development of nematodes. Hitherto, presence of these extremely conserved motifs in Mi-DPY-10 and Mi-DPY-31 suggests their role in cuticle formation and development in *M. incognita*.

The regulated spatial and temporal expression of *dpy* genes is very well established in *C. elegans* and has been described as early, intermediate or late expressing genes on basis of its mRNA abundance (Page and Johnstone, 2007). A higher transcript level of *Mi-dpy-10* in the J2 stage i.e. in early development in *M. incognita* is in good agreement with that observed in *Ce-dpy-10*, which is a typical trait of members belonging to subgroup *dpy-2*. Hence, significant role of *Mi-dpy-10* during moulting of J2 stage to form J3 in *M. incognita* has been demonstrated for the first time in root-knot nematodes. Unlike *dpy-10*, *dpy-31* is known to express throughout the life cycle of nematode, with specifically in early larval stages (Novelli et al. 2004; Stepek et al. 2015). In contrast to some reports in the literature, higher expression of *Mi-dpy-31* in the later stage of development i.e. in adult females in our expression analysis implies a species-specific role of *dpy-31* in parasitic-nematodes.

This research was not only restricted in indentifying new potential targets for silencing but was also intended to evaluate the silencing efficacy of few key genes for host-mediated RNAi approach. RNAi has revolutionized the control mechanisms for pests like plant-parasitic nematodes. Host-delivered RNAi-mediated root-knot nematode resistance is now an established technology. A few developmental genes, such as Rpn7

(essential for the integrity of the 26S proteasome), *nhr-48*, FAR-1, splicing factor and integrase genes, have been targeted using RNAi for controlling infection in the root-knot nematode *M. incognita* (Yadav et al. 2006; Niu et al. 2012; Iberkleid et al. 2015; Lu et al. 2016). Consequently there is always a need to identify better candidate genes. RNAi based silencing of dumpy genes showed cuticle alterations in *C. elegans* mutants. Dumpy genes have also been targeted for controlling animal-parasitic nematodes in animals (Steppek et al. 2015). Thus, we performed host-mediated RNAi experiments using *Mi-dpy-31* as target. But the infectivity of *M. incognita* in terms of equal number of galls produced, number of females developed and egg masses produced by nematode in both *dpy-31* RNAi lines and control plants clearly indicated a non-significant resistance against *M. incognita*. The finding proposes that silencing of *dpy-31* gene alone will not make much of the significance difference in controlling *M. incognita*. This inference is based on the findings of my study which are restricted to targeting single gene for host-delivered RNAi. Thus, what is required is the combinatorial silencing effect of more than one gene belonging to a multigene family that is detrimental to the growth of parasitic nematode. Clearly, further research is needed to validate this contention.

Pharynx gene and enhanced resistance of *glp-1* RNAi lines to *M. incognita* infection

This study also explores the role of *Mi-glp-1* in developing pharynx structure in *M. incognita* and its possibility as a potential target gene for host-mediated RNAi strategy. The genome-wide computational analysis revealed a single contig (MiV1ctg1087 or Minc16055) as a Notch receptor protein. Interestingly, to the authors knowledge this was the first time a gene involved in pharynx growth in *M. incognita* is identified and

reported except one study that reported Minc16055 as putative Mi-GLP-1 protein in the course of identifying microsatellite loci in *M. incognita* (Castagnone-Sereno et al. 2010).

The study attempts to evaluate the conservation of *Mi-glp-1* across nematode phylum. The phylogenetic analysis clearly demonstrated that Mi-GLP-1 product has putative functions closely related to the Ce-GLP-1 protein. Although a disparity in the nucleotide length of the mRNA sequences was revealed resulting in the overall different gene organization and structure of *Mi-glp-1*. One rational explanation of this difference in the exon/intron structure could be the scaffold form of *M. incognita* genome from which the sequence was retrieved and hence, a truncated protein was obtained. Intriguingly, this difference in mRNA length was also noticed while analysing *G. pallida glp-1* thus in consistent with that of *Mi-glp-1*. The presence of conserved domains such as LNR repeats known to mediate ligand-binding and ANK along with RAM requisite for signaling responses (Kelley et al. 1987; Rebay et al. 1991; Heitzler and Simpson, 1993; Artavanis-Tsakonas et al. 1999) further confirms the similarity in the property and structure to that of a receptor protein consisting of varied domains, each with a specific function. Thus, from the conserved domains including predicted transmembrane domain which is in concurrent with that of Ce-GLP-1 it appears that Mi-GLP-1 has a plausible role as a receptor protein, although a clear mechanism of interaction has not been determined. The absence of EGF domain in Mi-GLP-1 also divulges certain structural and functional differences of GLP-1 between *C. elegans* and *M. incognita*.

Since GLP-1 a receptor protein, it was hypothesized that certain DNA binding sequences for ligands might be present on GLP receptor. As observed from the motif

search analysis presence of LAG-1 ligand binding sequence at more than one site on Mi-GLP-1 supports our hypothesis. This finding is consistent with the previous report on Ce-LAG-1 DNA binding sites, implying its function in LIN-12/GLP-1 signaling pathways (Christensen et al. 1996). Experiments such as yeast two-hybrid assays and co-precipitation of proteins *in vitro* have demonstrated direct interactions between LAG-1 and the GLP-1 receptor via these domains in nematodes (Roehl et al. 1996). Thus, based on the *in silico* analyses and the available literature, it can be concluded that the deduced gene in this study is a Notch receptor protein present in *M. incognita*.

Another aim of the thesis was to explore whether *glp-1* exhibit differential expression as reported in *C. elegans* or is it ubiquitously present in all the stages of plant-parasitic nematode. The higher transcript level in egg masses suggests important role of *Mi-glp-1* during embryogenesis which is in good agreement with previous studies (Priess et al. 1987; Austin and Kimble, 1989). Although expression pattern of *Mi-glp-1* is generally in line with the reported studies there is one aspect in which it differs. A noticeable increase in *Mi-glp-1* transcript in mature females, suggests a possible role during later stages of RKN development as well. Future experiment determining localization of this gene product will confirm the role of GLP-1 during female development in *M. incognita*.

A dsRNA/siRNA strategy was also used for host-mediated RNAi-based suppression of *Mi-glp-1*, similar to that of *Mi-dpy-31*. Plant-mediated down regulation of putative *Mi-glp-1* provided resistance against *M. incognita* in stable transgenic *Arabidopsis* RNAi lines harbouring *glp-1*-specific dsRNAs. An approximately 47% reduction in the

infection level was recorded in two independent *glp-1* RNAi lines. Decrease in the gall formation, female infestation, and egg mass production were also observed in these RNAi lines. Transgenic *Arabidopsis* lines expressing dsRNA against *Mi-glp-1* subjected to *M. incognita* infection did not show any phenotypic changes compared to wild-type plants. The nematode females isolated from control plants had an average length and width similar to the reported body length (ranging from 510-690 μm) and width (300-430 μm) of a healthy mature *M. incognita* female (Whitehead, 1968; García and Sánchez-Puerta, 2012). However, a decrease in the overall body size was evident in RNAi females but whether this decrease was a direct result of the low expression of *glp-1* is not yet clear. Direct evidence supporting a role of *glp-1* in the growth of *M. incognita* at later stages in the life cycle has not yet been reported. These results unequivocally demonstrated the suppression of *glp-1* in females feeding on RNAi lines.

Additionally, to further confirm our claim of successful RNAi based silencing of *glp-1*, relationship between RNAi transgene, small RNA concentrations and *M. incognita* resistance were examined by detection of dsRNA molecules by Northern hybridization. We were able to confirm the presence of *glp-1*-specific dsRNA molecules in the transgenic lines, an important factor for successful host-mediated RNAi (Bass, 2000; Agrawal et al. 2003), but unfortunately could not verify *glp-1*-specific siRNAs despite numerous attempts. Several studies have reported a similar problem for other genes, which is most likely due to the low sensitivity of Northern blot analysis (Dinh et al. 2014a). The ability of *M. incognita* to ingest large molecules and the presence of four dicers in *Arabidopsis*, which might in all likelihood have processed *glp-1*-specific dsRNA (as shown in our Northern analysis) into siRNAs that could thereby trigger RNAi responses in *M. incognita* females feeding on transgenic RNAi lines may also have played a role.

These findings thus suggest suppression of *Mi-glp-1* in females feeding onto RNAi transgenic lines. But what effect does the suppression of *glp-1* eventually has on the phenotype of *M. incognita* females and their fecundity efficiency, structured the next aim of our study. To investigate this, hatching capability of egg masses hand-picked from all females infecting RNAi lines, control, and empty vector plants was determined and a decrease in J2s population was noticed. Reduced infectivity of *M. incognita* on RNAi lines compared to control plants was experimentally confirmed by calculating MF value which appeared lower in number. On the basis of reports in literature on maternal lineage of *glp-1* RNA in *C. elegans* (Evans et al. 1994), it was postulated that *glp-1*-dsRNA might have even affected the progeny produced from affected females. To prove our contention, next-generation J2s were observed for phenotype abnormalities. In these J2s, aberrations in the structures of meta-corporeal bulbs such as decrease in the length of a region from the stylet to the metacarpus was evident, along with some anomalies in their stylet discs, were clearly apparent. A similar degraded structure of intestinal tissues of *M. incognita*, wherein Sep1, a novel serine protease, was identified as a potent bio-agent from *Bacillus firmus* for controlling plant-parasitic nematode populations was described (Geng et al. 2016). Thus, it can be inferred that the females obtained from transgenic plants showed effects on the foregut region of their descendants. Our results offer suggestive transmission of dsRNA-mediated deleterious effects to the next generation of root-knot nematodes. A more detailed study of the observation is required.

Altogether, identifying and characterizing new development genes in *M. incognita* is the need of the hour. It would be interesting to investigate RNAi resistance on stable transgenic lines of other important crops such as tomato, potato and sugarcane against

M. incognita using these developmental genes in a plant-mediated RNAi approach. An extensive research for understanding the development and behaviour of these pathogens will enable researchers in selecting better targets for host-mediated gene silencing for controlling the nematode menace.

Chapter 6
Summary and Conclusion

6. SUMMARY AND CONCLUSION

The nematode cuticle acts as a defensive shield for both plant and animal-parasitic nematode by preventing them from phagocytosis. It is the cuticle that enables *M. incognita* to inhabit the host as sedentary endoparasites. On that account cuticle is indeed vital for nematode survival, consequently targeting genes that are involved in cuticle formation and development will be benefitted in combating such parasites. The present study reports the identification and characterization of two cuticle related genes namely, *dpy-10* and *dpy-31* in *M. incognita*. It also demonstrates the significance of these genes in organ development of RKN at its different life stages thereby imparting parasitism abilities to it. A highly conserved nature as exhibited from the phylogenetic analysis among different nematode phylum illustrate critical role of these genes in worms.

There are reports on dsRNA-mediated gene silencing administering cuticle genes as a target such as *dpy 2, 4, 10* and *11* in *Bursaphelenchus xylophilus* (Wang et al. 2016). Thus, potential of dumpy genes as a target in governing nematode infestation is very well understood by biologists. *Mi-dpy-10* and *Mi-dpy-31* identified in this study could be potent targets for developing transgenics conferring resistance against plant-parasitic nematodes using host-mediated RNAi approaches. However, the findings of this study suggest that *Mi-dpy-31* alone cannot serve as a successful target for mediating gene silencing in plant-parasitic nematode. One of the possibilities is since *dpy-31* belongs to a multigene family; a pyramidal effect of more than one dumpy gene together for developing transgenic might present a better solution to achieve a successful RNAi based nematode protection strategy in plant-parasitic nematode.

Another objective of the present research work was to characterize another key gene responsible for pharynx development namely, *glp-1*. *Glp-1* gene encoding a Notch receptor protein in *M. incognita* involved in pharynx development during embryogenesis. This gene is highly conserved in free-living as well as plant-parasitic nematodes suggesting its very critical role. Plant mediated down regulation of the *Mi-glp-1* provided resistance against *M. incognita* in stable RNAi transgenic lines of *Arabidopsis*. *In planta* production of RNAi resulted in reduced infectivity and the size of *M. incognita* females. Our results describe for the first time the deleterious effect of host-mediated RNAi in next-generation J2s obtained from females isolated from infected transgenic plants. Collectively, *glp-1* gene exhibits qualities for a good target gene for RNAi based administering of nematode infection.

From the research conducted in this study, it is possible to reasonably conclude that *glp-1* plays a significant role in pharyngeal development in plant-parasitic nematodes. The role of GLP-1 as a receptor protein has been well-characterized in *C. elegans*; however, its involvement in pathogenic nematodes has not been reported to date. An important implication of the study involves determining the silencing efficacy of *glp-1* against other root-knot nematode such as *M. hapla*, *M. floridensis* and *M. javanica*. This work was concerned with developing plant-mediated RNAi based resistance against root-knot nematodes; however, applicability of *glp-1* in managing other plant-parasitic nematodes viz. cyst nematodes for example *G. pallida* will involve a useful future research. Developing stable transgenic lines of major crops affected by root-knot nematode using *glp-1* as a target for host-mediated gene silencing approach will be an interesting research. Identifying genes downstream of the *glp-1* receptor and determining the ligands that bind to it will provide further insights into the various processes and

pathways in which *glp-1* is involved. These ligands and associated genes could then be targeted for understanding the cross-talk between different pathways and could eventually be used as targets for RNAi-mediated silencing for managing plant-parasitic nematodes, thereby improving overall crop productivity. However, several important questions remain unanswered. The nature of the study did not allow us to investigate whether role of *glp-1* in pharyngeal development is direct? Is the development of anterior region of the pharynx in plant-parasitic nematodes also involves interaction of *glp-1* with other genes as is the case in free-living nematodes or does it follows a different fate? Thus, to answer these questions future investigation for determining the phenotypic and molecular function(s) of *glp-1* gene in *M. incognita* is required.

References

REFERENCES

- Abad P, Favery B, Rosso MN, Castagnone-Sereno P (2003). Root-knot nematode parasitism and host response: molecular basis of a sophisticated interaction. *Molecular Plant Pathology* 4: 217–224.
- Abad P, Gouzy J, Aury JM, Castagnone-Sereno Pet al (2008). Genome sequence of the metazoan plant-parasitic nematode *Meloidogyne incognita*. *Nature Biotechnology* 26: 909–915.
- Agrawal N, Dasaradhi PVN, Mohmmmed A, Malhotra Pet al (2003). RNA Interference: biology, mechanism, and applications. *Microbiology and Molecular Biology Reviews* 67: 657–685.
- Aguinaldo AMA, Turbeville JM, Linford LS, Rivera MC et al (1997). Evidence for a clade of nematodes, arthropods and other moulting animals. *Nature* 387(6632): 489–493.
- Ahringer J, Rosenquist TA, Lawson DN, Kimble J (1992). The *Caenorhabditis elegans* sex determining gene *fem-3* is regulated post-transcriptionally. *The EMBO Journal* 11: 2303–2310.
- Albertson DG, Thomson JN (1976). The pharynx of *Caenorhabditis elegans*. *Philosophical Transactions of the Royal Society of London. Series B, Biological Sciences* 275: 299–325.
- Aleshin VV, Kedrova OS, Milyutina IA, Vladychenskaya NS et al (1998). Relationships among nematodes based on the analysis of 18S rRNA gene sequences: molecular evidence for monophyly of chromadorian and secernentian nematodes. *Russian Journal of Nematology* 6: 175–184.
- Artavanis-Tsakonas S, Rand MD, Lake RJ (1999). Notch signaling: cell fate control and signal integration in development. *Science* 284: 770-776.
- Atkinson HJ, Urwin PE, Mcpherson MJ (2003). Engineering plants for nematoderesistance. *Annual Review of Phytopathology* 41: 615–639.

- Atkinson NJ, Urwin PE (2012). The interaction of plant biotic and abiotic stresses: from genes to the field. *Journal of Experimental Botany* 63(10): 3523–43.
- Austin J, Kimble J (1987). *glp-1* is required in the germ line for regulation of the decision between mitosis and meiosis in *C. elegans*. *Cell* 51(4): 589–99.
- Austin J, Kimble J (1989). Transcript analysis of *glp-1* and *lin-12*, homologous genes required for cell interactions during development of *C. elegans*. *Cell* 58: 565–571.
- Bailey TL, Johnson J, Grant CE, Noble WS (2015). The MEME Suite. *Nucleic Acids Research* 43: W39–W49.
- Bakhetia MB, Urwin PE, Atkinson HJ (2007). qPCR analysis and RNAi define pharyngeal gland cell-expressed genes of *Heterodera glycines* required for initial interactions with the host. *Molecular Plant Microbe Interactions* 20: 306–312.
- Banerjee S, Banerjee A, Gill SS, Gupta OP et al (2017). RNA Interference: A Novel Source of Resistance to Combat Plant Parasitic Nematodes. *Frontiers in Plant Science* 8: 834.
- Banerjee S, Gill SS, Gawade BH, Jain PK et al (2018). Host Delivered RNAi of Two Cuticle Collagen Genes, *Mi-col-1* and *Lemmi-5* Hampers Structure and Fecundity in *Meloidogyne incognita*. *Frontiers in Plant Science* 8: 2266.
- Barber CA (1901). A tea-eelworm disease in South India. *Bulletin of the Department of Land Use and Agriculture, Madras* 2: 227–234.
- Bass BL (2000). Double-stranded RNA minireview as a template for gene silencing. *Cell* 101: 235–238.
- Berkeley MJ (1855). *Vibrio* forming excrescences on the roots of cucumber plants. *Gardener's Chronicle and Agricultural Gazette* 14: 220.
- Bert W, Karssen G, Helder J (2011). Phylogeny and Evolution of Nematodes. In: Jones J, Gheysen G, Fenoll C (eds) *Genomics and Molecular Genetics of Plant-Nematode Interactions*. Springer, Dordrecht.

- Bird AF (1971). The Structure of Nematodes. Academic Press, New York 1: 318.
- Bird DM, Opperman CH, Jones SJ, Baillie DL (1999). The *Caenorhabditis elegans* genome: a guide in the post genomics age. Annual Review of Phytopathology 37(1): 247–265.
- Bird DM, Williamson VM, Abad P, McCarter J (2009). The genomes of root-knot nematodes. Annual Review of Phytopathology 47: 333–51.
- Blaxter ML, De Ley P, Garey JR, Liu LX et al (1998). A molecular evolutionary framework for the phylum Nematoda. Nature 392: 71–75.
- Byrd Jr DW, Kirkpatrick T, Barker KR (1983). An improved technique for clearing and staining plant tissues for detection of nematodes. Journal of Nematology 15: 142–143.
- Cai DG, Kleine M, Kifle S, Harloff HJ et al (1997). Positional cloning of a gene for nematode resistance in sugar beet. Science 275: 832–834.
- Caillaud MC, Abad P, Favery B (2008). Cytoskeleton reorganization, a key process in root-knot nematode-induced giant cell ontogenesis. Plant Signaling and Behavior 3(10): 816–818.
- Castagnone-Sereno P (2006). Genetic variability and adaptive evolution in parthenogenetic root-knot nematodes. Heredity (Edinb). 96(4): 282–9.
- Castagnone-Sereno P, Danchin EGJ, Deleury E, Guillemaud T et al (2010). Genome-wide survey and analysis of microsatellites in nematodes, with a focus on the plant-parasitic species *Meloidogyne incognita*. BMC Genomics 11: 598.
- Charlton WL, Harel HY, Bakhetia M, Hibbard JK et al (2010). Additive effects of plant expressed doublestrandedRNAs on root-knot nematode development. International Journal for Parasitology 40: 855–864.
- Chattopadhyay SB, SK Sengupta (1955). Root knot diseases of jute in West Bengal. Current Science 24: 276.

- Chitwood DJ (2003). Research on plant-parasitic nematode biology conducted by the United States Department of Agriculture-Agricultural Research Service. *Pest Management Science* 59: 748–753.
- Christensen S, Kodoyianni V, Bosenberg M, Friedman Let al (1996). lag-1, a gene required for lin-12 and glp-1 signaling in *Caenorhabditis elegans*, is homologous to human CBF1 and Drosophila Su(H). *Development* 122: 1373–1383.
- Clough SJ, Bent AF (1998). Floral dip: a simplified method for *Agrobacterium*-mediated transformation of *Arabidopsis thaliana*. *The Plant Journal* 16: 735–743.
- Cosloy SD, Oishi M (1973). Genetic Transformation in *Escherichia coli* K12. *Proceedings of the National Academy of Sciences of the United States of America* 70(1): 84–87.
- Cotton JA, Lilley CJ, JonesLM, Kikuchi T et al (2014). The genome and life-stage specific transcriptomes of *Globodera pallida* elucidate key aspects of plant parasitism by a cyst nematode. *Genome Biology* 15: R43.
- Craig H, Isaac RE, Brooks DR (2007). Unravelling the moulting degradome: new opportunities for chemotherapy? *Trends in Parasitology* 23: 248–253.
- Crittenden SL, Rudel D, Binder J, Evans TC et al (1997). Genes required for GLP-1 asymmetry in the early *Caenorhabditis elegans* embryo. *Developmental Biology* 181: 36–46.
- Davis EL, Hussey RS, Baum TJ (2004). Getting to the roots of parasitism by nematodes. *Trends in Parasitology* 20: 134–141.
- Decraemer W, Hunt DJ (2006). Structure and classification. In: Perry RN, Moens M (eds) *Plantnematology*. CABI Publishing, Wallingford: 3–32.
- Dinh PTY, Brown CR, Elling AA (2014a). RNA interference of effector gene Mc16D10L confers resistance against *Meloidogyne chitwoodi* in *Arabidopsis* and Potato. *Phytopathology* 104: 1098–1106.

- Dinh PTY, Zhang L, Brown CR, Elling AA (2014b). Plant mediated RNA interference of effector gene Mc16D10L confers resistance against *Meloidogyne chitwoodi* in diverse genetic backgrounds of potato and reduces pathogenicity of nematode offspring. *Nematology* 6: 669–682.
- Dong K, Dean RA, Fortnum BA, Lewis SA (2001). Development of PCR primers to identify species of root-knot nematodes: *Meloidogyne arenaria*, *M. hapla*, *M. incognita*, and *M. javanica*. *Nematropica* 31: 273–282.
- Doyle JJ, Doyle JL (1990). Isolation of plant DNA from fresh tissue. *Focus* 12: 13–15.
- Dunn CW, Hejnol A, Matus DQ, Pang K et al (2008). Broad phylogenomic sampling improves resolution of the animal tree of life. *Nature* 452: 745–749.
- Edgar RC (2004). MUSCLE: multiple sequence alignment with high accuracy and high throughput. *Nucleic Acids Research* 32: 1792–1797.
- Eisenback JD, Hunt D (2009). General morphology. In: Perry RN, Moens M, Starr JL (eds) *Root-Knot Nematodes*. Wallingford: CAB International: 18–54.
- Eisenback JD, Hirschmann H, Triantaphyllou AC (1980). Morphological comparison of *Meloidogyne* female head structures, perineal patterns, and stylets. *Journal of Nematology* 12: 300–313.
- Elling AA (2013). Major emerging problems with minor *Meloidogyne* species. *Phytopathology* 103: 1092–1102.
- Elsworth B, Wasmuth J, Blaxter M (2011). NEMBASE4: the nematode transcriptome resource. *International Journal of Parasitology* 41: 881–894.
- Escobar LE, Peterson AT, Papeş M, Favi M et al (2015). Ecological approaches in veterinary epidemiology: mapping the risk of bat-borne rabies using vegetation indices and night-time light satellite imagery. *Veterinary Research* 46(1): 92.
- Evans TC, Crittenden SL, Kodoyianni V, Kimble J (1994). Translational control of maternal *glp-1* mRNA establishes an asymmetry in the *C. elegans* embryo. *Cell* 77: 183–194.

- Fanelli E, Di Vito M, Jones JT, De Giorgi (2005). Analysis of chitin synthase function in a plant parasitic nematode, *Meloidogyne artiellia*, using RNAi. *Gene* 349: 87–95.
- Finn RD, Coghill P, Eberhardt RY, Eddy SR et al (2016). The Pfam protein families database: towards a more sustainable future. *Nucleic Acids Research* 44: D279–D285.
- Fire A, Xu S, Montgomery MK, Kostas SA et al (1998). Potent and specific genetic interference by double-stranded RNA in *Caenorhabditis elegans*. *Nature* 391: 806–811.
- García LE, Sánchez-Puerta MV (2012). Characterization of a root-knot nematode population of *Meloidogyne arenaria* from Tupungato (Mendoza, Argentina). *Journal of Nematology* 44(3): 291–301.
- Gasteiger E, Hoogland C, Gattiker A, Duvaud S et al (2005). Protein Identification and Analysis Tools on the ExPASy Server. In: Walker JM (ed.) *The Proteomics Protocols Handbook*. Humana Press: 571–607.
- Geng C, Nie X, Tang Z, Zhang Y et al (2016). A novel serine protease, Sep1, from *Bacillus firmus* DS-1 has nematicidal activity and degrades multiple intestinal-associated nematode proteins. *Scientific Reports* 6: 25012.
- Gleason CA, Liu QL, Williamson VM (2008). Silencing a candidate nematode effector gene corresponding to the tomato resistance gene Mi-1 leads to acquisition of virulence. *Molecular Plant-Microbe Interactions* 21(5): 576–585.
- Handoo ZA (1998). Plant-parasitic nematodes. <http://www.ars.usda.gov/Services/docs/htm>.
- Hannon GJ (2002). RNA interference. *Nature* 418(6894): 244–251.
- Heitzler P, Simpson P (1993). Altered epidermal growth factor-like sequences provide evidence for a role of Notch as a receptor in cell fate decisions. *Development* 117: 1113–1123.

- Holterman M, van der Wurff A, van den Elsen S, van Megen H et al (2006). Phylum-wide analysis of SSU rDNA reveals deep phylogenetic relationships among nematodes and accelerated evolution toward crown clades. *Molecular Biology and Evolution* 23: 1792–1800.
- Hu B, Jin J, Guo AY, Zhang H et al (2015). GSDS 2.0: an upgraded gene feature visualization server. *Bioinformatics* 31(8): 1296–1297.
- Huang G, Allen R, Davis EL, Baum TJ et al (2006a). Engineering broad root-knot resistance in transgenic plants by RNAi silencing of a conserved and essential root-knot nematode parasitism gene. *Proceedings of the National Academy of Sciences of the United States of America* 103: 14302–14306.
- Hunter CP, Winston W, Molodowitch C (2002). Systemic RNAi in *C.elegans* requires the putative transmembrane protein SID-1. *Science* 295: 2456–2459.
- Hussey RS, Davis EL, Baum TJ (2002). Secrets in secretions: genes that control nematode parasitism of plants. *Brazilian Journal of Plant Physiology* 14: 183–194.
- Hussey RS, Janssen GJW (2002). Root-knot nematode: *Meloidogyne* species. In: Starr JL, Cook R, Bridge J (eds). *Plant Resistance to Parasitic Nematodes*. Wallingford, UK: CAB International: 43–70.
- Iberkleid I, Sela N, Brown MS (2015). *Meloidogyne javanica* fatty acid- and retinol-binding protein (Mj-FAR-1) regulates expression of lipid-, cell wall-, stress- and phenyl propanoid-related genes during nematode infection of tomato. *BMC Genomics* 16: 272.
- Johnstone IL (2000). Cuticle collagen genes expression in *Caenorhabditis elegans*. *Trends in Genetics*.16: 21–27.
- Johnstone IL, Barry JD (1996). Temporal reiteration of a precise gene expression pattern during nematode development. *The EMBO Journal* 15: 3633–3639.

- Jorgensen RA, Cluster PD, English J, Que Q et al (1996). Chalcone synthase co-suppression phenotypes in petunia flowers: comparison of sense vs. antisense constructs and single-copy vs. complex T-DNA sequences. *Plant Molecular Biology* 31: 957–973.
- Kaloshian I, Lange WH, Williamson VM (1995). An aphid-resistance locus is tightly linked to the nematode-resistance gene, Mi, in tomato. *Proceedings of the National Academy of Sciences of the United States of America* 92(2): 622–625.
- Kaur H, Attri R (2013). Morphological and morphometrical characterization of *Meloidogyne incognita* from different host plants in four districts of Punjab, India. *The Journal of Nematology* 45: 122–127.
- Kelley MR, Kidd S, Deutsch WA, Young MW (1987). Mutations altering the structure of epidermal growth factor-like coding sequences at the *Drosophila* Notch locus. *Cell* 57: 539–548.
- Ketting RF (2011). The many faces of RNAi. *Developmental Cell* 20: 148–161.
- Kidd S, Kelley MR, Young MW (1986). Sequence of the Notch locus of *Drosophila melanogaster*: Relationship of the encoded protein to mammalian clotting and growth factors. *Molecular Cell Biology* 6: 3094–3108.
- Kimber MJ, McKinney S, McMaster S, Day TA et al (2007). flp gene disruption in a parasitic nematode reveals motor dysfunction and unusual neuronal sensitivity to RNA interference. *The FASEB Journal* 21(4): 1233–43.
- Kohli D, Chidambaranathan P, Tej Kumar P, Singh AK et al (2018). Host-mediated RNAi of a Notch-like receptor gene in *Meloidogyne incognita* induces nematode resistance. *Parasitology* 145(14): 1896–1906.
- Kumar A, Kakrana A, Sirohi A, K Subramaniam et al (2017). Host-delivered RNAi-mediated root-knot nematode resistance in *Arabidopsis* by targeting splicing factor and integrase genes. *Journal of General Plant Pathology* 83: 91–97.
- Kumar S, Stecher G, Tamura K (2016). MEGA7: Molecular Evolutionary Genetics Analysis version 7.0 for bigger datasets. *Molecular Biology and Evolution* 33: 1870–1874.

- Kumari C, Dutta TK, Banakar P, Rao U (2016). Comparing the defence-related gene expression changes upon root-knot nematode attack in susceptible *versus* resistant cultivars of rice. *Scientific reports* 6: 22846.
- Kyte J, Doolittle R (1982). A simple method for displaying the hydropathic character of a protein. *Journal of Molecular Biology* 157: 105–132.
- Lambert K, Bekal S (2002). Introduction to Plant-Parasitic Nematodes. The Plant Health Instructor. doi: 10.1094/PHI-I-2002-1218-01.
- Li J, Todd TC, Lee J, Trick HN (2011). Biotechnological application of functional genomics towards plant parasitic nematode control. *Plant Biotechnology Journal* 9: 936–944.
- Li J, Todd TC, Oakley TR, Lee J et al (2010a). Host-derived suppression of nematode reproductive and fitness genes decreases fecundity of *Heterodera glycines* Ichinohe. *Planta* 232: 775–785.
- Lilley CJ, Bakhetia M, Charlton WL, Urwin PE (2007). Recent progress in the development of RNA interference for plant parasitic nematodes. *Molecular Plant Pathology* 8: 701–711.
- Livak KJ, Schmittgen TD (2001). Analysis of relative gene expression data using real-time quantitative PCR and the $2^{-\Delta\Delta C(T)}$ Method. *Methods* 25(4): 402–408.
- López-Pérez JA, Strange ML, Kaloshian I, Ploeg AT (2006). Differential response of *Mi* gene-resistant tomato rootstocks to root-knot nematodes (*Meloidogyne incognita*). *Crop Protection* 25(4): 382–388.
- Lu CJ, Tian BY, Cao Y, Zou CG et al (2016). Nuclear receptor *nhr-48* is required for pathogenicity of the second stage (J2) of the plant parasite *Meloidogyne incognita*. *Scientific Reports* 6: 34959.
- Lunt DH, Kumar S, Koutsovoulos G, Blaxter ML (2014). The complex hybrid origins of the root knot nematodes revealed through comparative genomics. *Peer-reviewed Journal* 2: e356.

- Majumdar R, Rajasekaran K, Cary JW (2017). RNA interference (RNAi) as a potential tool for control of Mycotoxin contamination in crop plants: concepts and considerations. *Frontiers in Plant Science* 8: 200.
- Mandel M, Higa A (1970). Calcium-dependent bacteriophage DNA infection. *Journal of Molecular Biology* 53: 109–118.
- Mango SE (2007). The *C. elegans* pharynx: a model for organogenesis. In: WormBook. The *C. elegans* Research Community, WormBook.doi/10.1895/wormbook.1.129.1.
- Martin J, Rosa BA, Ozersky P, Hallsworth-Pepin K et al (2015). Helminth.net: expansions to Nematode.net and an introduction to Trematode.net. *Nucleic Acids Research* 43(Database issue): D698–D706.
- Martinuz A, Schouten A, Sikora RA (2013). Post-infection development of *Meloidogyne incognita* on tomato treated with the endophytes *Fusarium oxysporum* strain Fo162 and *Rhizobium etli* strain G12. *BioControl* 58: 95–104.
- Mary P (1996). *Sustainable Practices for Vegetable Production in the South*. Focus Publishing, Newburyport MA: 75–77.
- McCarter JP (2009). Molecular approaches toward resistance to plant-parasitic nematodes. In: Berg RH, Taylor CG (eds) *Cell Biology of Plant Nematode Parasitism*. Berlin, Germany: Springer: 239–267.
- Milligan SB, Bodeau J, Yaghoobi J, Kaloshian I et al (1998). The root knot nematode resistance gene Mi from tomato is a member of the leucine zipper, nucleotide binding, leucine-rich repeat family of plant genes. *Plant Cell* 10: 1307–1319.
- Moens M, Perry RN, Starr JL (2009). *Meloidogyne* species: a diverse group of novel and important plant parasites. In: Perry RN, Moens M, Starr JL (eds) *Root-knot nematodes*. CABI Publishing, Wallingford, UK: 1–17.
- Mohrlen F, Hutter H, Zwilling R (2003). The astacin protein family in *Caenorhabditis elegans*. *European Journal of Biochemistry* 270: 4909–4920.

- Needham T (1743). A letter concerning certain chalky tubulous concretions called malm; with some microscopical observations on the farina of the red lily, and of worms discovered in smutty corn. *Philosophical Transactions of the Royal Society* 42: 173–174, 634–641.
- Nguyễn PV, Bellafiore S, Petitot A, Haidar R et al (2014). *Meloidogyne incognita* - rice (*Oryza sativa*) interaction: a new model system to study plant-root-knot nematode interactions in monocotyledons. *Rice* 7: 23.
- Nicol JM, Turner SJ, Coyne DL, Nijs LD et al (2011). Current Nematode Threats to World Agriculture. In: Jones J, Gheysen G, Fenoll C (eds) *Genomics and Molecular Genetics of Plant-Nematode Interactions*. Springer, Dordrecht (NL): 21–43.
- Niu J, Jian H, Xu J, Chen C et al (2012). RNAi silencing of the *Meloidogyne incognita* *Rpn7* gene reduces nematode parasitic success. *European Journal of Plant Pathology* 134: 131–144.
- Novelli J, Ahmed S, Hodgkin J (2004). Gene interactions in *Caenorhabditis elegans* define DPY-31 as a candidate procollagen C-proteinase and SQT-3/ROL-4 as its predicted major target. *Genetics* 168: 1259–1273.
- Nsengimana J, Bauters L, Haegeman A, Gheysen G (2013). Silencing of Mg-pat-10 and Mg-unc-87 in the plant parasitic nematode *Meloidogyne graminicola* using siRNAs. *Agriculture* 3: 567–678.
- Nykanen A, Haley B, Zamore PD (2001). ATP requirements and small interfering RNA structure in the RNA interference pathway. *Cell* 107: 309–21.
- Opperman CH, Bird DM, Williamson VM, Rokhsar D et al (2008). Sequence and genetic map of *Meloidogyne hapla*: a compact nematode genome for plant parasitism. *Proceedings of the National Academy of Sciences USA* 105: 14802–14807.
- Orion D, Kritzman G (1991). Antimicrobial activity of *Meloidogyne javanica* gelatinous matrix. *Revue de Nématologie* 14: 481–483.

- Page AP, Johnstone IL (2007). The cuticle. In: WormBook. The *C. elegans* Research Community, WormBook, doi/10.1895/wormbook.1.138.1,http://www.wormbook.org.
- Papolu PK, Gantasala NP, Kamaraju D, Banakar P et al (2013). Utility of host delivered RNAi of two FMRF amide like peptides, flp-14 and flp-18, for the management of root knot nematode, *Meloidogyne incognita*. PLoS ONE 8: e80603.
- Park JO, Pan J, Mohrlen F, Schupp MO et al (2010). Characterization of the astacin family of metalloproteases in *C. elegans*. BMC Development Biology 10: 14.
- Priess JR, Schnabel H, Schnabel R (1987). The *glp-1* locus and cellular interactions in early *C. elegans* embryos. Cell 51: 601–611.
- Priess JR, Thomson JN (1987). Cellular interactions in early *C. elegans* embryos. Cell 48: 241–250.
- Rastogi S, Borgo B, Pazdernik N, Fox P et al (2015). *Caenorhabditis elegans* *glp-4* encodes a valylaminoacyl tRNA synthetase. Genes Genomes Genetics 5: 719–728.
- Rebay I, Fleming RJ, Fehon RG, Cherbas L et al (1991). Specific EGF repeats of Notch mediate interactions with Delta and Serrate: implications for Notch as a multifunctional receptor. Cell 67: 687–699.
- Reddi AH (1996). BMP-1: resurrection as procollagen C-proteinase. Science 271: 463.
- Rich JR, Brito JA, Kaur R, Ferrel JA (2009). Weed species as hosts of *Meloidogyne* spp.: a review. Nematropica 39: 157–185.
- Roehl H, Bosenberg M, Blelloch R, Kimble J (1996). Roles of the RAM and ANK domains in signaling by the *C. elegans* GLP-1 receptor. The EMBO Journal 15: 7002–7012.
- Rosas-Cárdenas FdeF, Durán-Figueroa N, Vielle-Calzada JP, Cruz-Hernández A et al (2011). A simple and efficient method for isolating small RNAs from different plant species. Plant Methods 7: 4.

- Rosso MN, Dubrana MP, Cimbolini N, Jaubert S et al (2005). Application of RNA interference to root-knot nematode genes encoding esophageal gland proteins. *Molecular Plant-Microbe Interactions* 18: 615–620.
- Rosso MN, Jones JT, Abad P (2009). RNAi and functional genomics in plant parasitic nematodes. *Annual Review of Phytopathology* 47: 207–232.
- Rudel D, Kimble J (2001). Conservation of *glp-1* regulation and function in nematodes. *Genetics* 157: 639–654.
- Sambrook J, Fritsch EF, Maniatis T (1989). *Molecular cloning: a laboratory manual*, Cold Spring Harbor Laboratory Press, New York.
- Sambrook J, Russell DW (2001). *Molecular cloning: A laboratory manual*. 3rd ed. Cold Spring Harbor (NY): Cold Spring Harbor Laboratory Press: 132–150.
- Sasser JN (1980). Root knot nematodes: A global menace to crop production. *Plant Disease Journal* 64: 36–41.
- Sayre RM (1986). Pathogens for biological control of nematodes. *Crop Protection* 5: 268–276.
- Schacht H (1859). About some enemies and diseases of the sugar beet. *Zeitschrift Ver. Ru benzucker-Ind Zoolver* 2: 590.
- Sindhu A, Maier TR, Mittchum MG, Hussey RS et al (2009). Effective and specific *in planta* RNAi in cyst nematodes: expression interference of four parasitism genes reduces parasitic success. *Journal of Experimental Botany* 1: 315–324.
- Singh S, Singh B, Singh AP (2015). Nematodes: A Threat to Sustainability of Agriculture. *Procedia Environmental Sciences* 29: 215–216.
- Sobczak M, Avrova A, Jupowicz J, Phillips MS et al (2005). Characterization of susceptibility and resistance responses to potato cyst nematode (*Globodera* spp.) infection of tomato lines in the absence and presence of the broad-spectrum nematode resistance *Hero* gene. *Molecular Plant-Microbe Interaction* 18: 158–168.

- Steeves RM, Todd TC, Essig JS, Trick HN (2006). Transgenic soybeans expressing siRNAs specific to a major sperm protein gene suppress *Heterodera glycines* reproduction. *Functional Plant Biology* 33: 991–999.
- Stepek G, McCormack G, Winter AD, Page AP (2015). A highly conserved, inhibitable astacin metalloprotease from *Teladorsagia circumcincta* required for cuticle formation and nematode development. *International Journal of Parasitology* 45: 345–355.
- Stifani S, Blaumueller CM, Redhead NJ, Hill RE et al (1992). Human homologs of a Drosophila Enhancer of split gene product define a novel family of nuclear proteins. *Nature Genetics* 2: 119–127.
- Sulston JE, Schierenberg E, White JG, Thomson JN (1983). The embryonic cell lineage of the nematode *Caenorhabditis elegans*. *Developmental Biology* 100: 64–119.
- Suzuki M, Sagoh N, Iwasaki H, Inoue H et al (2004). Metalloproteases with EGF, CUB, and thrombospondin-1 domains function in molting of *Caenorhabditis elegans*. *Biological Chemistry* 385: 565–568.
- Tandingan De Ley I, De Ley P, Vierstraete A, Karssen G et al (2002). Phylogenetic Analyses of Meloidogyne SSU rDNA. *Journal of Nematology* 34: 319–331.
- Taylor AL, Sasser JN (1978). *Biology, Identification and Control of Root Knot Nematodes (Meloidogyne Species)*. A cooperative publication of North Carolina State University, Dept. of Plant Pathology, and USAID, Raleigh, NC, USA.
- Titani K, Torff HJ, Hormel S, Kumar S et al (1987). Amino acid sequence of a unique protease from the crayfish *Astacus fluviatilis*. *Biochemistry* 26: 222–226.
- Tytgat T, Vercauteren I, Vanholme B, Meutter DJ et al (2004). An SXP/RAL-2 protein produced by the subventral pharyngeal glands in the plant parasitic root-knot nematode *Meloidogyne incognita*. *Parasitology Research* 95: 50–54.
- Tamilarasan S, Rajam MV (2013) Engineering Crop Plants for Nematode Resistance through Host-Derived RNA Interference. *Cell Development Biology* 2: 114.

- Urwin PE, Lilley CJ, Atkinson HJ (2002). Ingestion of double-stranded RNA by pre-parasitic juvenile cyst nematodes leads to RNA interference. *Molecular Plant-Microbe Interactions* 15: 747–752.
- Vanholme B, De Meutter J, Tytgat T, Van Montagu M (2004). Secretions of plant-parasitic nematodes: a molecular update. *Gene* 332: 13–27.
- van Megen H, van den Elsen S, Holterman M, Karssen Get al (2009). A phylogenetic tree of nematodes based on about 1200 full-length small subunit ribosomal DNA sequences. *Nematology* 11: 927–950.
- Vieira P, Eves-van den Akker S, Verma R, Wantoch S et al (2015). The *Pratylenchus penetrans* transcriptome as a source for the development of alternative control strategies: mining for putative genes involved in parasitism and evaluation of *in planta* RNAi. *PLoS ONE* 10: e0144674.
- Von Mende N, Bird D, Albert P, Riddle D (1988). DPY-13: A nematode collagen gene that affects body shape. *Cell* 55: 567–576.
- Wallace RL, Ricci C, Melone G (1996). A cladistic analysis of pseudocoelomate (aschelminth) morphology. *Invertebrate Biology* 115: 104–112.
- Wang KH, McSorley R, Gallaher RN (2004). Effect of *Crotalaria juncea* amendment on squashinfected with *Meloidogyne incognita*. *Journal of Nematology* 36(3): 290–296.
- Wang M, Wang D, Zhang X, Wang X et al (2016). Double-stranded RNA-mediated interference of dumpy genes in *Bursaphelenchus xylophilus* by feeding on filamentous fungal transformants. *International Journal of Parasitology* 46: 351–360.
- Waterhouse PM, Graham MW, Wang MB (1998). Virus resistance and gene silencing in plants can be induced by simultaneous expression of sense and antisense RNA. *Proceedings of the National Academy of Sciences of the United States of America* 95: 13959–13964.

- Webster JM (1987). Introduction. In: Brown RH, Kerry BR (eds) Principles and practice of nematode control in crops. Academic Press, Melbourne: 1–12.
- Wharton KA, Yedvobnick B, Finnerty VG, ArtavanisTsakonas S (1985b). opa: A novel family of transcribed repeats shared by the Notch locus and other developmentally regulated loci in *Drosophila melanogaster*. Cell 40: 55–62.
- Whitehead AG (1968). Taxonomy of *Meloidogyne* (Nematodea: Heteroderidae) with descriptions of four new species. Journal of Zoology 131(3): 263–401.
- Williamson KJ, Fisher JM, Langridge P (1994a). Identification of RFLP markers linked to the cereal cyst nematode resistance gene(Cre) in wheat. Theoretical and Applied Genetics 89: 927–930.
- Xie J, Li S, Mo C, Wang G et al (2016). A Novel *Meloidogyne incognita* effector Misp12 suppresses plant defense response at latter stages of nematode parasitism. Frontiers in Plant Science 7: 964.
- Xue B, Hamamouch N, Li C, Huang G et al (2013). The 8D05 parasitism gene of *Meloidogyne incognita* is required for successful infection of host roots. Phytopathology 103: 175–181.
- Yadav BC, Veluthambi K, Subramaniam K (2006). Host generated double stranded RNA induces RNAi in plant parasitic nematodes and protects the host from infection. Molecular and Biochemical Parasitology 148: 219–222.
- Ye W, Zeng Y, Kerns J (2015). Molecular characterisation and diagnosis of root-knot nematodes (*Meloidogyne* spp.) from Turf grasses in North Carolina, USA.PLoS One10(11): e0143556.
- Yepsen RB (1984). The encyclopedia of natural insect and disease control.Revised Yepsen, R.B. Edition. Rodale press: 267–271.
- Yochem J, Greenwald I (1989). glp-1 and lin-12, genes implicated in distinct cell-cell interactions in *C. elegans*, encode similar transmembrane proteins. Cell 58: 553–563.

Appendices

Composition of media/ solutions

Table 1. Luria Broth medium (LB)

Components	Amount (g/100 ml)
Tryptone	1
Yeast extract	0.5
NaCl	1
pH 7 (adjusted prior to autoclaving)	

Table 2. Luria Agar medium (LA)

Components	Amount (g/100 ml)
Tryptone	1
Yeast extract	0.5
NaCl	1
Agar	1.5
pH 7 (adjusted prior to autoclaving)	

Table 3. Yeast extract peptone medium (YEP)

Components	Amount (g/100 ml)
Yeast Extract	1
Peptone	1
NaCl	0.5
pH 7 (adjusted prior to autoclaving)	

Table 4. Alkaline lysis solutions (plasmid extraction)

Components	Stock	Working
Solution I		
Tris-Cl, pH 8.0	50 mM	
EDTA	10 mM	
RNase A	100 µg/ml	
Solution II		
NaOH	200 mM	
SDS	1%	
Solution III		
Potassium acetate	3.0 M	

Table 5. M9 buffer

Components	Amount (g/100 ml)
Na ₂ HPO ₄ .7H ₂ O	5.8
KH ₂ PO ₄	3
NaCl	5
MgSO ₄ .7H ₂ O	0.25
dH ₂ O	Upto 1 litre

Table 6. Tris-acetate (TAE) buffer

Components	Amount (per litre) 50X
Tris	242 gm
Glacial Acetic Acid	57.1 ml
0.5 M EDTA (pH 8.0)	40.0 ml

Table 7. DNA Gel loading dye

Components	Amount (100 ml)
Tris-HCl (pH7.6)	10.0 mM
EDTA	60.0 mM
Bromophenol Blue	0.25%
Xylene Cyanol FF	0.25%
Glycerol	60% w/v

Table 8. 3-[N-morpholino]propanesulfonic acid (MOPS) buffer for RNA

Components	Amount (per litre) 10X
MOPS	200 mM
Sodium acetate	50 mM
EDTA (pH 7.0)	10 mM

Table 9. RNA gel loading buffer

Components	Amount (10 ml)
Formamide	9.5 ml (95%)
Bromophenol Blue	100 µl (0.025%)
EDTA	200 µl (0.5 mM)
Xylene Cyanol FF	100 µl (0.025%)
Glycerol	60%

Table 10. Plant genomic DNA isolation buffer (CTAB buffer)

Components	Amount (per 100 ml)
CTAB	2 g
Tris HCl (pH 8.0)	10 ml
EDTA (0.5M) (pH 8.0)	93.05 g
NaCl (5M)	146.1 g
PVP 40	1 g
pH 5 (adjusted prior to autoclaving)	
dH ₂ O	Upto 100 ml

Table 11. Buffers for small RNA isolation

1. LiCl Extraction Buffer

(Prepare fresh just before isolating RNA)

Components	Amount (ml/litre)
SDS (20%)	50
LiCl (8M)	12.5
EDTA (0.5M)	20
DEPC treated dH ₂ O	Upto 1 litre

2. 40% PEG (polyethylene glycol) 8000 w/v

Components	Amount (g/100 ml)
PEG (8000 w/v)	40
DEPC treated dH ₂ O	Upto 100 ml

3. Chloroform:Isoamyl alcohol (24:1)

Components	Amount (ml/100 ml)
Chloroform	96
Isoamylalcohol	4

4. 10X TBE

Components	Amount (per litre)
Tris base	108 g
Boric acid	55 g
EDTA (0.5M), pH8	40 ml
DEPC treated dH ₂ O	Upto 1 litre

Table 12. Buffers for Northern hybridization

1. 20X SSC (Saline-sodium citrate)

Components	Amount (per litre)
NaCl	175.3 g
Trisodium citrate	88.2 g
pH 7 (adjusted prior to autoclaving)	
DEPC treated dH ₂ O	Upto 1 litre

List of Publications

LIST OF PUBLICATIONS

1. Kohli, D., Chidambaranathan, P., Tej, J., Singh, A., Kumar, A., Sirohi, A., Srinivasan, R., Bharadwaja, N., Jain, P. (2018). Host-mediated RNAi of a Notch-like receptor gene in *Meloidogyne incognita* induces nematode resistance. *Parasitology*, 1-11. doi:10.1017/S0031182018000641.
2. Kohli D, Sirohi A, Srinivasan R, Bharadvaja N, Jain P (2018). Isolation, cloning and characterization of cuticle collagen genes, *Mi-dpy-10* and *Mi-dpy-31*, in *Meloidogyne incognita*. *IJ of Nematology* 48(1): 1-9.

Poster and Paper Presentations in the Conferences

1. Kohli D, Kumar A, Bharadvaja N, Subramaniam K, Sirohi A, Srinivasan R, Jain PK. Identification of a vital development gene, *glp-1*, and its utilization in RNAi mediated silencing for conferring resistance against root knot nematode in Arabidopsis. National Symposium on Germplasm to Genes: Harnessing Biotechnology for Food Security and Health. August 9-11, 2015. NASC, New Delhi, India. (Awarded first prize in poster presentation).
2. Kohli D, Srinivasan R, Jain PK, Bharadvaja N. Plant Parasitic nematode: management through RNA interference approach. India-Japan workshop on Biomolecular electronics and organic nanotechnology for environment preservation. December 13-15, 2013. Delhi Technological University, New Delhi, India.

Reprints of the Publications

Research Article

Cite this article: Kohli D *et al.* (2018). Host-mediated RNAi of a Notch-like receptor gene in *Meloidogyne incognita* induces nematode resistance. *Parasitology* 1–11. <https://doi.org/10.1017/S0031182018000641>

Received: 23 November 2017

Revised: 21 March 2018

Accepted: 21 March 2018

Key words:

Arabidopsis; double-stranded RNA (dsRNA); *glp-1* gene; *in vivo* RNAi; *Meloidogyne incognita*; pharynx development

Author for correspondence:

Pradeep K. Jain, E-mail: jainpmb@gmail.com

Host-mediated RNAi of a Notch-like receptor gene in *Meloidogyne incognita* induces nematode resistance

Deshika Kohli^{1,2}, Parameswaran Chidambaranathan¹, J. Prasanth Tej Kumar¹, Ashish Kumar Singh³, Anil Kumar¹, Anil Sirohi³, K. Subramaniam⁴, Ramamurthy Srinivasan¹, Navneeta Bharadvaja² and Pradeep K. Jain¹

¹ICAR-NRC on Plant Biotechnology, Pusa Campus, New Delhi 110012, India; ²Delhi Technological University, Shahbad Daultapur, Delhi-110042, India; ³Division of Nematology, ICAR-Indian Agricultural Research Institute, Pusa Campus, New Delhi 110012, India and ⁴Department of Biotechnology, Indian Institute of Technology, Madras, Chennai 600036, India

Abstract

GLP-1 (abnormal germline proliferation) is a Notch-like receptor protein that plays an essential role in pharyngeal development. In this study, an orthologue of *Caenorhabditis elegans glp-1* was identified in *Meloidogyne incognita*. A computational analysis revealed that the orthologue contained almost all the domains present in the *C. elegans* gene: specifically, the LIN-12/Notch repeat, the ankyrin repeat, a transmembrane domain and different ligand-binding motifs were present in orthologue, but the epidermal growth factor-like motif was not observed. An expression analysis showed differential expression of *glp-1* throughout the life cycle of *M. incognita*, with relatively higher expression in the egg stage. To evaluate the silencing efficacy of *Mi-glp-1*, transgenic *Arabidopsis* plants carrying double-stranded RNA constructs of *glp-1* were generated, and infection of these plants with *M. incognita* resulted in a 47–50% reduction in the numbers of galls, females and egg masses. Females obtained from the transgenic RNAi lines exhibited 40–60% reductions in the transcript levels of the targeted *glp-1* gene compared with females isolated from the control plants. Second-generation juveniles (J2s), which were descendants of the infected females from the transgenic lines, showed aberrant phenotypes. These J2s exhibited a significant decrease in the overall distance from the stylet to the metacarpus region, and this effect was accompanied by disruption around the metacarporeal bulb of the pharynx. The present study suggests a role for this gene in organ (pharynx) development during embryogenesis in *M. incognita* and its potential use as a target in the management of nematode infestations in plants.

Introduction

Meloidogyne incognita, the root-knot nematode, is a member of the group of sedentary plant-parasitic nematodes (PPNs) that cause serious damage (to the tune of hundreds of billions of dollars) to crop production worldwide (Elling, 2013). As an obligate endoparasite, *M. incognita* resides permanently inside the roots of its host throughout its lifecycle, and to derive nutrients, this organism has developed a specialized organ called the stylet. The pharynx of *M. incognita* is continuous with the stylet lumen and aids with the ingestion of food material into the intestine (Eisenback and Hunt, 2009). Pharyngeal development occurs during embryogenesis, and several genes responsible for its development, most of which belong to the Notch-like receptor family, have been identified in *Caenorhabditis elegans*. Notch pathways are known to regulate the aspects of growth and patterning in metazoans (Rudel and Kimble, 2001). Pharyngeal cells are produced by two distinct molecular pathways, ABa and EMS. The ABa pathway is dependent on the Notch receptor orthologue *glp-1* (abnormal germline proliferation) (Mango, 2007), which is a homologue of the *Drosophila* Notch gene (Roehl *et al.* 1996) and induces germline proliferation during pharyngeal embryonic development. *Glp-1* is structurally and functionally similar to another Notch-related receptor, *lin-12*, and these two proteins have similar conserved motifs that contribute to the functional roles of these proteins as membrane-bound receptors involved in Notch signalling (Yochem and Greenwald, 1989).

With recent advances in the generation of genomic datasets for nematodes, many studies have focused on identifying and characterizing genes with varied functional roles and determining their conservation throughout evolution. Various secretory and effector proteins have been characterized over the past few years (Banerjee *et al.* 2017). *Misp12* is a potential root-knot nematode effector expressed in the dorsal oesophageal gland (Xie *et al.* 2016). The SXP/RAL-2 secretory protein was identified in *M. incognita* and is expressed in the sub-ventral pharyngeal glands (Tytgat *et al.* 2004). However, there are limited reports concerning the identification and characterization of genes involved in nematode development. Among the genes involved in organ development in nematodes, collagen genes are the most studied, and the *M. incognita* collagen genes, *Mi-col-1* and *lemmi-5*, and the *Globodera pallida* collagen

genes, *col-1* and *col-2*, have been identified and characterized (Wang et al. 1998; Gray et al. 2001). Chitin synthase, which functions in the production of eggshells, has been reported in *C. elegans* and *Meloidogyne artiellia* (Veronico et al. 2001; Fanelli et al. 2005). However, with the exception of the study conducted by Calderón-Urrea et al. (2016), who studied and compared the early development of *M. incognita* with that of *C. elegans*, almost no detailed studies have investigated genes associated with the early development of *M. incognita*.

Several reports detail the RNAi-mediated knockdown of specific secretory genes that affect parasitism in PPNs (Rehman et al. 2016). However, only some of the known developmental genes have been targeted by host-mediated gene silencing in the management of PPNs. The *Rpn7* gene, which is essential for the integrity of the 26S proteasome, has been targeted in attempts to control the root-knot nematode *M. incognita*, and the silencing of this gene resulted in a reduction in nematode motility (Niu et al. 2012). Two genes essential for body wall formation in *Meloidogyne graminicola*, namely the *Mg-pat-10* and *Mg-unc-87* genes, which function in muscle contraction and the maintenance of structural myofilaments, have been identified and suppressed *in vitro* through soaking, resulting in 91% and 87% reductions in infectivity, respectively (Nsengimana et al. 2013). *nhr-48*, a nuclear receptor gene that regulates various developmental, reproduction and pathogenicity processes in nematodes, has been silenced in *M. incognita*, resulting in delayed development and reduced reproduction (Lu et al. 2016). Despite these efforts, few developmental genes have been targeted in nematode control efforts.

The present study reports the identification and characterization of the *glp-1* gene of *M. incognita*. A host-mediated RNAi silencing approach was adapted to determine the potential of *Mi-glp-1* as a candidate gene for the control of nematode infection.

Materials and methods

Genome-wide identification of the *glp-1* gene in *M. incognita*

The *M. incognita* genome database was downloaded from http://www6.inra.fr/Meloidogyne_incognita (Abad et al. 2008), and local nucleotide and protein *M. incognita* databases were created through a BioEdit local BLAST search for the identification of the *glp-1* gene in *M. incognita*. A tblastn search was conducted against these databases using the *C. elegans glp-1* (CAA79620.1) gene as the query and default parameters (expected threshold value 10; maximum number of aligned sequences displayed 100). All the sequences that met the requirements were subjected to gene predictions through GeneMark and FGENSH analyses, and the genes that did not contain the known conserved domains and motifs detailed in the Pfam database (<http://pfam.janelia.org/>) were removed (Finn et al. 2016). MiV1ctg1087 (Minc16055), the single contig obtained with the maximum possible score, was selected as the probable *Mi-glp-1* for further experimentation. In addition to Minc16055 in *M. incognita*, we identified *glp-1* orthologues in four other *Meloidogyne* species (spp.), namely *M. hapla* (Mh10g200_708_Contig1018), *M. floridensis* (contig nMf_1_1_scaf00321), *M. javanica* (MJ01378, MJ05005) and *M. chitwoodi* (MC01544, MC00257), and in *G. pallida* (GPLIN_000999900.1), a cyst nematode, using their genome, transcriptome and/or expressed sequence tag (EST) databases. The derived sequences were downloaded from their genome assembly or transcriptomic databases or EST clusters available at either NCBI, NEMBASE4 (www.nematode.org) and/or nematode.net V4.0 (Opperman et al. 2008; Elsworth et al. 2011; Cotton et al. 2014; Lunt et al. 2014; Martin et al. 2015).

Phylogenetic and gene structure analyses

The identified GLP-1 amino acid sequences in PPNs, including *M. incognita*, *M. hapla*, *M. floridensis*, *M. javanica*, *M. chitwoodi* and *G. pallida*, along with the reported GLP-1 sequences of free-living nematode species, e.g. *C. elegans*, *Caenorhabditis briggsae*, *Caenorhabditis japonica* and *Caenorhabditis remanei*, and the Notch-like protein of the marine worm *Priapululus caudatus* (retrieved from NCBI), were aligned in MUSCLE using the default parameters (Edgar, 2004). To analyse the clustering pattern, an unrooted phylogenetic tree was constructed based on the neighbour-joining (NJ) method using MEGA 7.0 software (<http://www.megasoftware.net/>), with Poisson correction, pairwise deletion and the bootstrap value set to 2000 replicates (Kumar et al. 2016).

The protein sequences were analysed with the Pfam (<http://pfam.sanger.ac.uk/>) and SMART (<http://smart.emblheidelberg.de/>) databases to confirm the presence of conserved motifs. SignalP3.0 and TMHMM server v. 2.0 were employed to predict the presence of signal peptide sequences and transmembrane domains (TMDs), respectively. Two other software programs (Kd and ProtScale) based on different algorithms were used to determine the presence of TMDs (Kyte and Doolittle, 1982; Gasteiger et al. 2005).

The motif-based sequence analysis tool MEME 4.11.2 (<http://meme.sdsc.edu/meme/meme.html>) (Bailey et al. 2015) with the following parameters was used to identify conserved motifs in the *glp-1* gene of *M. incognita*: optimal width, 10–300 amino acids and maximum number of motifs 10. The gene architecture of this gene, which depicts the exon/intron arrangement, gene length and upstream/downstream region, was designed using the online Gene Structure Display Server 2.0 (<http://gsds.cbi.pku.edu.cn/>) (Hu et al. 2015) with the coding sequences and corresponding genomic sequences.

Maintenance of pure cultures of nematodes

Tomato (*Solanum lycopersicum*) seeds were sterilized by soaking 20 min in sterile distilled water, 5 min in 70% ethanol and 15 min in 5% NaOCl and 0.1% Tween 20 followed by washing four times in sterile distilled water and germinated on a mixture of cocopeat, vermiculite and sand (1:1:1) in an Indian Agricultural Research Institute (IARI) glass house. Two-week-old tomato seedlings were infected with a pure culture of *M. incognita* maintained in our laboratory (Kumar et al. 2017). Egg masses of *M. incognita* were hand-picked from the roots of the infested plants and then maintained until hatching at 28 °C in Petri plates containing 10–15 mL of sterile water to collect second-stage juveniles (J2s) of *M. incognita*. These J2s were then used for subsequent inoculation assays using transgenic *Arabidopsis* lines.

Quantitative real-time PCR analyses

To evaluate the expression at different developmental stages, cDNA from the samples of *M. incognita* egg masses, infective J2s and mature females as well as roots of infected plants harvested at different time points after inoculation was subjected to quantitative real-time PCR (qRT-PCR). J2s were hatched from freshly picked egg masses, mature females were excised from infected roots, and other stages, namely third-stage juveniles (J3s) and fourth-stage juveniles (J4s), were analysed from nematodes within the roots of infected plants harvested at 10 and 21 days post-inoculation (dpi), respectively. The second molt, which gives rise to J3s, occurs 10 dpi, and the third molt, which yields J4s, occurs approximately 16 dpi (Moens et al. 2009; Martinuz et al. 2013). Total RNA was isolated using a Pure

Link RNA Mini Kit (Ambion, Carlsbad, CA, USA) according to the manufacturer's instructions and then subjected to DNase treatment using the Qiagen DNase enzyme. cDNA was synthesized using the SuperScript[®] III First-Strand Synthesis System (Invitrogen, USA). SYBR-based chemistry was adopted for the qRT-PCR, which was performed in a StepOne Plus[™] real-time PCR System. The primers for *M. incognita*-specific actin and 18S rRNA genes were used as references (Nguyễn *et al.* 2014; Ye *et al.* 2015) (Supplementary Table S1). Three biological and three technical replicates were included for each sample. The data were analysed using the $2^{-[\Delta\Delta C(T)]}$ method, and real-time data are reported as the means \pm standard error (S.E.) of three biological replicates per sample (Livak and Schmittgen, 2001). The data obtained were statistically analysed by analysis of variance (ANOVA), and the significance of the differences between sample means was then determined through Student's *t*-tests ($P < 0.05$).

A qRT-PCR analysis was also performed to determine the silencing efficacy of *glp-1* at the transcript level in *M. incognita*. Transgenic *Arabidopsis* RNAi lines were infected with *M. incognita* J2s, and the infected roots were harvested at 45 dpi. The mature females were isolated from these infected transgenic RNAi lines and compared with females from control (wild-type) *Arabidopsis* plants using the above-described protocol for qRT-PCR analysis.

In vivo RNAi silencing

A 419 bp fragment of the *Mi-glp-1* gene was amplified using gene-specific primers (Supplementary Table S1) in the sense and antisense directions for double-stranded RNA (dsRNA) construction. The primers were designed based on the region flanking the conserved Lin-12/Notch repeat (LNR) domain found in three tandem copies of Notch-related proteins encoded by the *glp-1* gene. The RNAi binary vector pBC6 was used for the design of dsRNA constructs (Yadav *et al.* 2006), and the positive dsRNA constructs were confirmed by double digestion of the sense strand with the *Bam*HI and *Xho*I restriction enzymes and of the antisense strand with *Kpn*I and *Sac*I. The integrity of the products was further confirmed by Sanger sequencing. A positive dsRNA construct and an empty vector construct were transferred into *Agrobacterium tumefaciens* GV3101. *Arabidopsis thaliana* (Col0) plants were then transformed with the designed RNAi constructs driven by the CaMV35S promoter using the floral dip method (Clough and Bent, 1998). T₁ seeds were selected on antibiotic selection medium containing kanamycin (50 $\mu\text{g mL}^{-1}$). Kanamycin-resistant plants were transferred to a greenhouse maintained at 22 °C with a 16 h light/ 8 h dark photoperiod, and the presence of the nematode gene in independent transgenic RNAi lines was confirmed by PCR.

Meloidogyne incognita infection bioassay for evaluating silencing efficacy

All the analyses of transgenic plants were performed with the T₃ generation, and 10–15 biological replicates of each line were used. Seeds of T₃ transgenic lines expressing *glp-1* dsRNA or empty vector and of control (wild-type) *Arabidopsis* plants were surface-sterilized with 70% alcohol for 2 min and 0.1% mercuric chloride +0.1% sodium dodecyl sulphate for 7 min and then washed in sterile distilled water. The seeds were then maintained on Murashige and Skoog media at 4 °C for vernalization prior to germination, and after germination, the plates were maintained at ± 22 °C under a 16 h light/8 h dark photoperiod. Twelve days after germination, the control seedlings and the transgenic seedlings expressing *glp-1* dsRNA or empty vector were uprooted from the medium, transferred to a suitable mixture of vermiculite,

cocopeat and sand (1:1:1), with one plant per slot (3 inches) in a 24-slot tray, and maintained in a growth chamber with a 16 h light/8 h dark photoperiod. After 1 week, each plant was inoculated with 1000 freshly hatched J2s to evaluate the silencing efficacy *in vivo*. Nematode infection bioassays were performed using mature females isolated from the root samples collected 45 dpi. The isolated females were used for qRT-PCR and morphometric studies. The number of galls per plant, the number of females and the egg mass per gram of root fresh weight were determined and used as measures for determining the degree of nematode infection. Specifically, the nematode multiplication factor (MF) of *M. incognita* was calculated as follows: (number of egg masses \times number of eggs per egg mass) \div nematode inoculum level. The statistical significance of the differences between the means of replicates of transgenic lines and wild-type control plants was determined by ANOVA and Student's *t*-tests ($P < 0.05$ or $P < 0.01$).

The nematodes within all the samples of infected roots were stained with acid fuchsin (Bybd *et al.* 1983) and photographed using a Nikon microscope. The size of the stained females isolated from the infected plant samples was measured using the 10 \times objective of a Nikon microscope equipped with the NIS-Elements D measurement software (Eisenback and Hunt, 2009; Kaur and Attri, 2013). The stylet and pharyngeal structures of the J2 progeny of females isolated from transgenic RNAi and control plants were also observed with a Zeiss AxioImager.M2m microscope coupled to an AxioCam with a 40 \times objective, and the data were subjected to statistical analyses as described above.

Detection of glp-1 by Northern hybridization

The small RNA fraction was isolated from the RNAi line, empty vector line and control plants using the LiCl method (Verwoerd *et al.* 1989). Twenty micrograms of the small RNA fractions were resolved on 15% polyacrylamide/1X MOPS urea gels and blotted onto a Hybond-N⁺ membrane (Amersham). The Block-It[™] RNAi designer (<https://rnaidesigner.thermofisher.com/rnaiexpress>), siRNA wizard (<http://www.invivogen.com/sirnazizard/>) and siDesign centre (<http://dharmacon.gelifsciences.com/design-center/>) tools were used to identify the most suitable regions for siRNA target design, and primers for probe preparation were designed based on the region that was deemed most suitable for siRNA targeting (Supplementary Table S1). To generate specific DNA probes (183 bp in size), ³²P- α -dCTP labelling was performed with a Megaprime DNA Labeling kit (GE Healthcare, Amersham) using gene-specific antisense fragments. Hybridization was performed using PerfectHyb[™] Plus according to the manufacturer's instructions (Sigma). The signals were detected by autoradiography.

Results

glp-1 orthologues among nematode species

The tblastn analysis performed against the *M. incognita* genome using the *C. elegans glp-1* protein as the query (retrieved from WormBase) and the subsequent Pfam analysis yielded various hits. Among these hits, MiV1ctg1087, the only contig with a high bit score, showed 100% similarity with Minc16055, which was identified through an OrthoMCL analysis of *M. incognita* as a *Ce-glp-1* orthologue by Abad *et al.* (2008). Thus, functional annotation studies of MiV1ctg1087 involving a Pfam analysis and computer simulation predictions were performed to determine its gene and protein structures. Mi-GLP-1 (Minc16055 or MiV1ctg1087) is a member of the LIN-12/Notch family of receptors and is composed of a series of motifs that are conserved among all Notch receptors. The *Ce-glp-1* and *Mi-glp-1* genes were nearly identical in size, 7.458 and 7.449 kb, respectively.

However, a computational analysis showed differences in the numbers of introns and exons in these orthologous genes: *Ce-glp-1* has only nine exons and eight introns (Rudel and Kimble, 2001), whereas *Mi-glp-1* has 18 exons and 17 introns. This finding indicates that the exon/intron structures of these orthologous genes are not well conserved among nematodes. At the mRNA level, *Mi-glp-1* is 3.252 kb in length, whereas *Ce-glp-1* comprises 4.326 kb (Fig. 1). The *Mi-glp-1* gene encodes a 1083-amino-acid-long truncated protein, as determined through the Pfam analysis, whereas *Ce-glp-1* is composed of 1295 amino acids. The gene encoding GLP-4, which is considered a member of the Notch GLP protein family, was recently identified in *C. elegans* (Rastogi *et al.* 2015), and to date, this new member has only been identified in *C. elegans* and *C. briggsae*. The genome-wide search performed in this study identified only a single *glp-1* contig, which is similar to the findings obtained for *C. japonica* and *C. remanei*, each of which has a single *glp-1*.

Because *glp-1* is a vital gene involved in pharyngeal development during embryogenesis, we also performed a comprehensive species-wide tblastn search for this gene in the genomes and ESTs of various other *Meloidogyne* species available in NCBI and/or Nematode.net. A *glp-1* homologue was identified in various *Meloidogyne* spp., namely, *M. hapla*, *M. floridensis*, *M. javanica* and *M. chitwoodi* and in *G. pallida*, another PPN (details in Supplementary Table S2). We also considered free-living nematodes, including *C. elegans*, *C. briggsae*, *C. japonica* and *C. remanei* and a marine worm (*P. caudatus*) Notch receptor gene in our phylogenetic study (Supplementary Fig. S1). The findings revealed that among the homologues identified in *Meloidogyne* spp., the *glp-1* homologue in *M. hapla* contains all the domains that are present in the *Ce-glp-1* gene, whereas *Mi-glp-1* does not have an epidermal growth factor (EGF) domain. A motif search including all the species analysed in this study (Supplementary Fig. S2) revealed a conserved ankyrin repeat (ANK).

Protein sequence analysis and phylogenetic analysis of Notch receptor orthologues in selected nematode species

An amino acid sequence analysis of the *M. incognita* GLP-1 protein revealed a single TMD, an extracellular domain containing the LNRs, the ANK, which is an intracellular domain, and a Pro-Glu-Ser-Thr (PEST) domain. The molecular and biological functions of the LNR and ANK in *C. elegans* have been described (Austin and Kimble, 1989; Roehl *et al.* 1996). Thus, the presence of these motifs in Mi-GLP-1 indicates its probable role in embryogenesis. Specific primers for the LNR were designed, and the region was successfully amplified, confirming the presence of the LNR in *M. incognita* (data not shown). Interestingly, the presence of a conserved cysteine ('C') as the first residue of the LNR was identified in the *glp-1* proteins of all nematode species evaluated in this study. Mi-GLP-1 contains one ANK with three copies,

three LNR domains at the 5' end, a TMD and an RAM domain but does not have an EGF domain (Fig. 2). GLP-1 induces downstream transcriptional regulators and interacts with them to mediate signalling. Our sequence analysis revealed an 'RTGGGAA' DNA-binding site and an RAM domain in *Mi-glp-1*. These sites have been proposed as binding sites for the LAG-1 (Lin-12 and Glp-1) protein, which is required during embryogenesis to regulate pharyngeal development (Christensen *et al.* 1996).

All identified GLP-1 protein sequences belonging to the different nematode species were aligned using MUSCLE (Fig. 2). This alignment revealed the presence of several conserved motifs in these parasitic and free-living nematodes, and the LNR and ANK motifs showed maximal amino acid conservation. A phylogenetic analysis using the amino acid sequences was performed to understand the patterns of relatedness among the *glp-1* genes of the nematodes analysed in this study. The phylogenetic analysis of GLP-1 in *Meloidogyne* and other species, which was conducted using the NJ method, revealed a separate cluster comprised of Mi-GLP-1, Gp-GLP-1, Mh-GLP-1 and Mf-Notch-like protein. As observed in the phylogenetic tree, Mi-GLP-1 appeared to be most closely related to the Mf-Notch-like protein, which lacks an ANK (as demonstrated in the Pfam analysis). However, a higher degree of similarity in the LNR, RAM domain and ANK was found between Mi-GLP-1 and Gp-GLP-1, conclusively demonstrating the close relationship between these two genes (Fig. 3).

Transcript abundance of Notch-receptor genes in the developmental stages of *M. incognita*

To study the expression pattern of *glp-1* in *M. incognita* development, five different stages were selected: egg masses, J2s, mature females, J3s and J4s (the last two were obtained from the samples of infected plant roots harvested 10 and 21 dpi). Interestingly, *glp-1* showed higher expression during early development in *M. incognita*, i.e. in egg masses (Fig. 4). This finding is consistent with those of previous studies that investigated *glp-1* abundance at early developmental stages in *C. elegans* embryos (Austin and Kimble, 1989; Crittenden *et al.* 1997). A qRT-PCR analysis also revealed that the *glp-1* transcript levels were increased in mature females, indicating a possible role for this protein at this developmental stage in *M. incognita*.

Determination of the efficacy of *glp-1* gene silencing

Nematode infection assay on *Arabidopsis* RNAi lines

A dsRNA expression construct of the *glp-1* gene was designed in the pBC vector (Yadav *et al.* 2006). The constructs were mobilized into *Arabidopsis* plants for the host-mediated delivery of RNAi of the *glp-1* gene. To evaluate the silencing efficacy of *Mi-glp-1*, T₃ seedlings of two independent transgenic lines were infected by

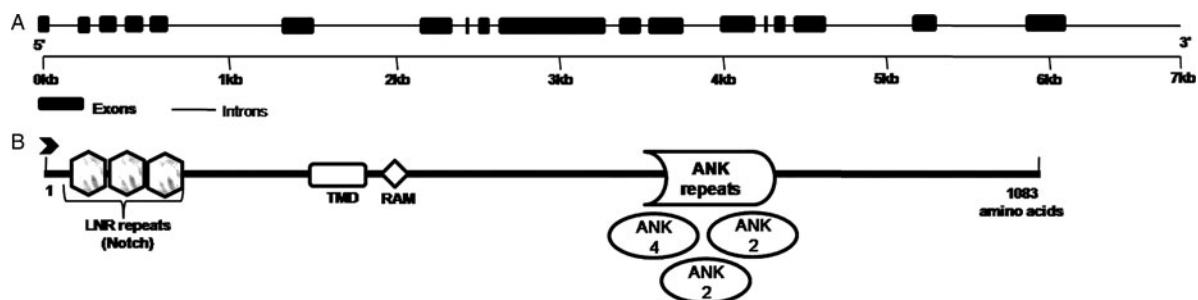


Fig. 1. Diagrammatic representation of the predicted structures of the *glp-1* gene and its encoded protein. (A) Exon/intron structure of *Meloidogyne incognita glp-1*. The boxes represent exons, and the black lines represent introns. (B) Architecture of the *M. incognita* GLP-1 protein. The functional domains are indicated as follows: ◻ LNR, ◻ TMD, ◻ RAM domain and ◻ ANK.

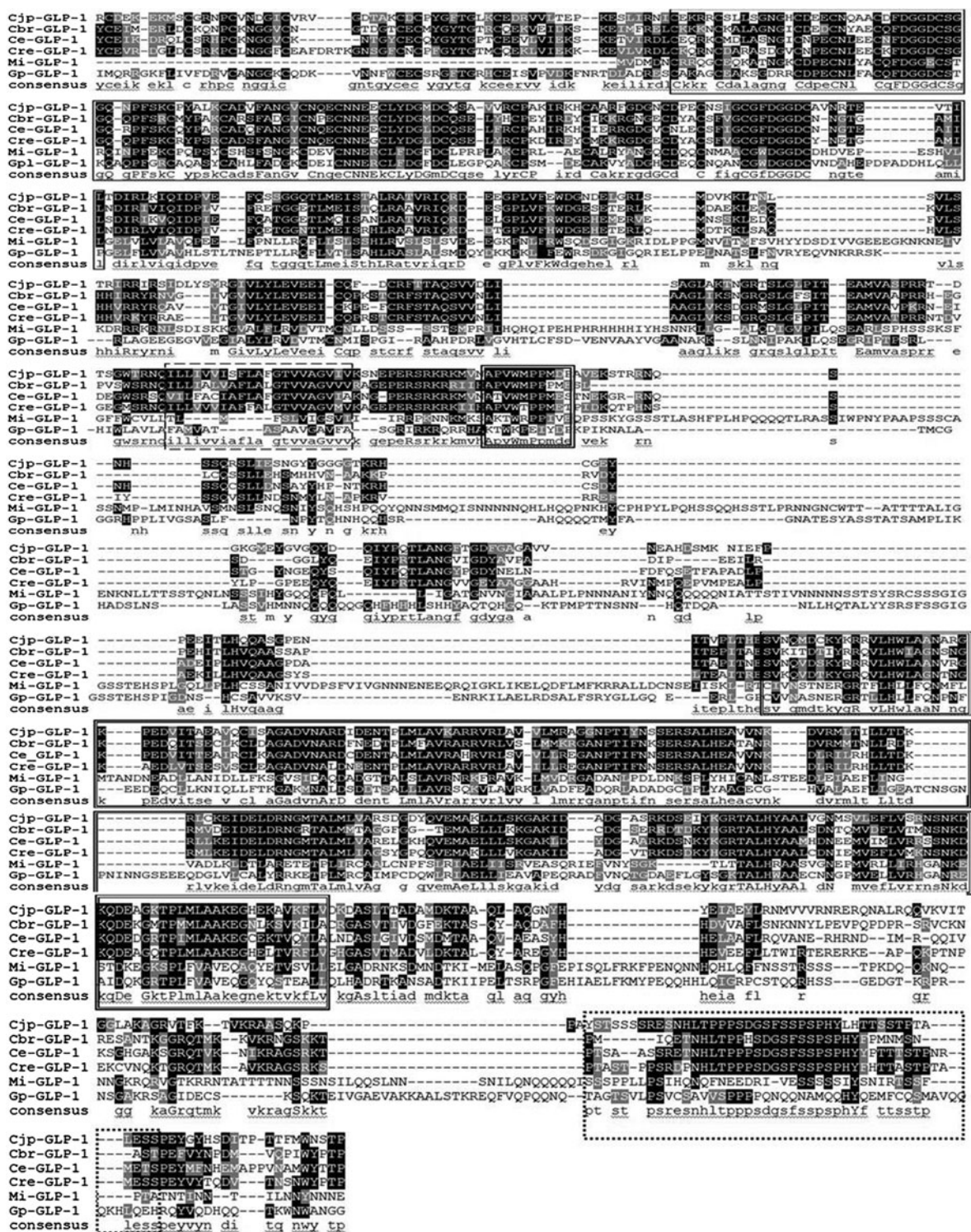


Fig. 2. Multiple sequence alignment of GLP-1 in free-living and plant-parasitic nematodes. Black shading indicates conserved amino acids. Rectangular boxes represent different motifs conserved in GLP-1 in these species (□ LNR, ▒ TMD, ■ RAM domain, □ ANK and ▫ PEST domain). Ce, *Caenorhabditis elegans*; Cbr, *Caenorhabditis briggsae*; Cjp, *Caenorhabditis japonica*; Cre, *Caenorhabditis remanei*; Mi, *Meloidogyne incognita*; Gp, *Globodera pallida*.

parasitic juveniles. Two *glp-1* RNAi lines (RNAi lines 1 and 2) were evaluated by staining the nematodes inside their roots and determining the infection level (Fig. 5A). Both *glp-1* RNAi lines exhibited reductions in the number of galls (47.8% and 51.3%), females (51.5% and 47.79%) and egg masses (49.3% and 59.4%) compared with the control plants and transgenic plants harbouring an empty vector (Fig. 5A–C). Altogether, both transgenic RNAi lines presented significant reductions in the number of galls, females and egg masses, indicating that the silencing of

this gene has a deleterious effect on the growth and development of nematodes. The adult female nematodes were isolated, and their sizes were analysed to determine any phenotypic effects, if any, on *M. incognita*. The length and width of randomly selected females were measured using a scale on a Nikon microscope (Supplementary Fig. S3). The average length and width of the females dissected from control plants were 396.27 and 248.18 μm , respectively, whereas the average length and width of the females isolated from the RNAi lines were significantly

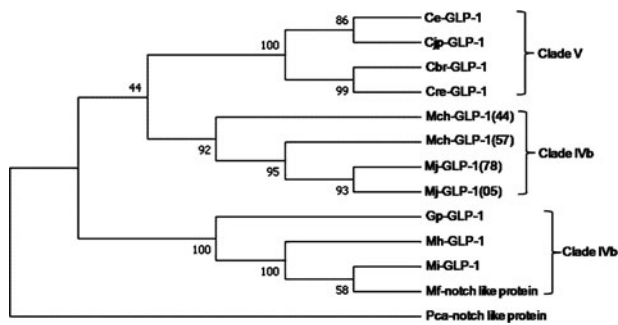


Fig. 3. Phylogenetic analysis of Notch-like receptors. Neighbour-joining phylogenetic tree of Notch-like receptors from *Caenorhabditis elegans* (Ce), *Caenorhabditis japonica* (Cjp), *Caenorhabditis briggsae* (Cbr), *Caenorhabditis remanei* (Cre), *Meloidogyne chitwoodi* (Mch), *Meloidogyne javanica* (Mj), *Globodera pallida* (Gp), *Meloidogyne incognita* (Mi), *Meloidogyne floridensis* (Mf), *Meloidogyne hapla* (Mhp) and *Priapulius caudatus* (Pca, as an outgroup). The percentage of replicate trees in which the associated taxa clustered together in the bootstrap test (2000 replicates) is shown next to the branches. The phylogenetic analysis was conducted using MEGA7.

decreased, with values of 231.9 and 140.36 μm , respectively (Supplementary Table S3). Therefore, the nematodes obtained from the RNAi lines showed reductions of 41.4% and 43.4% in their length and width, respectively.

Molecular analyses of RNAi lines through qRT-PCR and Northern blotting

The transcript abundance of the target gene in the females isolated from both RNAi lines showed an approximately 60% reduction compared with that in the females isolated from control plants (Fig. 6A). This decrease in the transcript levels of *glp-1* in females obtained from the RNAi lines demonstrated the effect of its silencing through host-delivered dsRNA. A Northern analysis was also performed, and the results confirmed the presence of *glp-1* dsRNA in RNAi line 1 (Fig. 6B). One of the key components of host-mediated RNAi was the 419 bp dsRNA of *glp-1*, which was detected in the transgenic RNAi line.

Effect of silencing on *M. incognita* fecundity and next-generation J2s

The females that fed on RNAi lines produced fewer numbers of egg masses compared with those that fed on wild-type plants. To further investigate the deleterious effects, if any, of the

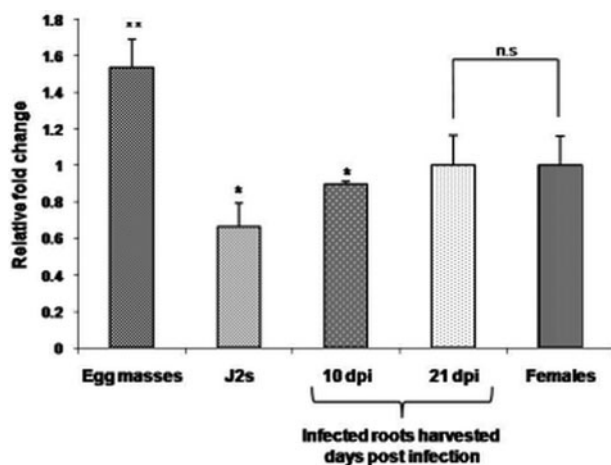


Fig. 4. Expression analysis of *Mi-glp-1* at different developmental stages in *Meloidogyne incognita*. The histogram indicates the relative fold change ($2^{-\Delta\Delta\text{CT}}$ value) normalized based on the actin gene as an endogenous gene and the female ΔCt value as a calibrator. The asterisks * and ** indicate significant differences at $P < 0.05$ and $P < 0.01$, respectively, and 'n.s.' indicates no significance.

silencing of the *glp-1* gene, the number of eggs present in these egg masses was evaluated, and these eggs were maintained for subsequent hatching. A 26% reduction in the number of eggs was noted in the RNAi lines, and the corresponding MF value was estimated to determine the nematode population. The estimated MF value for the infection of *M. incognita* in transgenic RNAi lines was calculated to equal 11.57, whereas that for wild-type plants was 31.1 (Supplementary Table S4A). Although J2s with well-developed pharynxes and stylet structures were observed in the samples isolated from the RNAi lines, several J2s showed aberrations around the metacarpus region as well as a shorter distance from the stylet to the metacarpus region of the pharyngeal structures (Fig. 7 and Supplementary Table S4B). Thus, it can be deduced that this effect on J2s is due to the nature in which RNAi is inherited from one generation to the next. Studies in *C. elegans* have shown inherited effects of silencing even in the absence of the original trigger (Bird *et al.* 2009), and the persistence of silencing effects has also been observed after suppression of the *Mi-1* gene of tomato (Gleason *et al.* 2008).

Discussion

Although several genes related to neuropeptides and secretory pathways involved in the parasitism of PPNs have been reported (Rehman *et al.* 2016), detailed information regarding the structural and functional roles of genes with functions in organ development in PPNs, including *M. incognita*, is lacking. Very few studies have identified genes that play a crucial role in organ development in a PPN. *Mi-glp-1*, a Notch family member, was identified in this study as an orthologue of *Ce-glp-1*. In our study, a genome-wide computational approach revealed MiV1ctg1087, a single contig, as *Mi-glp-1* in *M. incognita*. Interestingly, Minc16055 was also annotated as a Notch receptor protein in an identification of microsatellite loci in *M. incognita* (Castagnone-Sereno *et al.* 2010). A phylogenetic tree showed 12 orthologues originating from three clusters, all of which were branched, as well as one separate unbranched cluster (*P. caudatus*) as an outgroup. Notably, the branching of these three clusters originated from a common node. Thus, it could be hypothesized that the Mi-GLP-1 product has putative functions closely related to those of the Ce-GLP-1 protein. Nevertheless, further studies on the function of each conserved domain in Mi-GLP-1 will support its predicted role.

Mi-glp-1 is composed of 7.449 kb, which is similar to the size of *Ce-glp-1*. However, the corresponding mRNA sizes showed a difference of approximately 1.07 kb, which resulted from differences in the overall gene organization and structure. A similar size difference at the mRNA level was also observed with *G. pallida glp-1* (Supplementary Table S2). The observed difference in the exon/intron structure could be due to the scaffold form of the *M. incognita* genome, which resulted in the formation of a truncated protein. A genome-wide search to identify more members of *glp-1* in the *M. incognita* genome was attempted using *Ce-glp-1* as the query sequence, but only a single member was identified. To date, only one other member of the GLP protein family, named GLP-4, has been characterized in *C. elegans* and *C. briggsae* (Mango, 2007; Rastogi *et al.* 2015). At the protein level, Mi-GLP-1 has several conserved motifs that are also present in the corresponding protein in *C. elegans*. A Pfam analysis showed the presence of a TMD, LNR, an RAM domain and an ANK. The LNR mediates ligand-binding functions, and the ANK and RAM domain are needed for signalling responses (Kelley *et al.* 1987; Rebay *et al.* 1991; Heitzler and Simpson, 1993; Artavanis-Tsakonas *et al.* 1999). Based on previous experimental evidence, the ANK is thought to be critical for the function of Notch receptors (Roehl and Kimble, 1993; Diederich *et al.* 1994). In addition, three different software programs predicted

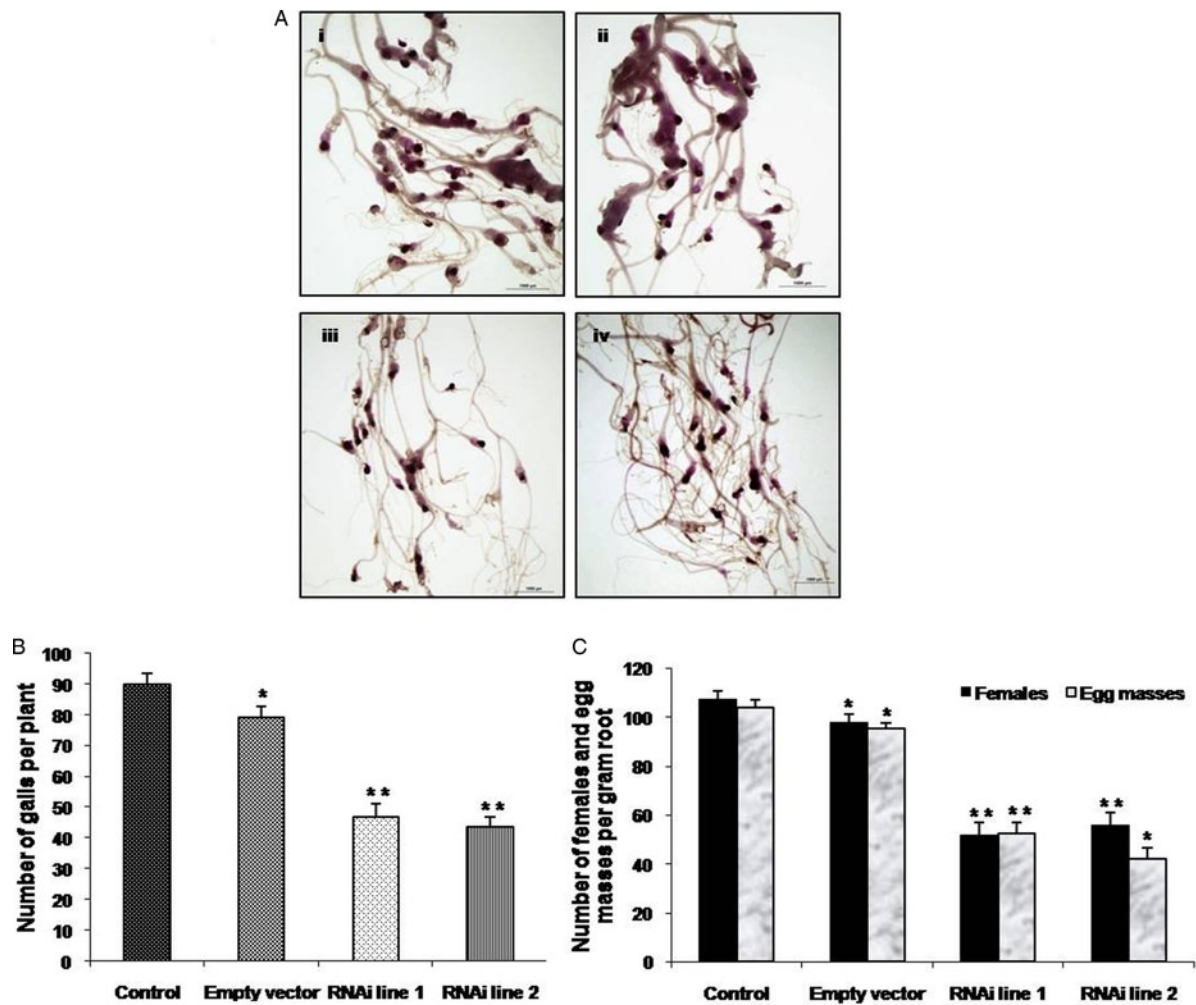


Fig. 5. Nematode infection assay. (A) Representative photograph depicting *Meloidogyne incognita* in infected roots stained with acid fuchsin: (i) wild-type plants, (ii) empty vector line, (iii) RNAi line 1 and (iv) RNAi line 2. (B) and (C) Histogram depicting the number of galls, females and egg masses in the RNAi lines, empty vector transgenic lines and control (wild-type) plants. The asterisks * and ** indicate a significant difference at $P < 0.05$ and $P < 0.01$, respectively.

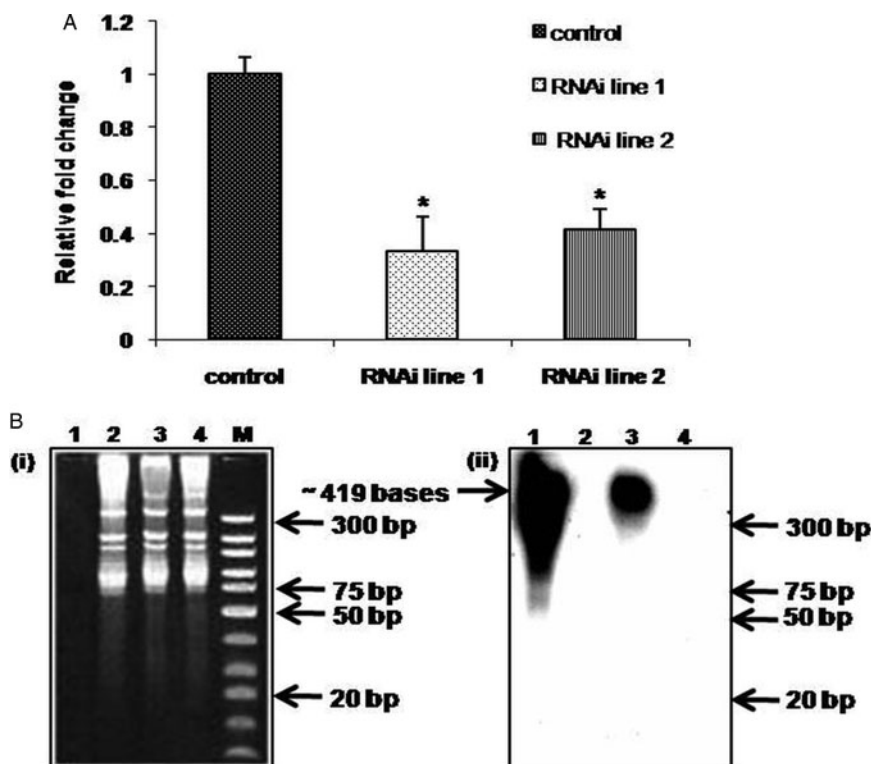


Fig. 6. Molecular analyses of *Meloidogyne incognita* isolated from transgenic *Arabidopsis* plants. (A) RT-qPCR-based *glp-1* expression analysis of *M. incognita* females isolated from infected roots of RNAi lines 1 and 2 and females isolated from control plants. (B) Ethidium bromide-stained PAGE gel (before transfer) showing the low-molecular-weight RNA fraction (i) and the corresponding Northern blot for detecting the presence of *glp-1* dsRNA (ii). The 183 bp probe corresponding to *glp-1* was designed from the LNR domain. In (i) and (ii), lane 1 - gene-specific PCR product as a positive control, lane 2 - empty vector line, lane 3 - RNAi line 1, lane 4 - wild type as a control and lane M - molecular marker.

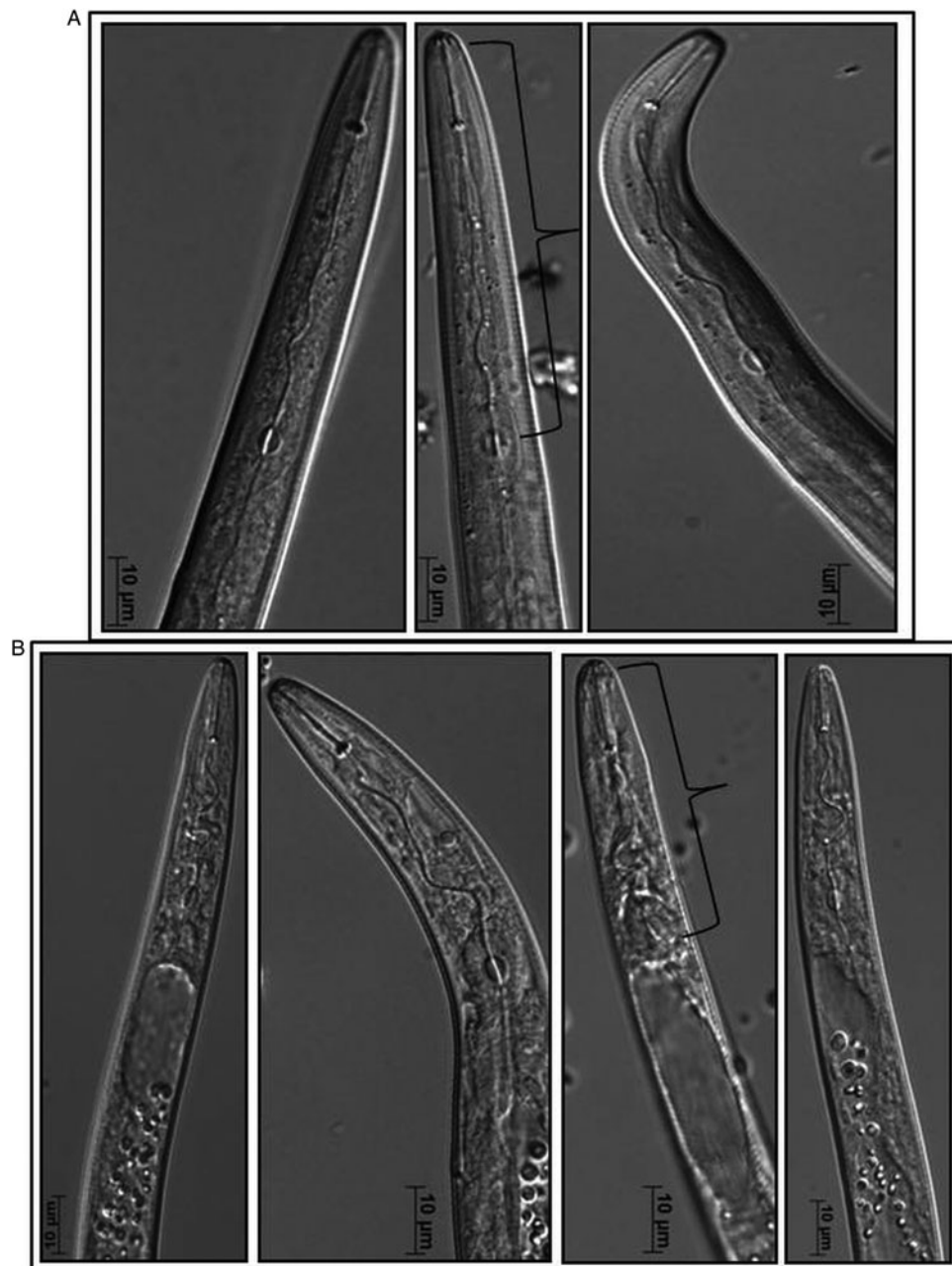


Fig. 7. Phenotypes of stylets and pharynxes of J2s descended from *Meloidogyne incognita* females isolated from infected plants: (A) wild-type (control) plants and (B) RNAi lines. Curly brackets indicate the length from the mouth to the metacarpus bulb in J2s. Please note shortening of length in few J2s from RNAi lines as compared to control plants.

the presence of a TMD, further indicating that Mi-GLP-1 most likely functions as a receptor protein (Supplementary Fig. S5A and B), although a clear mechanism of interaction has not been determined. A noticeable difference between Ce-GLP-1 and Mi-GLP-1 is the absence of an EGF domain at the 5' end of the Mi-GLP-1 amino acid sequence, suggesting certain structural and functional differences between the *glp-1* gene of *C. elegans* and that of *M. incognita*. Hence, the putative GLP-1 protein identified in this study has properties and structures similar to those of a receptor protein with varied domains, each with a specific function. In addition to these conserved domains, DNA-binding sites for ligands such as LAG-1 proteins were also found to be present in Mi-GLP-1. The presence of this type of motif at more than one site on the Mi-GLP-1 Notch receptor suggests that a vital function of GLP-1 is mediated through LAG-1 ligand binding to induce downstream reactions in the signalling pathway. Based on previous studies on Ce-LAG-1 DNA-binding sites, the potential function of

this protein in LIN-12/GLP-1 signalling pathways has been proposed (Christensen *et al.* 1996). Experiments including yeast, two-hybrid assays and *in vitro* protein co-precipitation have demonstrated direct interactions between LAG-1 and the GLP-1 receptor *via* these domains in nematodes (Roehl *et al.* 1996). Further studies are needed to determine the role of these domains in signalling processes. Thus, based on *in silico* analyses and the available literature, it can be concluded that the gene identified in this study is a Notch receptor protein present in *M. incognita*.

Our study revealed that *Mi-glp-1* is differentially expressed during different developmental stages of *M. incognita*. The increased transcript level observed in egg masses suggests an important role during embryogenesis. This observation was consistent with previous studies that suggested a possible role for this protein during embryogenesis in *C. elegans* (Priess *et al.* 1987; Austin and Kimble, 1989). However, a slight increase in the transcript level was detected in mature females, suggesting another

possible role for this protein during later stages of RKN development. Interestingly, similar reports regarding a possible role for *glp-1* in the adult stage of *C. elegans* have not been reported. Future studies examining the localization of this gene product will confirm the role of GLP-1 during female development in *M. incognita*.

Host-delivered RNAi-mediated root-knot nematode resistance is an established technology, but the identification of better candidate genes remains necessary. In addition, the identification of genes involved in different developmental pathways will enable the targeting of several vital genes. Parasitic and secretory genes have traditionally been the genes of choice in silencing studies. However, there are very few candidate genes from the perspective of nematode development. A few developmental genes, such as Rpn7 (essential for the integrity of the 26S proteasome), *nhr-48*, FAR-1, splicing factor and integrase genes, have been targeted using RNAi in efforts aiming to control infection with the root-knot nematode *M. incognita* (Yadav *et al.* 2006; Niu *et al.* 2012; Iberkleid *et al.* 2015; Lu *et al.* 2016). The *glp-1* gene, which was identified in this study, appears to be involved in the development, and a dsRNA/siRNA strategy was used for the host-mediated RNAi-based suppression of *Mi-glp-1* in *M. incognita*. Transgenic *Arabidopsis* lines expressing dsRNA against *Mi-glp-1* and infected with *M. incognita* did not show any phenotypic changes compared with wild-type plants. An approximately 47% reduction in the infection level was recorded in two independent *glp-1* RNAi lines, and decreases in the gall formation, female infestation and egg mass production were also observed in these RNAi lines. In addition, an overall decrease in the number of females feeding on RNAi lines was recorded compared with females isolated from control plants. These results unequivocally demonstrated that *glp-1* was suppressed in females that fed on the established RNAi lines. The nematode females isolated from control plants had an average length and width similar to the reported body length (ranging from 510 to 690 μm) and width (300 to 430 μm) of a healthy mature *M. incognita* female (Whitehead, 1968; García and Sánchez-Puerta, 2012). In contrast, the females isolated from the RNAi lines had average lengths and widths of 232 and 141 μm , respectively, indicating an evident decrease in the overall body size in the females that fed on the RNAi lines. However, whether this decrease was a direct result of the low expression of *glp-1* is unclear. Direct evidence supporting a role for *glp-1* in the growth of *M. incognita* at later stages in the lifecycle has not yet been reported. However, in this study, a 60% decrease in transcript abundance was noted in the adult nematode females that fed on the RNAi lines. Additionally, to confirm the reduction in expression due to dsRNA/siRNA effects, the dsRNA molecules in the control and transgenic plants (empty vector and RNAi lines) were detected by Northern hybridization. The results confirmed the presence of *glp-1*-specific dsRNA molecules in the transgenic lines, an important factor for successful host-mediated RNAi (Bass, 2000; Agrawal *et al.* 2003), but we were unable to identify *glp-1*-specific siRNAs despite numerous attempts. Several studies have reported a similar problem with other genes, and this difficulty is most likely due to the low sensitivity of the Northern blot analysis (Dinh *et al.* 2014). The ability of *M. incognita* to ingest large molecules, which has been well established, and the presence of four dicers in *Arabidopsis*, which likely processed the *glp-1*-specific dsRNAs (as shown in our Northern analysis) into siRNAs to trigger RNAi responses in *M. incognita* females feeding on the transgenic RNAi lines might also have played a role. However, future studies comparing the transcript and protein levels in progenies are required to confirm our observations.

To investigate the suppression effect of *glp-1* on the fecundity of *M. incognita* females, egg masses were hand-picked from all

females in the infected RNAi lines, control plants and empty vector lines and subsequently incubated to determine their hatching capability, and the number of J2s hatched from each sample was counted. A decrease in the population of J2s obtained from the RNAi lines was noted, and the lower estimated MF value for *M. incognita* in the transgenic RNAi plants compared with control plants suggested a reduced infectivity of *M. incognita* on the RNAi lines compared with the wild-type plants. In embryos, *glp-1* RNA is maternally donated (i.e. by the mother) in *C. elegans* (Evans *et al.* 1994); therefore, dsRNA appears to affect even the progeny produced from the affected females. In our J2s, aberrations in the structures of the metacorporeal bulbs and their stylet discs were clearly apparent. A noticeable and significant decrease in the length of the region from the stylet to the metacarpus was also evident. Our study showed an adverse effect of the suppression of the *glp-1* gene on the pharyngeal and stylet structures and thereby provides insight into the function of the *glp-1* gene in pharyngeal development in *M. incognita*. Similarly, Geng *et al.* (2016) reported a degradation of intestinal tissues of *M. incognita* and identified Sep1, a novel serine protease, as a potent bio-agent from *Bacillus firmus* for controlling PPN populations. Thus, it can be inferred that the females obtained from transgenic plants exerted effects on the foregut region of their descendants. Our results strongly suggest the transmission of dsRNA-mediated deleterious effects to the next generation of root-knot nematodes. Because a difference in the phenotype of J2s was observed, a decrease in the GLP-1 protein level is possible; however, a more detailed study is required to fully evaluate this hypothesis.

The present work identified and characterized a gene encoding a Notch receptor protein in *M. incognita* involved in the development of the pharynx during embryogenesis and investigated the evolutionary conservation of its function between free-living nematodes and PPNs. Several common features in the Mi-GLP-1, Ce-GLP-1 and Gp-GLP-1 amino acid sequences were revealed. The *in planta* production of RNAi has been shown to effectively reduce the infectivity and size of *M. incognita* females. Deleterious effects were also observed in later generations (J2s) obtained from females isolated from infected transgenic plants. Taken together, our results demonstrate that the host-mediated gene silencing of the nematode *glp-1* is an efficient method for inhibiting plant infection. The presence of *glp-1* homologues in other PPNs, such as *M. hapla*, *M. floridensis*, *M. javanica*, *M. chitwoodi* and *G. pallida*, suggests the wide potential applicability of the silencing of this gene using host-mediated gene silencing approaches for the control of these parasitic nematodes. However, several important questions remain unanswered: (1) Does the *glp-1* gene directly determine the pharyngeal development in PPNs or does it interact with other genes to define the development of the anterior region of the pharynx, as shown in free-living nematodes? (2) Does this gene have a specific role in other stages, such as the adult female stage, as indicated from our expression analysis? Providing answers to these questions requires experimental assessment of the phenotypic and molecular function(s) of the *glp-1* gene. Although further investigations are essential to fully determine the role of *glp-1* in parasitic nematodes, the observations obtained in this study provide a reasonable indication that *glp-1* plays a significant role in pharyngeal development in PPNs. The role of GLP-1 as a receptor protein has been well characterized in *C. elegans*, but its involvement in pathogenic nematodes has not yet been reported. Establishing the involvement of *glp-1* in pharyngeal development could further aid the elucidation of various pathways in PPNs, and the identification of genes downstream of the GLP-1 receptor and of its ligands will provide further insights into the various processes and pathways in which *glp-1* is involved. These ligands and associated genes can then be targeted to obtain a more in-depth

understanding of the cross-talk between different pathways and could eventually be used as targets in RNAi-mediated silencing approaches for PPN management to improve overall crop productivity.

Supplementary material. The supplementary material for this article can be found at <https://doi.org/10.1017/S0031182018000641>

Acknowledgements. The authors thank the staff of the National Phytotron Facility, IARI, New Delhi, India, for providing space in their greenhouse and growth chambers. The authors would also like to thank Dr Gautam Chawla, Division of Nematology, IARI, India, for providing the Zeiss Axio microscope used in this study and Mr Gaurav for assisting with the use of the Zeiss microscope.

Financial support. The present study was supported by a grant from the ICAR-NASF Project (formerly known as NFBSFARA; code: NFBSFARA/RNA-3022) during the years 2012–2015.

Conflicts of interest. None.

Ethical standards. Not applicable

References

- Abad P, et al. (2008) Genome sequence of the metazoan plant-parasitic nematode *Meloidogyne incognita*. *Nature Biotechnology* **26**, 909–915.
- Agrawal N, et al. (2003) RNA interference: biology, mechanism, and applications. *Microbiology and Molecular Biology Reviews* **67**, 657–685.
- Artavanis-Tsakonas S, Rand MD and Lake RJ (1999) Notch signaling: cell fate control and signal integration in development. *Science* **284**, 770–776.
- Austin J and Kimble J (1989) Transcript analysis of *glp-1* and *lin-12*, homologous genes required for cell interactions during development of *C. elegans*. *Cell* **58**, 565–571.
- Bailey TL, et al. (2015) The MEME Suite. *Nucleic Acids Research* **43**, W39–W49.
- Banerjee S, et al. (2017) RNA interference: a novel source of resistance to combat plant parasitic nematodes. *Frontiers in Plant Science* **8**, 834.
- Bass BL (2000) Double-stranded RNA minireview as a template for gene silencing. *Cell* **101**, 235–238.
- Bird DM, et al. (2009) The genomes of root-knot nematodes. *Annual Review of Phytopathology* **47**, 333–351.
- Bybd Jr. DW, Kirkpatrick T and Barker KR (1983) An improved technique for clearing and staining plant tissues for detection of nematodes. *Journal of Nematology* **15**, 142–143.
- Calderón-Urrea A, et al. (2016) Early development of the root-knot nematode *Meloidogyne incognita*. *BMC Developmental Biology* **16**, 10.
- Castagnone-Sereno P, et al. (2010) Genome-wide survey and analysis of microsatellites in nematodes, with a focus on the plant-parasitic species *Meloidogyne incognita*. *BMC Genomics* **11**, 598.
- Christensen S, et al. (1996) *lag-1*, a gene required for *lin-12* and *glp-1* signaling in *Caenorhabditis elegans*, is homologous to human CBF1 and *Drosophila* Su(H). *Development* **122**, 1373–1383.
- Clough SJ and Bent AF (1998) Floral dip: a simplified method for *Agrobacterium*-mediated transformation of *Arabidopsis thaliana*. *The Plant Journal* **16**, 735–743.
- Cotton JA, et al. (2014) The genome and life-stage specific transcriptomes of *Globodera pallida* elucidate key aspects of plant parasitism by a cyst nematode. *Genome Biology* **15**, R43.
- Crittenden SL, et al. (1997) Genes required for GLP-1 asymmetry in the early *Caenorhabditis elegans* embryo. *Developmental Biology* **181**, 36–46.
- Diederich RJ, et al. (1994) Cytosolic interaction between *deltex* and Notch ankyrin repeats implicates *deltex* in the Notch signaling pathway. *Development* **120**, 473–481.
- Dinh PTY, Brown CR and Elling AA (2014) RNA interference of effector gene *Mc16D10L* confers resistance against *Meloidogyne chitwoodi* in *Arabidopsis* and Potato. *Phytopathology* **104**, 1098–1106.
- Edgar RC (2004) MUSCLE: multiple sequence alignment with high accuracy and high throughput. *Nucleic Acids Research* **32**, 1792–1797.
- Eisenback JD and Hunt DJ (2009) General morphology. In Perry RN, Moens M and Starr JL (eds). *Root Knot Nematode*. Oxfordshire, UK: CAB International 2, pp. 18–50.
- Elling AA (2013) Major emerging problems with minor *Meloidogyne* species. *Phytopathology* **103**, 1092–1102.
- Elsworth B, Wasmuth J and Blaxter M (2011) NEMBASE4: the nematode transcriptome resource. *International Journal of Parasitology* **41**, 881–894.
- Evans TC, et al. (1994) Translational control of maternal *glp-1* mRNA establishes an asymmetry in the *C. elegans* embryo. *Cell* **77**, 183–194.
- Fanelli E, et al. (2005) Analysis of chitin synthase function in a plant parasitic nematode, *Meloidogyne artiellia*, using RNAi. *Gene* **349**, 87–95.
- Finn RD, et al. (2016) The Pfam protein families database: towards a more sustainable future. *Nucleic Acids Research* **44**, D279–D285.
- García LE and Sánchez-Puerta MV (2012) Characterization of a root-knot nematode population of *Meloidogyne arenaria* from Tupungato (Mendoza, Argentina). *Journal of Nematology* **44**(3), 291–301.
- Gasteiger E, et al. (2005) Protein identification and analysis tools on the ExpASY server. In Walker JM (ed). *The Proteomics Protocols Handbook*. Totowa, NJ: Humana Press, pp. 571–607.
- Geng C, et al. (2016) A novel serine protease, *Sep1*, from *Bacillus firmus* DS-1 has nematocidal activity and degrades multiple intestinal-associated nematode proteins. *Scientific Reports* **6**, 25012.
- Gleason CA, Liu QL and Williamson VM (2008) Silencing a candidate nematode effector gene corresponding to the tomato resistance gene *Mi-1* leads to acquisition of virulence. *Molecular Plant-Microbe Interactions* **21**(5), 576–585.
- Gray LJ, Curtis RH and Jones JT (2001) Characterisation of a collagen gene subfamily from the potato cyst nematode *Globodera pallida*. *Gene* **263**, 67–75.
- Heitzler P and Simpson P (1993) Altered epidermal growth factor-like sequences provide evidence for a role of Notch as a receptor in cell fate decisions. *Development* **117**, 1113–1123.
- Hu B, et al. (2015) GSDS 2.0: an upgraded gene feature visualization server. *Bioinformatics (Oxford, England)* **31**(8), 1296–1297.
- Iberkleid I, Sela N and Brown Miyara S (2015) *Meloidogyne javanica* fatty acid- and retinol-binding protein (Mj-FAR-1) regulates expression of lipid-, cell wall-, stress- and phenyl propanoid-related genes during nematode infection of tomato. *BMC Genomics* **16**, 272.
- Kaur H and Attri R (2013) Morphological and morphometrical characterization of *Meloidogyne incognita* from different host plants in four districts of Punjab, India. *The Journal of Nematology* **45**, 122–127.
- Kelley MR, et al. (1987) Mutations altering the structure of epidermal growth factor-like coding sequences at the *Drosophila* Notch locus. *Cell* **57**, 539–548.
- Kumar A, et al. (2017) Host-delivered RNAi-mediated root-knot nematode resistance in *Arabidopsis* by targeting *splicing factor* and *integrase* genes. *Journal of General Plant Pathology* **83**, 91–97.
- Kumar S, Stecher G and Tamura K (2016) MEGA7: Molecular Evolutionary Genetics Analysis version 7.0 for bigger datasets. *Molecular Biology and Evolution* **33**, 1870–1874.
- Kyte J and Doolittle R (1982) A simple method for displaying the hydrophobic character of a protein. *Journal of Molecular Biology* **157**, 105–132.
- Livak KJ and Schmittgen TD (2001) Analysis of relative gene expression data using real-time quantitative PCR and the 2^{(-Delta Delta C(T))} method. *Methods* **25**(4), 402–408.
- Lu CJ, et al. (2016) Nuclear receptor *nhr-48* is required for pathogenicity of the second stage (J2) of the plant parasite *Meloidogyne incognita*. *Scientific Reports* **6**, 34959.
- Lunt DH, et al. (2014) The complex hybrid origins of the root knot nematodes revealed through comparative genomics. *PeerJ* **2**, e356.
- Mango SE (2007) The *C. elegans* pharynx: a model for organogenesis. In *Wormbook*, The *C. elegans* Research community. WormBook. doi/10.1895/wormbook.1.129.1.
- Martin J, et al. (2015) Helminth.net: expansions to Nematode.net and an introduction to Trematode.net. *Nucleic Acids Research* **43**, D698–D706.
- Martinuz A, Schouten A and Sikora RA (2013) Post-infection development of *Meloidogyne incognita* on tomato treated with the endophytes *Fusarium oxysporum* strain Fo162 and *Rhizobium etli* strain G12. *BioControl* **58**, 95–104.
- Moens M, Perry RN and Starr JL (2009) *Meloidogyne* species: a diverse group of novel and important plant parasites. In Perry RN, Moens M and Starr JL (eds). *Root-knot nematodes*. Wallingford, UK: CABI Publishing, pp. 1–17.
- Niu J, et al. (2012) RNAi silencing of the *Meloidogyne incognita* *Rpn7* gene reduces nematode parasitic success. *European Journal of Plant Pathology* **134**, 131–144.
- Nguyễn PV, et al. (2014) *Meloidogyne incognita* – rice (*Oryza sativa*) interaction: a new model system to study plant-root-knot nematode interactions in monocotyledons. *Rice* **7**, 23.

- Nsengimana J, et al.** (2013) Silencing of Mg-pat-10 and Mg-unc-87 in the plant parasitic nematode *Meloidogyne graminicola* using siRNAs. *Agriculture* **3**, 567–678.
- Opperman CH, et al.** (2008) Sequence and genetic map of *Meloidogyne hapla*: a compact nematode genome for plant parasitism. *Proceedings of the National Academy of Sciences USA* **105**, 14802–14807.
- Priess JR, Schnabel H and Schnabel R** (1987) The glp-1 locus and cellular interactions in early *C. elegans* embryos. *Cell* **51**, 601–611.
- Rastogi S, et al.** (2015) *Caenorhabditis elegans* glp-4 encodes a valylaminoacyl tRNA synthetase. *Genes Genomes Genetics* **5**, 719–728.
- Rebay I, et al.** (1991) Specific EGF repeats of Notch mediate interactions with Delta and Serrate: implications for Notch as a multifunctional receptor. *Cell* **67**, 687–699.
- Rehman S, Gupta VK and Goyal AK** (2016) Identification and functional analysis of secreted effectors from phytoparasitic nematodes. *BMC Microbiology* **16**, 48.
- Roehl H and Kimble J** (1993) Control of cell fate in *C. elegans* by a GLP-1 peptide consisting primarily of ankyrin repeats. *Nature* **364**, 632–635.
- Roehl H, et al.** (1996) Roles of the RAM and ANK domains in signaling by the *C. elegans* GLP-1 receptor. *The EMBO Journal* **15**, 7002–7012.
- Rudel D and Kimble J** (2001) Conservation of glp-1 regulation and function in nematodes. *Genetics* **157**, 639–654.
- Tytgat T, et al.** (2004) An SXP/RAL-2 protein produced by the subventral pharyngeal glands in the plant parasitic root-knot nematode *Meloidogyne incognita*. *Parasitology Research* **95**, 50–54.
- Veronico P, et al.** (2001) Nematode chitin synthases: gene structure, expression and function in *Caenorhabditis elegans* and the plant parasitic nematode *Meloidogyne artiellia*. *Molecular Genetics and Genomics* **266**, 28–34.
- Verwoerd TC, Dekker BM and Hoekema A** (1989) A small-scale procedure for the rapid isolation of plant RNAs. *Nucleic Acids Research* **17**(6), 2362.
- Wang T, Deom CM and Hussey RS** (1998) Identification of a *Meloidogyne incognita* cuticle collagen gene and characterization of the developmental expression of three collagen genes in parasitic stages. *Molecular and Biochemical Parasitology* **93**, 131–134.
- Whitehead AG** (1968) Taxonomy of *Meloidogyne* (Nematodea: Heteroderidae) with descriptions of four new species. *Journal of Zoology* **131**(3), 263–401.
- Xie J, et al.** (2016) A novel *Meloidogyne incognita* effector Misp12 suppresses plant defense response at latter stages of nematode parasitism. *Frontiers in Plant Science* **7**, 964.
- Yadav BC, Veluthambi K and Subramaniam K** (2006) Host-generated double stranded RNA induces RNAi in plant-parasitic nematodes and protects the host from infection. *Molecular and Biochemical Parasitology* **148**, 219–222.
- Ye W, Zeng Y and Kerns J** (2015) Molecular characterisation and diagnosis of root-knot nematodes (*Meloidogyne* spp.) from Turf grasses in North Carolina, USA. *PLoS ONE* **10**(11), e0143556.
- Yochem J and Greenwald I** (1989) glp-1 and lin-12, genes implicated in distinct cell-cell interactions in *C. elegans*, encode similar transmembrane proteins. *Cell* **58**, 553–563.

Isolation, Cloning and Characterization of Cuticle Collagen Genes, *Mi-dpy-10* and *Mi-dpy-31*, in *Meloidogyne incognita*

DESHIKA KOHLI^{1,2}, ANIL SIROHI³, RAMAMURTHY SRINIVASAN¹, NAVNEETA BHARADVAJA²
AND PRADEEP K. JAIN^{1*}

¹ICAR-NRC on Plant Biotechnology, Pusa Campus, New Delhi 110012, India

²Delhi Technological University, Shahbad Daultapur, Delhi-110042, India

³Division of Nematology, ICAR-Indian Agricultural Research Institute, Pusa, New Delhi 110012, India

*Corresponding author; E-mail: jainpmb@gmail.com

Received on, Revised on, Accepted on

ABSTRACT: Endoparasitic plant-parasitic nematodes (PPN) including *Meloidogyne incognita* inhabit the host body due to their unique body surface, the outer layer of which is cuticle. The nematode cuticle is an extracellular matrix, majorly composed of collagens which are encoded by a large gene family. Nematode cuticle acts as a shield against host's defense system thereby protecting parasitic nematodes. The cuticle of PPN is a less studied area of research with only few cuticle genes identified till date. In this study two new cuticle genes viz. *dpy-10* and *dpy-31* have been identified in *M. incognita* as orthologs of *Caenorhabditis elegans dpy-10* and *dpy-31*, respectively. The partial mRNA sequences of *dpy-10* (1,031 bp) and *dpy-31* (1,116 bp) were cloned. The conserved collagen triple helix Gly-X-Y pattern in *Mi-dpy-10*; where proline was preferred as X amino acid and conserved catalytic (HEVAHALGFWHEQSRPDRD) and methionine-turn (SIMHY) sites in *Mi-dpy-31* classifies them in group Dpy-2 and subgroup V, respectively. A protein-protein interaction reveals a direct association between Mi-DPY-10, Mi-DPY-2, and Mi-DPY-7 together involved in post-embryonic development. While only a single Mi-SQT-3 (cuticle gene) was observed as the direct target for Mi-DPY-31 both involved in collagen processing. Phylogenetic analysis reveals a high order of conservation among the dumpy class of cuticle genes across phylum Nematoda. Since dumpy genes have a temporally regulated expression, qRT-PCR expression analyses of *Mi-dpy-10* showed higher expression at the J2 stage of the nematode development in comparison to eggs and adult females. However, *Mi-dpy-31* gene revealed higher expression in adult females in *M. incognita* suggesting different roles of dumpy genes during nematode development. Mutations in dumpy genes resulted in abnormal morphology in *C. elegans*; thus targeting such genes for developing resistance using Host-delivered RNA interference approach in *M. incognita* will be useful in managing these plant parasites.

Keywords: Cuticle superfamily genes, *Mi-dpy-10*, *Mi-dpy-31*, *Meloidogyne incognita*, Nematode cuticle

The nematode cuticle is a multifunctional exoskeleton which is a highly impervious barrier between nematode and its environment. It is an essential element for maintaining the body morphology and integrity. It is synthesized by an underlying ectodermal cell layer termed as the hypodermis. Interestingly, in a life cycle of plant-parasitic nematode synthesis of cuticle occurs five times during its development and the process is known as molting. It is required for the progression between the larval stages in the life cycle of nematodes (Davis *et al.* 2004). The cuticle synthesis occurring second round time and henceforth occurs underneath an existing cuticle unlike the initial round of synthesis.

The cuticle is an extracellular matrix, where collagen constitutes as one of the major components. Collagens are structural proteins with glycine-X-Y tripeptide repeats, where X- proline and Y- mostly hydroxyproline or proline. These proteins are encoded by over 170 members belonging to a gene family of cuticle collagen. In *C. elegans*, about 21 cuticle collagen genes were identified through mutants of these genes (Page & Johnstone 2007). These mutated genes include phenotype as DumPY (Dpy), Ray AbnorMal (Ram), RoLler (Rol), BLIster (Bli), SQaT (Sqt) and LONG (Lon). Some of the members belonging to the cuticle collagen family are expressed throughout the life cycle while many collagen

genes are required at a different time point of the molting stage thus exhibiting specific function at a specific time.

Root-knot nematode, *M. incognita*, is a plant-parasitic nematode and is a serious threat to agriculture worldwide resulting in millions of losses dollars round the year (Elling, 2013). *M. incognita* being sedentary endoparasites reproduces and feed on modified living plant cells within the plant roots. They produce galls (giant cells) inside the host and feed exclusively from these giant cells. With the time they undergo three molting to reach the adult stage thus, completing its entire life cycle inside its host body. It is the nematode body wall that protects it from the plant environment. The outer layer of the body wall is cuticle (composed of collagen) that provides protection to nematode and synthesized five times by molting in its life-cycle. Processing of collagen involves stages like catalytic events altering protein solubility and removal of N- and C- terminal teleopeptides (Page & Johnstone 2007). There are not many reports identifying cuticle genes in plant-parasitic nematodes. *Mi-col-1*, *Mi-col-5* and *lemmi 5* in *M. incognita* and COL-1 and COL-2 collagen genes in *Globodera pallida* were identified and characterized (Wang *et al.* 1998, Gray *et al.* 2001, Banerjee *et al.* 2017). Since cuticle is the major structure that is essential for *M. incognita* development and growth inside its host. Thus, the aim of this study was to focus on identifying critical cuticle genes that are involved in cuticle formation. This study involves identification of two such cuticle collagen genes viz. *dpy-10* and *dpy-31* in the *M. incognita*. Characterizing such developmental genes will help in understanding the mechanism of cuticle development in *M. incognita*. *dpy* genes have been well studied in *C. elegans* and animal-parasitic nematode but the role of these genes and their regulated expression in cuticle formation in *M. incognita* is yet to be deciphered.

MATERIALS AND METHODS

Identification of genes

Nucleotide and protein sequences of *M. incognita* genome were retrieved from NCBI and genome database

(http://www6.inra.fr/Meloidogyne_incognita) (Abad *et al.* 2008). The *C. elegans* sequences (retrieved from NCBI) were used as a query as it is a representative of nematodes. The local nucleotide and protein database was created in BioEdit (version 7.0.9.0) for identifying putative *M. incognita dpy-10* and *dpy-31* gene. An e-value and cut off (default parameters) was the selection criterion and hits with lower e-value were discarded. Further filtration was carried out on the basis of Pfam (<http://pfam.janelia.org/>) analysis using default parameters and removal of those genes that did not contain the known conserved domains and motifs (Finn *et al.* 2016). Thus, these two sequences were retrieved from the *M. incognita* database and their detailed study was carried out.

Gene structure and phylogenetic analyses

A gene prediction algorithm GeneMark and FGENSH were employed for prediction of the gene structure. The intron-exon structures were visualized using the online Gene Structure Display Server v 2.0 (GSDS) (<http://gsds.cbi.pku.edu.cn/>) (Hu *et al.* 2015) with the help of coding sequence and corresponding genomic sequences which depicts the exon/intron arrangement, gene length, and upstream/downstream region.

The identified DPY-10 and DPY-31 amino acid sequences in *M. incognita* were aligned in MUSCLE with default parameters with other DPY orthologues identified and also reported across the nematode phylum using tBLASTn with *C. elegans* DPY-10 and DPY-31 as a query (Edgar, 2004). Following are the nematodes used for constructing phylogenetic tree viz. *C. elegans*, *C. briggsae*, *C. japonica*, *C. brenneri* and *C. remanei* (retrieved from NCBI), *M. hapla*, *M. floridensis* (retrieved from our blast analysis), *Brugiya malayi*, *Pristionchus pacificus* and *Onchocerca volvulus* (retrieved from Wormbase). The unrooted phylogenetic tree was constructed by Neighbor-Joining (NJ) method using MEGA 7.0 software (<http://www.megasoftware.net/>), with Poisson correction, pairwise deletion and bootstrap value set to 2000 replicates for analyzing the clustering pattern as parameters (Kumar *et al.* 2016).

Identification of conserved motifs and protein structure

NCBI conserved domain database was used for identifying conserved domains within the *Mi-dpy-10* and *Mi-dpy-31* genes. Transmembrane domains and signal peptide sequences were detected using TMHMM server v. 2.0 and SignalP3.0, respectively. The Isoelectric Point (pI), molecular weight and grand average of hydropathy (GRAVY) of the amino acid sequences were predicted by Sequence Manipulation Suite (SMS) V2 available at gene infinity web server (<http://www.geneinfinity.org/index.html?dp=5>). The subcellular localization of DPY-10 and DPY-31 proteins was predicted using WoLFPSORT a protein Subcellular Localization Prediction Tool available at <http://www.genscript.com/wolf-psort.html>. The secondary structure of DPY-10 and DPY-31 were generated using Phyre² prediction pipeline and protein databases (Kelly *et al.* 2015).

Protein-protein interaction prediction

To better understand the functional interactions of DPY-10 and DPY-31 with other cuticle genes, we imported all the cuticle sequences identified through our computational approach from *M. incognita*, into the STRING database v10 (Szklarczyk *et al.* 2014). To construct the protein-protein interaction we retained an interaction from experiments, co-expression, and databases and also textmining (in case of DPY-31) that had a median confidence ≥ 0.4 .

Maintenance of nematode pure culture

The tomato (*Solanum lycopersicum*) seeds were sterilized (soaked for 20 min in sterile distilled water, 5 min in 70 % ethanol and 15 min in 5 % NaOCl and 0.1 % Tween 20, and washed four times in sterile distilled water) and germinated on cocopeat, vermiculite and sand (1:1:1) mixture in IARI glass house. Two-week-old tomato seedlings were infected with a pure culture of *M. incognita* maintained in our lab. Egg-masses of *M. incognita* were hand-picked from the roots of these infested plants and were then kept for hatching at 28 °C in Petri plates containing 10-15 ml of sterile water for

collecting second stage juveniles (J2s) of *M. incognita*. These J2s were then used for the subsequent inoculation and expression studies.

RNA isolation and expression analyses of cuticle collagen genes

Total RNA was isolated from egg masses, infective stage juveniles (J2s) and mature females. J2s were hatched from freshly picked egg masses and mature females were excised from infected roots. Total RNA was isolated using Pure Link RNA Mini Kit (Ambion) according to the manufacturer's instructions followed by DNase treatment using Qiagen DNase enzyme. cDNA was synthesized using SuperScript® III First-Strand Synthesis System (Invitrogen).

A quantitative real-time PCR (RT-qPCR) was performed on *M. incognita* RNA samples of egg masses, infective stage juveniles (J2s), and mature females for evaluating the expression at different development stages. SYBR based chemistry was adopted to operate RT-qPCR in a StepOnePlus™ Real-Time PCR System. The primers of *M. incognita* specific Actin and 18SrRNA genes were used as a reference (Table S1) (Nguy^Ån *et al.* 2014, Ye *et al.* 2015). Three biological and three technical replicates were used per sample. The data were analyzed using the 2^[-Delta Delta C(T)] method and reported as the means \pm standard errors (SE) of three biological replicates (Livak & Schmittgen 2001) and statistically analyzed by ANOVA followed by determining the significant difference between the sample means through student t-test ($p < 0.05$).

Isolation and cloning of cuticle collagen genes

The cDNA sample synthesized from the RNA isolated from the adult females was used for the cloning of pGEM-T Easy vector (Promega, USA). Gene-specific primers were designed for the amplification of the desired partial mRNA sequence and PCR product was purified using Qiagen gel extraction kit (Table S1). The initial screening for the recombinant clones was performed through colony PCR and further confirmation of the positive clones was done by Sanger-sequencing.

RESULTS

Identification, isolation and cloning of *M. incognita* cuticle collagen genes

We identified two cuticle collagen genes namely, *dpy-10* and *dpy-31* genes in *M. incognita* as the orthologs of *Ce-dpy-10* and *Ce-dpy-31* genes using in silico approach. The sequences were retrieved from the genomic database of *M. incognita* and were further analyzed. The local TBLASTN revealed a single hit for the *dpy-10* (Minc15911) gene and two hits for *dpy-31* (Minc01936 and Minc03986). The BLAST analysis revealed >95% similarity between Minc01936 and Minc03986 both at the gene as well as amino acid level despite showing different coordinates. Genes enlisted in OrthoMCL search database carried out by Abad *et al* also revealed *Ce-dpy-10* and *Ce-dpy-31* genes ortholog in *M. incognita* genome (2008). A recent report also predicted Minc01936 as *dpy-31* gene in *M. incognita* while identifying *dpy-31* in ovine gastrointestinal nematode *Teladorsagia circumcincta* (Stepek *et al.* 2015). At the gene level, *Mi-dpy-31* (Minc01936) is transcribed by a 3.328 kb long sequence, comprising of 12 exons and 10 introns and *Mi-dpy-31* (Minc03986) gene is 3.721 nucleotides long, comprising of 14 exons and 13 introns (as analyzed on G-browse available at *M. incognita* resources; http://www6.inra.fr/meloidogyne_incognita). Whereas its ortholog in *C. elegans* is a 5kb long gene, interestingly comprising of 8 exons and 7 introns. The 3.328 kb DNA segment of *dpy-31* is predicted to encode a 1.197 kb long mRNA and Minc03986 encoding a 1.148 kb long. While *Mi-dpy-10* showed gene length of 1.903 kb comprising of 8 exons and 7 introns and *Ce-dpy-10* is reported as 2.072 kb long interestingly comprising of only 4 exons and 3 introns. *Mi-dpy-10* mRNA is 1.181 kb long which is shorter in length in comparison to *Ce-dpy-10* mRNA which is 1.586 kb. Even with the disparity in the number of exons and coding length between *C. elegans* and *M. incognita* cuticle genes, gene structure analysis indicated the presence of a similar length of the conserved domains in both the cuticle genes identified in *M. incognita*. The partial mRNA sequence of *Mi-dpy-10* (1,031 bp) and *Mi-dpy-31* (1,116 bp) were successfully cloned in

pGEMT easy vector and both the sequences were confirmed by Sanger sequencing (Fig. 1 and 2). The sequencing result revealed 99% similarity to the *dpy-10* and *dpy-31* sequences that were enlisted in the OrthoMCL analysis reported by Abad *et al.* (2008).

Protein prediction and phylogeny analysis

Although the identified *dpy-10* and *dpy-31* genes in *M. incognita* are the orthologs of *C. elegans* genes due to the difference between the two in their habitat and lifestyle, former being endoparasites and latter a free-living nematode, we expected some difference in their cuticle protein composition. In order to analyze the biochemical properties of these two genes molecular weight, isoelectric point (pI) and subcellular localization were predicted. The identified *dpy-10* encodes a protein of 352 amino acids long (Fig. 3a). The two probable paralogs of *dpy-31* identified viz., Minc01936 and Minc03986 encode a protein of 391 and 375 amino acids, respectively (Fig. 3b). The molecular weight of DPY-10, DPY-31(Minc01936) and DPY-31(Minc03986) proteins is 36.83 kDa, 45.43 kDa and 43.44 kDa with isoelectric point (pI) of 5.20, 6.65 and 6.17, respectively. A negative grand average of hydropathicity (GRAVY) scores of -0.683, -0.808 and -0.771 of these identified DPY-10, DPY-31 (Minc01936 and Minc03986) proteins indicated the hydrophilic nature. The sub-cellular localization prediction of both the cuticle collagen genes revealed it to be a complex. The analysis showed both are majorly located in nuclear or extracellular (including cell-wall) regions. As reported earlier the expression of *dpy-31* in the hypodermis was noticed and is reported to process cuticle components (Mohrlen *et al.* 2003, Novelli *et al.* 2004, Suzuki *et al.* 2004, Park *et al.* 2010). The TMHMM prediction software indicated the presence of transmembrane domain in Mi-DPY-10 similar to that of Ce-DPY-10 protein (Fig. 4a). In case of Mi-DPY-31 no transmembrane domain was predicted in accordance with Ce-DPY-31 protein (Fig. 4b). But signal peptide prediction software revealed contrasting output between Mi-DPY-31 and Ce-DPY-31 where latter showed a presence of signal peptide and former absence (Fig. S1a). Whereas signal peptides were not found in Mi-DPY-10 and Ce-DPY-10 proteins (Fig. S1b).

The phylogenetic analysis of these genes was on the basis of high similarity within the conserved collagen domains. The phylogenetic tree indicates the presence of DPY-10 and DPY-31 throughout the different nematode phylum and its conserved function (Fig. 5 and 6). Phylogenetic tree involving Mi-DPY-10 formed two clusters. In case of DPY-31, both the probable paralogs of Mi-DPY-31 (Minc01936 and Minc03986) grouped together forming cluster II with other *Meloidogyne spp.* The analysis showed three clusters with DPY-31 belonging to *Meloidogyne spp viz., M. incognita, M. floridensis* and *M. hapla* placed in one cluster and hence, closely related. Cluster I and III comprised of cuticle genes from free-living and animal-parasitic nematodes, respectively.

Presence of conserved domains and secondary structure

Proteins of DPY family have a diverse role ranging from development to processes like extracellular matrix components. Protein structure analysis of DPY-10 reveals the presence of collagen superfamily domain which contains copies of Gly-X-Y to form a triple helix. The analysis revealed two copies of such collagen triple helix, a highly conserved 60 amino acid long sequence. The multiple sequence alignment showed that it is evolutionary conserved across nematode phylum (Fig. 7). It was reported to be 60 amino acids long in *C. elegans* and *B. malayi* having two copies in each. It was observed that in Mi-DPY-10, the Gly-X-Y repeats forming this triple helix are flanked by conserved cysteine residues as reported in Ce-DPY-10. The pattern of Gly-X-Y repeats of Mi-DPY-10 resembles that of Dpy-2 group as classified on the basis of the pattern of conserved cysteines (Johnstone, 2000). In Mi-DPY-10 the size of Gly-X-Y repeats between first and second cysteine cluster is 47 amino acids and between second and third cluster is 131 amino acids. It was also observed that proline content was more in the Gly-X-Y pattern in Mi-DPY-10 which is a typified character of nematodes. Secondary structure prediction exhibited that 18% amino acid residues were involved in alpha helices, 7% in TM helix (transmembrane), 4% comprises β -turn and rest 71% involved in the random coil (Fig. 8).

Astacin domain is a characteristic of members of DPY family proteins. In both the Mi-DPY-31 proteins (Minc01936 and Minc03986), astacin domain is comprised of 191 amino acid residues. Astacin containing proteins are proteases that require zinc for catalysis and hence, the name metalloprotease proteins. Presence of astacin domain indicates towards the peptide cleavage role of Mi-DPY-31. The motif search analysis showed same motifs of similar sizes in these two probable copies of DPY-31. Apart from astacin domain, motif analysis search also revealed the presence of CUB domain (for complement C1r/C1s, Uegf, Bmp1) at C-terminal of both the copies of Mi-DPY-31, thus classifying it under subgroup V according to the classification by Park *et al* (2010). It comprises of 110 amino acids, similar as observed in Ce-DPY-31 (Fig. 9). The proteins with astacin and CUB domain are generally membrane proteins known to be involved in development. Thus, Mi-DPY-31 could also be a membrane protein although no transmembrane domain was predicted in Mi-DPY-31 which is in accordance to Ce-DPY-31. DPY-31 is thought to be responsible for C-terminal cleavage of the cuticular collagen SQT-3 (Novelli *et al.* 2004), a function reminiscent of the role of BMP-1 in cleaving fibrillar collagens in vertebrates (Reddi, 1996, Park *et al.* 2010). Secondary structure prediction of Mi-DPY-31 revealed 21% of amino acid residues involved in alpha helices, 23% in β -strand and rest in the random coil (Fig. 10). On comparing the secondary structures of Mi-DPY-31 and Ce-DPY-31, not much deviation in the structures was noticed.

Protein-protein interaction

To determine the probable function of DPY-10 and DPY-31 in *M. incognita*; a protein-protein association network was carried out using STRING software. For this, we identified and retrieved other dumpy genes from the *M. incognita* genome using *C. elegans* dumpy genes as a query. The analysis revealed a direct interaction between Mi-DPY-2, Mi-DPY-7, and Mi-DPY-10 (Fig. 11). To further confirm our result we also performed protein-protein interaction analysis for Ce-DPY-10 and Ce-DPY-31 genes with other cuticle genes using STRING. The analysis revealed a direct interaction

between Ce-DPY-10, Ce-DPY-7, and Ce-DPY-2. However, an indirect network between Ce-DPY-10 and other proteins like NOAH-1, NOAH-2, MLT-11, DPY-3, ACN-1 and IPR-3 (Fig. S2) was noticed. Nevertheless, we were unable to identify these sequences in *M. incognita* genome and therefore no such network was established between Mi-DPY-10 and other respective protein sequences. Interestingly, Mi-DPY-31 displayed a direct interaction with only Mi-SQT-3 protein (sequence identified and retrieved in our BLAST analysis) similar to the predicted interaction network indicated by the Ce-DPY-31 (Fig. 12).

Transcript abundance of cuticle collagen genes during development stages of *M. incognita*

To study the expression pattern of *dpy-10* and *dpy-31* in *M. incognita* development, three different stages (eggs, J2s, and adult females) were selected. *dpy-10* showed higher expression at J2 stage (7.5 fold) indicating towards its possible role during an early stage of molting (Fig. 13). In *dpy-31* transcript levels were found higher in adult females as compared to early stages (Fig. 14). Thus, indicating its possible role during the fourth round of molting in its life cycle.

DISCUSSION

Earlier studies report the presence of similar cuticle synthesis enzymes in the free-living nematode *C. elegans* and parasitic-nematodes hence, this study reports the identification and characterization of two of the cuticle collagen genes viz., *Mi-dpy-10* and *Mi-dpy-31*, functioning in the cuticle formation of nematode, from *M. incognita* using *Ce-dpy-10* and *Ce-dpy-31* as orthologs. The complete nucleotide sequences of *dpy-10* and *dpy-31* genes have been characterized in *C. elegans*. These are collagen genes involved in cuticle structure development of nematodes. Gene structure analysis revealed a difference of 1 Kb in gene length between *Mi-dpy-10* and *Ce-dpy-10* gene. Although encoding a protein of a similar number of amino acids, Mi-DPY-10 lacks the presence of N-terminal domain that was reported in Ce-DPY-10. This might be due to the *M. incognita* genome assembly present in scaffold forms. Two hits of the *Mi-dpy-31* present at different scaffolds

were found in our analysis and both showed more than 70 % similarity to *Ce-dpy-31* isoform a. These two hits could be two copies of the *dpy-31* present at a different location in *M. incognita* genome which got duplicated during speciation. Another probable reason for obtaining two hits could be as stated above due to the *M. incognita* genome assembly in scaffold form. Nevertheless, both the hits showed more than 95 % similarity at gene as well as amino acid level among themselves.

Astacins are the class of metalloprotease proteins playing important role in structure development of nematodes. Recent review studies reported about 37 astacins present in *M. incognita*, 30 in *M. hapla*, 13 in *B. malayi* and some in *M. chitwoodi*, *Parastronglyoides trichosuri* and *Trichinella spiralis* on basis of in silico analysis indicating the conserved function and expansion of astacin protein family in nematodes (Craig *et al.* 2007, Park *et al.* 2010). *Mi-dpy-10* and *Mi-dpy-31* belong to group *dpy-2* and subgroup V, respectively as based on classification by Johnstone & Park (2000, 2010). There are only two members of group *dpy-2* and members of this group have a defined function in post-embryonic developmental stages. The members of subgroup V are known to express in hypodermis and have a role in cuticle components like collagen processing.

DPY-10 enzymes are characterized to have a longer C-terminal tail than average similar observation was made in Mi-DPY-10. A negative GRAVY value of Mi-DPY-10 implies hydrophilic nature of this protein thus suggesting the enzymatic role of Mi-DPY-10. The presence of conserved Gly-X-Y repeats interrupted by cysteines residues was in accordance with Ce-DPY-10 with proline as the major preference in position X. In Mi-DPY-31 conserved zinc-binding active site (HExxHxxGFxHExxRxDRD) and methionine-turn (SxMHY) domain which are characteristic of astacin protein was found in our motif search. Interestingly, the multiple sequence alignment analysis revealed a 100 % identity in these two sites among all the nematodes across different phylum. Thus, the conserved catalytic and methionine-turn sites were HEVAHALGFWHEQSRPDRD and SIMHY, respectively found in our analysis. All the domains

present in DPY-10 and DPY-31 have been well characterized in cuticle development in nematodes. Thus, the presence of collagen triple helix in Mi-DPY-10 and astacin and CUB domain in Mi-DPY-31 suggests their role in cuticle formation and development in *M. incognita*. Further, the protein network analysis reveals both the direct as well as the indirect associations based on functional roles of Mi-DPY-10 and Mi-DPY-31. Interestingly, the direct and major role of Mi-DPY-10 is observed with the member of its own group viz., Mi-DPY-2. Together, these two play a vital role in post-embryonic body morphogenesis and development besides constituting collagen and cuticulin-based cuticle in *M. incognita*. Additionally, Mi-DPY-10 and Mi-DPY-7 form the structural constituent of the extracellular cuticle. Alternatively, Mi-DPY-31 is shown to have a direct interaction with only Mi-SQT-3 as indicated by the prediction analysis which is a substrate for DPY-31 procollagen C-proteinase as reported in *C. elegans*. However, future work involving yeast two-hybrid assay is required to fully evaluate this contention.

Genes belonging to the *dpy* family are known to have a regulated spatial and temporal expression, each expressing at a different time in nematode life cycle. These genes have been described as early, intermediate or late expressing genes on basis of mRNA abundance in *C. elegans* (Page & Johnstone 2007). The RT-qPCR based expression of *Mi-dpy-10* in this study is analogous to that observed in *Ce-dpy-10*. *Mi-dpy-10* showed highest expression in the J2 stage which is an early development stage in *M. incognita*. The higher expression during early stage is the characteristic of *dpy-2* subgroup class of genes. Thus, indicating its role during the second molting of cuticle from J2 to J3 in *M. incognita*. Unlike *dpy-10*, *dpy-31* is known to express throughout the life cycle of nematode, with specifically in early larval stages (Novelli *et al.* 2004, Stepek *et al.* 2015). However, *Mi-dpy-31* showed different expression pattern than that reported in other nematodes, expressing higher in the later stage of development i.e. in adult females. This variation in the expression pattern of *Mi-dpy-31* might indicate its specific role during later stages of the life cycle in *M. incognita* thus, a species-specific role.

Nematode cuticle is encoded by multigene family among which dumpy (DPY) class of proteases are one

such member having a vital role in cuticle formation and development. Members of this family are known to contain some but not all the regions, each member is required at different time of cuticle formation. In conclusion, this study reports the presence of *dpy-10* and *dpy-31* in *M. incognita*. It also demonstrates the role of these genes at the different time of nematode development through RT-qPCR based expression studies. Conserved nature and the critical role of these genes can be seen from the phylogenetic analysis performed among different nematode phylum. The nematode cuticle acts as a defensive shield for both plant and animal-parasitic nematode by preventing them from phagocytosis. The cuticle is indeed vital for nematode survival thus, targeting genes that are involved in cuticle formation and development will aid in combating such parasites. Dumpy genes have been targeted in animal-parasitic nematodes for controlling their infection in hosts. *Tc-dpy-31* in sheep gastrointestinal nematode, *T. circumcincta* is considered a new target for drug development to manage nematode infection (Stepek *et al.* 2015). *dpy 2, 4, 10* and *11* have been identified in *Bursaphelenchus xylophilus* and targeted for dsRNA-mediated gene silencing (Wang *et al.* 2016). Cuticle collagen genes are interesting for biochemists and molecular biologists. Dumpy genes have been identified by the reverse genetic approach in *Pristionchus pacificus* (Kenning *et al.* 2004). These genes have a potential to be a target for nematode control. The identification of dumpy genes through RNA interference (RNAi) based mutation in *C. elegans* in itself indicates the crucial role played by these genes. Hence, *dpy-10* and *dpy-31* is a potent target for host-mediated RNAi approaches for developing transgenics conferring resistance against plant-parasitic nematodes by interrupting the nematode cuticle development.

CONFLICTS OF INTEREST

On behalf of all authors, the corresponding author states that there is no conflict of interest.

ACKNOWLEDGEMENTS

The authors thank the staff of the National Phytotron Facility, IARI, New Delhi, India for providing space in the greenhouse and in the growth chambers.

FINANCIAL SUPPORT

The present study was supported by a grant from the ICAR-NASF (formerly known as NFBSFARA) (code: NFBSFARA/RNA-3022) project during the years 2012-15.

REFERENCES

- Abad, P., Gouzy, J., Aury, J.M., Castagnone-Sereno, P., Danchin, E.G.J., Deleury, E., Perfus-Barbeoch, L., Anthouard, V., Artiguenave, F., Blok, V.C., Caillaud, M.C., Coutinho, P.M., Dasilva, C., De Luca, F., Deau, F., Esquibet, M., Flutre, T., Goldstone, J.V., Hamamouch, N., Hewezi, T., Jaillon, O., Jubin, C., Leonetti, P., Magliano, M., Maier, T.R., Markov, G.V., McVeigh, P., Pesole, G., Poulain, J., Robinson-Rechavi, M., Sallet, E., Ségurens, B., Steinbach, D., Tytgat, T., Ugarte, E., van Ghelder, C., Veronico, P., Baum, T.J., Blaxter, M., Blevé-Zacheo, T., Davis, E.L., Ewbank, J.J., Favery, B., Grenier, E., Henrissat, B., Jones, J.T., Laudet, V., Maule, A.G., Quesneville, H., Rosso, M.N., Schiex, T., Smant, G., Weissenbach, J. & Wincker, P. (2008). Genome sequence of the metazoan plant-parasitic nematode *Meloidogyne incognita*. *Nature Biotechnology* **26**: 909-915.
- Banerjee, S., Gill, S.S., Jain, P.K. & Sirohi, A. (2017). Isolation, cloning, and characterization of a cuticle collagen gene, *Mi-col-5*, in *Meloidogyne incognita*. *3 Biotech* **7**: 64.
- Craig, H., Isaac, R.E. & Brooks D.R. (2007). Unravelling the moulting degradome: new opportunities for chemotherapy? *Trends Parasitol* **23**: 248-253.
- Davis, M.W., Birnie, A.J., Chan, A.C., Page, A.P. & Jorgensen E.M. (2004). A conserved metalloprotease mediates ecdysis in *Caenorhabditis elegans*. *Development* **131**: 6001-6008.
- Edgar, R.C. (2004). MUSCLE: multiple sequence alignment with high accuracy and high throughput. *Nucleic Acids Research* **32**: 1792-1797.
- Elling, A.A. (2013). Major emerging problems with minor *Meloidogyne* species. *Phytopathology* **103**: 1092-1102.
- Finn, R.D., Coggill, P., Eberhardt, R.Y., Eddy, S.R., Mistry, J., Mitchell, A.L., Potter, S.C., Punta, M., Qureshi, M., Sangrador-Vegas, A., Salazar, G.A., Tate, J. & Bateman, A. (2016). The Pfam protein families database: towards a more sustainable future. *Nucleic Acids Research*. **44**: D279-D285.
- Gray, L.J., Curtis, R.H. & Jones, J.T. (2001). Characterisation of a collagen gene subfamily from the potato cyst nematode *Globodera pallida*. *Gene* **263**: 67-75.
- Hu, B., Jin, J., Guo, A.Y., Zhang, H., Luo, J. & Gao, G. (2015). GSDS 2.0: an upgraded gene feature visualization server. *Bioinformatics* **31**: 1296-1297.
- Johnstone, I.L. (2000). Cuticle collagen genes: Expression in *Caenorhabditis elegans*. *Trends Genetics* **16**: 21-27.
- Kelley, L.A., Mezulis, S., Yates, C.M., Wass, M.N. & Sternberg, M.J. (2015). The Phyre2 web portal for protein modeling, prediction and analysis. *Nature Protocols* **10**: 845-858.
- Kenning, C., Kipping, I. & Sommer, R.J. (2004). Isolation of mutations with dumpy-like phenotypes and of collagen genes in the nematode *Pristionchus pacificus*. *Genesis* **40**: 176-183.
- Kumar, S., Stecher, G. & Tamura, K. (2016). MEGA7: Molecular Evolutionary Genetics Analysis version 7.0 for bigger datasets. *Molecular Biology Evolution* **33**: 1870-1874.
- Livak, K.J. & Schmittgen, T.D. (2001). Analysis of relative gene expression data using real-time quantitative PCR and the 2(-Delta Delta C(T)) Method. *Methods* **25**: 402-408.
- Mohrlen, F., Hutter, H. & Zwilling, R. (2003). The astacin protein family in *Caenorhabditis elegans*. *European Journal of Biochemistry* **270**: 4909-4920.
- Nguy^âân, P.V., Bellafiore, S., Petitot, A., Haidar, R., Bak, A., Abed, A., Gantet, P., Mezzalana, I., Engler, J.D.A. & Fernandez, D. (2014). *Meloidogyne incognita* - rice (*Oryza sativa*) interaction: a new model system to study plant-root-knot nematode interactions in monocotyledons. *Rice* **7**: 23.
- Novelli, J., Ahmed, S. & Hodgkin, J. (2004). Gene interactions in *Caenorhabditis elegans* define DPY-31 as a candidate procollagen C-proteinase and SQT-3/ROL-4 as its predicted major target. *Genetics* **168**: 1259-1273.
- Page, A.P. & Johnstone, I.L. (2007). The Cuticle. *WormBook* **19**: 1-15.

- Park, J.O., Pan, J., Mohrlen, F., Schupp, M.O., Johnsen, R., et al.** (2010). Characterization of the astacin family of metalloproteases in *C. elegans*. *BMC Development Biology* **10**: 14.
- Reddi, A.H.** (1996). BMP-1: resurrection as procollagen C-proteinase. *Science* **271**: 463.
- Suzuki, M., Sagoh, N., Iwasaki, H., Inoue, H. & Takahashi, K.** (2004). Metalloproteases with EGF, CUB, and thrombospondin-1 domains function in molting of *Caenorhabditis elegans*. *Biology Chem* **385**: 565-568.
- Stepek, G., McCormack, G., Winter, A.D. & Page, A.P.** (2015). A highly conserved, inhibitable astacin metalloprotease from *Teladorsagia circumcincta* is required for cuticle formation and nematode development. *International Journal of Parasitology* **45**: 345-355.
- Wang, M., Wang, D., Zhang, X., Wang, X., Liu, W., Hou, X., Huang, X., Xie, B. & Cheng, X.** (2016). Double-stranded RNA-mediated interference of dumpy genes in *Bursaphelenchus xylophilus* by feeding on filamentous fungal transformants. *International Journal of Parasitology* **46**: 351-360.
- Wang, T., Deom, C.M. & Hussey, R.S.** (1998). Identification of a *Meloidogyne incognita* cuticle collagen gene and characterization of the developmental expression of three collagen genes in parasitic stages. *Molecular Biochem Parasitology* **93**: 131-134.
- Ye, W., Zeng, Y. & Kerns, J.** (2015). Molecular characterization and diagnosis of root-knot nematodes (*Meloidogyne* spp.) from Turfgrasses in North Carolina, USA. *PLoS One* **10**: e0143556.